Investigating the Production of Multiple Bio-Products from Cassava Peel and Date Seed through an Integrated Biorefinery Approach

A Thesis Submitted in Fulfilment of the Requirements for the Degree of

Doctor of Philosophy (PhD)

Alla Alrefai

BEng, MSc (Mechanical and Manufacturin Engineering)

Supervisors

Prof. Joseph Stokes & Dr. Khaled Benyounis

School of Mechanical and Manufacturing Engineering

Dublin City University

September 2021

Declaration

I hereby certify that this material, which I now submit for assessment on the programme of study leading to the award of PhD is entirely my own work, and that I have exercised reasonable care to ensure that the work is original, and does not to the best of my knowledge breach any law of copyright, and has not been taken from the work of others save and to the extent that such work has been cited and acknowledged within the text of my work.

Signed:  Student ID no.: 59210679 Date: 09/09/2021

Acknowledgment

In the beginning, all of my praise goes to ALLAH and his blessing to help me complete this thesis. I thank ALLAH for the opportunity, strength and patience during my studies.

I would like to express my gratitude and appreciation to my supervisor Prof. Joseph Stokes for providing guidance, support, enthusiasm, encouragement, feedback and patience throughout this project.

I would like to gratefully thank Dr. Khaled Benyounis for his time in helping me in completing my experimental work, continued support, advise, patients and willingness to impart his knowledge throughout this project.

From the bottom of my heart, I would like to say a big thank you to my parents (Mohammed and Kadeja), who set me off on the road to this PhD. Your prayers and encouragement had a great impact on me in completing my PhD.

My wife Ghaida, my daughters Wareef and Seba and my son Mohammed, thanks for your support, you have been amazing. Thank you for enduring my absence for such long periods.

I would like to express my gratitude and appreciation to my brothers (Hussam, Raid and their families) for your support, wishes and prayers.

My biggest thanks to my family and friends for your support that have shown through out this research.

I would like to express my sincere gratitude to the Saudi Government and Saudi Cultural Bureau in Ireland, for their funds and giving me this opportunity.

I am also thankful to Dublin City University, the staff members of the School of Mechanical and Manufacturing Engineering for all their guidance.

Table of Contents

Nomenclature

AD	Anaerobic digestion
N	Nitrogen
P	Phosphorous
K	Potassium
DM	Dry matter
DOE	Design of experiment
RSM	Response surface methodology
α	Significance level
VS	Volatile solid
TS	Total solid
MS	Moisture content
ANOVA	Analysis of variance
BBD	Box-Behnken design
Pred. R^2	Predicted R^2
Adj. R^2	Adjusted R^2
Adequation Precision	Adequate Precision
Cor total	Total sum of the squares corrected for the mean
df	Degree of freedom
B_s	The energy content of Biogas produced by substances in [kW h/m3]
9.67	The energy content of 1 Nm^3 (Normal cubic meter) of biogas
E_p	The energy gained from a gram of volatile solid of substances from the biogas produced in [Wh/g-VS]
B_p	The biogas volume produced from each gram of volatile solid of substances.
E_c	The energy consumed by the water bath to digest the gram volatile solid of substances in [Wh/g-VS].
E_{pt}	The electric energy consumed in the digestion process, which was measured by a prodigit kilowatt-hour meter.
VS_m	The total amount of volatile solid in the water bath

List of Figures

List of Tables

Publications

The to date list of publications arising from this research are as follows:

Published Journal Paper

1. Alrefai, A.M., Alrefai, R., Benyounis, K.Y. and Stokes, J., 2021. Biogas Produced by Anaerobic Digestion Process and Biodiesel from Date Seed. Energies, 14(16), p.4851.

2. Alrefai, A.M., Alrefai, R., Benyounis, K.Y. and Stokes, J., 2020. Impact of Starch from Cassava Peel on Biogas Produced through the Anaerobic Digestion Process. Energies, 13(11), p.2713.

Published Book Chapter

1. Alrefai, A.M., Alrefai, R., Benyounis, K. Y., and Stokes, J, Bio-Based Polymer Adhesive Material: Properties and Applications, Reference Module in Materials Science and Materials Engineering, Elsevier, 2020.

2. Alrefai, A.M., Alrefai, R., Benyounis, K. Y., and Stokes, J, The Environmental Challenges Associated With the Anaerobic Digestion Process when Applied Extensively, 2019, in Encyclopedia of Renewable and Sustainable Materials., Elsevier. p. 279-286.

International Conference Paper:

1. Alrefai, A.M., Alrefai, R., Benyounis, K. Y., and Stokes, J, Impact of Cassava's Peel Starch on the Biogas Produced Through Anaerobic Digestion Process, in Sustainable Development of Energy, Water and Environment System (SDEWES 2019), October 1-6. 2019: Dubrovnik.

Investigating the Production of Multiple Bio-Products from Cassava Peel and Date Seed through an Integrated Biorefinery Approach

Alla Alrefai

Abstract

The environmental damage from fossil fuels due to harmful emissions and the desire to find alternative sustainable energy sources led to this investigation of utilising biomass energy. Food wastes are considered one of the important sustainable sources of energy. Exploiting them in the production of energy may lead to avoiding the damage resulting from their accumulation. In this study, the possibility of exploiting the waste/unused product from cassava and date were explored as they are an important food used by many nations. Globally about 550 million metric tons of cassava and 9 million tons of dates are produced annually. Several bio-products can be produced from cassava peel starch and date seed oil, in addition, biogas can be produced through the anaerobic digestion process. The cassava peels have a considerable amount of starch and date seeds contain oil, so this study aims to explore the effect of starch and oil extracted from them on the quantity and quality of the resulting biogas. It also contributes to demonstrating the possibility of benefiting from producing bio-products from extracted starch and oil such as adhesive, biodiesel and glycerine. Overall this research has investigated the production of multiple bio-products from cassava peel and date seed using an integrated biorefinery approach.

Cassava peel was treated by beating pre-treatment process to chop and slice the peel and extract the starch at the same time. The date seeds were treated using a grains and stones grinding machine. The digestate resulting from the anaerobic digestion was tested to determine starch and oil extraction effects on the resulting digestate. The influence of temperature, volatile solid and sludge quantity were investigated with the aid of Design of Experiments (DOE). An optimisation process was carried out to calculate the energy balance at the optimal results and evaluate the impact of the extraction process on the biogas and digestate produced, calculating the production costs of biodiesel, the adhesive and the preliminary analysis of process boundary, thus to evaluate its biorefinery applications.

The study revealed that the influence of the starch on the biogas quantity and quality was quite low. Simultaneously, the oil extraction process contributed to the decrease in the amount of biogas and methane. The addition of cassava peels and date seeds before and after starch and oil extraction contributed to increase biogas and methane yields. The highest biogas volume obtained from the cassava peel, date seed and extracted oil date seed was 3830 ml, 4140 ml and 3534 ml respectively. The maximum methane per gram volatile solid added was 850 ml /g-VS, 1143.8 ml /g-VS and 949.6 ml /g-VS respectively. The percentage of oil extracted from date seeds was approximately 16% of the date seed weight, while the biodiesel and glycerine accounted for 79% and 9% of it. The starch-based adhesives showed high adhesion strength to the plywood and paperboard specimens. The laboratory tests of the resulting digestate proved that the anaerobic digestion process contains the necessary elements in fertiliser, so this test aims to gain more knowledge about the digestate. Overall, the study investigated the feasibility of an integrated biorefinery approach to the use of cassava peel and date seeds; to produce several bio-products and proper waste management with promising results.

Chapter 1

1 INTRODUCTION

1.1 Introduction

Energy generation and consumption play a major role in developing and improving the economics of countries and societies [1]. The need for energy has increased due to technological development, population growth, urbanisation and industrial investment [2]. It is estimated there has and will be an increase in energy demand by 85% from 2010 to 2030 worldwide. More than 80% of global energy is produced from non-renewable sources such as oil and gas [3]. The non-sustainable and destructive nature of fossil fuels issues such as harmful emissions and price fluctuation have led to find safer and more efficient energy sources [4, 5]. In addition to that, many studies of researchers and interested people focus on finding solutions to overcome difficulties in increasing energy productivity, diversifying energy sources, overcoming environmental issues and the fair use of the energy. Large amounts of carbon dioxide (CO_2) and other harmful emissions have increased concerns about resulting environmental damage [6, 7]. Furthermore, there are concerns about future shortage of these sources for several reasons, such as natural disaster [8].

The search for alternative solutions to oil, began in the late last century as a result of the rise in oil prices [9]. Natural sources of energy such as; bioenergy, solar energy and wind energy are appropriate solutions to overcome the environmental issues caused by oil extraction/use. Renewable energy from natural resources, which are renewed constantly, can be derived directly or indirectly. Clean energy enhances environmental safety and thus supports society's needs from energy [10, 11]. 20% of the world’s energy is supplied from renewable sources, 10.4% of these sources were from modern sources such as wind, solar and biomass [12]. In 2017, a significant support for the renewable energy sector led to 70% of net added energy capacity around the world, which were from renewable sources, with an investment of more than 275 billion USD [12]. Figure 1 illustrates a representation of sustainable development known as doughnut economics [10].

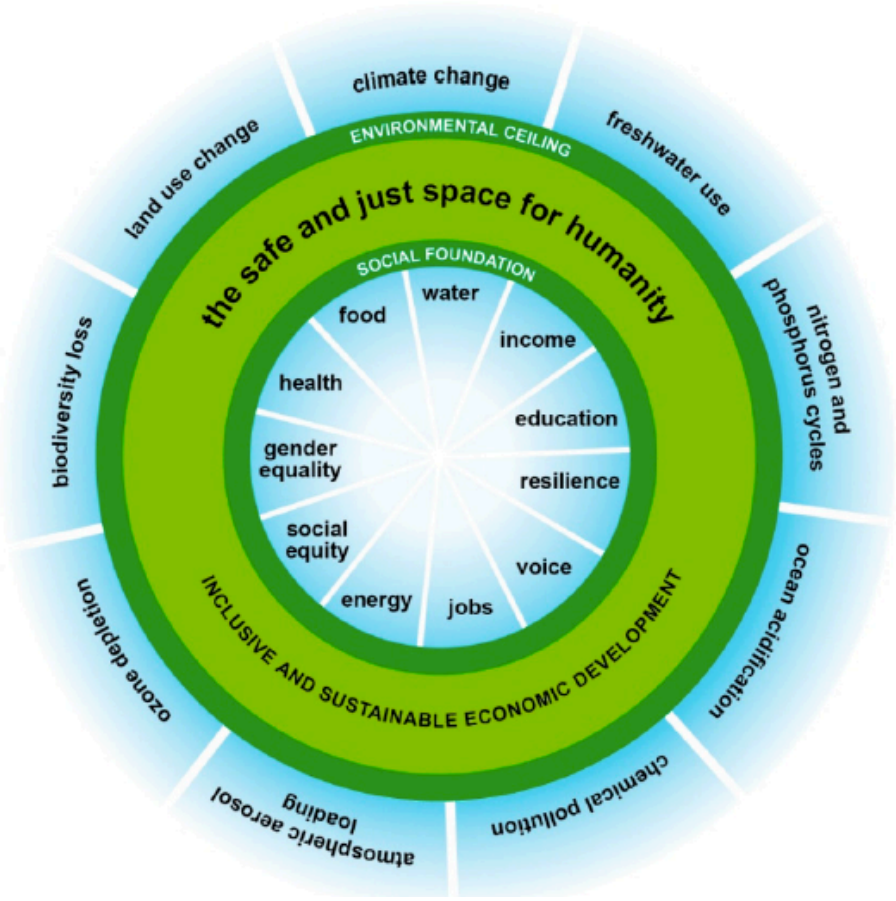

Figure 1: The doughnut economics [13].

The majority of renewable energy worldwide is from biomass fuel such as wood that used for cooking and heating. It is estimated the percentage of renewable energy needs to increase to 50% by the second half of the century [14, 15]. The full utilisation of these massive sources has the ability in principle to provide the world demands from the energy. Where that sustainable energy can be provided by continues utilising several energy sources such as hydropower, wind energy, solar energy, geothermal energy and biomass [16]. Some of renewable energy costs continue to fall down compared to the variability of fossil fuel price. All of these causes, in addition to reaching zero emissions and increasing their sustainability, indicate a promising future for renewable energy within the world markets [17, 18]. The low percentage of harmful emissions from renewable energy reduces the impact of climate change and environmental pollution [19]. In 2016, more than 170 countries employed their effort to reach to the ambitious of renewable energy [20]. The worldwide acceleration of innovation in renewable energy reflects the challenge among nations. Some countries such as Germany, Spain and Denmark are interested in

innovation in wind energy, while countries such as South Korea and Taiwan are interested in innovation in solar energy. Other countries such as America and Japan are also intensifying their effort in developing renewable energy [21]. It is expected that 70-85% of electricity may be generated from renewable energy sources by 2050 [22]. According to International Energy Agency (IEA), renewable energy will cover around 40% of energy demand in 2040 [23, 24].

CO_2 in the atmosphere has increased by 30% over the last five decades, with a dramatically rise of other harmful gases. In addition to these harmful emissions and the use of fossil fuels, temperatures have increased by 0.6 °C during last century [25]. Studies indicate that an increase in temperature by 0.2 °C per decade [25]. Reducing the number of forests and replacing them with buildings, has contributed to quadrupling climate change and increasing emissions by 15% during the 30 years proceeding in 2010. The number of deaths in Europe from diseases that related to the temperature increasing was estimated at 70,000 in 2003 [25, 26]. Belt and Road countries are responsible for more than 60% of CO_2 emotions [27]. The Belt Road Initiative includes 68 countries (about 65% of the world's population) that aim to increase their economic growth and enhance their industrial capabilities by sharing technologies, skilled labour and resources [28].

Energy is considered the basis of economic growth and makes social life more well-being. Sustainable sources of energy are a major element for energy sustainability to obtain an energy security and economic development. Energy participates in most of life aspects such as in education, health, transport and agriculture. These contribute in the creation of Jobs [29]. In addition they contribute to the welfare of people in rural areas, by increasing their economic activities by taking advantage of their own resources [30]. Many nations are transforming from non-renewable energy to renewable energy to overcome the sustainability and environmental issues [20]. Several factors influence the energy development process, such as lack of community awareness about renewable energy and slow demand [31]. The improvement in renewable energy sector, will support in reaching many of people living in poverty by providing more available affordable energy. Governments in some countries support the approach to renewable energy, they providing supported programs through subsidies, tax exemption and other incentives to increase competitiveness. Recently, expansion in renewable energy for developing countries is grown faster than in developed countries [32]. 80% of the produced

energy is renewable in developed countries and 35% in developing countries [32]. For the period from 2004 to 2014, developed and developing countries spent about $ 270 billion on renewable energy. Support in developing countries increased 14 times, while in developed countries it increased fourfold [32, 33]. Worldwide, energy generated from renewable sources in 2017 was 20.9% and It is expected to reach 50% in 2030 [34, 35]. European countries were to produce 20% of total renewable energy by 2020 to meet rising demand [36]. The European Union reached the target since 2017, as the energy and carbon intensity decreased by more than 14.6% and 8.6% compared to 2008 [34, 37]. More than 50 countries worldwide have adopted laws and policies to develop renewable energy [38]. There are different types of energy sources depending on weather alone, such as wind and solar energy [17]. Biomass is another source of renewable that is receiving high attention [39]. They are developing and growing rapidly and it is expected to play a major role in the transformation process to renewable energy [17]. To meet the growing energy demand, which is expected to rise by more than 35% by 2040, the exploitation of renewable energy sources is increasing and it is expected to continue into the future [40, 41].

Anaerobic digestion (AD) is a mature technology for utilising food waste, and converting sewage and grass to biofuel in several stages [42-44]. Currently, AD is not fully utilised in terms of food waste and products due to the lack of knowledge about this technology in addition to the contrast in the feedstock composition. The process needs further exploration of products that can be produced and the resources available [45]. AD is distinguished by its high organic load treatment, low cost and less energy demand [46, 47]. It is more feasible and economical than other biogas production processes despite the pre-treatment processes [48]. The main process faults are its poor stability and low conversion efficiency [47, 49]. Reactors regulation and parameters optimisation are some of the procedures that can lead to more effective AD process [50, 51]. The AD process usually uses one-digestion substances, while using two or more digestion substances is called co-digestion process [52].

The use of biomass has derived from ancient times to use today. Some differences in the current use, compared to the past are the multiplicity of biomass sources and more attention to the environment by controlling harmful emissions [53]. Biomass accounts for about 14% of global renewable energy consumption, increasing the dependence on these vital renewable resources reduces dependence on fossil fuels [54]. Three-quarters of this percentage is used in developing

countries, for example for heating, while the quarter remained is used in industrialised countries for energy production. It is converted to several forms of energy such as biofuels or to bio-products for example bio-plastic and starch-based adhesive material by different methods. Many forms of energy can be produced from biomass such as electricity, heat and other fuels [54, 55]. Figure 2 shows the procedure of producing energy from biomass and its products [56].

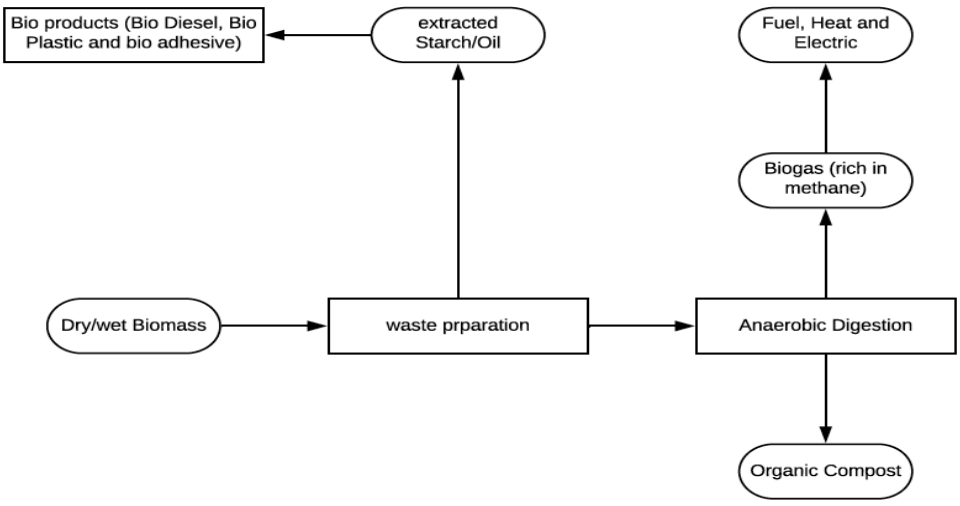

Figure 2: AD process and resulted bio-products [56].

1.2 Contribution to the Science of Biomass Energy

In light of the increasing environmental and health risks resulting from the accumulation of waste in general and food waste in particular, in addition to the emissions of fossil fuels, this study provides some novelty in this regard. The study seeks to provide some solutions to overcome some of the obstacles that hinder the AD process and expand the rely on bio-products. It also seeks to provide some solutions and options for managing food waste instead of using improper disposal. It is possible to exploit the waste of some food even before anaerobic digestion (AD), by extracting some compounds to produce other bio-products.

The study sought to produce numerous bio-products: biogas, digestate, biodiesel, glycerine, and starch-based adhesive from two types of food waste (cassava peel and date seed). The study introduces the principle of an integrated approach, by using the Hollander beater for the first time in pre-treating the cassava peel, plus extracting starch from it at the same time. No other studies were found, demonstrating the extraction of starch from cassava peel, using it to produce starch-

based adhesive material, or using the residue in the AD process for biogas and methane production. Also, the effect of starch extraction from cassava peel on the quantity and quality of biogas produced, was equally not previously studied. So in this work, the effect of starch extraction from cassava peel on the quantity and quality of the biogas produced was analysed. Equally this study is unique to the study of biogas production from Sagai date seeds, before and after extracting oil from it, directly after grinding pre-treatment without additional heating or crushing processes, and its effect on the quantity and quality of the resulting biogas. The study shows the effect of starch and oil extraction on the digestate resulted from the AD of cassava peels and date seeds and gains more knowledge about it components and properties. The effect of temperature, volatile solid and sludge quantity was studied and analysed in terms of its effect on the quantity and quality of biogas. The optimisation process was performed in the study to calculate the energy balance at optimal settings. Moreover, the biodiesel produced from the Sagai Date Seed oil through Soxhlet extraction method was tested and compared with the standards and biodiesel formed from other date seed types. The resulting glycerine also was tested to determine its properties and compliance with standards. Furthermore, the starch extracted from cassava peel was utilised for the first time to produce starch-based adhesives from two types of gelatinisation (base and acid) in the adhesion of plywood, plastic and paperboard specimens, to determine its properties The energy balance calculations, the bio-product production cost and the preliminary analysis of process boundary were presented in this project as well.

This study will answer the following questions:

1- What is the effect of starch extraction from cassava peels on the quantity and quality of biogas?

2- What is the effect of extracting oil from the Sagai Date Seed on the quantity and quality of the biogas?

3- Is there an effect on extracting starch from cassava peel and oil from date seed on the resulting digestate?

4- What are the energy balance calculations resulting from the production of biogas from cassava peel and Sagai Date Seed after extracting starch and oil from them?

5- To what extent the production of starch-based adhesive material, biodiesel and glycerine from food waste would be feasible?

1.3 Objective and Aims of the Research

The main objective of this study is to provide alternative uses for the accumulated food waste and the obstacles facing the process of anaerobic digestion through the exploitation of food waste in the production of multiple bio-products in addition to the biogas resulting from them. Some of food wastes contain starch within its waste, such as cassava peel. Exploiting the presence of starch in food waste in producing several bio product such as starch-based adhesive material and bioplastic may enhance the anaerobic digestion process without affecting the quantity and quality of biogas and digestate generated. Extracted starch cassava peels were used as a feedstock in the AD to produce biogas. The starch-based adhesive were subsequently produced from cassava peels starch, tested to determine its properties and calculate its production cost.

The study also aimed to explore the quantity and quality of biogas produced from date seeds after grinding pre-treatment without exposing them to any other treatment such as heating or crushing. The effect of oil extraction from the date seed on biogas quality and quantity will also be examined. The ability of biodiesel and glycerine from dates seed oil to enhance the AD process will be investigated as well in this study. Moreover, the effect of starch and oil extraction on the resulting digestate will be clarified as well, to gain more knowledge about its components and suitability for agriculture applications as a biofertiliser and soil amendment.

The effect of some factors affecting AD process, such as temperature, volatile solid concentration and sludge quantity, were analysed during this study. The effect of interaction of these factors on the biogas produced were analysed to reach to the optimal composition to maximise the biogas and methane (CH_4) percentage and to calculate the energy balance at the optimal settings.

1.4 Thesis Outline

The thesis is organised as follows:

- Chapter 1: This chapter provides an introduction to the work in this study followed by the contributions and objective of the study.
- Chapter 2: The literature review section highlights the background of waste management, waste biomass to produce energy, food waste, pre-treatment, AD process and some of AD products: (biogas, biodiesel, glycerine, starch-based adhesive material and digestate).
- Chapter 3: The substances and inoculum used in this work in addition to the experiment design and equipment used in the experimental works are presented in this chapter.
- Chapter 4: The fourth chapter illustrates and discusses the results of the AD experiments of cassava peels and date seeds before and after oil extraction, biodiesel and glycerine properties and the results from the adhesion of plywood and paperboard specimens with the adhesive obtained from acid and base gelatinisations.
- Chapter 5: Describes the energy balance calculations of the optimal settings, calculates the production cost of biodiesel and glycerine and starch-based adhesive and the preliminary analysis of process boundary assessment.
- Chapter 6: Provides a summary of main conclusions and future works.

Chapter 2

2 LITERATURE REVIEW

2.1 Waste Management

The incentive for waste minimisation and management has become essential, as waste accumulations lead to growing environmental hazards. This involves the recycling, reuse or application of waste via various waste generation techniques. Dealing with waste properly helps to reduce greenhouse gases and thus works to reduce global warming. The UK Climate Change Act of 2008 recommended a reduction of the amount of harmful emissions by 80% by 2050 [57]. Figure 3 shows the EU and other countries hierarchy of waste disposal priorities by rethinking, reducing, reusing, recycling or utilising them in energy production and finally disposal, (which is the least favoured option) [58-60]. The waste management system is an integrated waste management process that begins with waste handling and ends with recycling or destruction. The waste management process goes through several steps, Table 1 clarifies these steps in addition to the energy used in food waste management [61-63]. Failure to exploit and properly utilise waste leads to loss of a source of energy in addition to the other damages causes by its accumulated [64].

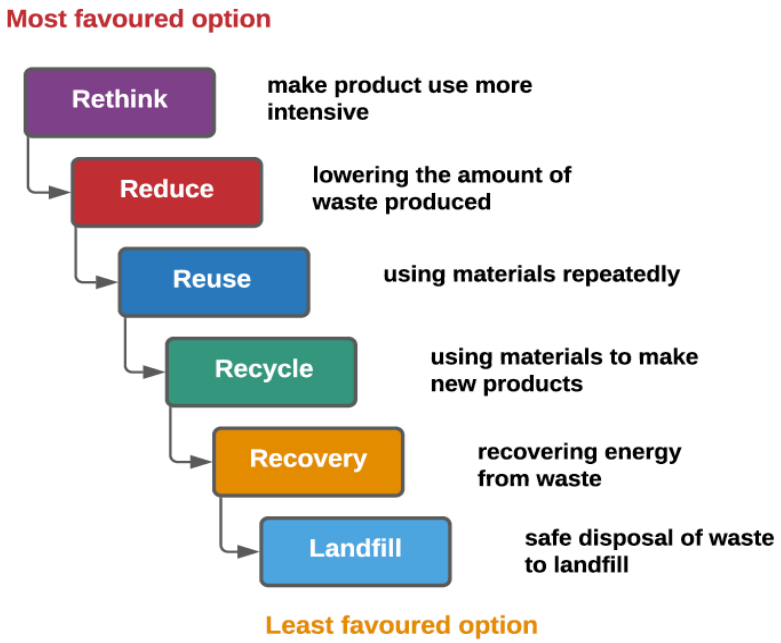

Figure 3: Waste hierarchy [58, 60].

Table 1: Steps involved and energy consumed of food waste in a waste management system [62, 63].

Initial step	Sub step	Energy consumed of food waste management system [MJ/fu]				
		Process	FWT*	AN*	CC*	CD*
Production of materials	Waste sources Source separation	Capital equipment (material)	24	47	53	54
	Internal collection Production rates	Collection of organic waste	_	_	487	147
	Waste types	Avoided Transportation	-2.3	-6.8	-6.8	_
Collection and transport	Collection	Transportations	57	_	4.9	
	Transport	Water supply	15	_		1.0
	Transfer	Wastewater treatment	15	_	0.20	0.0007
Treatment	Physical: Shredding, Thermal: Incineration, Biological: Anaerobic digestion, aerobic	Waste pre-treatment	38	_	122	17
Final disposition	Recycling Land filling	Total	146	40	661	218

** FWT: Food waste treatment, AN: Aerobic and anaerobic digestion, CC: Centralised composting, CD: Co-disposal.*

2.2 Waste Biomass to Produce Energy

Biomaterials derived from all parts of living plants such as fruits, trunks and tree leaves are biomass [54]. This Lignocellulose biomass, in addition to wood and grass, are suitable sources to convert to renewable energy [65]. Biomass is sustainable source, with annual production estimated at about 100 billion metric tons annually around the world [66]. One of the most important challanges facing the AD plants is the process of moving low density and large quantities biomass (as it contains high water content), as the only way to minimise this challenge is to use biomass in the vicinity of the AD plant. Supply operations account for the largest share

of the biomass energy cost [67]. It is worth reducing these costs by working with supply operations, due to the low cost of biomass energy [68, 69]. The supply of biomass includes the processes of collection, transportation, storage and utilisation. Figure 4 demonstrates the general supply operation of biomass [70, 71]. In an analysis study of the supply chain of wood biomass found that the transportation process has the largest share in energy consumption and harmful emissions [72].

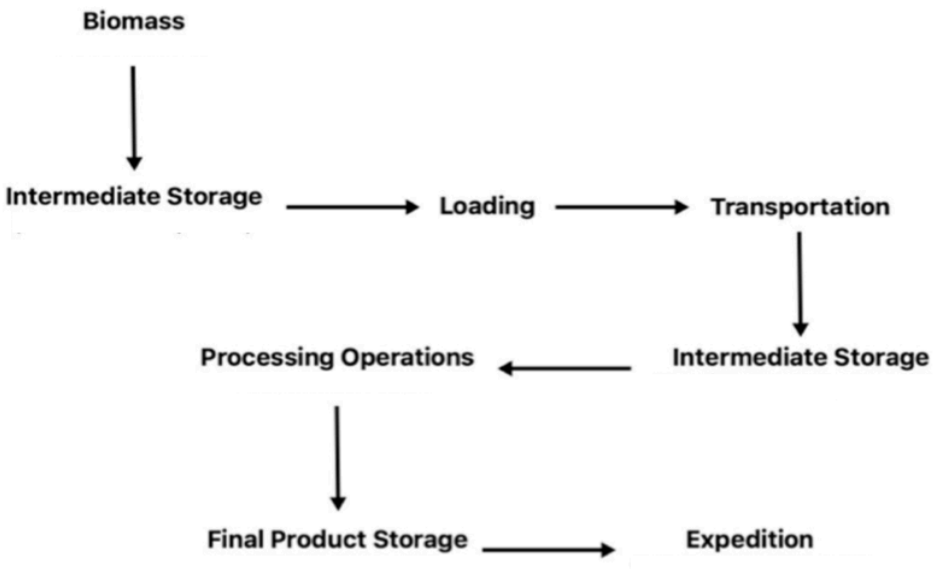

Figure 4: Supply operation of biomass in general [70].

Muscat, et al. (2019) [73] identified the most important factors that have a positive or negative affect on the use of the biomass. One of the factors affecting the use of biomass is the increase in demand for bioenergy, due to the fact that its sustainability is linked to many other factors such as increasing food prices and water consumption. Working to increase the quantities of agricultural crops without expanding the agricultural areas helps in reducing the effects of the increased demand for biomass [73]. The study also indicated that the effectiveness of supply processes contributes to reducing food waste and enhance the sustainability of biomass energy. [74]. The type of biomass used in the production of bioenergy determines its sustainability. It also determines whether it is possible to produce additional bio-products [73, 75].

Biomass energy contributes to energy security and sustainability, which reduces concerns about the greenhouse emissions to near zero. That would be achieved for the small amount of

emissions from biomass recourses, which reduces harmful effects on the environment and health [76, 77]. Zero emissions can be achieved by balancing biomass production and use [78].

2.3 Food Waste

Food waste is the material that is produced of, when preparing food in homes or commercial settings. These wastes consist of vegetables and fruits wastes, grain waste, animal waste and other food waste [79]. A third of this excess food waste that is disposed to landfill, which results in environmental damage and negative climate change [80, 81]. Therefore, minimising food waste has a role in the improving welfare, economy, sustainability and environment of developing countries [82]. Other ways to dispose of waste include burning or storage in landfill, which cause pollution and/or harmful emissions such as CO_2, resulting from storage or during transportation. These damages effect negatively on human life and pose a threat to the environment [83, 84]. Landfills may not be able to handle the increasing number of food waste in the future, so it is necessary to find sustainable ways to dispose of waste [85]. Utilising these wastes to produce or recycle bio-products is an appropriate, environmentally friendly and sustainable choice [86].

The management of food waste in retail stores has become an important issue because of its influences on the efficiency of the commercial process [87, 88]. Food waste from stores represents 5% of total food waste in Europe, while it reaches 13% in the United State [89, 90]. One of the reasons for the accumulation of waste in retail stores is related to the poor packaging process. Inadequate and excessive storage also contributes to waste [91]. Food waste in Europe for the year of 2012 was estimated at 88 million tons. The share of each person was more than 170 kg of food waste per year which counts about 20% of the total food of 865 kg/person of food produced for each person [89]. While food waste in 2019 was estimated at more than 119 million ton in the EU [92]. Table 2 and Figure 5 shows the share of sectors and people in the accumulation food waste in Europe in 2012 [89]. Ireland produces nearly one million metric tons of food waste from individual consumer and the commercial sector waste, even though approximately 10% of the population is undernourished [93]. The per capita quantity in Saudi Arabia from the food waste was estimated between 1.2-1.4 kg/day, or approximately 511 kg annually [94]. The value of these food wastes was estimated at 70 million SR daily or 8 million meals/day, which means disposing of 1.65 million tons annually of food in the landfill [95, 96].

Table 2: The sectors and person share in accumulation food waste [89].

Sector	Food waste	
	Million ton	Kg/person
Primary production	9.1	18
Processing	16.9	33
Wholesale and retail	4.6	9
Food service	10.5	21
Household	46.5	92
Total food waste	87.6	173

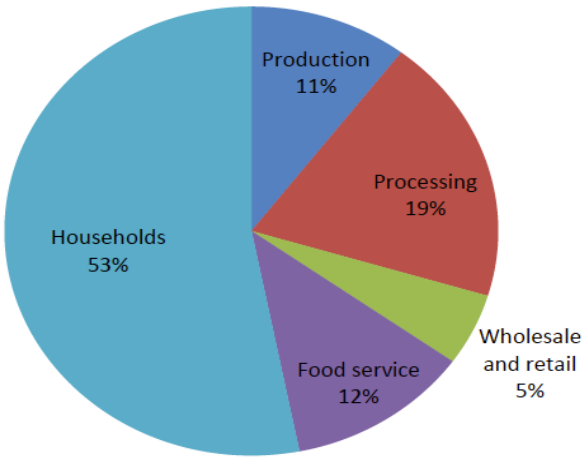

Figure 5: The sectors share in accumulation food waste [89].

The amount of surplus food around the world is estimated at 1.3 billion ton annually [97]. While, currently more than 690 million (8.9% of the world population) hungry people exist in the world. It is expected that in 2030 these number will reach to 840 million of hungry people which represent approximately 10% of the world's population [97, 98]. This large amount of food waste, which accounts for a large proportion of food production, contribute to many environmental, health and social issues [82, 97]. In order to reduce the issue of disposal of surplus food to landfill, their re-use must be exploited. Exploiting waste can be achieved by raising awareness consumers about the harmful effects of food disposal, managing the waste generated by residential complexes, public places such as restaurants and hospitals would also assist in the reduction of waste accumulation in landfill [99-101]. Additionally, energy plants play an important role in waste management when the waste used in renewable energy

production processes [102]. Food and agricultural waste, which are the most important biomass waste resources, contribute in increasing environment and health risks. The exploitation and treatment of these wastes to produce bio-products, producing energy and fertilisers contributes to promote the renewable energy, and thus sustainability [102, 103].

Population growth has led to more energy consumption from fossil fuels, accompanied by increased harmful emissions and global temperatures. Population growth and rising temperatures rely on clearing land by deforestation. By the end of the last century, deforestation contributed to more than 35% of global warming. Continued deforestation at the same rate is expected to cause an increasing the world's population to more than 14 billion in 2100 [104]. Simultaneously, a decrease in the rate of deforestation may keep the population at around 10.3 billion [104]. Factors such as agricultural expansion, infrastructure development and exploration for oil and minerals constitute further deforestation [105-107]. The unjust cutting of forests for the production of fuelwood and charcoal contributes to this deforestation [108]. Among the factors that threaten the existence of forests is the fires due to human caused climate change [105].

A study on deforestation in 28 tropical areas found that the motives for deforestation lie in commercial and subsistence farming, in addition to the desire for expansion and development. Cassava cultivation was one of the major deforestation crops. The agricultural expansion of cassava cultivation in tropical regions is a major driver of deforestation. Although cassava is a staple crop in many tropical cities, its effect on deforestation has not received attention [109]. On the other hand, globally there has been an increased demand for palm oil production from Southeast Asia, Africa and Latin America, which calls for the sustainability of palm oil production. This could lead to more deforestation and consequently environmental damage. The proportion of land used to cultivate oil palms around the world has increased nearly six-fold, reaching more than 21 million hectares from 1961 to 2017 [110, 111]. Oil palm cultivation has been associated with many negative impacts on the environment and society due to sustainability and the resulting greenhouse gas emissions [112]. Also, oil palm plantations carry out many other harmful operations, such as the use of wastewater, fertilisers and petrol (gasoline) to remove weeds [113]. Several measures are being worked on to reduce these impacts, such as oil palm cultivation in areas with less carbon pollution, avoiding deforestation and the use of bio fertilisers and biodiesel [114-116]. There is an urgent need to develop solutions to reduce the

impact of oil palm cultivation sustainability on the environment and human health, by creating an environmentally friendly supply chain that reduces the negative effects on human health [117]. Despite this, the cultivation of oil palm trees has positive effects on the producing countries, such as improving income, providing job opportunities and economic growth [118, 119]. The composition of the oil palm differs from date palm, as in the date palm contains 100 times more sugars than the oil palm, which contains more oil, despite both trees appearing to be same, as shown in Figure 6 [120].

Forests in Saudi Arabia, which constitute 1.3% of the total area, are facing degradation due to lack of rain, high temperatures and natural factors. Urban expansion in addition to deforestation represents major challenges to sustaining forest development. Recently, there has been a lot of interest placed on many projects to plant trees and restore forests. It is imperative to raise people's awareness of the importance of preserving forests and trees for the success of these initiatives [121-123].

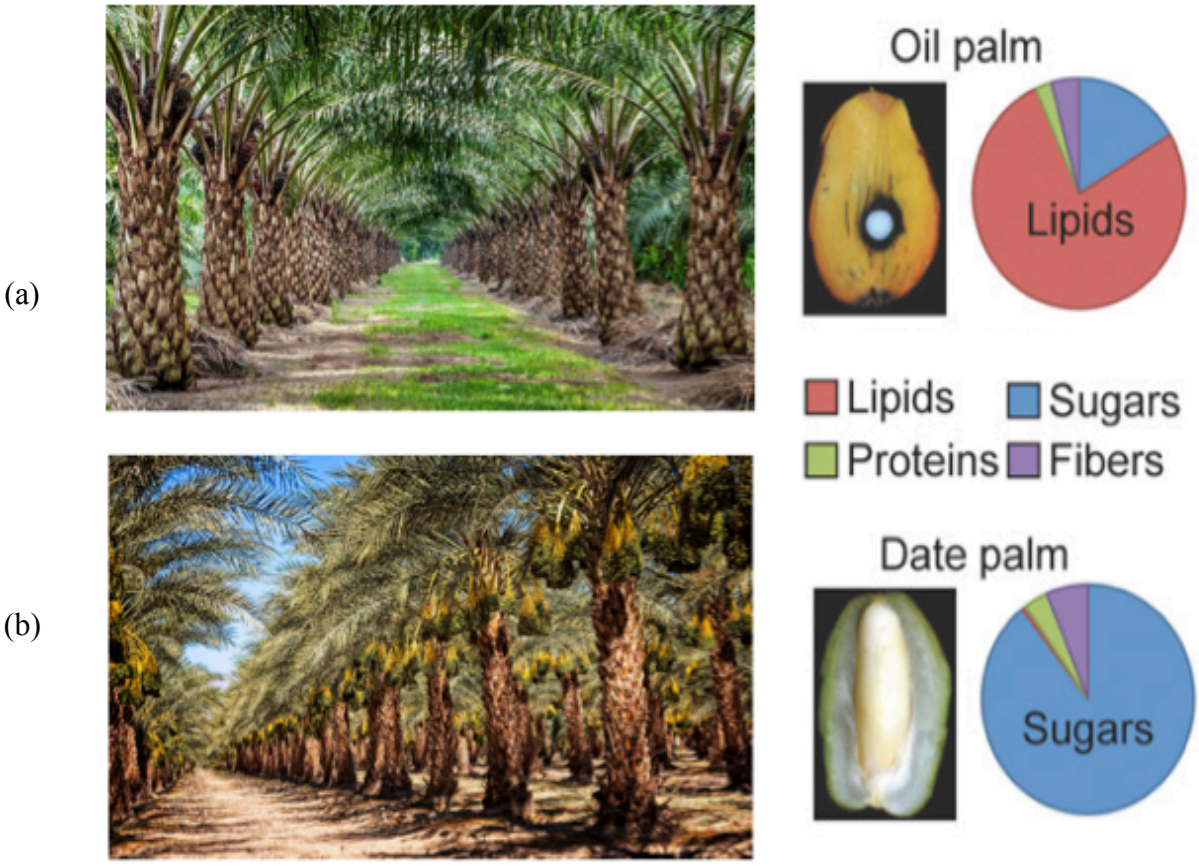

Figure 6: (a) Oil palm and (b) date palm trees and fruits compositions [120, 124, 125].

2.3.1 Cassava

Cassava shown in Figure 7 is a tropical plant that grows in many countries in Asia, Africa and South America and in low-fertility soils [126, 127]. Its length reaches to 35 cm and diameter up to 10 cm, it is also known as manioc, tapioca and yucca [128, 129]. It is harvested after 8-24 months after planting and does not depend on fertilisers or any other materials in its production [129, 130]. Globally, more than 200 million metric ton a year were produced from cassava in 2015, so it is considered one of the most important food sources that are rich in carbohydrates [131]. In 2018, cassava yields rose by almost three fold to reach to 550 million metric ton; about 350 million metric ton [132] of them are cassava waste (peel, leaf, bagasse and stem). More than two-thirds of the annual cassava crop is waste including peel, leaves and stem [132]. Approximately half a ton of cassava peel and pulp produced per ton of processed cassava is used to produce ethanol and starch in some Asian countries such as Indonesia and Thailand [131, 133]. The cassava peel counts up to 20% of its fresh weight. Table 3 shows the main composition of cassava [129]. That cassava peel percentage could reach up to 30% by hand peeling [134]. Many products can be produced from cassava peel, which made it an area of interest for researchers [135]. The cassava peel is rich in starch [136]. In fact, one of the cassava peel uses has been the production of biogas and bio-fertiliser by AD process [132, 137].

Figure 7: Cassava.

Table 3: Composition of cassava [129].

Composition	% of Fresh Weight
Moisture	62-66
Total Solids	38
Volatile Solids	99
Ash	0.9-1
Peel	10-20
Starch	18-32

Cassava is not cultivated in Saudi Arabia due to its large abundant need for water, rain and tropical climate. Nevertheless, for the plant diversity in Saudi Arabia, a study was conducted for the purpose of cultivating cassava in Saudi Arabia and studied its potential to adapt in the environmental and regional conditions. It showed a vigorous and rapid growth after exposed to hardened process adaption [138]. Saudi Arabia imported approximately 535 metric tons of cassava in 2019 from many countries such as India, which has the largest share of cassava exported to Saudi Arabia [139]. However, cassava is not grown in the Arabian Peninsula, except it grows in Zanzibar and in some lands in Oman [140].

The highest biogas yield was of a study on the production of biogas from cassava peel with urea under mesophilic condition at 80.79 ml/g.TS added [141]. The cassava peel was treated by soaking it in water for 7 days. The study concluded that the 0.01 of urea with cassava peel increases the biogas volume by 24.33% [141]. Jekayinfa and Scholz [142] found that, the highest biogas volume and methane content volume produced from cassava peel were 660 ml/g-VS and 280 ml/g-VS respectively at 35°C.

2.3.2 Palm Date

The palm tree has existed for more than 5,000 years ago. It grows in extreme climatic conditions, which normally not ideal for the growth of many other plants [143, 144]. It can grow and survive in arid, semi-arid and hot climate regions [143]. A palm date is scientifically known as “phoenix dactylifera L.”. It is an essential food for many countries such as the Middle East, North Africa. It is one of the oldest and main staple food in this region due to its content of several nutrients [144]. Its composition and other contents of vitamins and minerals make it a highly nutritional and health value products. Many people worldwide depend on the date for their daily diet as a main source of food. Although dates are rich in sugars, the Glycaemic Index of date is low and

therefore, their regular consumption do not lead to health worries [145]. That is due to the high quality of carbohydrates in dates which resulting in a low glycaemic response [146]. Some of the well-known types of dates are Sagai, Ajwa and Sukkary [147]. The Sagai Date is illustrated in Figure 8 and the date composition is shown in Figure 9. Dates are processed in mass production to produce many products such as date syrup and date paste [148, 149]. The seed is one of the wastes produced from the date, which annually estimated at more than 960 thousand tons. It is a solid rectangular body inside the dates, tends to be brown in colour [150, 151]. The date seed is used as a source of energy, nutritious drinks and polymer components [152-154]. In addition, some studies extract oil from the date seed in order to produce biodiesel [155-158]. Date Seed Oil is also used in cosmetic industries such as creams, shampoos and soaps [159]. It consists of more than 90% carbohydrate, protein and lipids and this enhances its use as a source of biogas production through the AD process [160]. This high carbohydrate percentage is a catalyst for microbial fermentation in the AD process [161]. Date palm tree produces many other wastes such as leaves and fibre [162]. Date palm fibre can be used as a filler and reinforcement material [163, 164].

The annual production of dates in 2004 was estimated at approximately 7 million ton, while the value of the resulting waste was estimated at 2 million ton [165]. The total production reached more than 9 million tons annually in 2019, which harvested in approximately 1.4 million ha [166]. The disposal of these wastes in landfill has contributed to increasing the harmful emissions into the air, resulting in the increment of global warming across the globe [167]. The structure of date fruit is known to consist of three parts: seed, skin or date flesh (pulp) and endocarp (Figure 9). The largest share of date seed weight is for the skin while the seed represents 10-15% [148] of the whole date weight. Table 4 shows the components and proportions of dates for a type date seed (Dalaki). The seed is the main waste of dates and is often used as animal feed [148, 168]. Egypt, Iran, Saudi Arabia, Algeria and Iraq are the most prolific producers of dates in 2012. The total production of dates in the world was estimated at 7,500,000 mt (metric ton). The share of the five countries of total production was about two third of the world's production. Table 5 shows the largest producing countries dates for the year 2012 and the share of each country [169, 170]. In 2018, Egypt, Saudi Arabia, and Iran produced nearly half of the world's production, by an increase of about 25%. In contrast, Tunisia is the world's largest exporter of dates, with more than 17.5% of global production in 2018 [154].

Figure 8: Sagai date

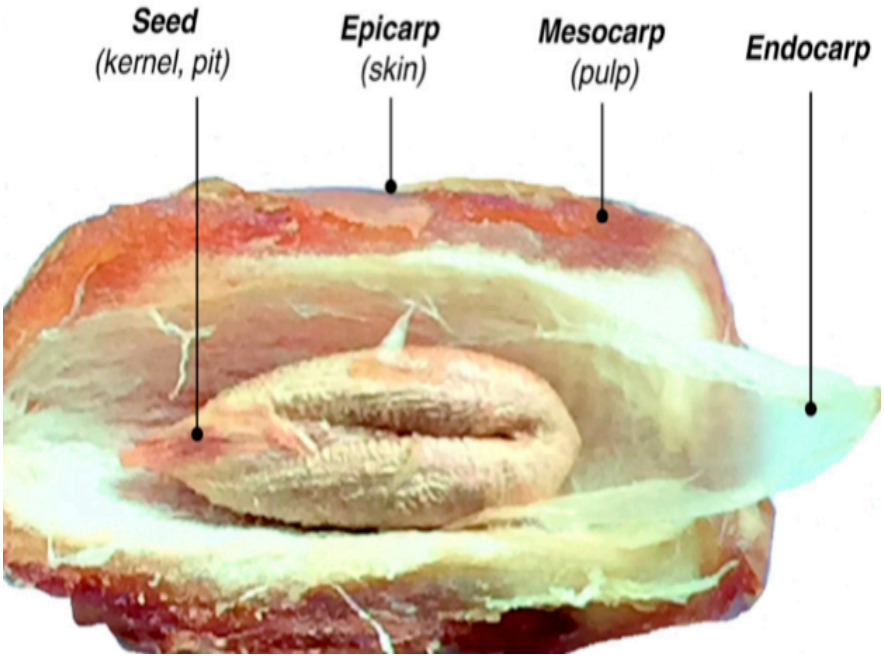

Figure 9: Date composition [148].

Table 4: Dalaki date components proportions [168].

Date Part	Content (% dry basis)
Flesh	85.7 ± 0.12
Seed	13.8 ± 0.29
Skin	0.50 ± 0.15

Table 5: The top 10 countries producing dates and their share in 2012 [169].

Rank	Country	Date Yield (mt)
1	Egypt	1400000
2	Iran	1069655
3	Saudi Arabia	1031082
4	Algeria	789357
5	Iraq	655450
6	Pakistan	524612
7	Sudan	433500
8	Oman	281000
9	United Arab Emirates	221529
10	Tunisia	192000

Dates in Saudi Arabia consider as one of the most important food crops. The number of palm trees was estimated at more than 25 million palm trees cultivated in 107,281 ha. The total production of dates in 2016 was more than 1.1 million tons of dates [171]. While the number of palm trees increased in 2019 to more than 30 million palm trees, producing more than 1.4 million tons annually [172]. Palm trees can withstand water stress and dryness for long periods of time, as their roots spread across the ground to reach wet areas [173]. Half of the palm trees in Saudi Arabia are irrigated by drip irrigation, which reduces water consumption, while the rest of the trees are irrigated by flood irrigation [171]. The regions of Riyadh and Al-Qassim are the largest areas for growing dates in Saudi Arabia, with 39,301 ha under cultivation, with an estimated production of 190,000 tons of dates in 2011 [174]. Saudi Arabia's export of dates increased from 108,000 tons in 2015 to 130,000 tons in 2019 [175]. There are about 29 types of dates grown in Al-Qassim region [176]. In Saudi Arabia, there are more than 300 types of dates, each has a different shape and taste. Moreover, the chemical composition and sugar content of each type is a bit different. Table 6 shows the chemical compositions and sugar content of some date seeds [177]. Figure 10 illustrates the different shapes for several date types [178].

Table 6: Chemical compositions for different date seed types (g/100 g dry weight).

Date type	Chemical composition				Total Sugar	Ref
	Moisture	Protein	Lipid	Ash		
Zahdi/Zahidi	26.1± 0.0	3.38 ± 0.00	N/A	2.53 ± 0.00	68.5±0.00	[179, 180]
Digal	10.0 ± 0.0	2.00 ± 0.00	8.00 ± 0.00	25.0 ± 0.00	55.0± 0.00	[167]
Khalas	14.2 ± 3.7	7.61 ± 0.00	N/A	1.10 ± 0.00	82.5±0.00	[181, 182]
Sagai/Segae	14.5 ± 0.1	2.73 ± 0.04	0.41 ± 0.005	2.29 ± 0.03	79.7± 0.20	
Ajwa	22.8 ± 0.1	2.91 ± 0.02	0.47 ± 0.001	3.43 ± 0.01	74.3± 0.20	
Shalaby	15.2 ± 0.2	4.73 ± 0.01	0.33 ± 0.005	3.39 ± 0.01	75.9± 0.50	
Khodari	19.5 ± 0.1	3.42 ± 0.03	0.18 ± 0.004	3.42 ± 0.04	79.4± 0.30	
Anabarah	29.5 ± 0.2	3.49 ± 0.01	0.51 ± 0.004	2.33 ± 0.01	78.4± 0.20	[177]
Sukkari	21.2 ± 0.1	2.76 ± 0.01	0.52 ± 0.001	2.37 ± 0.05	78.5± 0.10	
Safawy	23.6 ± 0.3	2.48 ± 0.02	0.12 ± 0.003	1.68 ± 0.01	75.3± 0.10	
Burni	24.4 ± 0.1	2.50 ± 0.04	0.67 ± 0.001	2.02 ± 0.01	81.4± 0.04	
Labanah	10.5 ± 0.1	3.87 ± 0.05	0.72 ± 0.002	3.94 ± 0.02	71.2± 0.10	
Mabroom	21.3 ± 0.1	1.72 ± 0.05	0.27 ± 0.001	2.79 ± 0.05	76.4± 0.07	

N/A: Not Available

Figure 10: Different types of dates [178].

Jaafar [183] showed that the amount of biogas produced from AD in thermophilic conditions at 55 °C was estimated to be 570 ml/g-VS. The methane percentage was found to be 67%. Zahdi Date Seed was treated by boiling it in water and then allowed to cool down wherein the resulted feedstock was washed and filtered twice. Lattieff [167] found that 15% of Digal Date Seed/water produced the highest amount of biogas of 182 ml/g-VS at 37 °C and for 28 days. The biogas volume was increased to 203 ml/g-VS when using recycled digestate waste. In his study, the pre-treatment process for date seed was not discussed in detail. The researcher mentioned that the date seed were pitted and shredded before the AD process.

The studies on AD of oil-extracted dates are scarce, where only one study looked at the production of biogas from extracted oil of two types (Khalas and Khudari) of date seed [181]. There are some studies which researched extracting oil from date seeds to produce biodiesel [167, 183]. In one study [181] of biogas production from raw and oil-spent date palm seeds, two types of date seeds (Khalas and Khudari) were mixed with wastewater treatment sludge. The seeds were washed by water to remove the remains and dried in oven for 24 h at 50 °C. The seeds were crushed using a steel hammer, then ground by using a household mixer and sieved into three different sizes 1.18-3.75, 0.6-1.18, and 0.425-0.6 mm. Grounded date seeds co-digested with wastewater sludge at seed/sludge total solids ratios of 0%, 2.5%, 5%, 7.5%, 10%, 20% and 40%. The incubation period for the reactors was 14 weeks. There was no significant effect of the date seed grain size on the biogas volume produced, although the smallest grains size produced slightly more biogas. The study found that there was no significant difference in the biogas produced from the raw date seeds and extracted oil date seeds. The highest biogas volume reached was 390 ml/g-VS when the seed/sludge ratios were 0-10%. Mixtures containing higher percentages of date seeds/sludge (20% and 40%), they provided higher amounts of VS, however the yield of biogas was lower than that for the sludge alone. The reason for this, was due to inhibition and acid accumulating which was determined as a result of low pH. The oil extracting process improved digestion efficiency and decreases the inhibition of biogas production. The average methane ratio from the total biogas was about 65%. A Soxhlet extraction method (an effective oil extraction method that will explain later in the next chapter) was used to extract oil from the date seeds with a solvent mixture with methanol, chloroform and water volume ratio of 2:1:0.8 respectively [181].

2.4 Anaerobic Digestion

AD is an efficient and reliable method to produce energy from natural sources. It produces more net energy than many other energy-producing techniques from microorganisms such as gasification and consumes less energy [184, 185]. The AD process is the process of converting organic matter into biogas in the absence of oxygen (O_2) by different types of bacteria. Biogas contains different gases in different percentages. Methane is the main component of biogas, generally reaching up to 70%. The remaining gases containing up to 45% of CO_2 and the balance includes O_2 and hydrogen sulphide (H_2S) [186, 187]. Several types of inoculum, such as sludge from wastewater treatment plants and sludge of manures are used in the AD process. The process of producing biogas through AD goes through four stages as shown in Figure 11 [188]. There are many factors that influence the AD process, for example, the temperature; its effect in the thermophilic (50-60 °C) condition is different than in mesophilic condition (30-40 °C) [189]. The result of a fast reaction rate in thermophilic, results in a biogas that is higher than in mesophilic with the potential for acidification, which affects the AD production. The rise in temperature leads to an increase in the energy used and thus raising the production cost. Mesophilic conditions are less sensitive to environmental changes and have better stability, however the methane yield is lower than that for in thermophilic conditions [190, 191].

Moreover, the pH, Carbon/Nitorgen ratio (C/N), retention time and the organic load rate also have an effect on the AD process and thus affect the quantity and quality of the process output [190]. The bacteria growth process is affected by the pH, so the optimal value of the pH is 6.5-7.2 [192]. Adjusting the C/N ratio between 16.5-24.9 found the optimal range for food waste [193]. The time required to keep the organic material in the reactor to complete the biogas production process is known as the retention time. The retention time depends on the temperature used and is associated with the organic load rate. The time required for completing the degradation process and producing the biogas within a mesophilic condition is typically 15-30 days while it is a little shorter under thermophilic condition [194]. A two-stage digestion process can reduce the retention time to 12 days without affecting the process or the quantity of energy produced [44].

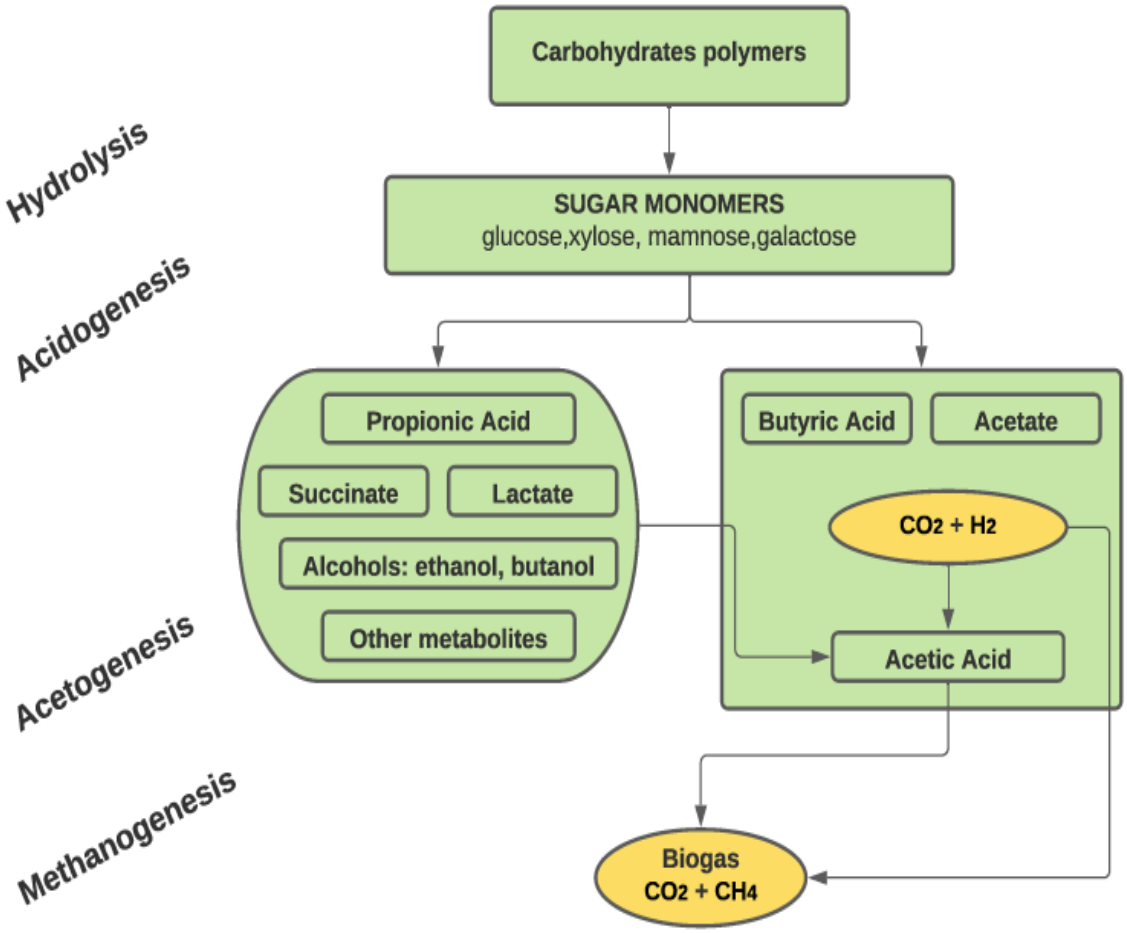

Figure 11: AD stages [188].

In addition to biogas, a rich nutrient digestate can be produced from an AD process. Figure 12 shows an overview of the resulted products and their use [195]. The exploitation of this digestate leads to enhance the benefit of using the AD process, by increasing the process products value. The resulting digestate can be used in many fields such as a bio-fertiliser or soil amendment in agriculture or reuse it in a two-stage AD process [196, 197].

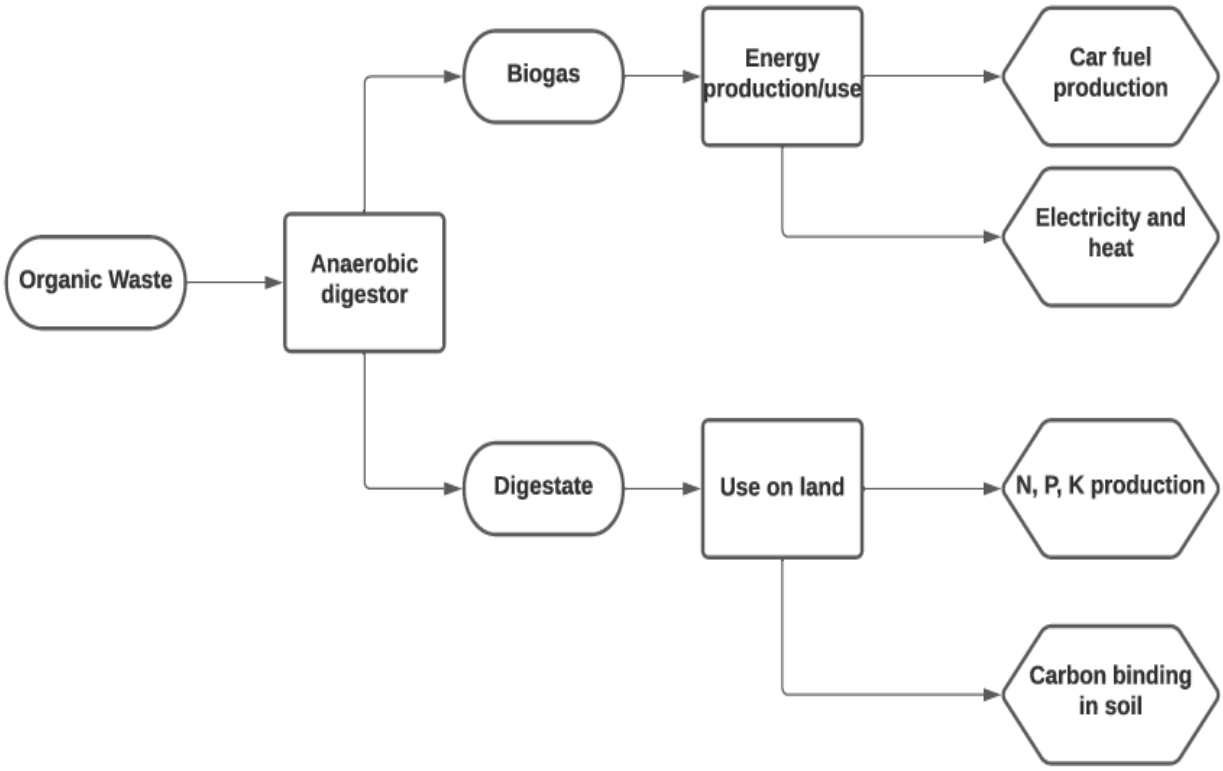

Figure 12: AD products and uses [195].

The AD process faces many challenges that limit its further exploitation and use. Among these challenges is the instability of the process due to inhibition of substrates that disrupt the stability of AD and inhibit methane production. The presence of some elements in large quantities such as protein, fats, minerals, pesticides and other organics in the substrates inhibits the AD process by inhibiting microbial activity [198]. Controlling the factors affecting the process such as, temperature, pH and organic loading provide process stability [198, 199]. Digestate quality is another issue that faces the AD process, as the dehydration of digestate leads to the loss of large amounts of the necessary elements that it contains, such as nitrogen and phosphorous [200]. The recovery of these elements leads to more costs [201]. Digestate can be recycled and reused in AD processes [167, 202]. Although mechanical pre-treatments effectively treat substrates to increase biogas production, they are costly in terms of energy consumption [203].

2.5 Pre-treatment

Biomass consists of complex compositions that make analysing and decomposing them difficult [204]. Breaking up these complex compositions helps in converting some of the compounds into

simple sugars. The pre-treatment process aims to disassemble the protective layer of sugary compounds and increases the porosity of the biomass to facilitate their digestion [205]. Fruits biomass contain inhibitors that may reduce yield despite their easy degradation [206]. Bacteria actions that are in the sludge causes the release of compounds inside the cells, which helps to improve biodegradation, thereby enhancing the AD and increasing the resulting biogas [207]. The pre-treatment process enhances the hydrolysis and methanogenesis in the AD process with increases in resulting methane yield [208]. The biogas from food waste is associated with the cellulose (either total solids or carbohydrates) amount presented in the waste. Therefore, the pre-treatment of these wastes makes the conversion of cellulose into simple sugars in addition to the lignin compounds easier. These simple sugars make their hydrolysis less complicated as shown in Figure 13 [86, 209]. Non-biological pre-treatments, despite their efficiency, they are expensive, consume high energy and producing a considerable amount of harmful chemical wastes. Therefore, biological pre-treatments are more desirable as they are cost less and have less harmful emissions [210, 211].

There are several methods of biomass pre-treatment that are used to make it digestible by microbes. Pre-treatment is accomplished under certain conditions to prevent degradation processes. There are different types of pre-treatments for biomass, including physical/mechanical pre-treatments e.g. (beating, grinding and milling), thermal pre-treatment such as (microwave), chemical pre-treatment e.g. (alkali) and biological pre-treatment e.g. (microorganism) [206, 212-214].

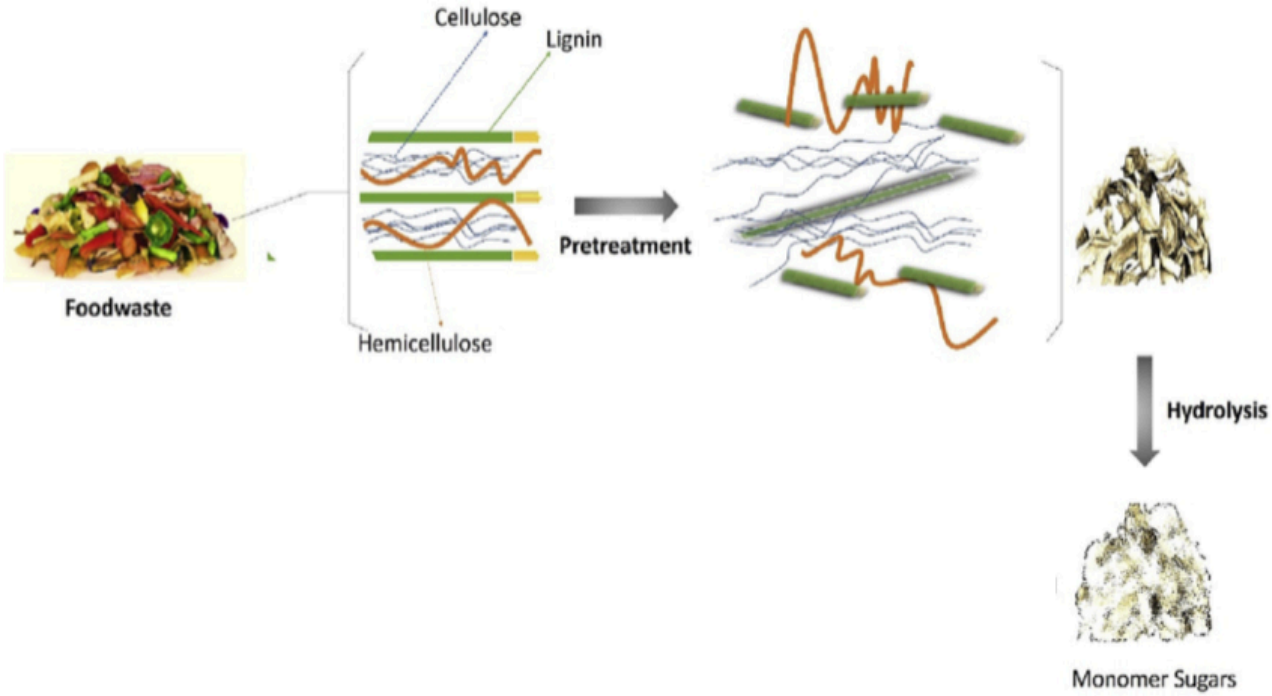

Figure 13: The pre-treatment effects on food waste [86].

2.5.1 Mechanical Pre-treatment

Several studies have demonstrated the need of substances for pre-treatment due to the effect of their partical size on the AD outcomes [215-217]. Mechanical pre-treatment includes chipping, grinding and milling processes. They perform to increase the susceptibility biodegradation of substances before the AD process [218]. It also helps in reducing polymerisation and crystallisation of cellulose [219]. Mechanical pre-treatment of substances especially that rich in fibres and seeds helps in improving the biogas volume than untreated substances [220]. However, it modifies the substances physical properties, such as increasing the surface area. This facilitates digestion and microbial feeding in AD. Moreover, it contributes to reducing the retention period for biogas production [221]. The particle sizes produced vary according to the treatment method, for example the sizes ranging between 10-30 mm as a result of the chipping pre-treatment, while, in milling and grinding pre-treatment it is between 0.2 and 2 mm. However reducing the practical size to less than 0.4 mm has been shown to have no effect on the volume of biogas produced [216, 222]. The required particles size and the energy consumed depend on several factors, including the type of substances and the treatment time, as the treatment of woody materials requires more energy than agricultural materials [219, 223].

A) Beating Pre-treatment

Beating treatment is a treatment method used to treat substances to improve the AD Process. The bioenergy group at DCU introduced this treatment method using Hollander beater device in the last decade. The beating treatment process breaks down the substances and increases their surface area. This increases the chances of microbes feeding and thereby increasing the biogas yield. Beating pre-treatment has been applied in many previous studies to produce biogas on food waste, algae and paper [224-226].

In a study [224] of producing biogas from sludge with silage corn, fresh grass and potato peels, the feedstock was pre-treated with a Hollander beater before being mixed with sludge. It was found that beating pre-treatment has a positive effect on the volume of biogas resulting from the AD of these substances. The yield of biogas from silage corn increased by approximately 27%, while it increased with fresh grass to more than 38% and 31% with potato peel compared with untreated feedstock. The pre-treatment time for silage corn was 20 minutes while it was 5 minutes for both fresh grass and potato peel [224].

A study conducted by Tedesco (2014) [226] showed the effect of algae beating treatment on biogas and methane production. Whereas, the beating treatment increased the yield of biogas by 52% and increased the volume of methane by 53% compared to untreated algae [226]. Rodriguez (2017) [225] found that beating treatment of paper contributed to a 21% increase in methane yield. In this study, it was found that treating the paper with a Hollander beater for 60 minutes produced the best volume of methane. The methane yield did not raise much when the paper was treated for 30 minutes. In order to reduce the operating costs by reducing treatment time and increasing methane yield, an optimisation process was applied. It was found that the optimum methane was increased 17% at 245 ml for 55-minute of treatment time [225].

B) Grinding Pre-treatment

Milling and grinding are common pre-treatment processes that are used in treating lignin biomass. The choice between them is made based on the wet content of the biomass [227]. In the grinding pre-treatment the surface area, the polymerisation and the porosity of the substances are modified which helps in improving their degradability. These properties could be changed based on the type and conditions of grinding [223, 228, 229]. The particle size from the grinding

process ranges between 0.2-2 mm [230]. The surface area of the material increases with increasing the degree of grinding, accompanying with an increase in energy consumption [231]. The grinding machine supply by feedstock into the grinding chamber and inserted in batches by rapid mechanical effects. Grinding occurs when materials collide with rotating teeth or a sieve [232]. Several studies conducted on the impact of the grinding/milling pre-treatment on the biogas and methane yield. Table 7 illustrates some of these studies and their effect on Biogas/Methane yield and AD conditions [48].

Table 7 : Effects of grinding/milling pre-treatment on the biogas/methane yield [48].

Biomass	AD Conditions	Effect on Biogas%	Effect on Methane%	References
Elephant grass, Mexican sunflower, Siam weed	37 °C, 30 days	-	22	[233]
Meadow grass	54 °C, 27 days	27	-	[234]
Wheat straw	37 °C, 28 days	-	49.3	[235]
Ensiled meadow grass	54 °C, 20 days	-	25	[236]
Rice straw	35 °C, 25 days	17.5	-	[237]

2.6 Biogas

The biogas resulted from the AD of organic waste is flammable, colourless and contains several gases at different percentages. The highest biogases percentages reached more than 60% of CH_4 and up to 40% of CO_2 [238]. Oxygen (O_2), Hydrogen Sulfide (H_2S) and nitrogen (N) are the other gases that produced at a lower percentage of 1-5% [239, 240]. Biogas has been used as a primary source of energy for households from the past in some countries in Asia and Africa. It was then used to produce energy in Western Europe and Northern America. Biogas is currently used in many countries for heating, electricity production and to produce transport fuels (i.e. converted to methane) [241]. Using the biomethane from food waste as vehicles fuel could reduce harmful emissions [242]. Several factors affect the production of biogas such as temperature, retention time, mixing, substances volatile concentration and pH. These factors may slow or reduce the biogas yield [243].

The temperature plays an important role in the biogas production process. In thermophilic, the methane yield enhances, while in the mesophilic, less methane yield [244, 245]. The reaction temperature should be monitored and controlled to maintain the temperature constant, especially when climate changes affect the reactor [240]. Retention time is the time required for the

decomposition of organic matter during the AD process. It is also related to the temperature, as in the mesophilic conditions the retention time for organic waste is between 15 to 30 days, while it is up to 14 days in the thermophilic conditions [224, 246]. Mixing (shaking) process stabilises the digester and increases the methane volume [247, 248]. It also increases the possibility of contact between bacteria and feedstock, distributes bacteria and temperature eventually in the reactor and prevents deposits. Slow mixing is recommended to avoid disrupting the bacteria [224]. The mixing process can be achieved by using mechanical mixers, reactor recirculation or by bumping back the biogas to the reactor [249, 250]. Improper adjusting of volatile solids added value leads to instability and hence a decrease in the biogas produced [251]. Also, increasing the volatile concentration inhibit the reaction and reduces the biogas volume [160]. Therefore, adjusting the volatile solid added value is a major factor in determining the amount of biogas produced [251]. The optimum pH for biogas production is between 6.5 and 7.2. It is also an indicator of the reaction stability. The pH value affects the AD process and digestion efficiency as low pH inhibits digestion process and methane production [252, 253]. Table 8 below shows the different types of food waste and the percentage of methane produced from these wastes [254].

Table 8: The methane percentage produced from different food wastes [254].

Substrates	Inoculum	Conditions	Methane (ml/ g-VS)	References
Cucumber residues + pig manure + corn stover	Sludge	Temperature= 35 °C	305.4	[255]
Potato waste + cabbage waste	Sludge	Temperature= 37 ± 1 °C,	360	[256]
Kitchen waste + cow manure	Sludge	Temperature= 35 °C, pH=7.5	179.8	[257]
Organic fraction of municipal solid waste + fruit and vegetable waste	Sludge	Temperature= 35 °C, pH=7.4-8.2,	396.6	[258]
Food waste + wheat straw	Sludge	Temperature= 35 ± 1 °C, pH=7.1-7.5	344	[259]
Food waste + wheat straw	Sludge	Temperature= 55 ± 1 °C, pH=7.1-7.5	370	

2.7 Digestate

The digestate consist of the residues of the AD process. The digestate can be used for several applications rather than just disposal [260, 261]. Due to the availability of several techniques to improve digestion that can be implemented in an integrated approach for AD plants, digestate management with integrated solutions received more attention. The solid digestate can use to produce biochar or recovered for cultivating insects or fungal [262, 263]. Promising alternative applications can be created to increase the system's efficiency by integrating AD processes with digestate processing processes [264]. Where biochar can be used as a solid fuel or as a soil amendment, liquid digestate can be reused in biogas production [265, 266]. Nitrogen (N), phosphorus (P) and potassium (K) exist in the feedstock reside in digestate, this presence is essential when used in agriculture [267]. Digestate contains carbon, which ends up been stored in the soil, thus preserving the environment from global warming [195]. The use of inorganic fertilisers with pesticides may lead to soil and agricultural crops damage [268]. Bio-fertilisers are more favoured than chemical fertilisers as they help in improving the soil and thus increase water retention of soil and thus reduced irrigation. This leads to a reduction in water consumption used during an irrigation process. Moreover, the need to use pesticides with bio-fertiliser is less than that with chemicals, leading to improved soil. The digestate represents a significant percentage of the AD residues [195].

The bio-fertilisers are evaluated based on the amount of necessary minerals they contain or by comparing them with the available organic or inorganic fertilisers [269, 270]. The optimal composition of the essential elements (NPK) differs in the digestate, so the ideal way to determine it is based on what the soil lacks from that composition because the plant derives its food from the soil [271]. Despite this, some standards values are: 2,300-4,200 mg/kg of N, 200-1,500 mg/kg of P and 1,300-5,200 mg/kg of K [272]. Table 9 shows a comparison of several available fertiliser sources. The use of digestate, which contains the necessary nutrients as organic fertiliser, has a clear value. N is available in bio-fertiliser at high rates, especially if it is not lost during the AD process, but less than that found in compost. The availability of P and K is similar to that found in compost. Compared with compost, the use of digestate, which contains a high percentage of N as a bio-fertiliser, leads to an increase in their value in the short term [273]. Fertiliser standards differ between some countries [270], Whereas, the European Union

developed legislation to implement the use of digestate of numerous sources under the standards stipulated [274]. Several studies concluded that the digestate produced from some animal manure and organic household waste is suitable for agricultural use [270, 275]. Digestate significantly reduced the rate of nutrient loss compared to conventional fertilisers [276]. The contribution of the AD process in reducing emissions, is not only associated with the production of biogases. Maintaining the carbon in the soil for use as natural fertiliser is another factor in reducing harmful emissions [195].

Table 9: Fertiliser components from different sources [270, 277].

Organic source	N	DM (%)	Biodegrability	Fertiliser Value (%)
Solid manure	6 kg m^{-3}	25	Low	10-20
Sewage sludge (high DM)	4-5 kg t^{-1}	25	Medium	15-30
Sewage sludge (low DM)	1-2 kg m^{-3}	5	Medium	45-55
Digestate from biomass plant	2-3 kg m^{-3}	8	Low	40-60
Digestate with co-fermentation	3-15 kg m^{-3}	5	Low	50-70
Poultry slurry	10 kg m^{-3}	15	Medium	70-85
Cattle slurry	4 kg m^{-3}	7.5	Low	34-45

2.8 Biodiesel

The increasing demand for energy in addition to environmental pollutants from fossil fuels has contributed to the search for more environmentally friendly and less harmful fuel. Many countries have turned to produce biofuels (includes bioethanol etc.) in different quantities, as shown in Figure 14 [278]. Therefore, biodiesel may be considered as one of such appropriate solutions [279]. Biodiesel is a fuel that could be derived from vegetable oil, animal oil and fats and cooking oil waste. It is renewable and suitable for diesel engines [280-283]. It is non-toxic, biodegradable and does not contain sulphur and aromatics [284]. Biodiesel has fewer CO_2 emissions compared to conventional diesel, however if it replaced the biodiesel from fossil fuel, it is expected that the dependence on biodiesel will be more in the future [279, 285, 286]. Clean and inexpensive biodiesel is produced by conversion technologies from bio-waste oils [287]. The cost of substrates, i.e. bio-waste oils, the produced energy efficiency and the conversion process time are some of the most important challenges and factors in determining the cost of biodiesel [288, 289]. The cost of substrates accounts about 75% of the total cost of producing biodiesel, the use of low-cost substrate reduces the process cost [290, 291]. About 350 substrates have been

identified for the production of biodiesel that is extracted from crop oils, algae oils, waste cooking oil and animal fats [283].

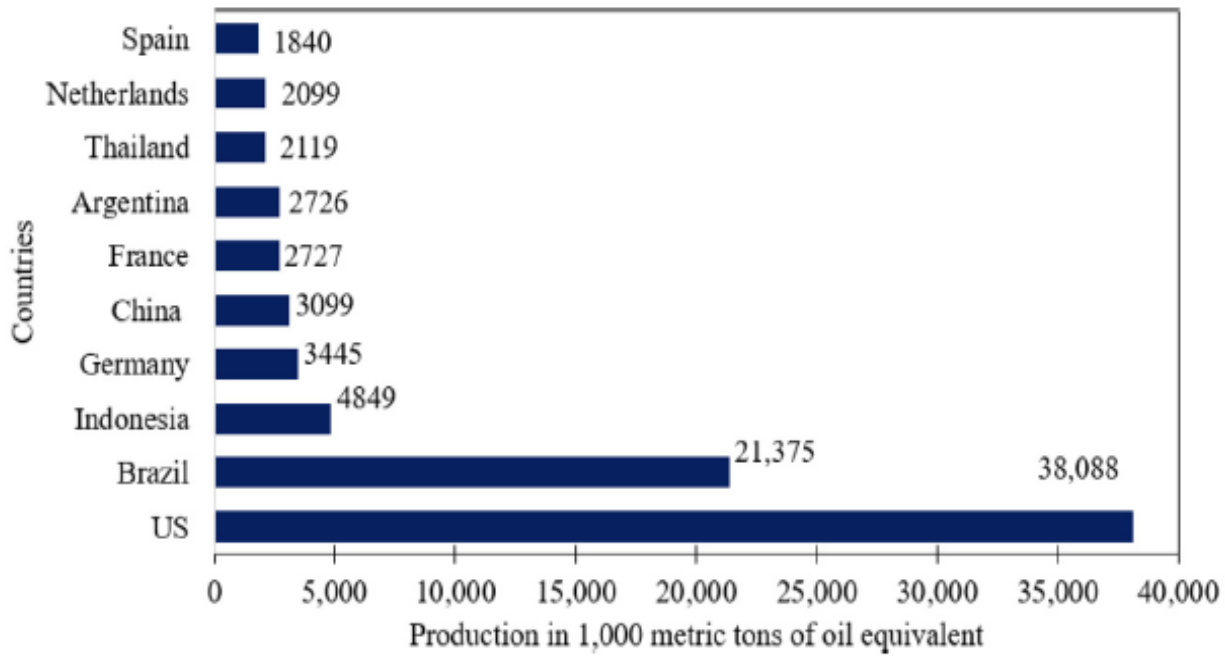

Figure 14: Quantities of several biofuels types produced by the leading countries in 2018 [278].

Table 10 demonstrate some of the substrates for biodiesel production and its region. The oil share of each substrate is illustrated in Table 11 [285]. There are several techniques for extracting oil from the seeds; mechanical (laboratory Soxhlet extraction), chemical and enzymatic techniques. Mechanical and chemical techniques are the most used. The seeds are separated from the fruits and then dried either in the oven or by placing them in the air before the extraction process [283]. Soxhlet extraction is an extraction method used widely in several studies [155, 156, 292, 293]. Figure 15 shows the laboratory Soxhlet extraction device and its oil extraction method.

Table 10: Some of substrates for biodiesel production [283].

Countries	Substrates
China	Jatropha, Waste cooking oil, Rapeseed
Indonesia	Palm oil, Jatropha/Coconut
India	Jatropha, Pongamia Pinnata (Karanja), Soybean, Rapeseed, Sunflower
Japan	Waste cooking oil
Malaysia	Palm oil
Philippines	Coconut, Jatropha
Bangladesh	Rubber seed, Pongamia Pinnata
Pakistan	Jatropha curcas*
Thailand	Palm, Jatropha, Coconut
Iran	Palm, Jatropha, castor, Algae
Singapore	Palm oil
Ghana	Palm
Zimbabwe	Jatropha
Kenya	Castor
Mali	Jatropha curcas
Norway	Animal fats
Sweden	Rapeseed
France	Rapeseed, Sunflower
Germany	Rapeseed
Greece	Cottonseed
Spain	Linseed oil, Sunflower
Italy	Rapeseed, Sunflower
Turkey	Sunflower, Rapeseed
UK	Rapeseed, Waste cooking oil
Ireland	Frying oil, Animal fats
Canada	Rapeseed, Animal fat, Soybeans, Yellow grease and Tallow, Mustard, Flax
Mexico	Animal fat, Waste Oil
USA	Soybeans, Waste oil, Peanut
Cuba	Jatropha curcas, Moringa, Neem
Argentina	Soybeans
Brazil	Soybeans, Palm oil, Castor, Cotton oil
Peru	Palm, Jatropha
Australia	Beauty leaf, Jatropha curcas, Pongamia, Waste cooking oil, Animal tallow waste
New Zealand	Cooking oil, Tallow

** Jatropha curcas is a specie of Jatropha [294]*

Table 11: The oil share of substrates [285].

Substrate	Oil%	Substrate	Oil%	Substrate	Oil%	Substrate	Oil%
Jatropha	50-60	Coconut	63-65	Rice bran	15-23	Palm oil	30-60
Calophyllum	65	Rapeseed	38-46	Sunflower	25-35	Corn (germ)	48
Moringa	40	Cottonseed	18-25	Jojoba	45-50		
Soybean	15-20	Olive oil	45-70	Microalgae	30-70		

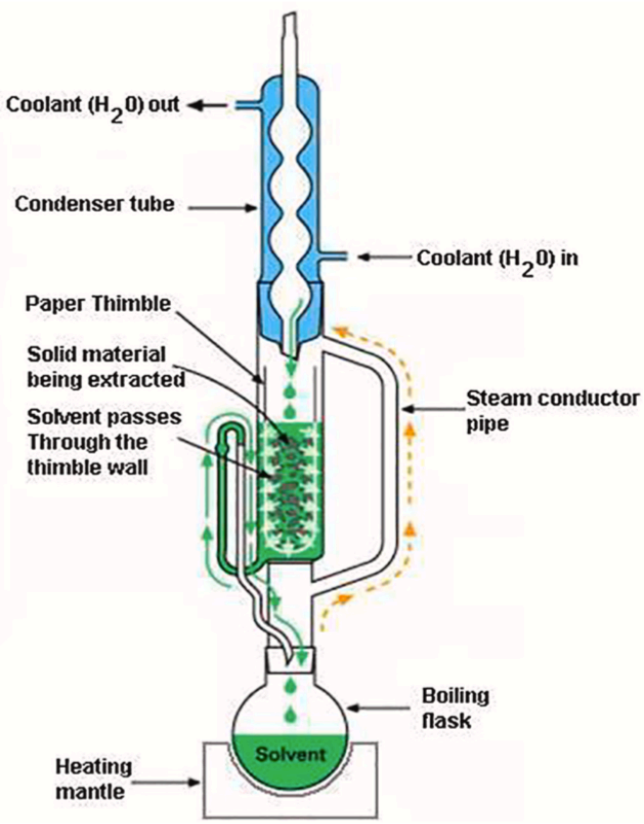

Figure 15: The Soxhlet extractor device and its mechanism [295].

N-Hexane is widely used as an organic solvent during Soxhlet extractor and in the industrial sectors, it is one of the most important solvents for oil extraction [296, 297]. It is also used in many other fields such as; printing, cleaning, food processing, petroleum and the plastics industry [298]. It is characterised as a non-polar solvent, with high selectivity for oils and a low boiling point at 69 °C, easily evaporated due to its low latent heat of evaporation at 29.74 kJ/mol, has high extraction efficiency and low energy consumption. It has been blamed for being unsafe, harmful and causing some damage to health and the environment when it is emitted into the air, however, this is not associated with the production of date seed oil, biodiesel and glycerine as a result of under reflux reactions conditions that have been performed. Figure 16 shows the process of separating n-hexane from the oil by rotary evaporator after extracting the oil from the base compound by the Soxhlet extractor [297].

Several techniques are used to recover the N-Hexane and reuse it, such as solvent extraction, evaporation, air stripping and thermal distillation [299, 300]. In a study by Xiao et al. (2007), doing n-hexane solvent recovery, they found that thermal distillation was suitable for recovering

the n-hexane solvent at a rate of 81-85% and restoring the same efficiency of use when heated for 90 seconds at 80-85 °C [296]. Wu et al. (2001) found that water washing technology is an appropriate technology to recover more than 97% of n-hexane organic solvent at optimal conditions of 40 °C, where the water volume used was recommended to be 3-4 times the volume of organic solvent and 5 min washing time [301].

Moreover, the amount of methanol used in the transesterification process was more than that required to complete the reaction. This excess quantity can be separated and reused, contributing to preserving the environment from the surplus quantities, reduced costs, and improved biodiesel quality to meet standards [302]. Al-Mawali et al. [303] found that a ratio of 15:1 of oil to methanol weight was the optimal ratio for the transesterification process, when producing large quantities of biodiesel (1,000 kg biodiesel from 1,111.11 kg of oil with 74.07 kg of methanol). 95% of the methanol used in the reaction can be recovered and reused. Figure 16 shows a schematic of the separation process of N-hexane from the oil.

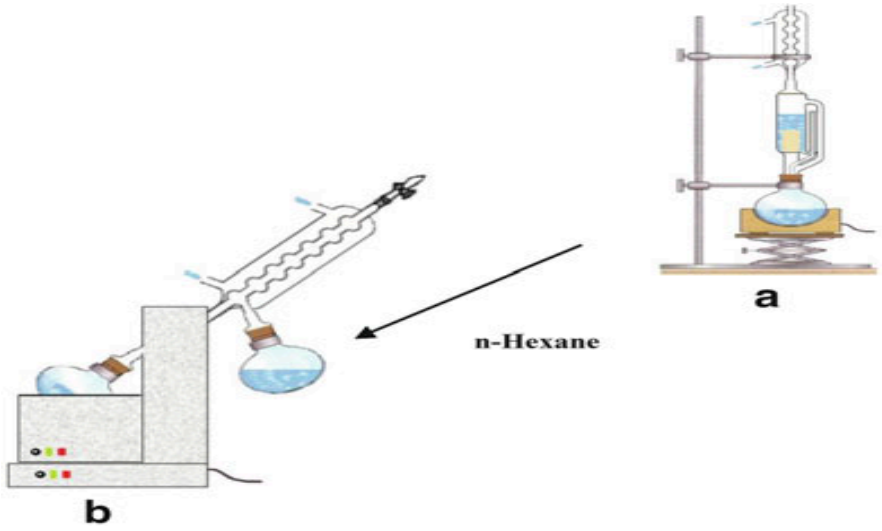

Figure 16: (a) Extracting the oil by n-hexane solvent in Soxhlet extractor (b) Separating the n-hexane solvent from the oil by the rotary evaporator [297].

Hydrolysis and transesterification are two of the main processes involved in biodiesel production. Hydrolysis is a chemical reaction in which water molecules are divided into oxygen and hydroxide anions. The reaction process between fats and alcohols to form biodiesel and glycerine is based on the transesterification process. The ratio of alcohol to fat in the transesterification process should be 3:1 and may reach 6:1 to achieve higher yield. Ester forms by replacing triglyceride molecules with alcohol molecules. Due to the splitting of alcohol, this

process is also called alcoholises. Sodium hydroxide and potassium hydroxide are used as a catalyst [304]. Methanol and ethanol are often used in esterification processes, which are considered environmentally friendly processes. The methanol is used for its cheap price, high polarity and short alkyl chain, while ethanol is chosen as it can be extracted from agricultural products and renewable resources [305]. Table 12 depicts the percentage range of the products as a result of the transesterification process. Figure 17 shows a simple process diagram used in the production of biodiesel and glycerine from vegetable oil [306].

Table 12: Percentages range of transesterification process [306].

Product	Percentages	References
Biodiesel	90-91	[307-309]
Glycerol	9.0-9.6	[308-312]
Unreacted products	0.4-1.0	[307, 310, 313, 314]

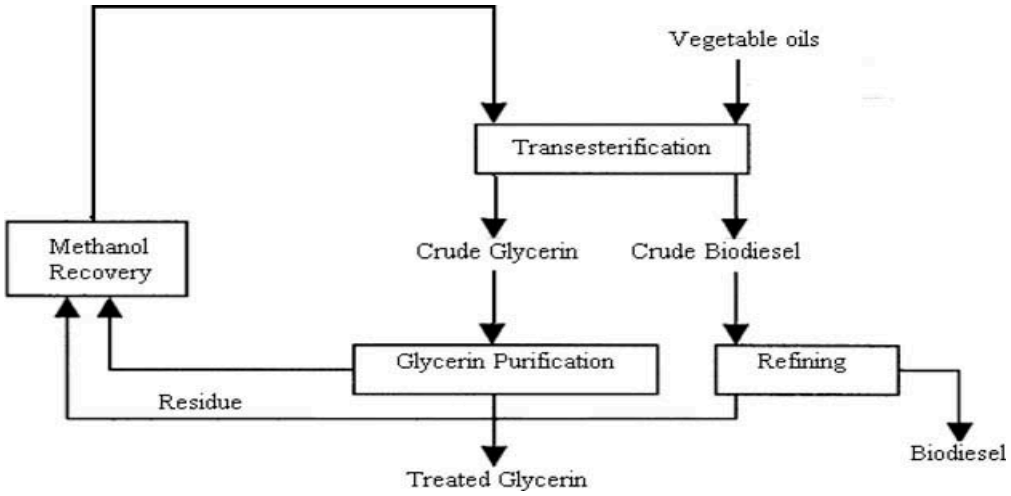

Figure 17: Biodiesel and glycerine production process flowchart [306].

Amani et al. (2013) [292] found that the properties of biodiesel extracted from date seed oil were optimal when the cetane number was 60.3, the iodine value was 46, the viscosity was 3.48 mm/s and at a flashpoint temperature of 140 °C. The biodiesel resulting from this study was affected by its high pouring point which was -1 °C, which limits its use in cold regions. In this study the seeds were ground using a heavy-duty grinder. The oil was extracted by using a Soxhlet extractor and n-hexane solvent for 4 hours. The solvent was separated from the resulting oil by using a rotary evaporator and passing it through a filter for purification. Methanol and sodium hydroxide were added to the date seed oil and reacted for two hours at 60-65 °C using reflux and constant

stirring. The reaction resulted in a mixture of biodiesel and glycerine that was separated by a separating funnel based on their different densities. To remove impurities from biodiesel, it was washed with hot water at (70 °C) and dried with a rotary evaporator.

Jamil et al. (2016) [293] found during their study in producing biodiesel from date seed oil that the highest yield of date seed oil was 16.5% (the weight difference between a pre-dried sample and extracted sample divided by dried sample). The date seeds were washed to remove impurities and dried in air for 6-7 days, prior being dried in the oven for 12 hours at 70 °C. The date seeds were ground in a mechanical grinder to obtain the required particles sizes of 250-300 nm. The optimal conditions for producing oil, whilist using the Soxhlet device, were at a reaction temperature of 70 °C, a ratio of solvent to seeds 4:1 and for 7 hours of extraction. To produce biodiesel, a reaction was conducted using methanol for one hour at 65 °C, where the ratio of methanol to oil was 6:1. It was found that the biodiesel produced had a cetane number of 58.23, density of 870 kg/m^{-3}, cloud point of 4 °C, pour point of -1 °C, and viscosity of 3.97 mm^2/s at 40 °C.

Ali et al. (2015) [155] studied the effect of particles size of Zahdi date seed on the oil produced volume. They used the Soxhlet device with several solvents to extract the oil. The study found that the highest percentage of oil was 8.5% (the weight of oil extracted divided by weight of date seed used) for 2 hours, when the particles size of the date seed was 0.425 mm and using n-hexane as a solvent. The seeds were washed, dried in the air and milled using a mechanical grinder to several sizes (0.425 and less, 1 mm and less and 1.2 mm and less). Five different solvents (n-hexane, methanol, 2-propanol, chloroform and toluene) were used to find the best solvent that provided the highest oil percentage and for extraction time 1, 2, 4 and 6 hours. In a study by Elnjjar et al. (2018) [156] in the production of biodiesel from the seeds using the Khalas and Allig date, the Soxhlet and Folch methods were used to extracted oil from the date seeds. Date seeds were washed and dried in the oven at 80 °C for 12 hours. The date seeds were then milled to five different sizes (300 nm, 0.1-0.3 mm, 0.3-0.85 mm, 0.85-1.18 mm, and > 1.18 mm) and compared to the whole date seeds. The study found that the particle size of the date seed has a noticeable effect on the percentage of oil produced. Where the oil percentage produced increased with the decreasing date seed particles size, except for the particles sizes of 300 nm. The oil produced from both date seeds using the Soxhlet method was 10.4% and 10.5% of the

date seed mass, while the ratio was 9.0% and 9.7% using the Foch method for extracting oil. The percentage of oil produced was determined by dividing the mass of extracted oil by the mass of dried sample used. They also found that the Soxhlet extraction method was more productive than the Folch method, for all particle sizes and both date seeds types. Table 13 illustrates the biodiesel characteristics of different date seed types.

Table 13: The Characteristics of biodiesel obtained from date seed oil from previous studies.

Feed stock	AN (mgKOH/g)	CN	BP (°C)	CP (°C)	D (kg/m^3)	FP (°C)	PP (°C)	Vs (mm^2/s)	Ref.
Multiple date seed	N/A	60.3	N/A	4	877	140	-1	3.84	[292]
Unknown date seed	0.21	58.23	N/A	4	870	137	-1	3.97	[293]

AN: Acid Number, CN: Cetane Number, BP: Final boiling point, CP: Cloud point, d: Density, FP, Flash point, PP: Pour point, Vs: Viscosity, N/A: not available.

2.9 Glycerine

Glycerol or as typically known as glycerine is formed during the transesterification process with ethanol or methanol [315]. Producing biodiesel from natural oils, also produces glycerine as a by-product of up to 10% [316]. Many previous studies indicated that the percentage of glycerine from the biodiesel transesterification process ranges between 9-9.6% of the total product [308-312]. Glycerine is environmentally friendly, harmless to human health, soluble in water, and is colourless and odourless [317]. Glycerol does not mix with biodiesel, it polymerises at high temperatures resulting in the emission of a toxic gas [318]. Therefore, it is more expedient to exploit the glycerol produced from the production of biodiesel [319]. The price of glycerine ranges from 0.33 USD/Ib (0.7277 USD/kg) for pure glycerine to 0.055 USD/Ib (0.1213 USD/kg) for crude glycerine, according to the United State National Biodiesel Board (NBB) in 2017 [278, 320]. Glycerine is available in different forms as shown in Table 14 [321]. The purity of glycerine affects its final use. Crude glycerine is less preferred in use, so it is sold to large refineries to purify it. Purified glycerine is preferred in food, pharmaceutical and cosmetic manufactures, while commercial glycerine is considered optimal in medical applications [278, 306].

Table 14: Glycerine types and propitiates [321].

Types	Crude	Purified	Commercial
Glycrine (%)	60-80	99.1-99.8	99.2-99.98
Moisture content (%)	1.5-6.5	0.11-0.8	0.14-0.29
Soap content (%)	3.0-5.0	0.56	N/A
Ash (%)	1.5-2.5	0.054	<0.002
Acidity pH (%)	0.7-1.3	0.10-0.16	0.04-0.07
Colour (APHA)	Dark	34-35	1.8-10.3
pH Values	9.8-11.2	6.7-6.9	6.7-6.8
Gross energy (Cal/g)	3685-3825	5810-5831	5832

Globally, glycerine production from bio-oil increased threefold, from 200,000 tons to 600,000 tons between 2003-2006. Based on the European Biodiesel Board (EBB) report, the European Union increased its glycerine production from 2015 to 2017 by 84%. The volume of glycerine produced in the European Union increased from 1.16 million tons in 2015 to 2 million tons in 2017. According to the NBB in the United States, glycerine production recorded a dramatic increase from 25 million gallons to 289 million gallons from 2006 to 2016. Figure 18 shows the expected growth in glycerine production over the period from 2001 to 2026 worldwide. A report issued by the Organisation for Economic Cooperation and Development (OECD) in 2017 indicated that the global glycerine production is expected to reach more than 4000 million litres in 2026. Crude glycerine that produces from biodiesel transesterification process contains some impurities such as alcohol, soap, water and ash that limit its direct use. The cost of purifying the crude glycerine and the abundance of pure glycerine drove the crude glycerine price down significantly. Therefore, many studies seek to reduce these costs by finding suitable alternatives to convert crude glycerine into useful products [278]. Figure 19 illustrates some industries that use glycerine in their processes. The chemicals emanating from fossil fuels result in many environmental damages such as greenhouse gases and carbon dioxide. Greenhouse gases from these chemicals constitute approximately 7% of total emissions and 5.5% of carbon dioxide emissions. It also results in harmful water discharges and many other harmful chemical wastes [322].

The glycerine that results from the biodiesel transesterification process is not pure enough and requires further purification [323]. The type of catalyst used in the esterification process, its quantity, recovery methods, unreacted methanol and other impurities are factors that effect the quality of the crude glycerine produced. The purification cost of glycerine is estimated at

approximately 0.15 USD/kg [306]. Glycerine extracted from sunflower oil is composed (w/w) of 30% glycerine, 50% methanol, 13% soap, 2% moisture, 2-3% salts and 2-3% other impurities [306]. While in a study by Hansen et al. [324] of 11 samples from 7 producers, they found that the percentage of glycerol ranged between 38-96%, where the methanol and ash ratios reached more than 14% and 29% respectively.

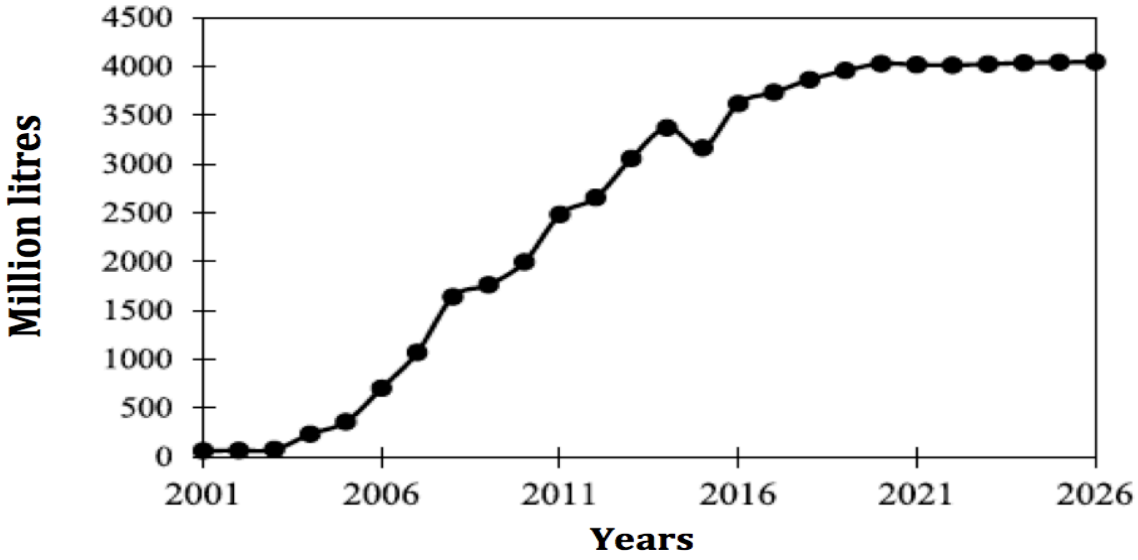

Figure 18: Global glycerin production [278].

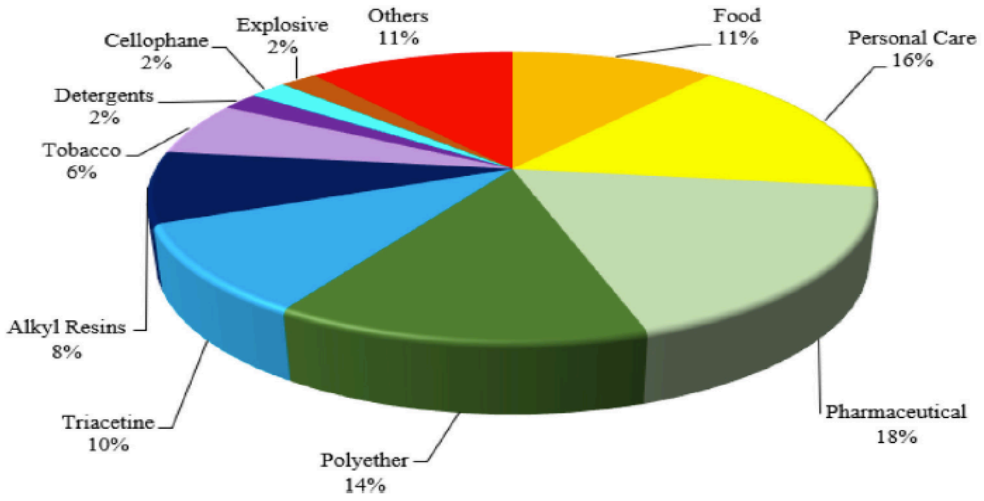

Figure 19: Industries usage of glycerine [325].

2.10 Starch-based Adhesive

Starch-based adhesive that produces from several food wastes is abundant, cheap and easy to use. The adhesive is characterised by its high quality and ability to degradable. It is usually in

powder form and mixed with water before use. Starch is extracted from some rich starch food such as potatoes, corn and cassava [326]. Adhesives are used in several applications such as woody composites, plastic and paper [261, 327, 328]. The properties of Adhesive starch appear after heating them at certain temperatures to break down the starch granules. The heating process breaks down the starch granules, and this process is known as gelatinisation [329]. The gelatinisation temperatures vary according to the starch type used, as shown in Table 15 [330, 331].

Table 15: The gelatinisation temperature of different starches [330, 331].

Starch Source	Gelatinisation Temperature ºC
Corn	62-72
Wheat	58-64
Oat	56-61
Rice	68-78
Potato	59-68
Cassava	49-70

Some modification compounds are added to the adhesive to improve its efficiency and properties, such as borax (sodium tetraborate), which uses as a viscosity enhancer. Also adding sodium hydroxide (NaOH) and hydrogen chloride (HCl) enhancing the gelatinisation of adhesive produced [332-334]. Urea-formaldehyde or melamine-formaldehyde with an acid catalyst is added to the adhesive to increase the adhesive water resistance. Since formaldehyde is not safe, its use is not attractive [330]. Several responses help determine the adhesive quality, such as adhesion strength, viscosity, density, pH and roughness [332].

Cassava starch is abundant, low cost, safe, biodegradable, and characterised by its ability to paste, which makes it suitable for applying as an adhesive [335]. The process of cassava starch sustainability faces some difficulties such as high cost and problems associated with waste management. Researchers seek to manage cassava waste by turning it into biological products of more valuable and reduce the damage resulting from its accumulation in the landfill [336]. The temperature required for the gelatinisation process for cassava starch is quite low comparing to the starch produced from other food sources. That contributes to reducing the heating temperature and thus saving the energy used [331]. Gunorubon (2012) found that the temperature and adding viscosity enhancer and gelatinisation enhancers have different effects on adhesive properties from cassava-based (viscosity, density, acidity, dry time and adhesion strength). The

study concluded that the temperature was indirectly proportioned with the viscosity and density. The temperature had a slight influence on the pH; at high borax concentrations, the pH was almost stable. While increasing the temperature, the pH slightly decreases at lower concentrations of borax. Using sodium hydroxide improves the gelatinisation rate of the adhesive and has a stronger bond than using hydrogen chloride. On the other hand, the drying time for the adhesive with sodium hydroxide has a longer drying time than with the hydrogen chloride. The study also showed that adding borax increased viscosity, density and pH [333]. Oghenejoboh (2012) in his study of cassava starch-based adhesive, conclude that the cassava starch which contains a high concentration of cyanohydric acid and has a lower pH value produce stable and high-quality adhesive and the longer drying time leads to a longer life [331].

Sun et al. [337] produced as adhesive from cassava starch with an esterification modifier (dodecenyl succinic anhydride) for use with plywood. A polyvinyl alcohol solution, deionised water and cassava starch were mixed at certain quantities. Dodecenyl succinic anhydride was added to the mixture at different quantities (0-8%wt of starch) and heated at 55 °C. The pH of the mixture was set at 8-8.5 and stirred for 45 minutes. Polyaryl polymethylene isocyanate was added to the adhesive as a crosslinking and stirred until it became homogenous. The study showed that the adhesive viscosity increased by increasing dodecenyl succinic anhydride concentration from 101 mPa.s at 0% dodecenyl succinic anhydride to 5,830 mPa.s at 8%. The shear strength of the plywood glued with produced adhesive increased from 1.51 MPa at 0% dodecenyl succinic anhydride to 2.61 MPa at 2% dodecenyl succinic anhydride. Subsequently, the shear strength of the plywood decreased with an increase of the modifier concentration. Table 16 shows the viscosity and shear strength values of plywood and the effect of adding the esterification modifier.

Table 16: Effect of esterification modifier on adhesive properties [337].

Modifier concentration (%)	Viscosity (mPa.S)	Shear strength (MPa)
0	101	1.51 ± 0.10
2	318	2.61 ± 0.23
4	367	2.23 ± 0.30
6	5510	1.77 ± 0.17
8	5830	1.73 ± 0.11

In another study [338] to produce starch-based adhesive material to be used with plywood, corn starch was used in combination with polyvinyl alcohol, borax, hydroxyel (polyethylene glycol 400) and different concentrations of thickening factor (concentrations of carboxymethyl cellulose (CMC)) (0, 0.25, 0.75 and 0.75%). Isocyanate prepolymers were added to the adhesive as a cross-linking and to enhance the water resistance. The study found that adding carboxymethyl cellulose increased the viscosity of the starch-based adhesive. Increasing this percentage by a large amount made it difficult to distribute the adhesive evenly over the plywood surface. The highest viscosity achieved was a little more than 450 mPa.s at 0.75% of carboxymethyl cellulose, while it was around 25 mPa.s at 0% of carboxymethyl cellulose. Figure 20 illustrates the change in viscosity with different carboxymethyl cellulose amounts. The bonding strength of plywood at different concentration of carboxymethyl cellulose and different ratios of Isocyanate prepolymers to hydroxyel is shown in Table 17. The relationship between bonding strength, carboxymethyl cellulose concentration and hydroxyl ratio was complicated. The lowest bonding strength attained was 1.39 MPa at 0% carboxymethyl cellulose concentration and Isocyanate prepolymers and hydroxyl ratio. In comparison, the highest bonding strength found was 3.78 MPa at 0.75% at 100 molar ratio of isocyanate to hydroxyel.

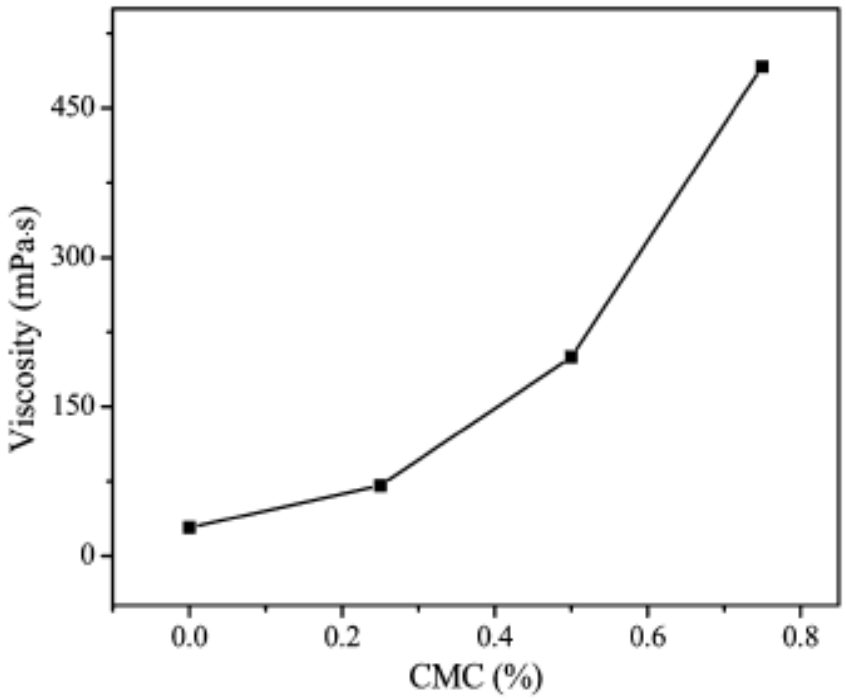

Figure 20: The effect of thickening factor on the adhesive viscosity [338].

Table 17 : Plywood shear strength [338].

Bonding strength (MPa)					
	Ratios of Isocyanate prepolymers to hydroxyel				
CMC (%)	0	15	25	50	100
0.00	1.39 ± 0.07	2.29 ± 0.09	3.14 ± 0.15	3.44 ± 0.16	2.99 ± 0.06
0.25	2.03 ± 0.08	2.80 ± 0.09	2.41 ± 0.10	3.58 ± 0.18	2.87 ± 0.14
0.50	1.69 ± 0.12	2.67 ± 0.22	2.84 ± 0.11	3.01 ± 0.12	3.37 ± 0.46
0.75	1.53 ± 0.13	2.80 ± 0.18	2.20 ± 0.12	3.25 ± 0.10	3.78 ± 0.13

Yap et al. [328] studied the use of a commercial adhesive with 3-D printed ASA plastic. Two commercial adhesives (epoxy and cyanoacrylate) were used to determine the plastic specimens' adhesive properties with and without heat treatment. Samples surfaces were cleaned with isopropyl alcohol, before adhesion with the commercial glue. The samples were clamped with spacers and left for 24 hours to cure either at room temperature or some samples were placed in the oven at 80 °C to explore the effect of heat treatment on adhesive. Two types of failure appeared for all of the adherent samples. Failure was in the substrate for all samples adherent with the cyanoacrylate, while failure was in the adhesive for all samples of plastic adherent with epoxy. The heat treatment affected the strength of the epoxy glue while increasing the failure load of the cyanoacrylate adherent samples. Surface treatment of ASA plastic with sandpaper of 320 grit led to a significant improvement in the adhesive shear strength, as a result of the improvement of surface conditions. The failure load increased from 473 N to 808 N (70%) after the sanding process.

In a study to overcome the issue of removing the adhesive from the paper during the recycling process, it was found that adding hyperbranched polyester (H_{102}) to the adhesive material acts as a dispersant and leads to stabilising the performance of the adhesive and extends its shelf life [261]. The adhesive was produced from corn starch, where the starch was dissolved in water, then added ammonium persulfate (APS) (oxidizing agent to catalyze the polymerization), sodium lignin sulfonate (polymerized) and $H_{10}2$ (dispersant). The study showed that the adhesive was well suited to the paper and resisted humidity to a certain extent. The paper was affected by the increase in humidity, the paper's shear strength was affected as well. The fracture occurred in the paper without the adhesive being affected. Moreover, the addition of H_{102} led to a decrease in the adhesive viscosity, thus stabilising the adhesive and extending its shelf life. The shear strength of

the paper was approximately 1.07 MPa (20% humidity), higher than 0.3 MPa at 100% humidity [261].

2.11 Adhesive Bond Strength

The adhesion properties can be evaluated through several methods, including lab shear test, pull off test, torque test, etc. Failure can occur in several locations of the substrate or adhesive, as will be explained later. These tests provide quantitative or qualitative data for adhesion not physical analysis [339]. The shear test provides a quantitative description of adhesion performance as it measures the ability of a material to withstand stresses by moving the shear force in opposite directions. Its low cost and simplicity characterise this test [340]. Figure 21 shows a schematic of samples used in a lap shear strength test. This test has been used to explore the properties of adhesive strength by several researchers [261, 328, 341]. Many factors affect the adhesive shear strength, such as the type of substrate, the adhesive used, the surface treatment and thickness of the adhesive [342].

Figure 21: Schematic drawing of lap shear strength test [343].

2.11.1 Surface Preparation

Surface pre-treatments and optimisation of substrate parameters improve the adhesive's bond strength [342]. Surface properties, mechanical interlocking and chemical bonding can be improved between the adhesive and the substrate by surface pre-treatment process that removes contaminants and adjusts the surface topography and wetting properties [344, 345]. Different surface treatment can be used such as grinding, sandblasting and anodising, which affect the bonding strength [346, 347]. Moreover, the surface roughness affects the surface adhesion strength due to the decrease in the actual contact area and increased distance between surfaces compared to smooth surfaces. Roughness causes a force of friction between the contacted surfaces [348]. Surface roughness can be adjusted by several ways, such as mechanical polishing, which is easy to use and effective for improving the roughness of surfaces, different sizes sandpaper and sandblasting that changes the substrate's topography [342, 349]. The relationship between surface roughness and adhesion is variable, and there is no specific trend to

link this relationship. Furthermore, The optimum surface roughness values vary according to the adhesive and adherent, therefore this relationship is complex [350]. In studying the effect of surface roughness on the bonding shear strength of aluminium and wood panels after being treated with emery and sandpaper respectively, Budhe et al. [350] found that the surface roughness affects the adhesion strength. Figure 22 (a and b) shows adhesive strength values againest the change of surface roughness. The adhesive strength of aluminium increases with the increase in surface roughness and then begins to decrease with a further increase in roughness. In contrast, wood exhibit high adhesion strength as the surface smoothness increases. The adhesive strength decreases with the increase in surface roughness, as shown in Figure 22 (b) [350]. Generally, the adhesion strength is also affected by the particle size and shape, in other words, the particle size has a large effect on the adhesion strength [351].

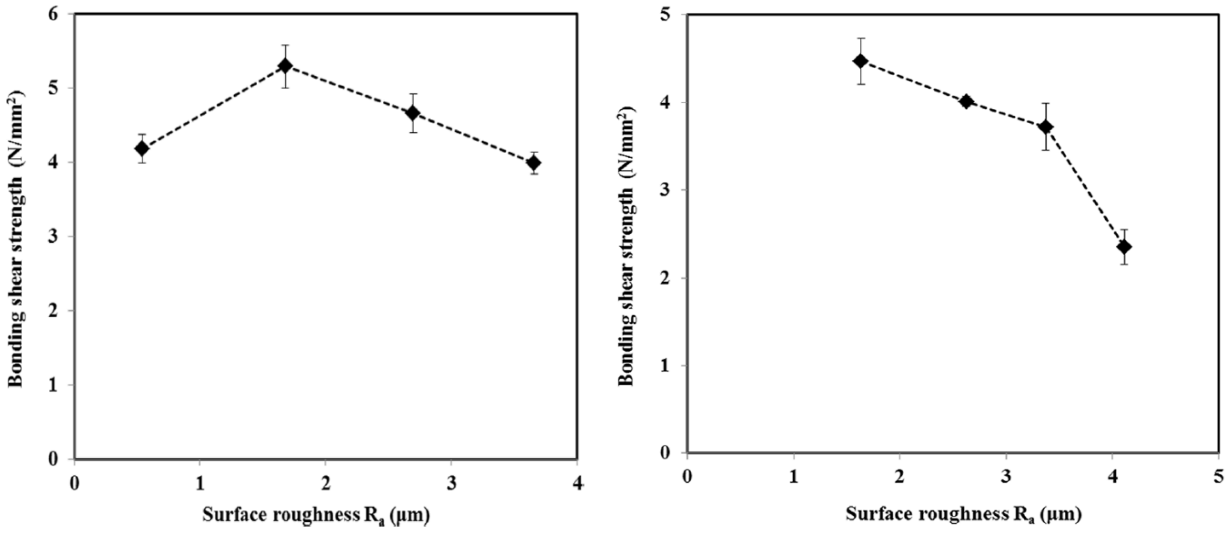

(a) (b)

Figure 22: Relationship between bonding shear strength and surface roughness of (a) Aluminium (b) Wood [350].

The poor surface properties of polymers, such as ineffective adhesion to polymers, are amongst the issues that limit their wide application. That has led to research to modify polymers surfaces such as plasma treatment, acid etching, machining and other processes to increase the adhesion strength [343, 352]. Failure to adhere polymeric materials can also occur based on weak cohesion forces connecting molecules of similar materials. Mechanical bonding, which depends on surface roughness, is one method for bonding substrates with adhesives. The adhesive

penetrates the pores, cracks, and other surface residues, forming mechanical interlocking between the adhesive and the substrate [353]. Optimal rheological properties of the adhesive to penetrate small cavities and wet the surfaces help in performing good mechanical bonding. Chemical bonding is another method that can be used to bond materials by forming covalent bonds between the adhesive and the substrate [343]. Figure 23 depicts the mechanical and chemical bonding.

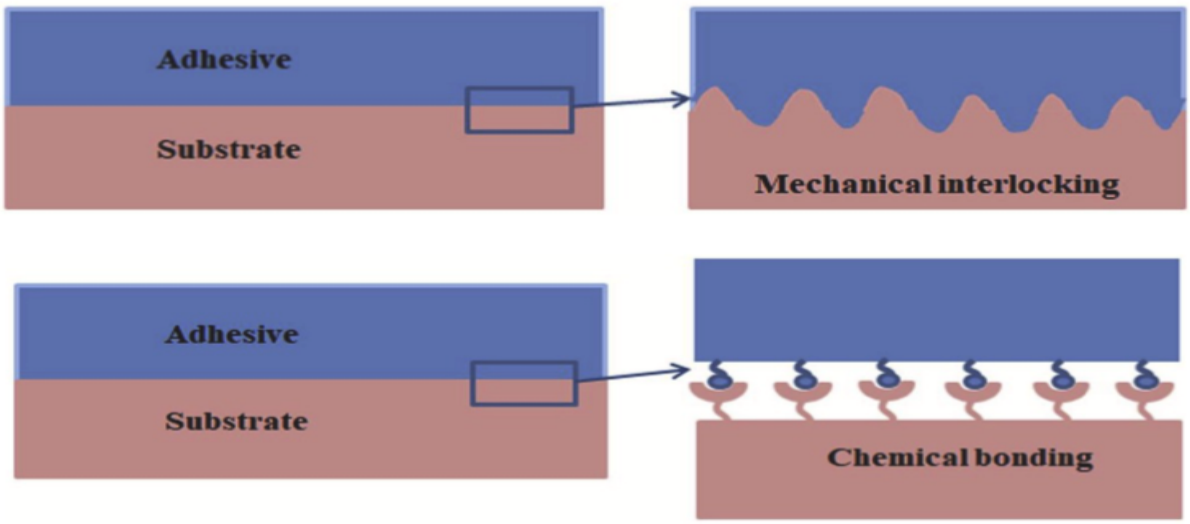

Figure 23: Mechanical interlocking and chemical bonding [343].

2.11.2 Adhesive Thickness

The bonded area and the thickness of the adhesive layer constitute the size of the adhesive. Although increasing the bonded area may increase the bond strength, increasing the adhesive layer's thickness may weaken the performance of the adhesive strength. Generally the adhesive thickness is often tens of microns [354]. Shokrian et al. [342] found that the shear strength decreased slightly with the difference in the adhesive thickness from 0.3, 0.5 and 1 mm, consistent with what stated in the study of Silva et al. [355], where the thickness of the adhesive was inversely proportional to the strength of the adhesive. The shear strength was affected by the difference in the adhesive thickness, as shown in Figure 24, which shows a scattered data, depicting a downtrend with increasing thickness. The reason for the scattered data may be due to errors in fabrication and sample testing. The epoxy adhesive was used to adhere aluminium specimens. Moreover, increasing the thickness of the adhesive material weakens the adhesive strength, as it increases the possibility of adhesion failure [342, 356]. In contrast, Liao et al.

[357] mentioned that the thickness and type of adhesive affect the adhesive strength and the failure of brittle adhesive increases with the decrease in the adhesive thickness. [357].

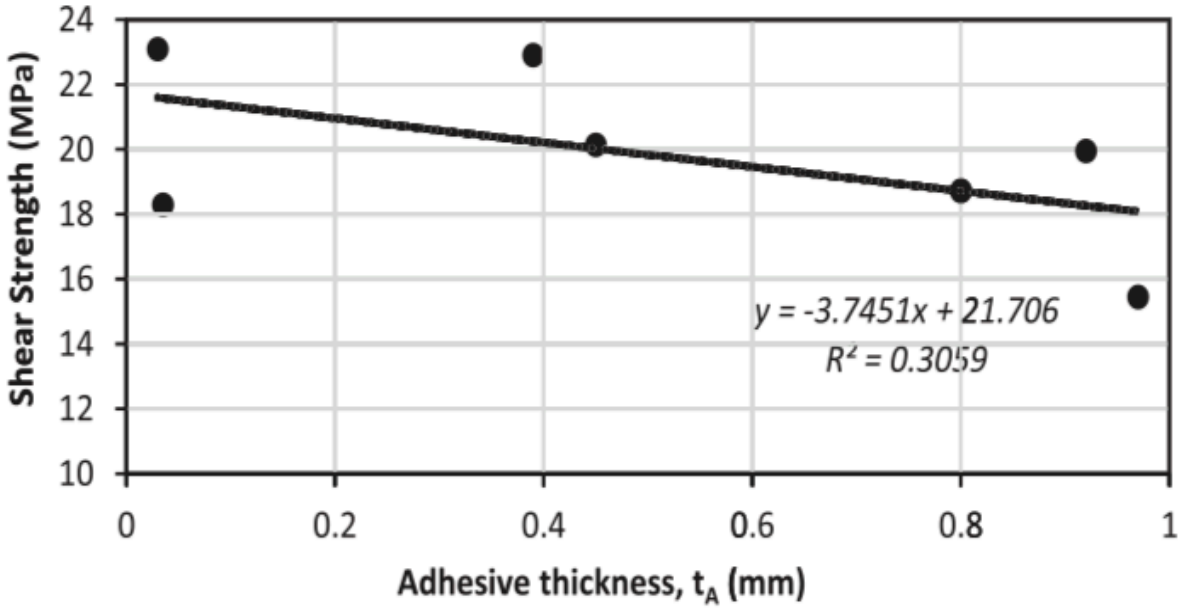

Figure 24: The effect of adhesive thickness on the bond shear strength [342].

2.11.3 Adhesive Failure

There are three forms of adhesion failure: (1) Adhesive failure, (2) Cohesive failure and (3) Substrate (adherent) failure as illustrated in Figure 25 [343]. Adhesive failure (1) forms in the layer between the adhesive and substrate surface (separating layer between the adhesive and adherent) due to insufficient surface preparation or using inappropriate adhesive for a substrate. Also, the lack of covalent activities between the adhesive and the surfaces leads to adhesive failure. Cohesive failure (2) is where adhesive remains on both surfaces of the substrate when the failure occurs. It is determined based on the rate of failure to bond and accordingly, the adhesive's effectiveness is determined. The greater the cohesive failure value indicates the weakness and inefficiency of the adhesive. Factors such as adhesive type and insufficient adhesion lead to cohesive failure. The cohesive failure indicates the suitability of the adhesive to the adherent surfaces and result in failure occuring inside the adhesive [358, 359]. Fractures that occurs in the substrate (3), before or not in the adhesive, are known as substrate failure [359]. This type of failure occurs for the low tensile strength substrates, where the strength of the adhesive greater than the tensile strength of the substrate. It occurs inside the substrate [360]. Figure 26 shows the different adhesive failures [361].

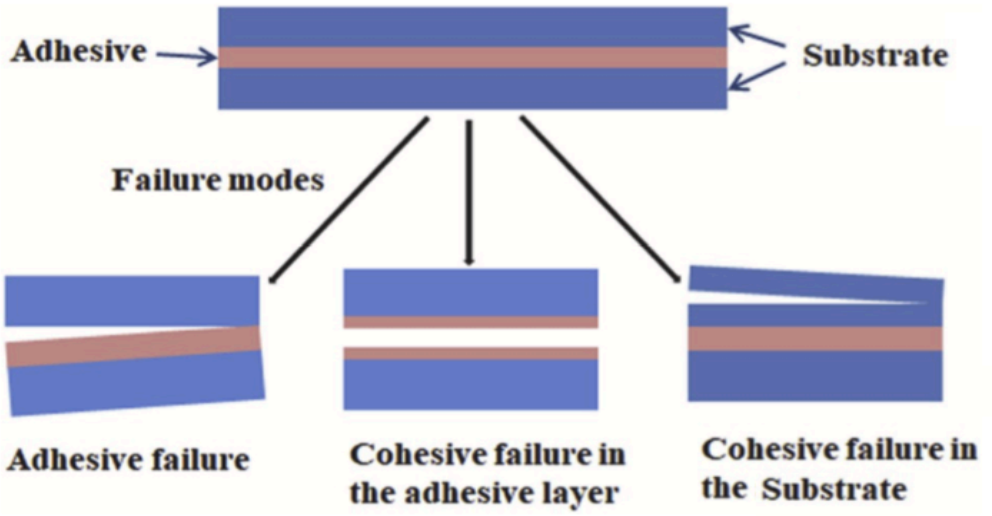

Figure 25: Adhesive failure forms [343].

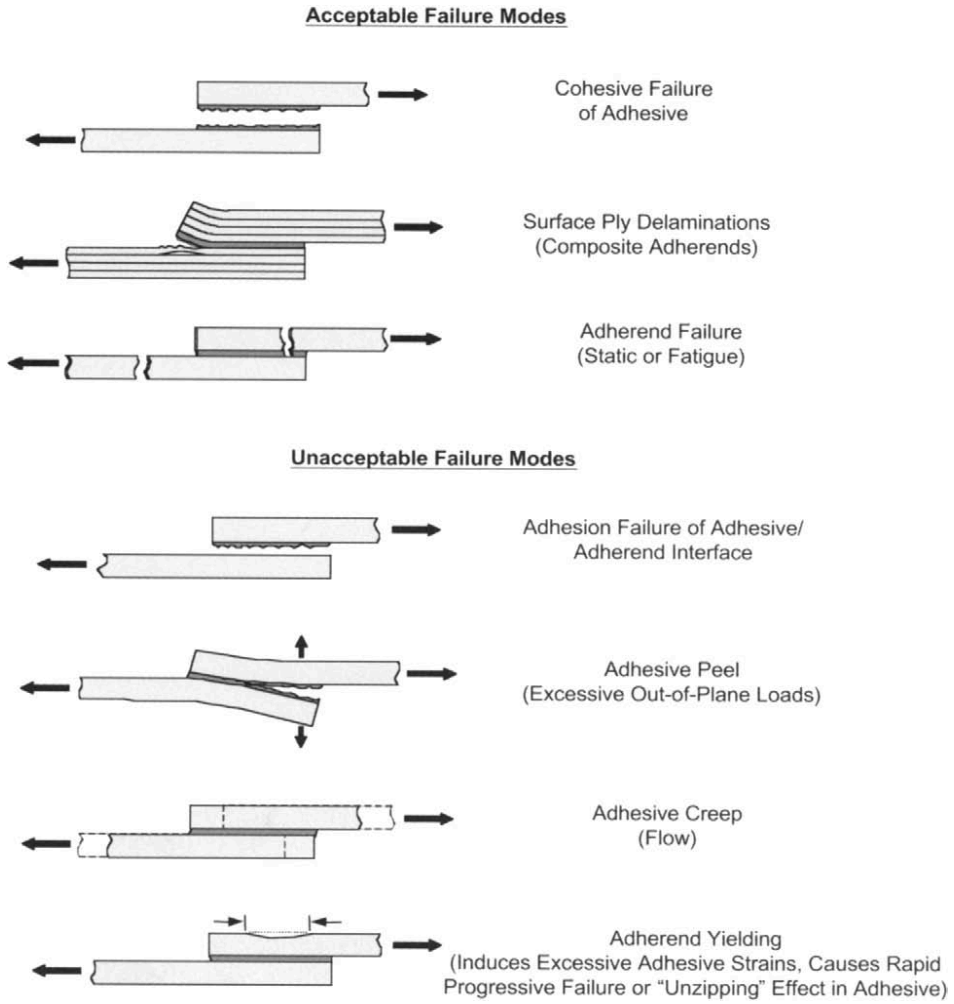

Figure 26: Acceptable and unacceptable adhesive failures [361].

2.11.4 Substrates of Adhesive Process

Many materials such as plywood, plastics, paperboard and paper are commonly used in several fields that required adhesion processes in some of their uses, applications and assembling [362, 363].

(A) Plywood

Plywood is one of the most common types of wood used in different fields, such as in the furniture and cabinet industries, engineering floors manufacturing and construction. Wood panels are bonded with many types of formaldehyde-based adhesives, such as urea-formaldehyde resin and resin phenolic-formaldehyde due to their lower cost and high performance. However, it is not resistant to external factors such as humidity, resulting in harmful formaldehyde emissions. Wood composite materials are the most harmful sources of formaldehyde emissions [362, 364]. There are many types of plywood such as birch and beech, which are used in many countries worldwide [365]. The global production of plywood panels in 2019 was approximately 163 million m^3 [166, 365]. Birch wood is a hardwood that is mostly used for indoor applications due to its low dimensional stability [366]. Cakiroglu et al. [365] found that birch wood had almost the same mechanical strength as other wood panels such as beech. Therefore, relying on it instead of beech wood in their applications would reduce manufacturing costs.

(B) Plastic

Plastic composed of several organic polymers such as polyethylene, nylon and polyvinyl chloride, which can be formed and modified into several flexible and rigid shapes. Daily life has many requirements of plastic products to meet the purposes and needs. Plastic is produced from various materials of fossil origin, renewable or mineral base. Plastic is used in many fields such as medical delivery systems, automotive and packaging industries. Plastic is characterised by its low cost, strength, low density, adjustable and ease of design and uses. Table 18 shows some types of plastics with their description and potential applications [363, 367, 368], however it is numerous.

Table 18: Several plastics types, descriptions and usage [363].

Type	Description	Applications (Virgin or recycle plastic)
PET: Polyethylene Terephthalate	Fiber, Clear tough plastic	Detergent bottles, soft drink bottles, fleecy jackets and mineral water

UPVC: Unplasticised Polyvinyl Chloride	Clear, hard rigid plastic	Detergent bottles, plumbing pipe fittings, tiles, juice bottles and clear cordial, plumbing pipes fittings and blister packs
HDPE: High Density Polyethylene	Very common plastic, usually white or coloured	Detergent bottles, compost bins, crates, mobile rubbish bins, freezer bags, crinkly shopping bags, milk and cream bottles
LDPE: Low Density Polyethylene	Flexible, soft plastic	Industry, packaging and plant nurseries, film for builders, bags, garbage bags, garbage bins, lids of ice-cream containers and black plastic sheet
PPVC: Plasticised Polyvinyl Chloride	Elastic plastic, flexible and clear	Industrial flooring, hose inner core, shoe soles, garden hose, tubing and blood bags
PS: Polystyrene	clear, glassy, rigid, brittle plastic	Office accessories, coat hangers, spools and rulers, clothes pegs, plastic cutlery, yoghurt containers and imitation crystal ‘‘glassware”
PP: Polypropylene	Many uses, flexible and hard plastic	Kerbside recycling crates, compost bins, potato crisp bags drinking straws and ice-cream containers
EPS: Expanded Polystyrene	Lightweight, foamed, thermal insulation and energy absorbing	Meat trays and packaging, takeaway food containers and hot drink cups
ABS: Acrylonitrile Butadiene Styrene	iRigid, opaque, glossy tough, good low temperature properties	Furniture such as chairs and tables, Luggage cases containers, telephone handsets, rigid luggage, electroplated parts, radiator grills
PC: polycarbonate	Transparency, strong, thermal stability, stiff, hard, tough and very rigid.	Data storage including, CD and DVD, construction materials such as dome lights, sound walls, automotive, glazing, electronic, business machine, optical media and medical and lighting
HIPS: Polystyrene (High Impact)	Hard, rigid, translucent, high impact strength	Countertop point of purchase displays, indoor signs, yoghurt pots, refrigerator linings, vending cups, bathroom cabinets, toilet seats and tanks
PA: Polyamides (Nylon)	Very tough materials with good thermal and chemical resistance	Hair combs, machine screws, gaskets, other low-to-medium-stress components, fishing line, carpets, food packaging, offering toughness and low gas permeability
TPE: Thermoplastic Elastomers	Flexible, clear, elastic, wear resistant and impermeable	Damping elements, grip surfaces, design elements, back-lit switches and surfaces, soles and heels for sports shoes, hammer heads, seals, gaskets and skate board wheels
EP: Epoxies	Rigid, clear, very tough, chemical resistant and good adhesion properties	Adhesives, coatings, encapsulation, electrical components and aerospace applications

(C) Paperboard

The recycling process of paperboard and paper is considered one of the major issues in the sustainable development process. Paper recycling faces some issues such as chemically complex, ink and papermaking chemicals and adhesive sticking to the equipment during the recycling process. These adhesives are not degradable and insoluble in water. Through their ability to dissolve and degrade, bio adhesive can provide a solution to the problem of adhesive adhesion to recycling equipment [261, 369]. Papers are used for a variety of uses, such as writing, wrapping and many other purposes [370].

2.12 Summary

The increasing negative impact on the environment and climate change due to fossil fuels has led to more research and studies to convert to alternative energy sources that are environmentally friendly, sustainable and renewable. Renewable sources provide large amounts of clean energy that can help to overcome the environmental issues caused by fossil fuels. Biomass energy is one of the renewable resources that may generate considerable amounts of energy when applied widely. Biomass energy needs more attention, research, and study on using available resources to make it more efficient and economical and become more reliable and sustainable. Food waste quantity, which is increasing dramatically, is one of the most important renewable energy sources that have not yet been fully exploited. It has the potential to produce many forms of energy and products from one feedstock.

AD is one of the most important and efficient ways to convert biomass into energy. Many factors affect the efficiency of the process, such as temperature, volatile solid and inoculums. It also requires pre-treating the raw materials to make the digestion process easier and effective. Pre-treatment processes include mechanical pre-treatment process, in which feedstock is sliced or ground. Some raw materials contain different components that may enhance the AD process when exploited. For example, some substances contain starch or oil in their waste. In this study, cassava peel and date seeds were selected as feedstock in the AD process. As the cassava peel is rich in starch and the date seed contains oil, they are two of the food sources consumed heavily in Asia, Africa and South America. Extracting starch and oil from them before placing the residue into the AD reactor to produce other energy sources or bio-products may enhance the AD

uptake. The starch can be converted into several bio-products such as bio-plastic or starch-based adhesive material, while biodiesel and glycerine can produce from date seed oil.

In this study, the cassava peels will mechanically pre-treat by beating the pre-treatment process to slice the cassava peel and extract the starch at the same time using a Hollander beater. Simultaneously, the date seed will be pre-treated by a mechanical grinder to convert it to powder. The effect of this extraction on the quantity and quality of the resulting biogas will be investigated and determine the optimum setting for biogas production based on the required criteria. Bio adhesive material from the starch of cassava peel will be generated for adhering plywood, paper, and plastic samples. Several tests such as viscosity, density, pH and shear strength will be conducted to analyse the adhesive properties, quality and conformity to the standards. The oil will extract from the date seed by the Soxhlet method with n-hexane. The transesterification process to produce biodiesel and glycerine from date seed oil will be implemented using methanol and sodium hydroxide. Digestate resulting from the AD process will test to determine its components and properties to gain more knowledge about its potential to use different applications and the effect of the extractions process on its component. The bio-products production costs will be calculated to assign the production cost of each product separately on a lab scale. Finally, the preliminary analysis of process boundary assessment on a lab scale will also be clarified later in this study.

After reviewing the literature, it has become clear that there is a huge amount of food waste that is not utilised, which leads to environmental damage due to the accumulation of these wastes. There is also diversity in the study of factors affecting the quantity and quality of biogas. Many studies have not focused on finding solutions to the AD process's difficulties, such as instability of the AD process, residual digestion and reducing pre-treatment costs. Cassava and dates are an important food in many nations worldwide, which produce significant amounts of waste. Many studies researched several methods of pre-treating cassava and date wastes before the AD process. Studies on extracting starch from cassava peels and producing biogas from them are scarce or absent. The same applies to the date seeds, in which most studies are subjected to prior softening processes before grinding, which leads to them losing their weight and thus changing their properties.

In this study, cassava and date waste represented in cassava peels and date seed will be used to produce several bio-product such as biogas, biodiesel, glycerine, adhesive and digestate, in an attempt to reduce production costs, overcome some of its environmental issues and increase its sustainability. Furthermore, applying an integrated approach, pre-treating the cassava peel and separating the starch from it using the Hollander beater and grinding the date seeds without exposing them to pre softening processes to reduce the pre-treatment processes and subsequently reduce the operation cost, which leads to proper waste utilisation and producing bio-products without significant effect on their quantity and quality. To provide solutions to the above-mentioned gaps, three main factors will be studied: temperature, the volatile solid added value, and sludge quantity to determine the optimum combinations and results according to the criteria set, which will be explained later in Chapter 5. Controlling these factors may contribute greatly in stabilising the AD process. The diversity of bio-product resulting from the food waste from extracting the starch and oil may play an important role in reducing the operational costs of the process. This study also seeks to learn more about the characteristics of the resulting digestate from the AD processes and its content from the necessary elements to utilise them in various fields.

Chapter 3

3 Materials, Methods and Experimental Design

This chapter describes the feedstock wastes (cassava and date seeds), inoculum and the Design of experiment software (Design Expert) applied in designing experiments and analysing the results. The experimental procedures used to produce biogas from cassava peel and date seed, extraction the oil from the date seed, producing biodiesel and glycerine from date seed oil and producing starch-based adhesive material will be explained in this chapter. Furthermore, the substrates used in the adhesion process and their preparation methods will be described in this section. The equipment and materials used in the study will be detailed in this chapter and in Appendix (A). The accuracy of the devices and their calibration methods will be noted for each instrument used. Figure 27 provides an overview for this chapter.

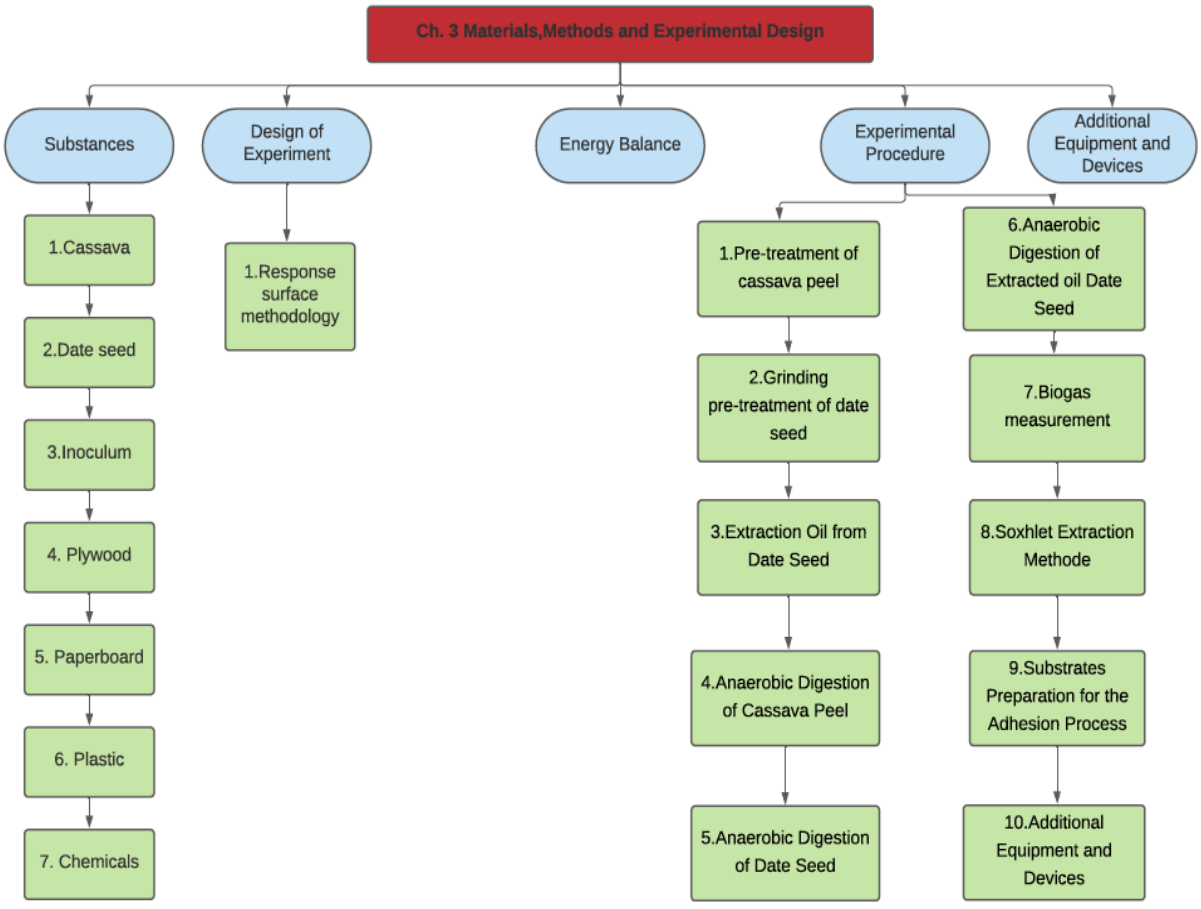

Figure 27: Flowchart of Methodology and Materials used.

3.1 Feedstock

In this study, two types of food waste were chosen, namely: cassava peel and date seed. The reason for choosing these food wastes because they are rich in starch and oil. In Asia, Africa, and South America, cassava is consumed in large quantities, while dates are consumed more in the Middle East.Their wastes are not exploited instead of being thrown in landfill. Cassava is a starch-rich food that can be used to produce several bio-products. Oil can be extracted from date seed, biodiesel and glycerine can be produced from that extracted oil.

3.1.1 Cassava

Cassava was purchased from Veg-ex shop, Dublin, Ireland. The cassava was peeled manually and cut into small pieces to facilitate the treatment process. The volume of 2.22 kg of cassava peel treated by beating pre-treatment process with a Hollander beater for 5 minutes with 20 L of water. The starch was isolated from the mixture, dried and then stored for future use. The feedstock was distributed in three containers and the volatile solid (VS) of each container was adjusted to 4.2, 2.65 and 1.1 g-VS.

3.1.2 Date Seed

Date seed (Sagai) was brought from Saudi Arabia. A kilogram of date seed was prepared and washed with water to remove impurities and remaining date flesh. It was left for three days in air to dry.

3.1.3 Inoculum

The sludge was collected from Green Generation Ltd., Nurney, Co. Kildare, Ireland in a 20L container. The sludge was brought on the same experiment day to maintain its properties.. The total solid (TS) of the sludge was 6.5%, the volatile solid was 4.51% and its pH was 8.1.

3.1.4 Plywood

Birch plywood sheet was purchased and prepared by Woodworkers Ireland. The plywood was cut into 100×25×4 mm pieces. The average surface roughness of the plywood pieces was 2.983 μm.

3.1.5 Paperboard

A4 Eco Craft brown card sheets (paperboard), 400 g were purchased and cut by Klee paper, Ireland. The paperboard sheets were cut into 100×25×4 mm pieces, with a paperboard roughness was 4.084 μm.

3.1.6 Plastic

Radionics Ireland provided ABS plastic sheet of 1,220×610×3 mm size. The tensile strength of the plastic sheet was 50 MPa. The sheet was cut into pieces 100×25×4 mm by Plastic Craft Limited using a CNC machine. The surface roughness measurement carried out of the plastic was 1.457 μm. The plastic surface was prepared using sandpaper grit 100 to increase the surface roughness, thus increase the plastic samples' potential to glued and enhance the adhesion strength.

3.1.7 Chemicals

Sigma Aldrich Ireland provided chemicals used in the study such as (n-hexane, methanol, NaOH, HCl and borax).

3.2 Design of Experiment (DOE)

DOE was introduced in the early 1920s by Sir R. Fisher to determine the effects of various fertilisers on different ranges of plots of land. DOE has been utilised in different fields such as biological, pharmaceutical and engineering, etc. [42]. The design of experiments is a statistical method that helps to identify the significant parameters and their interactions that influence a process. Mainly, DOE provides numerical, categorical, and graphical results. The latest version of DOE Design-Expert software version 12, was used in this study [44].

3.2.1 Response Surface Methodology (RSM)

A Box-Behnken design (BBD) with three numeric factors was conducted during this study. The AD studied factors were (temperature, volatile solid concentration and sludge quantity). They were designed as RSM to describe and evaluate the performance of the process and to provide the optimal combinations and results, based on ranges found from literature and pre-studied trials. RSM identifies the relationships between the resultant responses and the input variables. The levels of each factor were set as shown in Table 19. The ranges of the three factors were set based on carrying out a number of preliminary trials and in accordance to previous studies [160,

167, 183, 371-373]. The results were statistically analysed using the Design-Expert software, which determines the relationship between factors and responses using mathematical models, predicting and optimising responses. Furthermore, the software also tests the adequacy of models, the overall models, each term and the lack of fit by using statistical significance tools.

Table 19: Factor levels in coded and actual values.

Factors	Symbol	Unit	Type	Lower value	Higher value	Lower code	Higher code	Mean value
Temperature	(A)	ºC	Numeric	34	40	-1.00	1.00	37
Volatile solid	(B)	g	Numeric	1.1	4.2	-1.00	1.00	2.65
Sludge quantity	(C)	%	Numeric	25	50	-1.00	1.00	37.5

The interaction, perturbation between factors and responses and the adequacy of the process were determined by the analysis of variance (ANOVA). The statistical significance of the models developed and each term in the regression equation were also tested using the sequential lack-of-fit test and F-test. The confidence level (95%) of the model (α=0.05) was tested using the p-value.

3.3 Energy Balance

The energy balance based on mechanical processing is calculated using the following formula as shown in equation:

$$B_s = (CH_4\%) \times (9.67) \qquad \text{Equation (1)}$$

While; B_s is the energy content of biogas produced by cassava peel/date seed in [kW h/m^3], CH_4% is the average of methane percentage of each sample. The value 9.67 is a reference value and indicates the energy quantity of 1 Nm^3 of biogas [213]. The energy gained from a gram of volatile solid of feedstock from the biogas produced is calculated by the following formula:

$$E_p = B_p \times B_s \qquad \text{Equation (2)}$$

Where, E_p is the energy gained from a gram of volatile solid of feedstock from the biogas produced in [Wh/g-VS] while B_p is the biogas volume produced from each gram of volatile solid

of feedstock. The formula to calculate the electricity consumed by pre-treatment to treat a gram of volatile solid of cassava peel is:

$$E_c = E_{pt} / VS_m \quad \text{Equation (3)}$$

Where, E_c is the electricity consumed by pre-treatment to treat a gram of volatile solid of feedstock in [Wh/g-VS] and E_{pt} is the electricity consumed in the pre-treatment process that measured by a prodigit kilowatt-hour meter. The total amount of volatile solid in the machine indicated as VS_m. The net energy produced by a gram of volatile solid of treated feedstock ($\text{Net } E_p$) in [Wh/g-VS] was calculated by the formula:

$$\text{Net } E_p = E_p - E_c \quad \text{Equation (4)}$$

The energy gain percentage is the difference between the energy gained by the biogas from treated feedstock ($E_{p\text{-treated}}$) and the energy produced from the biogas from untreated feedstock ($E_{p\text{-untreated}}$). When the energy gain% is negative, it indicates that the mechanical pre-treatment of feedstock caused loss of energy compared to untreated feedstock. The energy gain% was calculated by the following formula:

$$\text{Energy balance\%} = \text{Net } E_p / E_c \quad \text{Equation (5)}$$

3.4 Experimental Procedures

The experiment procedure is divided into four stages: (1) Pre-treatment of feedstock, (2) measuring the dry solid weight of treated samples, (3) performing the AD process for cassava peel and date seed and (4) measuring and analysing the biogas released. Figure 28 shows the flowchart of accomplished and PhD experimental procedure. Table 19 shows the critical factors affecting on the AD process. The design matrix for cassava peel and date seed designed by RSM technique based on the critical factors is illustrated in Table 20 in their actual and code values.

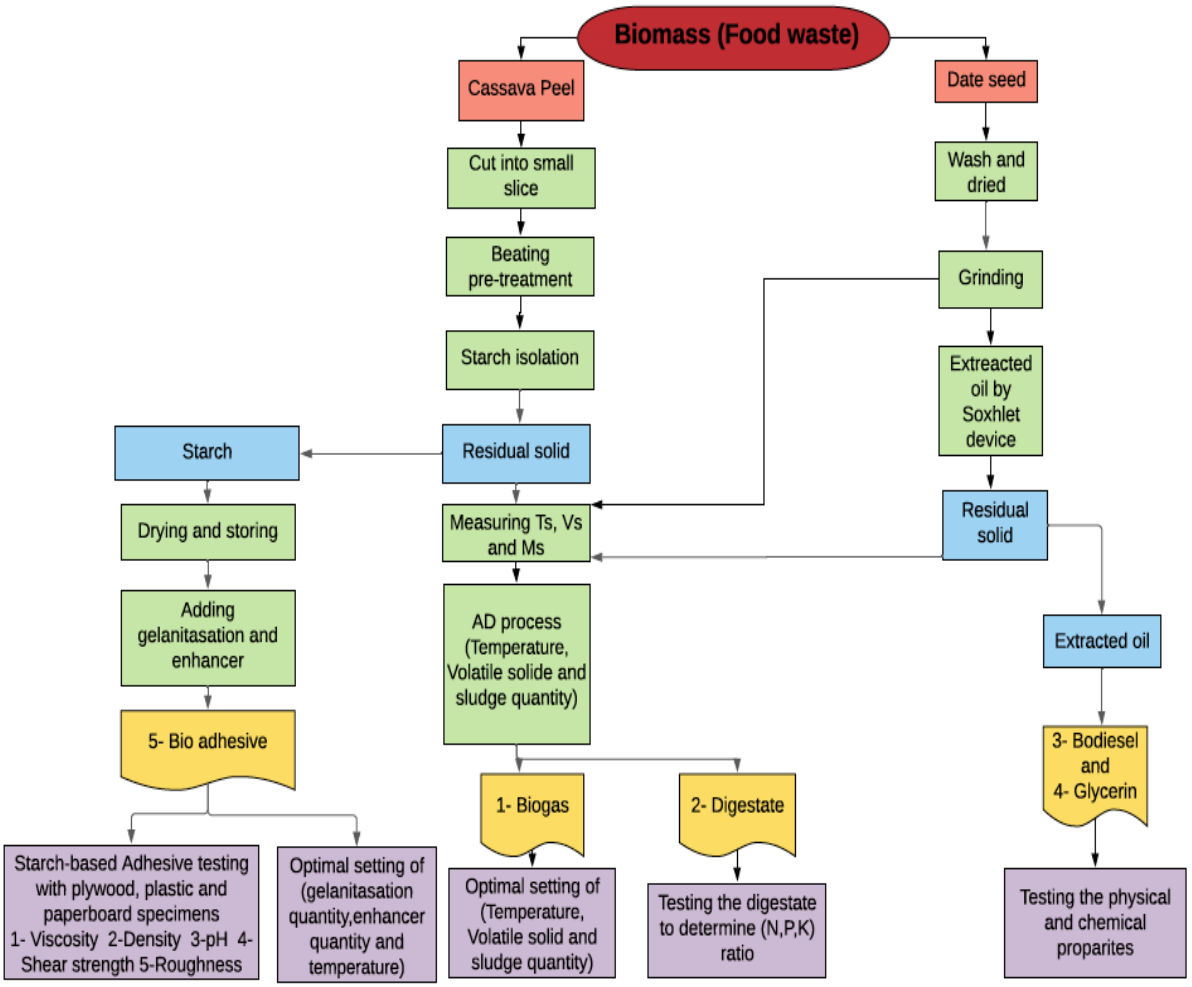

Figure 28: The experimetal procedure flowchart.

The coded models describe the factors symbolised by letters A, B and C, which are A: temperature, B: volatile solid and C: sludge quantity. While in the actual models, the factors names are used. The coefficient of the factors in the coded model illustrates the effect of each factor and the greatest effect of any factor is the one with the largest coefficient. While the coefficient sign indicates whether the effect is positive or negative. The positive sign means an upward effect and the negative sign means the opposite. The actual models can be used to predict the response at a given factor level within their range used in the study.

The perturbation plots help in determining the influence of each factor on the response of interest and compare the effects of all factors. While the effect of the interaction between factors on the responses are illustrated in associated interactions graphs. Interaction occurs when one factor

depends on another factor. This is indicated in the plots by two non-parallel lines. The contour plot is a 2-D graph that illustrates all points that have the same responses and connecting them by contour lines. All graphs are constructed from all the designed spaced values used in the study.

Table 20: Design factors matrix at their coded and actual values.

Std.	Factor 1	Factor 2	Factor 3	Factor 1	Factor 2	Factor 3
	A	B	C	A	B	C
	°C	g-VS	%	°C	g-VS	%
	Code value			Actual value		
1	-1	-1	0	34	1.10	37.5
2	1	-1	0	40	1.10	37.5
3	-1	1	0	34	4.20	37.5
4	1	1	0	40	4.20	37.5
5	-1	0	-1	34	2.65	25.0
6	1	0	-1	40	2.65	25.0
7	-1	0	1	34	2.65	50.0
8	1	0	1	40	2.65	50.0
9	0	-1	-1	37	1.10	25.0
10	0	1	-1	37	4.20	25.0
11	0	-1	1	37	1.10	50.0
12	0	1	1	37	4.20	50.0
13	0	0	0	37	2.65	37.5
14	0	0	0	37	2.65	37.5
15	0	0	0	37	2.65	37.5
16	0	0	0	37	2.65	37.5
17	0	0	0	37	2.65	37.5

3.4.1 Pre-treatment of Cassava Peel

Beating pre-treatment was employed in the study using a Hollander beater device (see Appendix A). A volume of 2.22 kg of cassava peel with 20L of water with ratio 1:9 [371-373] was placed into the beater for 5 minutes. This was done to slice the cassava peel into small slices and isolate the starch from the peel. Beating pre-treatment was applied immediately after slicing the

feedstock by high-pressure beating against inclined blades. The mixture was discharged into a large container through a sieve to isolate the cassava peel from the mixture. It was left for 3-4 hours for the starch to settle down in the container [374]. The water at the top was decanted off and added to the pre-treated peel.

A) Total Solids and Volatile Solids

The TS and volatile solids were measured and adjusted as designed in the experiment matrix according to the standard methods (NREL/MRI LAP 1994, 2008) [375]. Three samples were taken directly from the beater (prior to starch separation). Three other samples were also taken after starch isolation to measure the TS and volatile solid. The samples were dried in a drying oven at 105 °C for 24 hours to calculate the moisture content (MS) and the TS. Thereafter, the samples were burned at 575 °C for 4 hours to calculate the ash weight and thus the volatile solid amounts. According to previous studies [371-373], the preliminary trials which were conducted to set the ranges of the volatile solid added, (1.1-4.2 g-VS were found to be ideal). The preliminary trials revealed that the volatile solid higher than 4.2 could lead to a system failure, while lower values of volatile solid led to a starving condition [376].

3.4.2 Grinding Pre-treatment of Date Seed

A kilogram of the date seed was prepared and washed with water to remove impurities and flesh. It was left for three days in the air to dry. The date seeds were then ground by using a grains and stones grinding machine which is ground them efficiently in ideal sizes. The grinding process was performed without any additional process to soften the seeds such as heating or hammed to ensure that the seeds are not affected (losing weight) [303] by any external factors as well as to reducing the operational costs. The grinding process resulted in a powdered date with a practicle range of 800-355 μm, post sieving, as shown in Figure 29.

Figure 29: Date seed Powder with particle size 800-355 µm.

A) Total Solid and Volatile Solids

According to standard methods (NREL/MRI LAP 1994, 2008), the TS and volatile solid were measured and adjusted as designed in the experiment matrix [375]. The volatile solid value of the grounded date seeds was calculated by taking three samples and placing them in the oven at 105 °C. The MS and the TS of all the samples were calculated then they were burned in the oven at 575 °C for 4 hours. Thereafter, the volatile solid was determined based on the resulting ash weight. Consequently, based on the previous studies [167, 181, 183] and the preliminary experiments, found that the optimal value of the volatile solid lies between 1.1 and 4.2 g-VS.

3.4.3 Extraction of Oil from Date Seed

The Sagai date seeds were brought from Saudi Arabia. About 2 kilograms of date seeds were prepared and washed with water to remove the date flesh and impurities. It was then left in air for 72 hours to dry. The date seeds were ground by a grinding machine without subjecting them to any softening or prior preparation processes to reduce preparation costs. The oil extraction process for the production of biodiesel and glycerine was carried out using the Soxhlet device, according to the AOCS official method Am 2-93 [377]. Each time 20 g of date seed powder was placed in a paper thimble and covered with a piece of cotton to prevent the feedstock from leaking into the extraction device. The n-hexane organic solvent was used for the extraction

process at a ratio of 1:4 (seed/n-hexane). The mixture was left to react at 70 °C for 5 hours under reflux and continuous stirring. The n-hexane solvent was separated from the oil by a rotary evaporator. To produce biodiesel and glycerine, Amani (2013) [292] method was followed. The date seed oil was heated at 60 °C, then methanol was added to the oil at a ratio of 1:5 (methanol to oil) and approximately 0.4 g of sodium hydroxide. The components were left to react for 2 hours under constant stirring and reflux. After producing the biodiesel and glycerine, the alcohol was extracted from the mixture using a rotary evaporator. Biodiesel and glycerine were placed in a separating funnel to separate them from each other due to their differences in densities. The impurities and remaining glycerine were removed from biodiesel using hot water and then dried in a rotary evaporator [292, 293].

(A) Total Solids and Volatile Solids

Three samples were taken and placed in the oven at a temperature of 105 °C to calculate the TS value of the date seed powder according to standard methods (NREL/MRI LAP 1994, 2008) [375]. The moisture content and the TS were calculated as shown in Table 21. The samples were placed in an oven at 575 °C for burning. The weight of the resulting ash was measured and accordingly the volatile solid value was calculated as shown in the same table. It was noticed that each gram of date seed powder would give 0.867 g-VS. It was found from previous studies, that the optimal value of the volatile solid was between 1.1 and. 4.2 g-VS [160, 167, 183]. Accordingly, the volatile solid was measured and adjusted [375] as designed in the experiment matrix as follows: 4.85 g of date seed powder to yield 4.2 g-VS. As well, 3.06 g of date seed powder gave 2.65 g-VS, and 1.27 g of the date seed powder provided 1.1 g-VS. Date seed powders were placed in a 500 ml flask and sludge was added to the flask at different quantities (25%, 37.5% and 50%) from the total of 400 ml. Water was added to the mixture in a variable ratio to raise the flask to 400 ml.

Table 21: Date seed powder sample specifications

Sample specifications	Unit	Value
Wet weight	g	1
Moisture content	%	13
Total solid	%	87
Ash weight	%	1.53
Volatile solid	g	0.867

3.4.4 Anaerobic Digestion of Cassava Peel

Water was added to each container at a different ratio to adjust the value of volatile solids added in each container. The ratio of water to cassava peel was 9:1,18:1 and 27:1, respectively. The volatile solid added value of each container was 4.2, 2.65 and 1.1 g-VS. The 500 ml glass flask was filled by cassava peel and inoculum at different values 25, 37.5 and 50%. Factor levels in coded and actual values are shown in Table 19.

The sludge quantity varied in each flask (50%, 37.5% and 25%) of the total volume of the flask (400 ml) (Appendix A). The remainder of the 400 ml was filled with pre-treated cassava peel after were mixed well to ensure that the solids were not deposited at the bottom of the container. The samples that contained starch were used as controls. The same procedure was followed with the controls (samples that were not extracted starch). In order to allow comparison with the predicted values at the same conditions, the controls were digested at the volatile solid of 4 g-VS, sludge quantity of 50% and at each of three temperature levels. However, the ratio of water to cassava peel varied due to the presence of starch. The ratio of water to cassava peel in the control samples were 5.75:1, 9.7:1 and 23:1 respectively. Each sample was connected to an aluminium gas-bag (Appendix A), the nitrogen was pumped into the system and pulled out twice to ensure that the system was free of O_2. Each sample was carried out in triplicate. The control samples conditions are shown in Table 22.

Table 22: Control sample conditions.

Sample No.	Factor 1	Factor 2	Factor 3
	A: Temperature	B: volatile solid	C: Sludge quantity
	°C	%	%
1	34	4.0	50
2	37	4.0	50
3	40	4.0	50

Samples were placed in water baths at mesophilic operation temperatures that were set based on previous studies and pilot tests (34°C, 37°C and 40°C).The incubation time was 21 days. The flasks were shaken on a daily basis throughout the period of the experiment. The biogas produced from each sample was measured twice (on day 9 and day 21). The biogas volume was

measured using volumetric flask (Appendix A). It uses gas-sampling tubes that were installed in a gas jar with confining tab water. A biogas analyser (biogas5000 Geo-tech) (Appendix A) was used to measure the concentration of the gases: CH_4, CO_2, O_2, and H_2S. The pH of the digestate resulted from each sample was measured by a Hanna Precision pH meter (accuracy ± 0.01), model pH 213 (Appendix A) and examined to confirm the suitability of applying it in agricultural settings. Figure 30 illustrates the flow chart of the experimental work of the study.

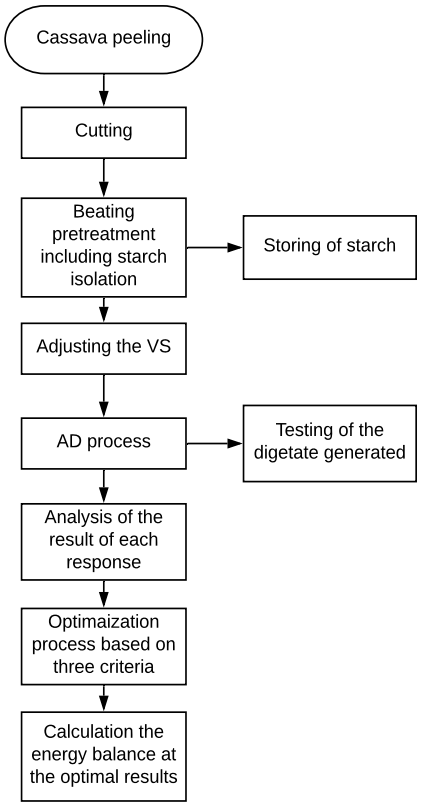

Figure 30: The flowchart of the AD of cassava peel experiment.

3.4.5 Anaerobic Digestion of Date Seed

For each reactor a specific amount of date seed powder, which would give the required amount of volatile solid was placed in a 500 ml flask (Appendix A). This was performed according to Table 19. Sludge was added to the mixture with different percentages (25%, 37.5% and 50%) from the total sample size of 400 ml. Then, completing the volume to 400 ml by adding water. The flasks were connected to aluminium gasbags (Appendix A) to form the reactor. Then the O_2 was withdrawn from the reactor by flushing nitrogen gas into it. A vacuum pump (Appendix A) was used to pump out the gases from the reactor. This process was repeated twice to ensure that

the reactor is nearly free of O_2. Reactors were placed in three water baths with three different temperatures. Each sample was replicated three times. The incubation period was set to 21-days. The reactors were shaken on a daily basis. The produced biogas volume was measured using a volumetric cylinder (Appendix A). It uses gas-sampling tubes that were installed in a gas jar with confining liquid. The biogas was measured twice during the experiment period (in day 9 and at the end of the incubation period). Figure 31 shows the flowchart of performing the AD experiment of date seeds.

The biogas analyser (Appendix A) model biogas5000 Geo-tech was used again to measure percentages of the biogases produced (mainly: CH_4, CO_2, O_2 and others gases). The pH of each reactor was measured at the end of the period using Hanna Precision pH meter (Appendix A). In addition, the residue of the process was tested to determine its validity to be used as an organic fertiliser. This test was carried out at Advance Laboratory Testing Ltd, Newbridge, Ireland.

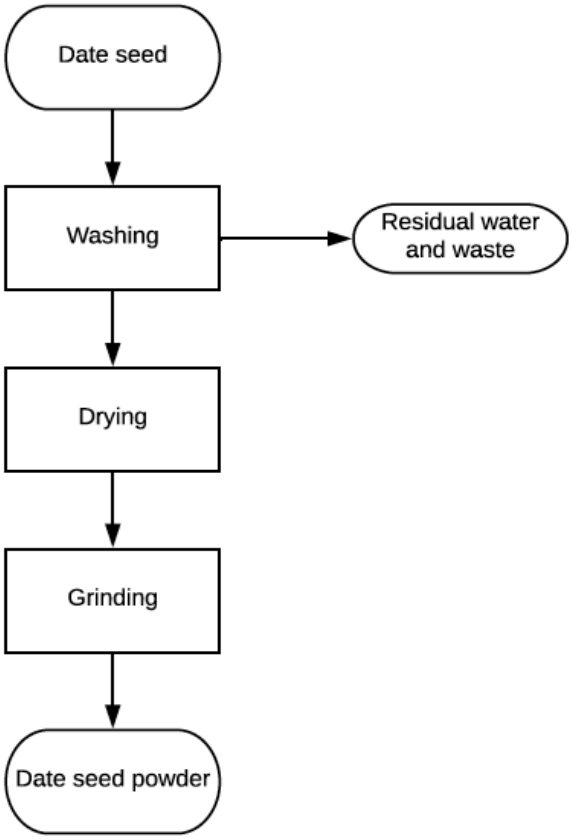

Figure 31: Flowchart of performing the AD of date seed experiment.

3.4.6 Anaerobic Digestion of Extracted Oil Date Seed

A specific amount of extracted oil date seed powder (as mentioned in section 3.4.3 part (A)) was placed in a 500 ml flask to give the required amount of volatile solid added. Sludge was added in different proportions (25%, 37% and 50%) as shown in the experiment matrix Table 21. With the further adding of water to the mixture to raise the mixture to 400 ml of the flask. The reactor was formed by connecting the flask to an aluminium gasbag. The oxygen was withdrawn from the reactors by pumping Nitrogen to the reactor and withdrawal using a vacuum pump. This process repeated twice to ensure that the reactor was free of oxygen. The reactors were placed in three water baths at specified temperatures that were determined from previous studies and preliminary experiments (34 °C, 37 °C and 40 °C) as illustrated in Table 20. Each sample was repeated three times. The retention time for the experiment was 21 days and the reactors were shaken daily. The resulted biogas was measured using a volumetric cylinder twice during the experiment on day nine and day twenty-one. The proportions of the gases that form the biogases: methane (CH_4), carbon dioxide (CO_2), hydrogen sulphide (H_2S) and oxygen (O_2) were measured by using a Biogas analyser model Biogas5000 Geo-Tech. The pH was measured for all samples at the end of the experiment using a Hanna Precision pH meter (accuracy ± 0.01), model pH 213. The resulting digestate from the AD process was tested to investigate the effect of oil extraction on the N, P and K components. The tests were carried out at Advance Laboratory Testing Ltd., Newbridge, Ireland.

3.4.7 Biogas Measurement

The resulting biogas was measured twice during the experiment on day 9 and day 21 at room temperature. Due to that some bags are almost full on the eighth/ninth day. The volumetric flask was filled with a specific amount of tap water for comparison. An inverted cylinder of 250 ml was placed in the volumetric flask and the biogas is pumped into it. The water level increased to reach a new level. The difference between the two levels represented the volume of the biogas produced.

3.4.8 Soxhlet Extraction Methods

Franz von Soxhlet designed the Soxhlet extractor in 1879. It consists of a round bottom flask, siphon tube, adapter, condenser, cooling water inlet and outlet, thimble and heat source. The substrate powder is placed in the strong fibre porous thimble and placed inside the extractor. The

solvent is placed in the bottom round flask with specific ratio to the powder and heated at a certain temperature using the heating source. The solvent evaporated by heat to the condenser, then returned to the extractor until it reaches the siphon arm. The content is emptied into the round bottom flask again loaded with the extracted oil. This process is repeated for a specified period of time to extract the optimum percentage of crude oil [378]. Figure 32 shows the Soxhlet extractor device [379]. The oil extracted from the solvent by rotary evaporator [295]. Methanol is often used in the transesterification process because of its lower cost compared to other catalysts [303]. Methanol and sodium hydroxide are added to the extracted oil and heated at a certain temperature to produce biodiesel and glycerin. The alcohol isolated by rotary evaporator. Biodiesel is isolated from glycerin by separating funnel [295].

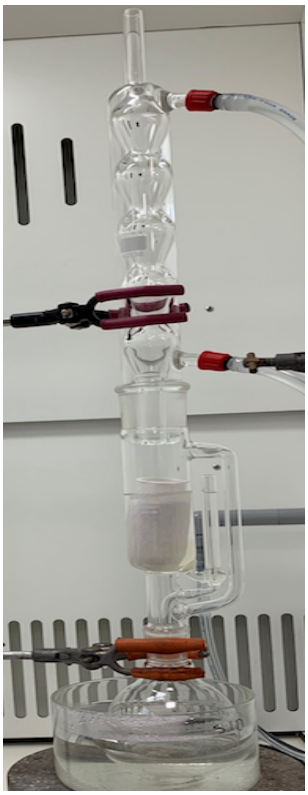

Figure 32: The Soxhlet extractor.

3.5 Substrate Preparation for the Adhesion Process

Table 23 shows the studied factors in the adhesive production process and their values. Different amounts (40, 45 and 50 ml) of two type of gelatinisation NaOH or HCl (base or acid) were added to a fixed amount of starch (1.5 g) in a glass beaker. The mixture was stirred continuously at the target temperatures (65, 75 and 85 °C). When the mixture became sticky, borax (0.1, 0.2 and 0.3

g) was added to the mixture during constant stirring. The adhesive material was left to cool, and then it was used in adhering the specimens. 0.15-0.2 mg/mm^2 of the adhesive was put on to each sample surface. The samples were prepared according to ASTM D 907, ASTM D 3163 and the method used by Wu et al. (2020) [261, 380, 381]. Each sample was cut to 100 × 25 × 4 mm with a bonding area of 25 ×25 mm^2. The samples were clamped with a force of 1.15 N at room temperature and left to dry. The adhesive viscosity was measured in line with the method used by Mahrdt et al. (2016) [382] using a rheology international viscometer (cone and plate measuring geometry) with a cone diameter of 30 mm, fixed lower plate 50 mm at 18 °C, where the gap between cone and plate was 0.1 mm and measured at 10 r.p.m. The adhesive density was measured using a density kit at 18 °C according to ASTM D792-20 standard [383]. The pH of all samples was measured at 18 °C by a Hanna Precision pH meter. The shear strength of all of the samples were measured on the next day of adhering at 60% humidity using a Zwick Roell machine at 1.3 mm/min. Figures 33 illustrates prepared samples for adhesion.

Table 23: Actual factors values.

Factors and codes	Unit	Lower level	Centre point	Upper level
Gelatinisation, (A)	ml	40	45	50
Borax, (B)	g	0.1	0.2	0.3
Temperature, (C)	°C	65	75	85

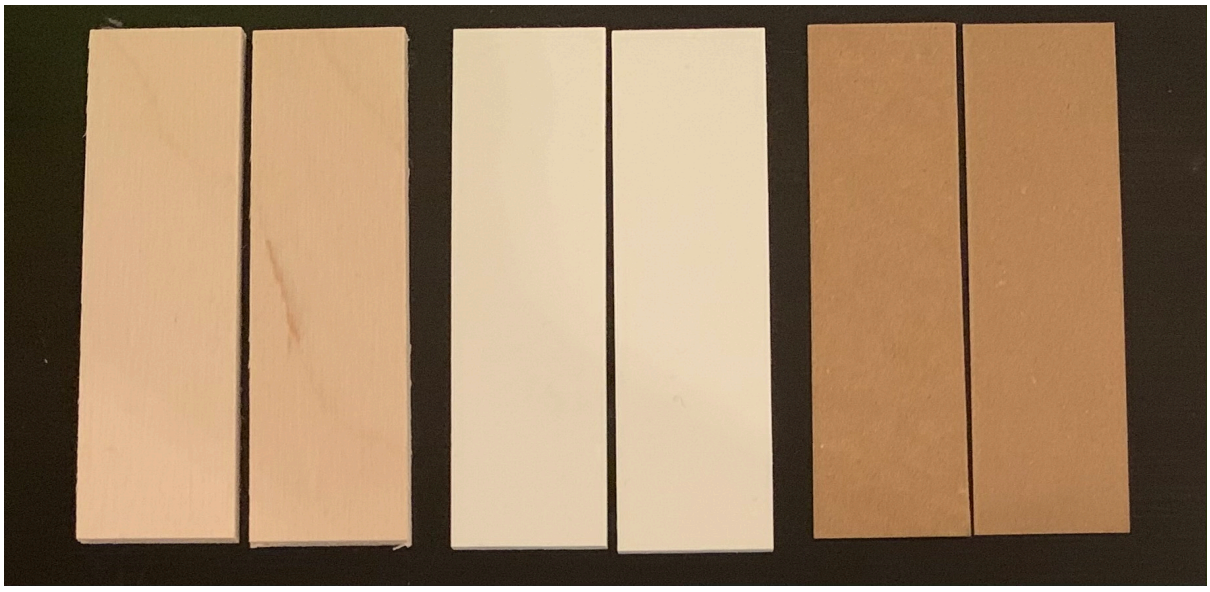

(a) (b) (c)

Figure 33: (a) Plywood, (b) Plastic and (c) Paperboard prepared samples.

3.6 Additional Equipment and Devices

Several devices and equipment were used during this study. Some were used in the preparation and pre-treatment process and some were used to calculate the total solid, volatile solid and moisture content. Other equipment and devices were used during AD and biogas measurement. Such equipment and devices are presented in Appendix A. The equipment used in preparing and producing biodiesel, glycerine and adhesive material also described in Appendix A.

Chapter 4

4 RESULTS AND DISCUSSION

4.1 Introduction

Chapter 4 is divided into ten main sections as shown in Figure 34. Sections 2-7 discusses the general results achieved from the AD experiments of cassava peel, date seed and extracted oil date seed then each experiment will be detailed separately. The results of the AD of date seeds before and after oil extraction will be compared in this section in addition to the digestates resulting from all AD processes. The remaining sections are concerned about the production of biodiesel, glycerine and adhesive material. The last section of this chapter is the results summary.

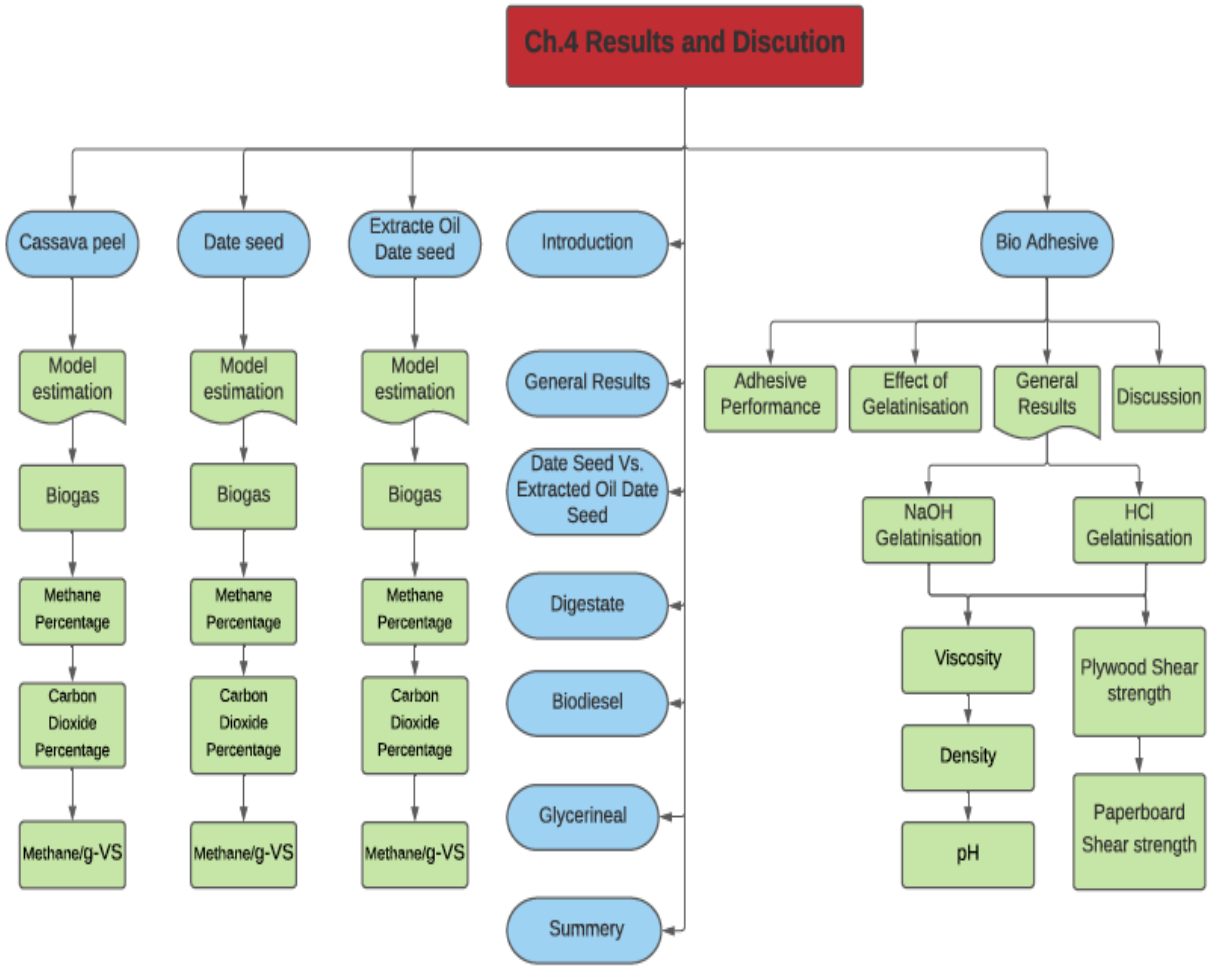

Figure 34: Results structure flowchart.

4.2 General Results of AD processes

The p-value of all models throughout this chapter indicated the significane of models (P-values of overall model were less than α where (α=0.05). The impact of each factor, the interaction between factors and the checked probability ("p-value") of them are described in the ANOVA tables. These tables illustrate significant model terms. The tables also show that all models were adequate as all values of R^2, predicted R^2 and adjusted R^2 were close to 1. For all models the Predicted R^2 was in reasonable agreement with the Adjusted R^2 as the difference between them was less than 0.2. When the Adjusted R^2 and Predicted R^2 values are lower than 1, this does not affect the significance of the model as long as the difference between them is less than 0.2. The model graphs aid in illustrating the behaviour of each response as the factors vary. In Figures 35 to 40 (probability graphs) all of the points were close to the distribution line, this indicates that the distribution was normal and that the adaptation of the model was adequate, which shows the normal probability and predicted volatile solid actual residual values. As the majority of the points did not deviate from the line, the agreement between the actual and predicted response was excellent.

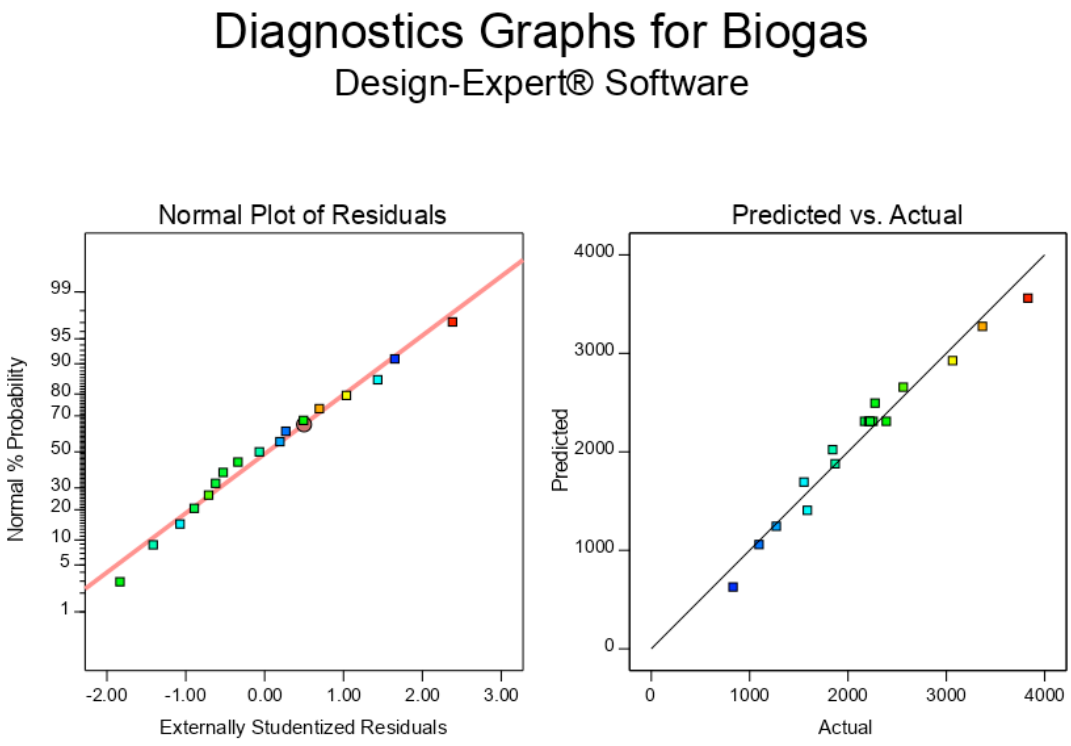

Figure 35: Normal probability and predicted versus actual residuals plot of Biogas produced from cassava peel.

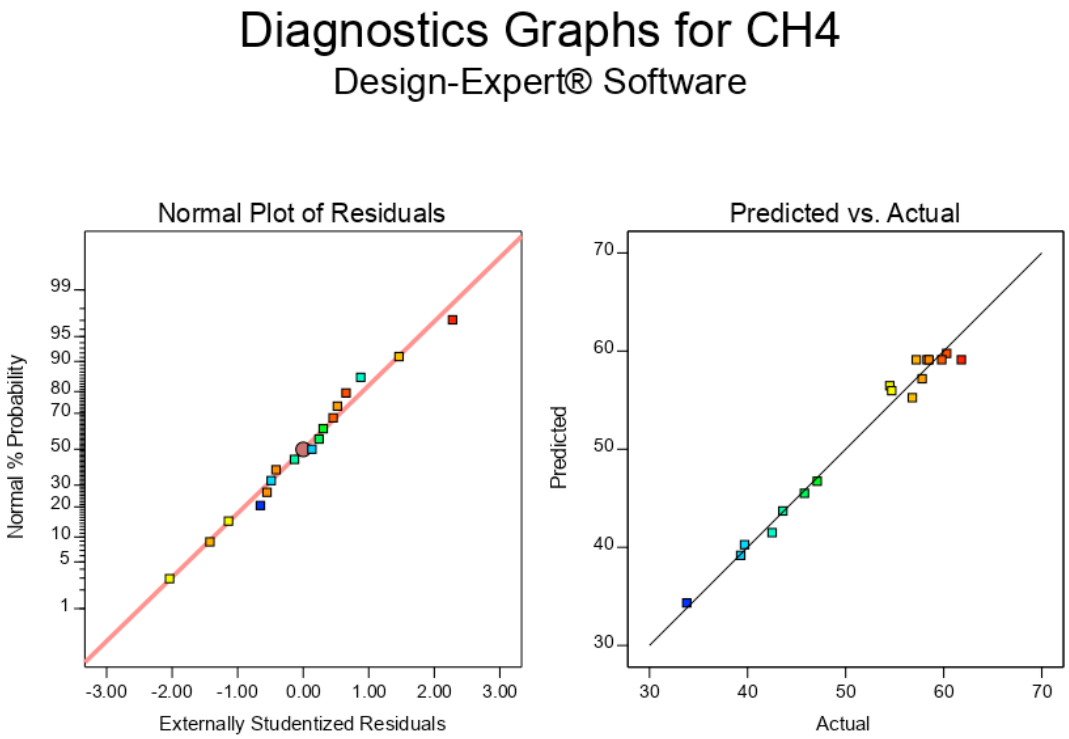

Figure 36: Normal probability and predicted versus actual residuals plot of CH_4% produced from cassava peel.

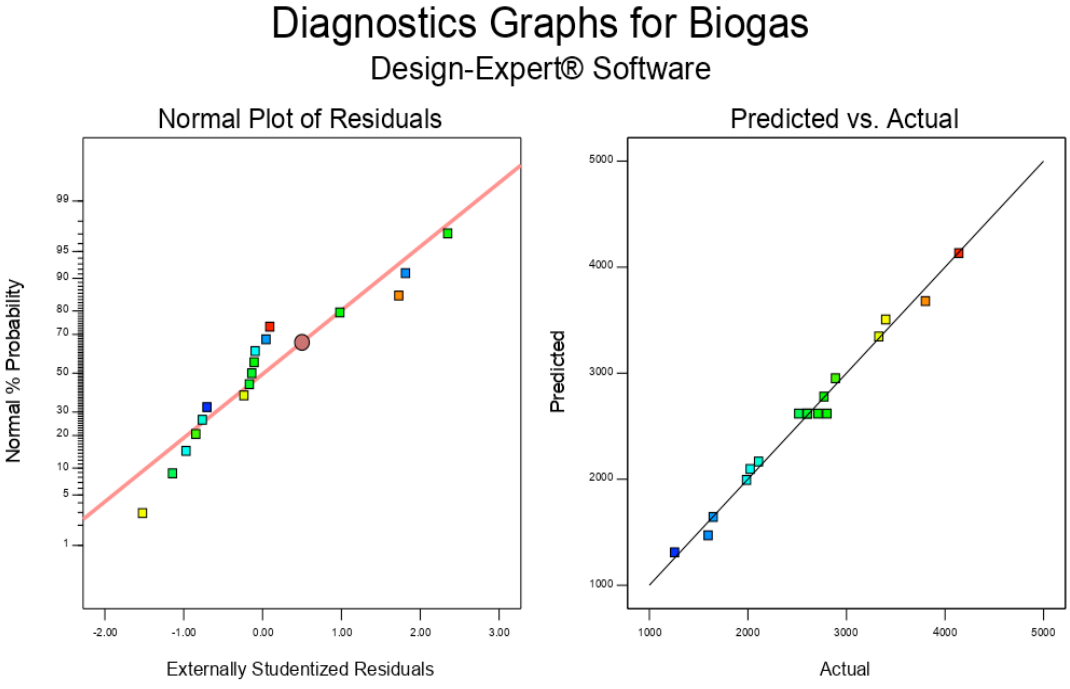

Figure 37: Normal probability and predicted versus actual residuals plot of Biogas produced from date seed.

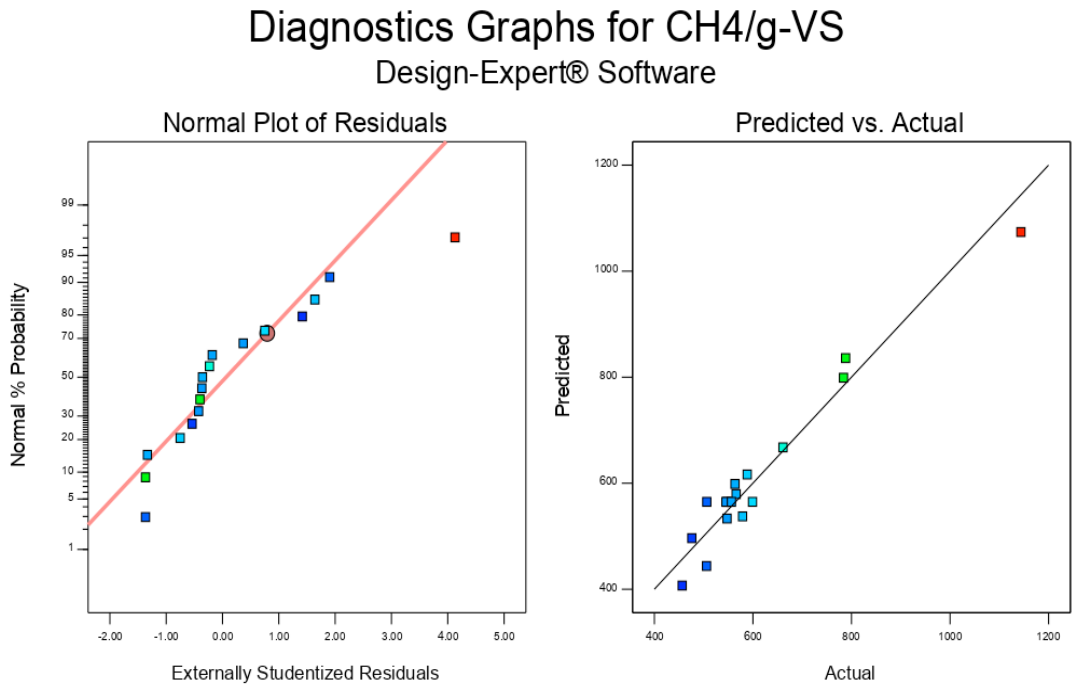

Figure 38: Normal probability and predicted versus actual residuals plot of CH_4/g-VS produced from date seed.

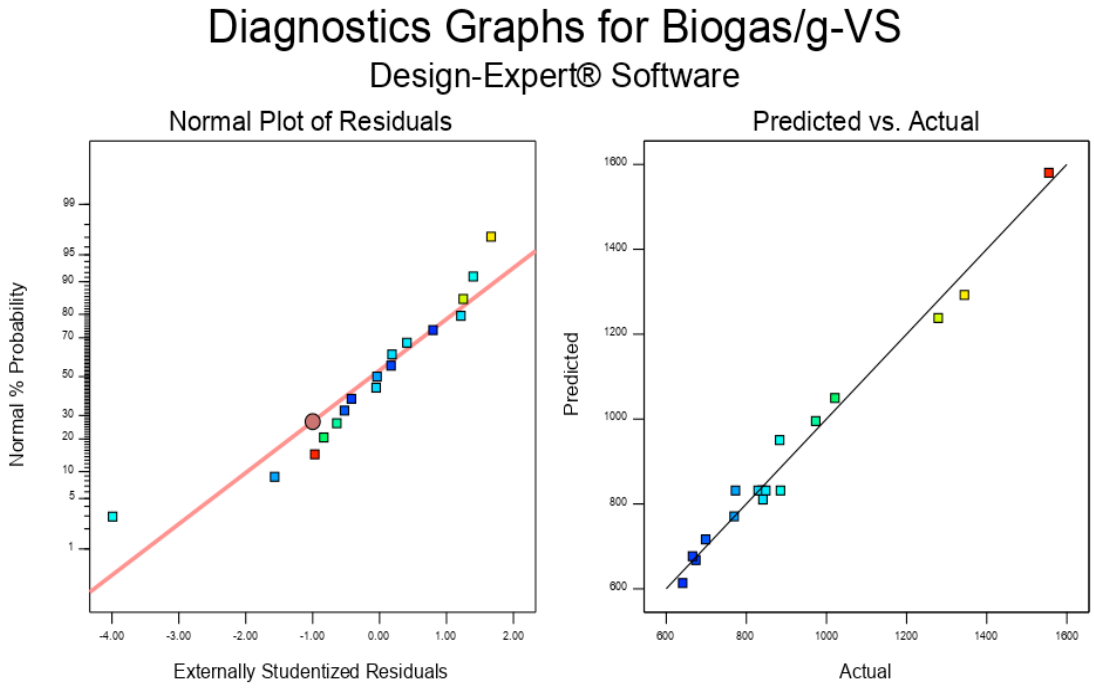

Figure 39: Normal probability and predicted VS actual residuals plot of biogas/g-VS produced from extracted oil date seed.

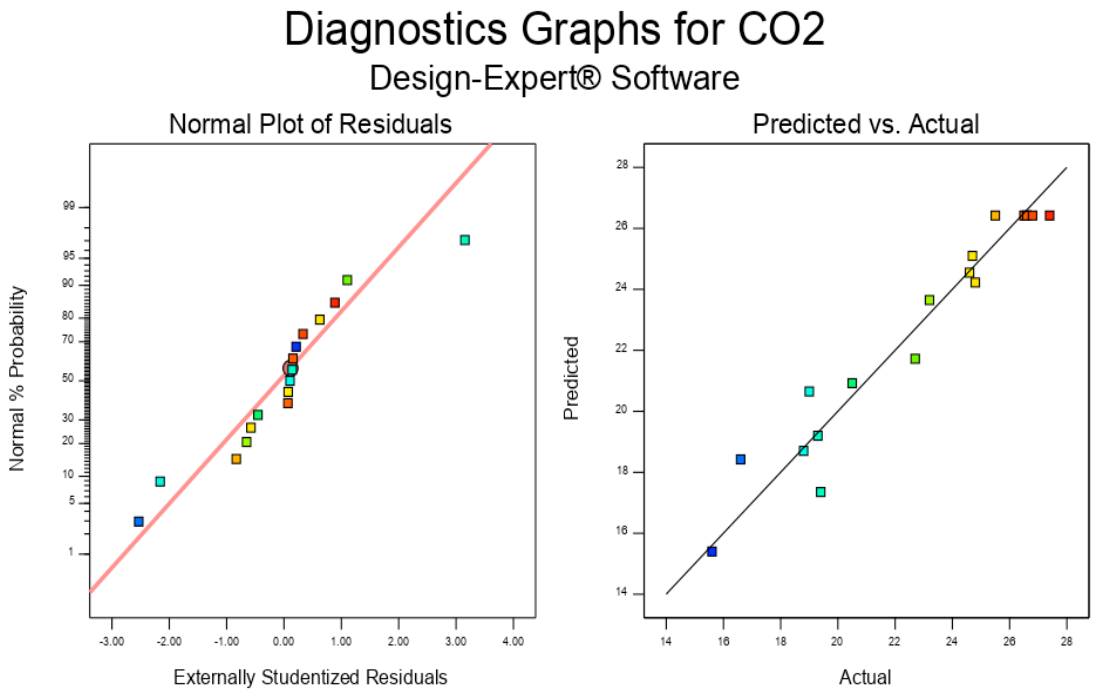

Figure 40: Normal probability and predicted VS actual residuals plot of CO_2% produced from extracted oil date seed.

4.3 Cassava Peel Results

The cassava peel constitutes approximately 20-25% of cassava weight which corresponds to what is mentioned in the study of Eziekiel and Aworh [135]. According to a study in 2018, 5% of the cassava weight is peel [384], this percentage can be raised to 20% by using one of the efficient peeling methods (mechanical, chemical and manual) [384-386]. In contrast, the current study found that, starch represented between 17-20% of the cassava peel. This is less than half of what Sivamani et al. mentioned in (2018) [136]. Table 24 illustrates the Biogas and CH_4% from the sludge.

Table 24: Biogas, CH_4% and methane resulted from sludge only.

Temperature (°C)	Biogas (ml)	CH_4 (%)	CH_4 (ml)
34	997	53.9	537
37	813	52.3	425
40	721	52.9	382

Furthermore, the experimental works of the study revealed that the effect of starch on the quantity of the biogas produced from the AD of cassava peel was relatively low, which ranged between 1.4% and 3.4%. While, the difference between methane percentages did not exceed

0.66%. Tables 25 and 26 show the results of all experiment responses and the comparison between actual and predicted values of the control samples.

Table 25: The experiment responses results for cassava peel.

Std.	Run	Factor 1	Factor 2	Factor 3	Resp. 1	Resp. 2	Resp. 3	Resp. 4	Resp. 5
		A*	B*	C*	Biogas	Biogas/g-VS	CH_4	CO_2	CH_4/g-VS
		°C	g-VS	%	ml	ml/g-VS	%	%	ml/g-VS
1	14	34	1.10	37.5	831	755.4	56.8	19.6	428.8
2	7	40	1.10	37.5	1587	1442.5	54.5	21.0	786.7
3	1	34	4.20	37.5	2275	541.7	39.7	36.1	214.9
4	5	40	4.20	37.5	3367	801.6	42.5	33.7	340.9
5	9	34	2.65	25.0	1271	479.7	45.8	29.2	219.8
6	4	40	2.65	25.0	1844	695.8	47.1	28.3	327.7
7	17	34	2.65	50.0	1870	705.7	54.7	22.5	386.3
8	16	40	2.65	50.0	2562	966.9	57.8	20.4	559.2
9	6	37	1.10	25.0	1096	996.0	43.6	32.0	434.2
10	3	37	4.20	25.0	3064	729.5	33.8	37.8	246.6
11	11	37	1.10	50.0	1552	1411.0	60.3	15.9	850.8
12	12	37	4.20	50.0	3830	911.9	39.3	35.7	358.7
13	8	37	2.65	37.5	2390	928.2	58.3	23.4	540.8
14	2	37	2.65	37.5	2169	818.6	59.8	22.9	489.8
15	10	37	2.65	37.5	2210	833.8	61.8	22.7	515.0
16	13	37	2.65	37.5	2255	851.0	58.5	24.6	497.5
17	15	37	2.65	37.5	2225	839.5	57.2	22.5	480.4

* *A= Temperature, B= Volatile solid, C= Sludge quantity.*

Table 26: Comparison between actual and predicted values of control samples (before starch extraction).

Resp.	Control samples					Predicted value				
	Biogas	Biogas /g-VS	CH_4	CO_2	CH_4 /g-VS	Biogas	Biogas /g-VS	CH_4	CO_2	CH_4 /g-VS
T (°C)	ml	ml/g-VS	%	%	ml/g-VS	ml	ml/g-VS	%	%	ml/g-VS
34	2766.1	691.5	40.5	35.0	280.1	2727.7	667.3	40.2	35.2	243.0
37	3558.7	889.7	42.9	33.3	381.4	3479.2	882.8	42.7	33.9	365.2
40	3630.5	907.6	41.7	32.3	378.8	3505.9	837.3	41.5	32.6	333.2

The highest biogas amount achieved was 3,830 ml at 37 °C, 4.2 g-VS and 50% sludge. At the same (run #12), the concentration of the CH_4 and CO_2 were 39.3% and 35.7% respectively. On the other hand, the lowest amount of biogas produced was 831 ml at the lowest temperature, lowest volatile solid added value, and 37.5% of sludge. While, the CH_4 concentration resulted from this (run #14) was 56.8% and 19.6% of CO_2. The highest percentage of the biogas yield per g-VS (run #7) was 1,442.5 ml/g-VS that achieved at 40 °C, 1.1 g-VS and 37.5% of sludge. In addition, the lowest volume of the biogas/g-VS achieved (run #9) was 479.7 ml/g-VS at 34 °C, 2.65 g-VS and 25% of sludge, from run #9.

Figure 41 shows the effect of adding cassava peel to the sludge, on biogas production compared to biogas produced from sludge only. The figure shows that cassava peel addition significantly increased the amount of biogas in all samples except for the sample #1, which was at the lowest temperature and volatile solid added values. This may be due to the bacteria being starved and inactivated due to the low temperature of the reaction. At 37 °C, the highest biogas quantity was achieved for the sludge/cassava compared to the sludge only (sample #12), the biogas volume rose by more than four times from approximately 813 ml to 3,830 ml.

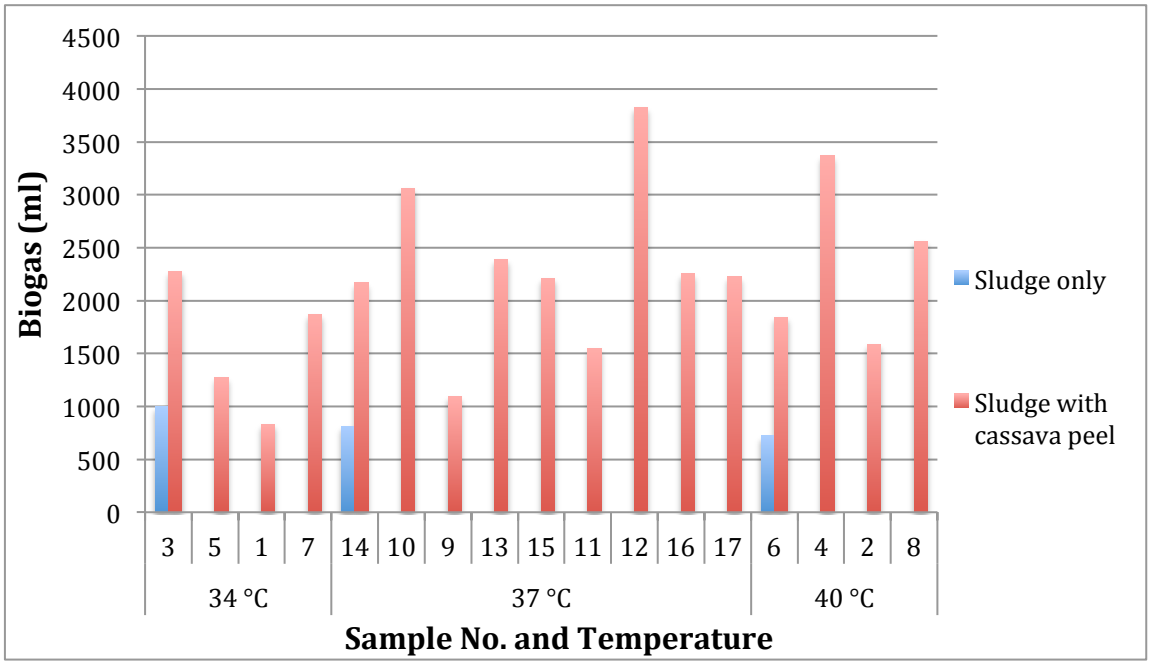

Figure 41: The amount of biogas produced from sludge before and after adding cassava peels.

Moreover, there was an inversely relationship between the percentage of the CH_4 resulted and CO_2. From Table 25, the CH_4 percentages ranged from 33.8% to 61.8%. The lowest percentage of CH_4 and the largest CO_2 were found for run #3 of 37 °C, 4.2 g-VS and 25% sludge. While the highest CH_4% (run #10) was 61.8% at 37°C, 2.65 g-VS and 37.5% of sludge. While, based on table 25 it is the case the highest CH_4/g-VS produced was 850.8 ml/g-VS at 37 °C, 1.1 g-VS and 50% sludge (run #11). In contrast, at 34 °C, 4.2 g-VS and 37.5% sludge, the CH_4/g-VS was 214.9 ml/g-VS which was the lowest yield (run #1). The pH value ranged between 7.7 and 8 for all samples.

Figures 42-43 show the effect of adding cassava peel on the resulting biogas quality in terms of the methane percentage and methane volume. The graph shows the varying effect of temperature on the CH_4% and methane. Figure 42 shows an increase in CH_4% to 61.8% (sample #15) compared to about 53% from the sludge only. The methane produced (Figure 43) after adding the cassava peel increased dramatically for the majority of samples. It rose from approximately 425 ml to about 1,505 ml (sample #12) at 37 °C and from 381 ml to 1,393 ml at 40 °C (sample #8). The methane in both cases increased by more than 3 times.

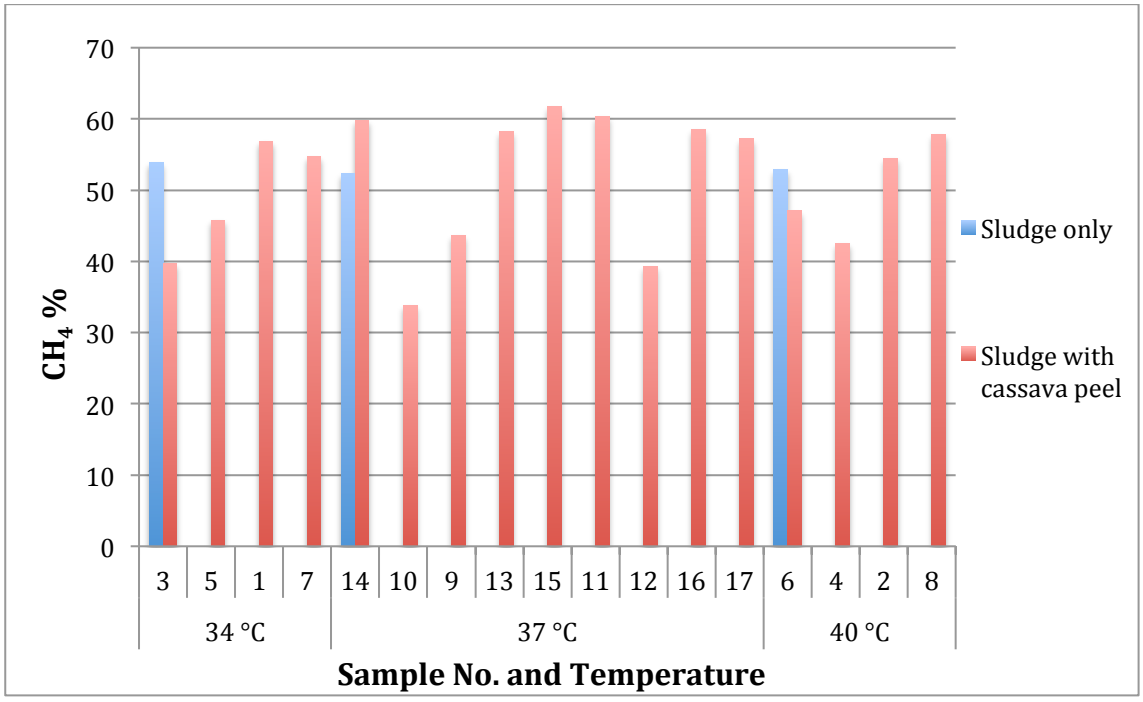

Figure 42: The effect of adding cassava peel on CH_4%.

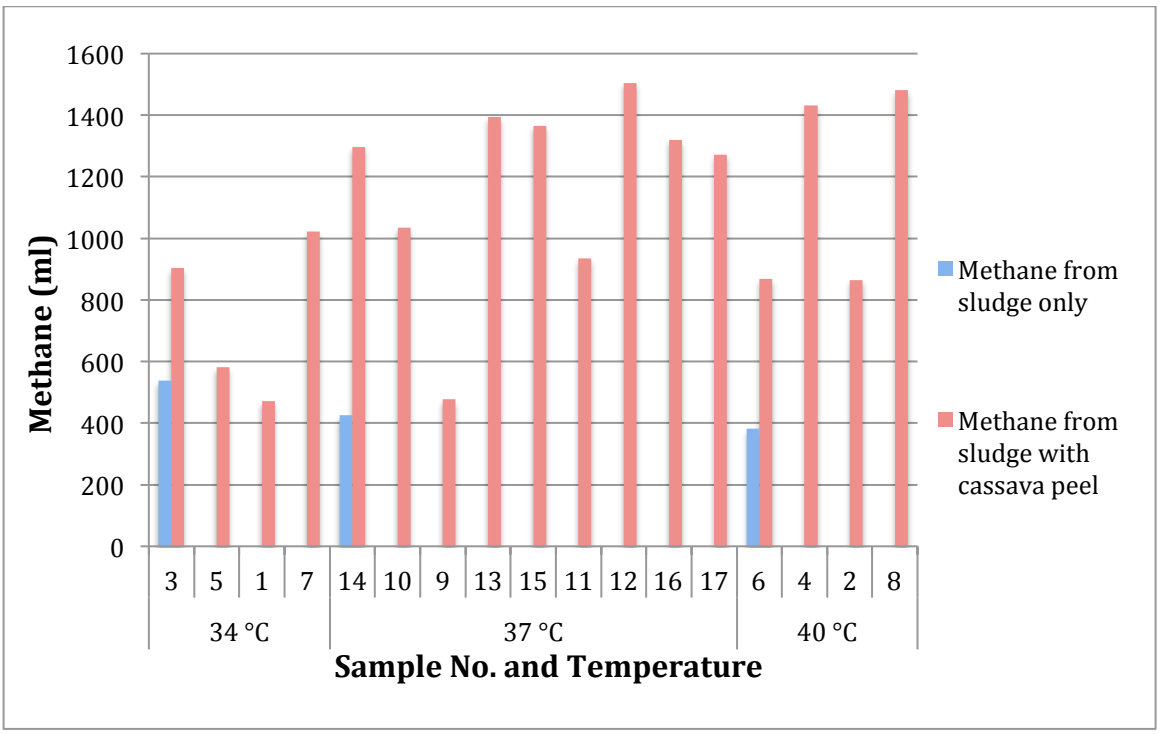

Figure 43: The effect of adding cassava peel on methane volume

Additionally, the actual and predicted values for the control samples are illustrated in Table 26. It highlights the difference between the percentages of biogas/g-VS; the biggest difference was 7.7% at 40 °C. The maximum reduction in the CO_2 amount was -1.8% at 37 °C. The difference between CH_4/g-VS values was the highest, as it reached 13.2% at 34 °C and 12.0% at 40 °C while it was 4.2% at 37 °C.

The highest biogas yield from a study on the production of biogas from cassava peel with urea under mesophilic condition was 80.79 ml/g-TS added. The cassava peel was treated by soaking it in water for 7 days. The study concluded that the 0.01 of urea with cassava peel increased the biogas volume by 24.33% [141]. Jekayinfa and Scholz [142] found that, the highest biogas volume and methane content volume produced from cassava peel were 660 ml/g-VS added and 280 ml/g-VS added respectively at 35 °C. Compared to the previous studies, the results of the proposed study showed an increase in the volume of biogas produced. This increase confirms the potential benefit of subjecting cassava peel with beating pre-treatment. The study also revealed that, there was no obvious impact of the isolated starch on the quantity and quality of the biogas produced.

Comparing the volume of produced biogas from the control samples at 34 °C with the studies described above, a significant increase in the volume of biogas reached more than 4.5%. This could potentially be an illustration of the positive effect of beating pre-treatment on cassava peel. While the ratio decreased to 1.1 % when compared with other samples (Starch-free samples), which confirms the limited effect of starch on the resulted biogas. The use of starch in producing more bio-products such as bio-plastic and bio adhesive material may enhance the efficiency of AD process and increase the reliance on it in the future.

4.3.1 Model Estimation

Figures 44-46 show the influence of each factor considered in this study on quantities of Biogas, Biogas/g-VS and CH_4/g-VS respectively. While Figures 47-49 describes each factor effect separately on the quality of the biogas. It is evident from Figure 44 that the highest value of CH_4/g-VS was attained at 37 and 40 °C. Figures 45 and 46 indicate that the highest values of CH_4/g-VS can be attained at 1.1 g and 37.5 °C and 50% of sludge.

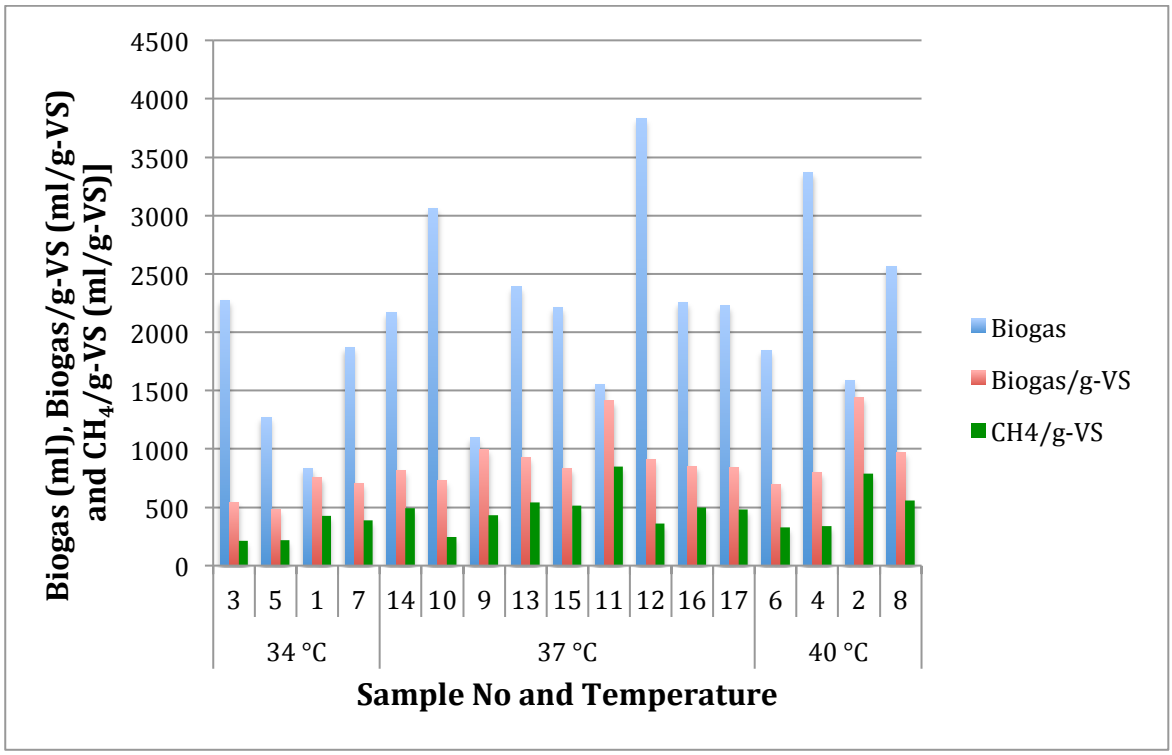

Figure 44: The impact of tempreture variance on the Biogas, Biogas/g-VS and CH_4/g-VS.

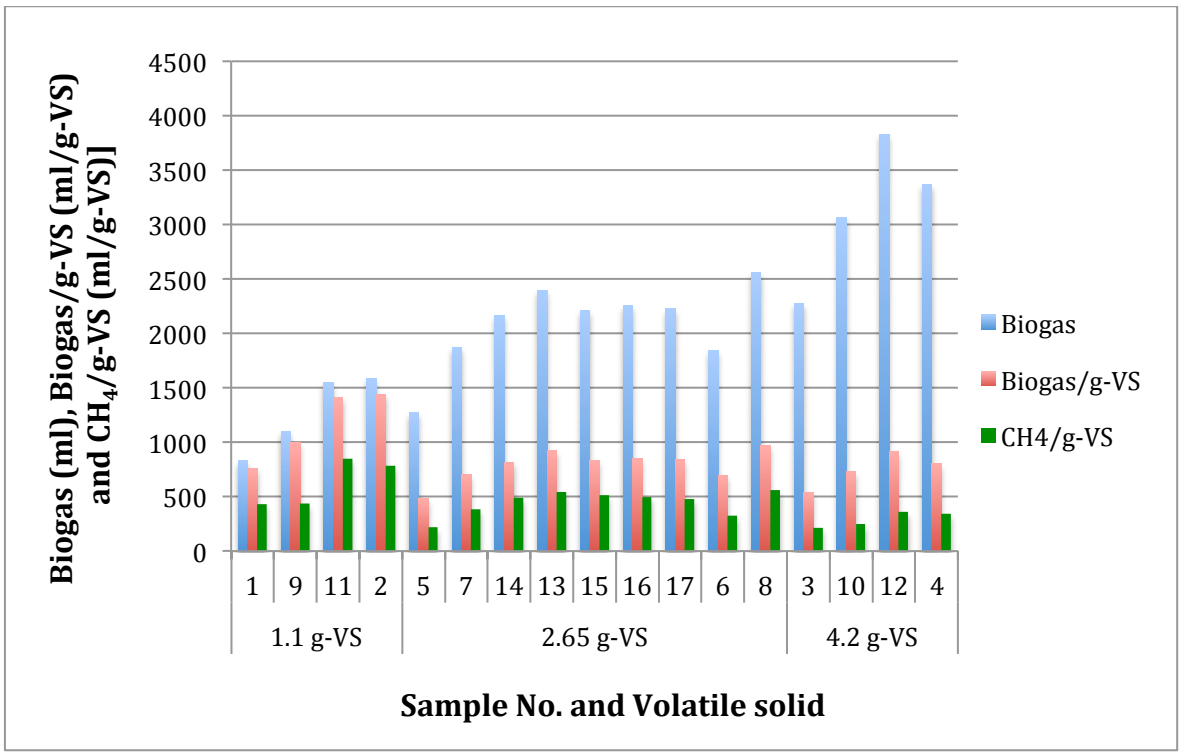

Figure 45: Effect of volatile solid added value change on the Biogas, Biogas/g-VS and CH_4/g-VS.

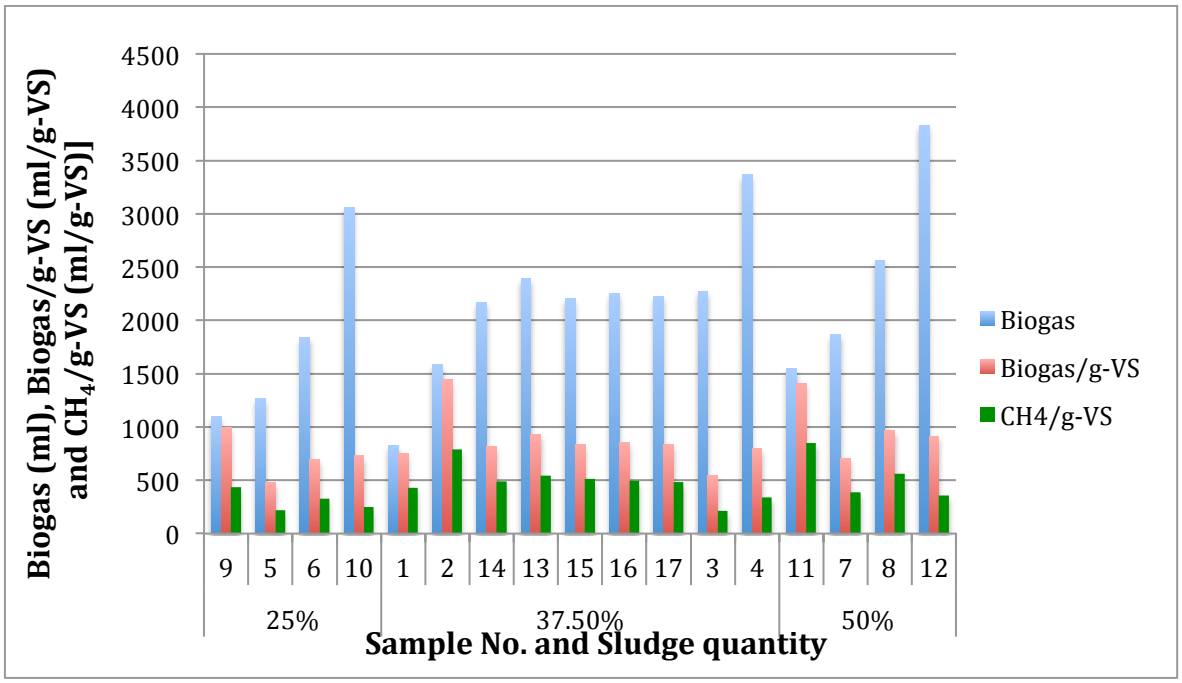

Figure 46: The influence of increasing sludge quantity on the Biogas, Biogas/g-VS and CH_4/g-VS.

Figures 47-49 show the effect of each factor on methane and carbon dioxide percentage. Figures 47 and 48 shows an increase of CH_4% and a decrease of CO_2% for all temperatures, at 2.65 g-VS and 1.1 g-VS. On the other hand, increasing the amount of sludge to 37.5% and 50% increased the CH_4% and reduced CO_2% in the resulting biogas for most of the samples, as clear in Figure 49.

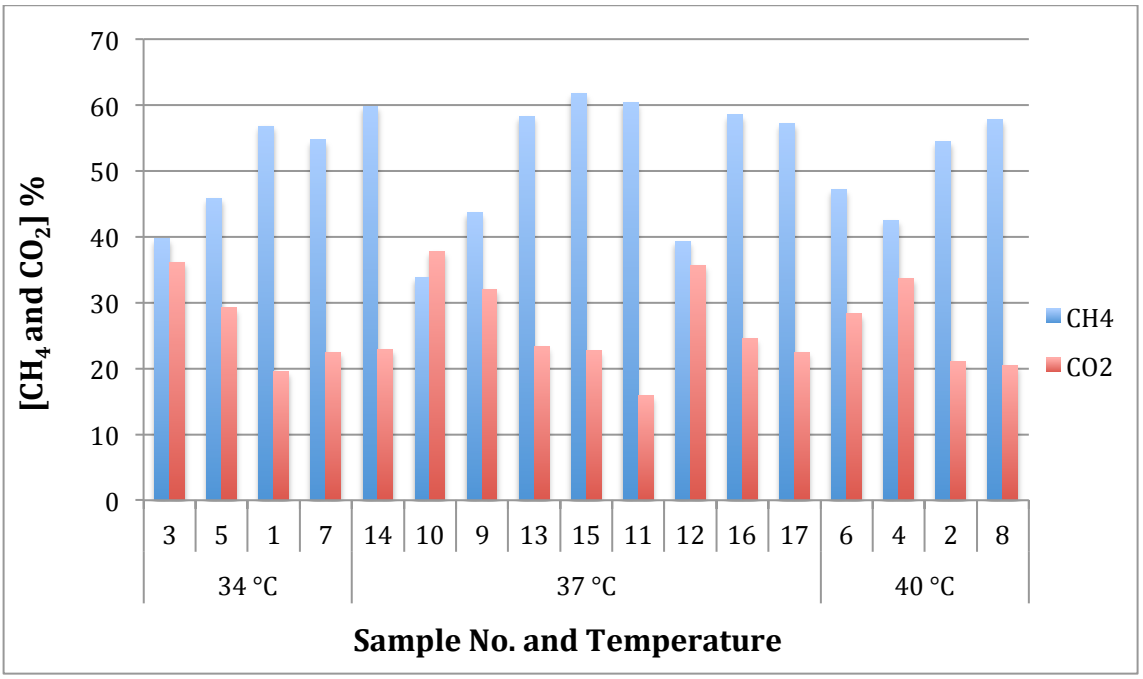

Figure 47: The temperature effects on biogas quality.

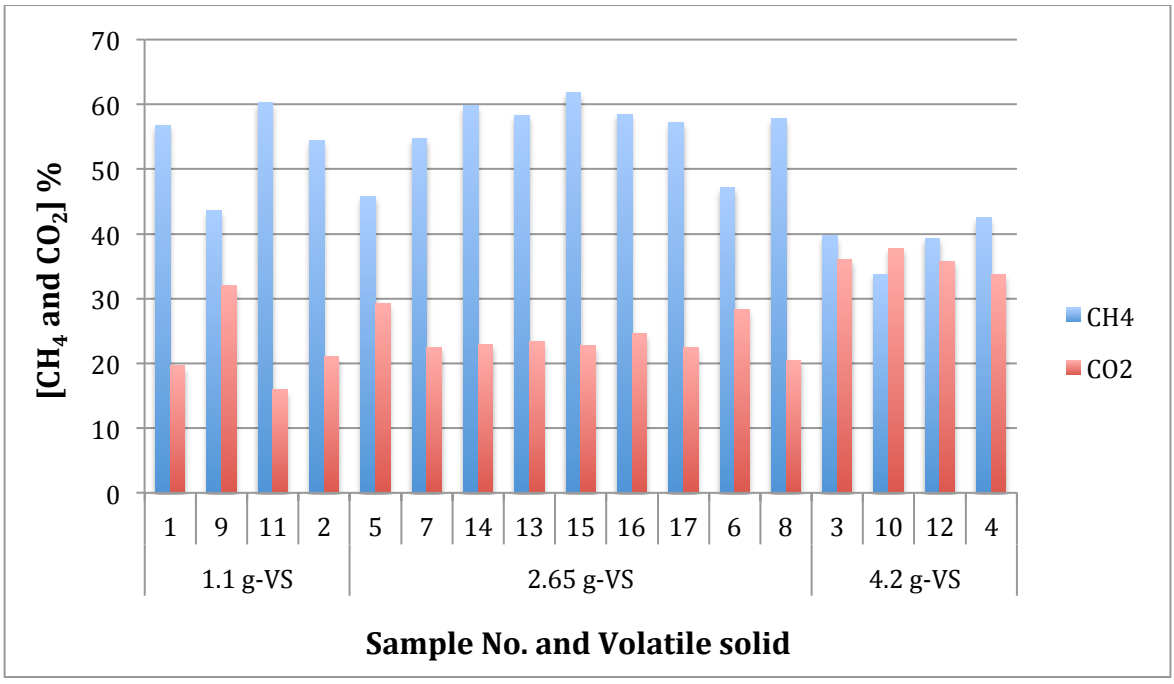

Figure 48: Changes in CH_4% and CO_2% with volatile solid added value change.

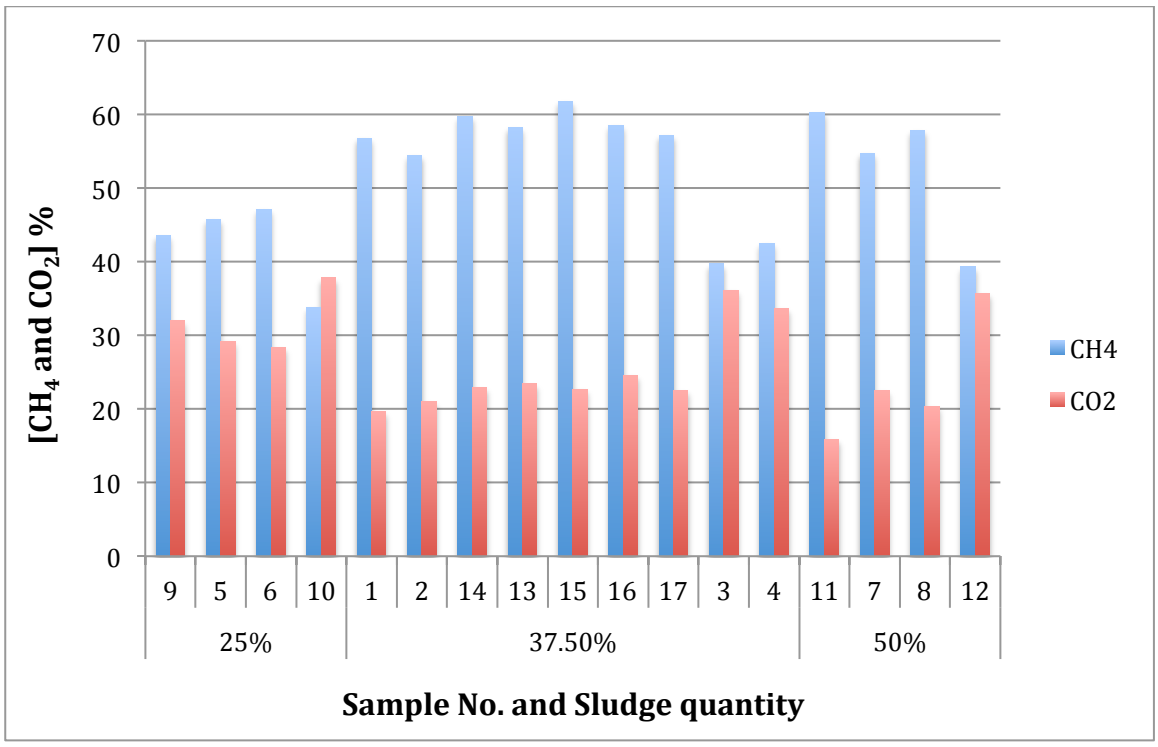

Figure 49: CH_4% and CO_2% Values with different sludge quantity.

As per section 4.2, the ANOVA Tables 27-31 for each response show that all developed models were significant. The coded equations (6, 8, 10 ,12 and 14) and the actual equations (7, 9, 11, 13 and 15) are shown below with each response. The influences of volatile solid (B) and sludge quantity (C) were significant for all responses, while there was no significant influence of temperature (A) on the CH_4% and CO_2%. The interaction of (BC) had a significant influence on the CH_4%, CO_2% and CH_4/g-VS responses. In contrast, the biogas/g-VS and CH_4/g-VS were significantly affected by the interaction of temperature and volatile solid (AB). There was no significant influence for the interaction between the temperature and the amount of the sludge (AC) on all responses.

4.3.2 Biogas

As shown in Figure 50 the direct proportions between the three factors and the biogas produced. The biogas volume increased with increasing of all factors. These results correspond to several studies about the AD of cassava [371, 372]. In a study of AD of cassava with sludge, it was found that the volume of biogas increased slightly when shifting from the mesophilic condition to thermophilic condition [371]. The effects of temperature remain directly until it reached to

around 38°C after that it became steady before it reduced slightly. The highest biogas volume was achieved when the sludge quantity at 50% at temperature between (36-40) °C and volatile solid of more than 4 g-VS according to Figure 51. The coefficients of coded equation (6) clarifies that the highest positive influence of volatile solid on the biogas followed by temperature and sludge quantity:

$$\text{Biogas} = 2310.11 + 389.13*A + 933.75*B + 317.38\ C - 359.24*A^2 \qquad \text{Equation (6)}$$

The actual equation (7) for Biogas is:

$$\text{Biogas} = -59681.43752 + 3083.42747\ *\text{Temperature} + 602.41935\ *\text{Volatile Solid} + 25.39000*\text{Sludge Quantity} - 39.91512*\text{Temperature}^2 \qquad \text{Equation (7)}$$

Table 27: ANOVA table for the Biogas response.

Source	Sum of Squares	df	Mean Square	F-value	p-value	
Model	9.539E+06	4	2.385E+06	86.14	< 0.0001	Significant
A-Temperature	1.211E+06	1	1.211E+06	43.76	< 0.0001	
B-Volatile Solid	6.975E+06	1	6.975E+06	251.97	< 0.0001	
C-Sludge Quantity	8.058E+05	1	8.058E+05	29.11	0.0002	
A^2	5.466E+05	1	5.466E+05	19.74	0.0008	
Residual	3.322E+05	12	27682.67			
Lack of Fit	3.038E+05	8	37972.65	5.35	0.0614	Not significant
Pure Error	28410.80	4	7102.70			
Cor Total	9.871E+06	16				
Adequacy measuring tools	R^2= 0.9663		Adjusted R^2= 0.9551		Predicted R^2= 0.9212	

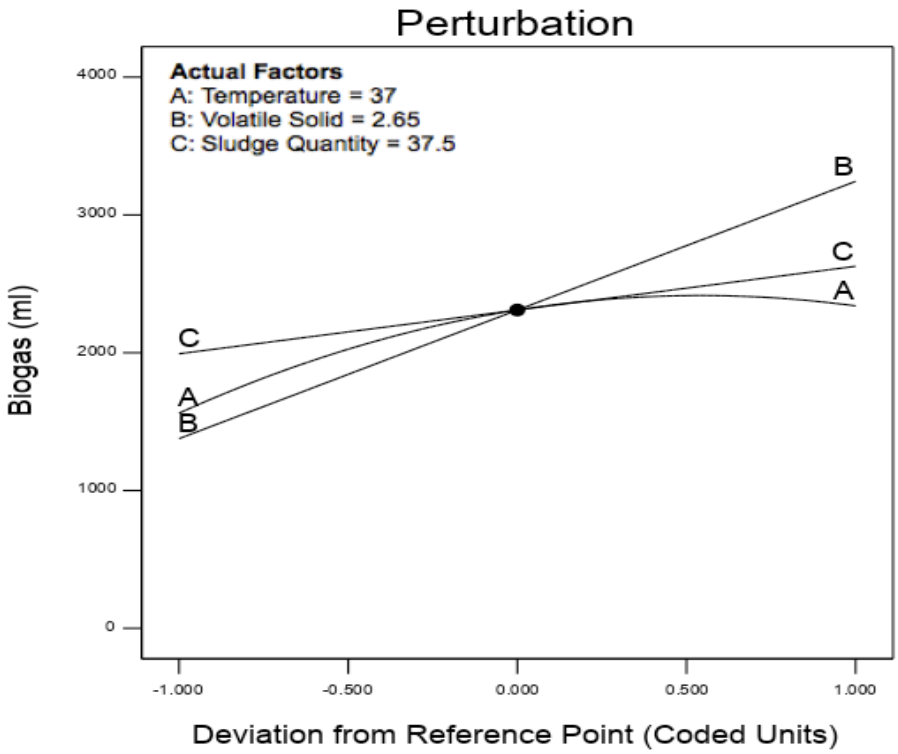

Figure 50: Perturbation plot shows the effect of all factors on Biogas volume.

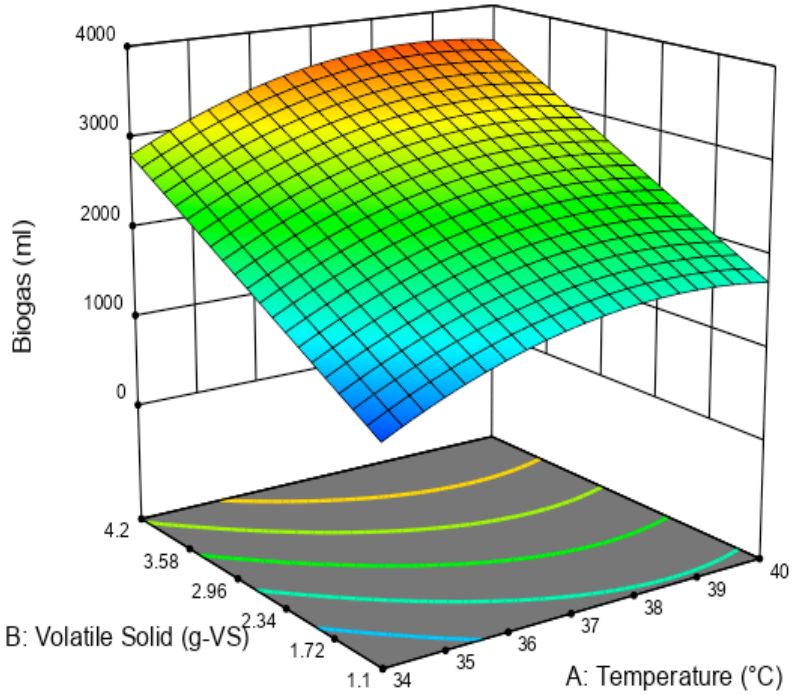

Figure 51**:** 3-D surface plot views the effect of temperature and volatile solid on Biogas volume at sludge quantity of 50%.

4.3.3 Biogas/g-VS

It is evident from Figure 52 that the highest Biogas/g-VS added produced was at its lowest volatile solid amount of 1.1 g-VS, this is because when calculating the Biogas/g-VS, the biogas volume divides the volatile solid added value. The higher the volatile solid value, the less volume of Biogas/g-VS that results and vice versa. In contrast, the same Figure 51 illustrates the direct relationship between Biogas/g-VS and both temperature and sludge quantity. As with the biogas impacts above, the effect of temperature increased until 38 °C, then it began to reduce slightly again. The interaction impacts of temperature and volatile solid added on the Biogas/g-VS is shown in Figure 53. The response increased slightly by increasing the temperature when using volatile solid of 4.2 g-VS. In contrast it significantly increased using a volatile solid of 1.1 g-VS. The response was at its minimum values at 34 °C, noticing as there was no significance difference when using both volatile solid values. This is due to the fact that the high volatile solid values of cassava requires higher temperatures to fully digest [371]. The contour graph in Figure 54 illustrates that the highest Biogas/g-VS was found at a volatile solid less than 1.3 g-VS and temperature between 38-40 °C. The coded Equation (8) clarifies the highest negative effect of volatile solid on the Biogas/g-VS:

$$\text{Biogas/g-VS} = 850.98 + 178.04*A - 202.53*B + 136.81\,C - 106.80*AB - 134.90*A^2 + 165.17*B^2 \quad \text{Equation (8)}$$

The actual equation (9) for Biogas/g-VS is:

$$\text{Biogas/g-VS} = -23698.37993 + 1229.40976*\text{Temperature} + 354.76907*\text{Volatile Solid} + 10.94500*\text{Sludge Quantity} - 22.96774*\text{Temperature} * \text{Volatile Solid} - 14.98918*\text{Temperature}^2 + 68.75021*\text{Volatile Solid}^2 \quad \text{Equation (9)}$$

Table 28: ANOVA table for Biogas/g-VS response.

Source	Sum of Squares	df	Mean Square	F-value	p-value	
Model	9.592E+05	6	1.599E+05	31.05	< 0.0001	Significant
A-Temperature	2.536E+05	1	2.536E+05	49.24	< 0.0001	
B-Volatile Solid	3.281E+05	1	3.281E+05	63.72	< 0.0001	
C-Sludge Quantity	1.497E+05	1	1.497E+05	29.08	0.0003	
AB	45624.96	1	45624.96	8.86	0.0139	
A^2	76839.04	1	76839.04	14.92	0.0031	
B^2	1.152E+05	1	1.152E+05	22.37	0.0008	
Residual	51494.42	10	5149.44			
Lack of Fit	44108.57	6	7351.43	3.98	0.1011	Not significant
Pure Error	7385.85	4	1846.46			
Cor Total	1.011E+06	16				
Adequacy measuring tools	R^2=0.9491	Adjusted R^2=0.9185			Predicted R^2=0.7554	

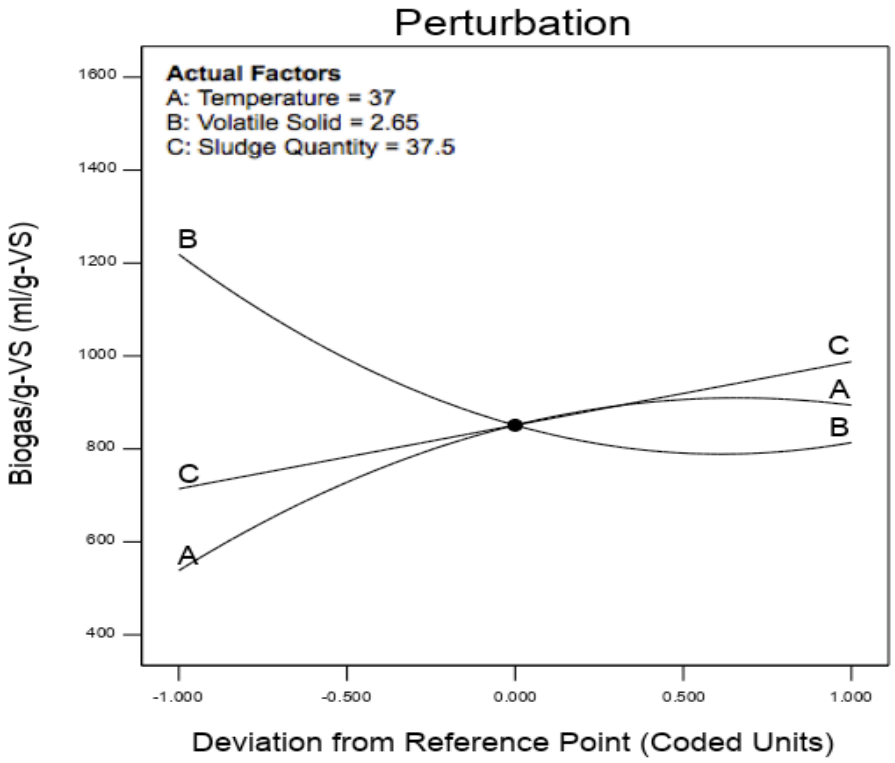

Figure 52: Perturbation plot shows the effect of all factors on Biogas/g-VS volume.

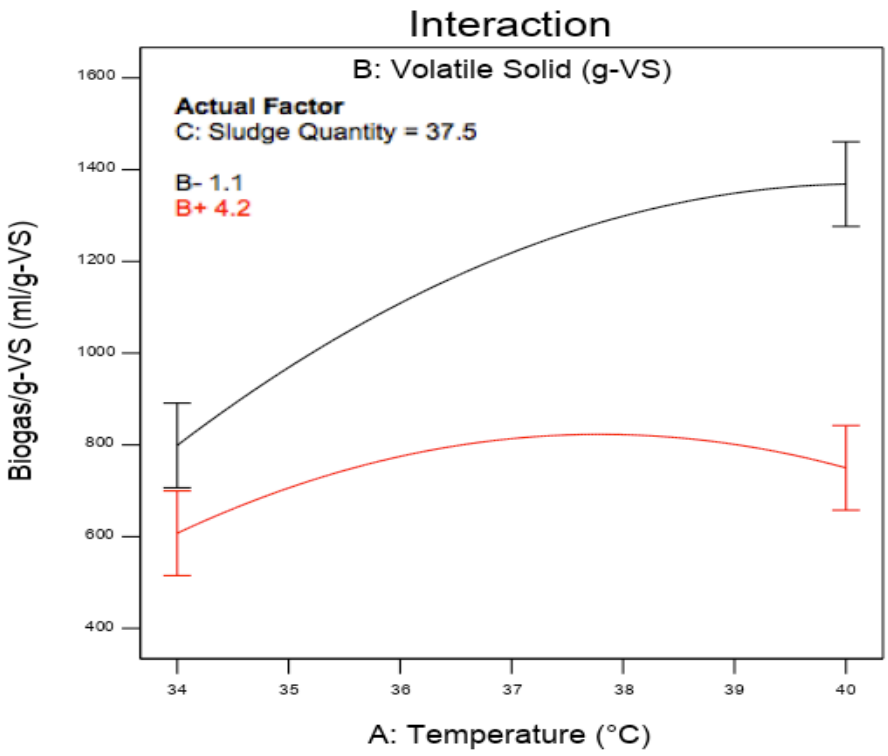

Figure 53: Interaction plot clarifies the effect of interaction between temperature and volatile solid on Biogas/g-VS.

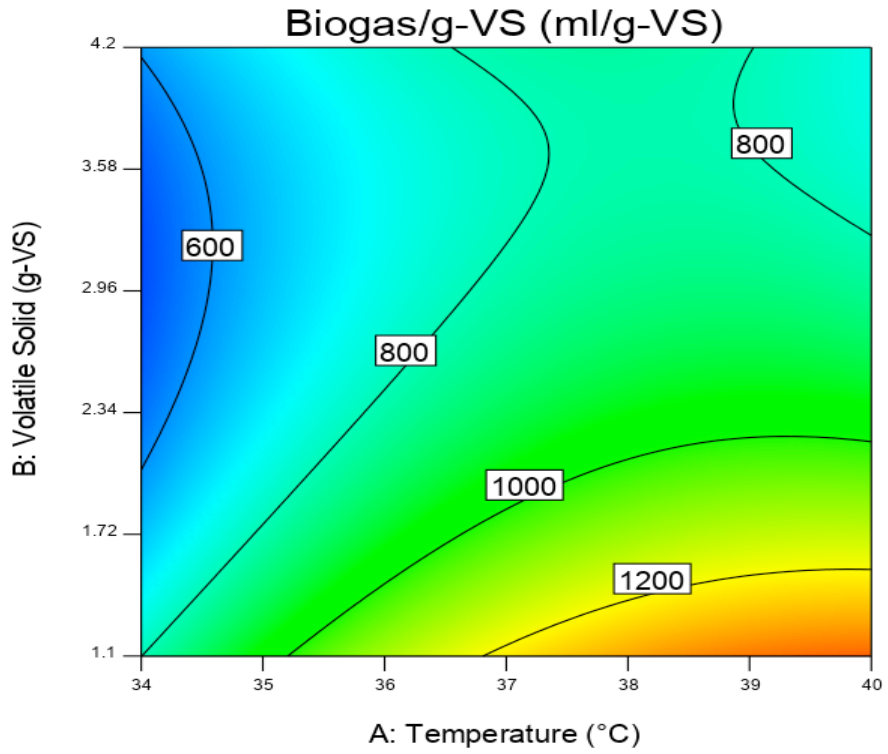

Figure 54: Contour plot views the effect of temperature and volatile solid on Biogas/g-VS volume at sludge quantity of 37.5%.

4.3.4 Methane Percentage

According to Figure 55, the influence of temperature was quite low on the methane percentage. Volatile solid slightly affects positively on the methane percentage and then decreases dramatically by further increasing the volatile solid value. On the contrary, the effect of the sludge quantity affects positively on the response and decreases slightly at sludge quantity of 38.5%. Figure 56 shows the influence of the interaction of volatile solid and sludge quantity on the response. The CH_4% significantly increased when changing sludge quantity from 25% to 50%. This is because the promotion of inoculum in the AD process, consequently affects the activity of bacteria to increase the methane yields [371, 387, 388]. The lowest CH_4% was found at 4.2 g-VS and at both sludge quantities. The 3-D surface plot in Figure 57 illustrates the wide area for the highest CH_4% achieved when using volatile solid less than 2.5 g-VS and sludge quantity of 37.5% and more. The highest factor effect on the methane percentage was volatile solid value followed by sludge quantity as demonstrates in the coded equation (10). The volatile solid affects negatively on the response while the sludge quantity positively affects the response.

The coded equation (10) for CH_4% is:

$$CH_4\% = 59.12 + 0.6125*A - 7.49*B + 5.23*C - 2.80*BC - 1.82*A^2 - 8.92*B^2 - 5.95*C^2 \quad \text{Equation (10)}$$

The actual equation (11) for CH_4% is:

$$CH_4\% = -322.49969 + 15.18917*\text{Temperature} + 20.27206*\text{Volatile Solid} + 3.65577*\text{Sludge Quantity} - 0.144516*\text{Volatile Solid} * \text{Sludge Quantity} - 0.202500*\text{Temperature}^2 - 3.71384*\text{Volatile Solid}^2 - 0.038064*\text{Sludge Quantity}^2 \quad \text{Equation (11)}$$

Table 29: ANOVA table for CH_4% response.

Source	Sum of Squares	df	Mean Square	F-value	p-value	
Model	1240.05	7	177.15	69.90	< 0.0001	Significant
A-Temperature	3.00	1	3.00	1.18	0.3048	
B-Volatile Solid	448.50	1	448.50	176.98	< 0.0001	
C-Sludge Quantity	218.40	1	218.40	86.18	< 0.0001	
BC	31.36	1	31.36	12.37	0.0065	
A^2	13.99	1	13.99	5.52	0.0434	
B^2	335.20	1	335.20	132.27	< 0.0001	
C^2	148.94	1	148.94	58.77	< 0.0001	
Residual	22.81	9	2.53			
Lack of Fit	10.42	5	2.08	0.6729	0.6674	Not significant
Pure Error	12.39	4	3.10			
Cor Total	1262.86	16				
Adequacy measuring tools	R^2=0.9819	Adjusted R^2=0.9679			Predicted R^2=0.9459	

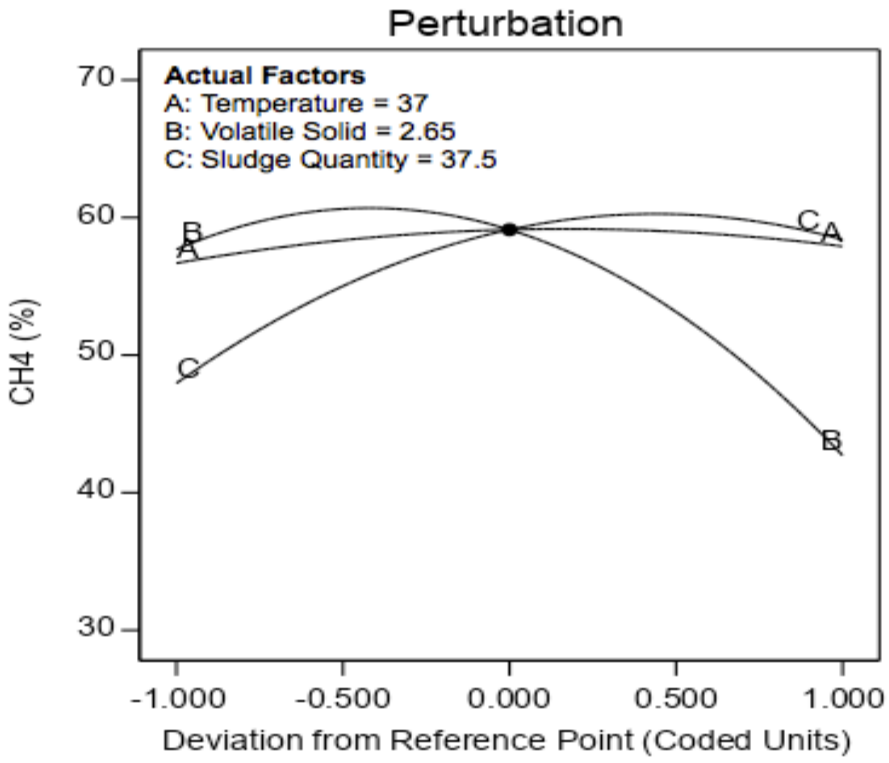

Figure 55: Perturbation plot shows the effect of all factors on CH_4%.

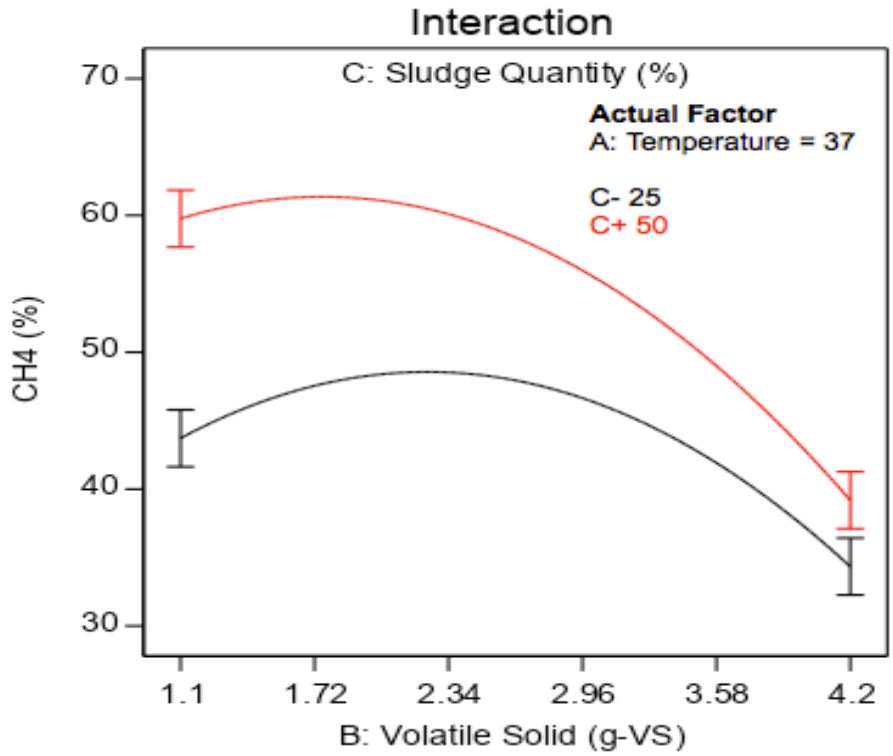

Figure 56: Interaction plot clarifies the effect of interaction between volatile solid and sludge quantity on CH_4%.

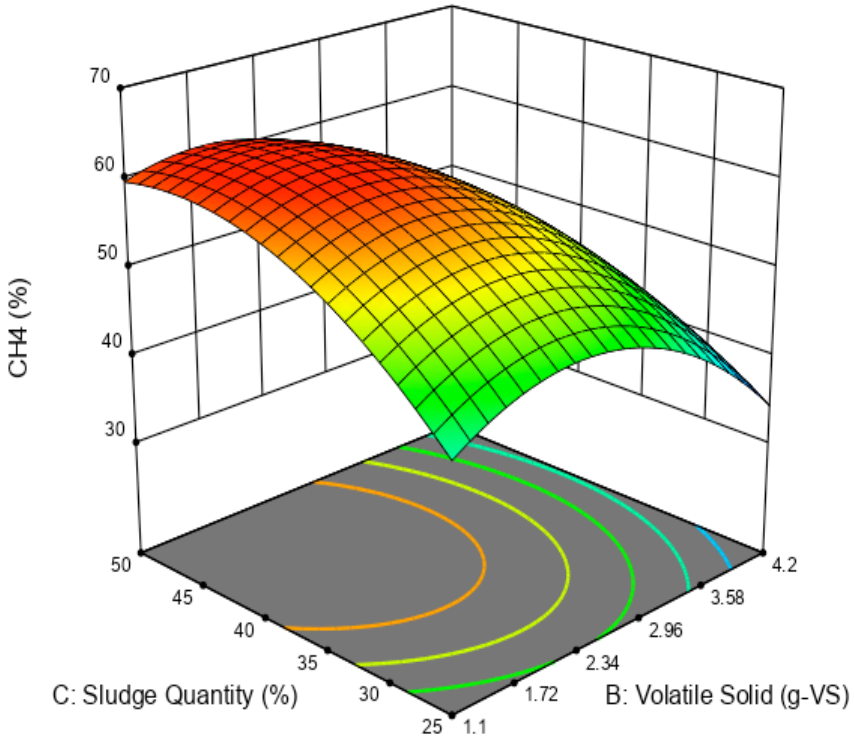

Figure 57: 3-D surface plot views the effect of volatile solid and sludge quantity on CH_4% volume at temperature of 37°C.

4.3.5 Carbon Dioxide Percentage

The impact of temperature was quite low on the CO_2% according to Figure 58. Whereas, it increased significantly by increasing the volatile solid and decreasing the sludge quantity. The response slightly increased by increasing the volatile solid at a sludge quantity of 25% (Figure 59). In contrast, CO_2% rises rapidly with increasing of volatile solid at sludge quantity of 50%, plus there was no difference in CO_2% when using volatile solid of 4.2 g-VS and both sludge quantities. Figure 60 demonstrate the lowest CO_2% achieved at the same wide area of highest CH_4% was found which illustrates the inverse relationship between CH_4% and CO_2%. The coded equation (12) shows the positive highest effect of the volatile solid added value on the response, followed by the negative effect of the sludge quantity:

$$CO_2\% = 23.04 - 0.5000*A + 6.85*B - 4.10*C - 0.9500*AB + 3.50*BC + 4.79*B^2 + 2.29C^2 \quad \text{Equation (12)}$$

The actual equation (13) for CO_2% is:

$$CO_2\% = 62.34837 + 0.374731*\text{Temperature} - 5.36725*\text{Volatile Solid} - 1.90692*\text{Sludge Quantity} - 0.204301*\text{Temperature} * \text{Volatile Solid} + 0.180645*\text{Volatile Solid} * \text{Sludge Quantity} + 1.99463*\text{Volatile Solid}^2 + 0.014669*\text{Sludge Quantity}^2 \quad \text{Equation (13)}$$

Table 30: ANOVA table for CO_2% response.

Source	Sum of Squares	df	Mean Square	F-value	p-value	
Model	689.15	7	98.45	114.70	< 0.0001	Significant
A-Temperature	2.00	1	2.00	2.33	0.1612	
B-Volatile Solid	375.38	1	375.38	437.35	< 0.0001	
C-Sludge Quantity	134.48	1	134.48	156.68	< 0.0001	
AB	3.61	1	3.61	4.21	0.0705	
BC	49.00	1	49.00	57.09	< 0.0001	
B^2	96.96	1	96.96	112.97	< 0.0001	
C^2	22.18	1	22.18	25.84	0.0007	
Residual	7.72	9	0.8583			
Lack of Fit	4.90	5	0.9793	1.39	0.3873	Not significant
Pure Error	2.83	4	0.7070			
Cor Total	696.88	16				
Adequacy measuring tools	R^2=0.9889	Adjusted R^2=0.9803			Predicted R^2=0.942	

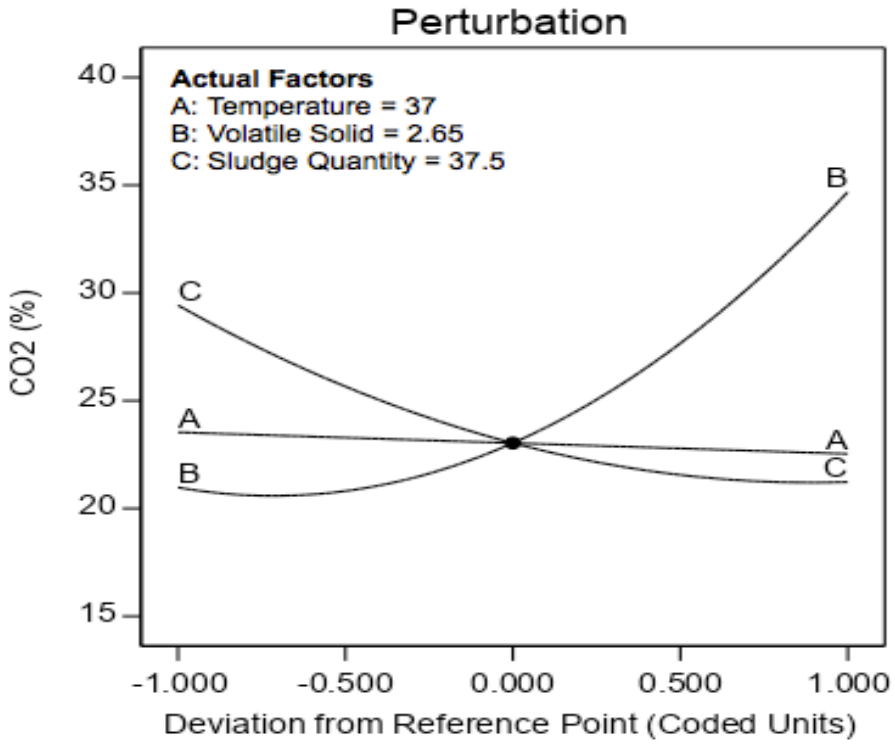

Figure 58: Perturbation plot shows the effect of all factors on CO_2%.

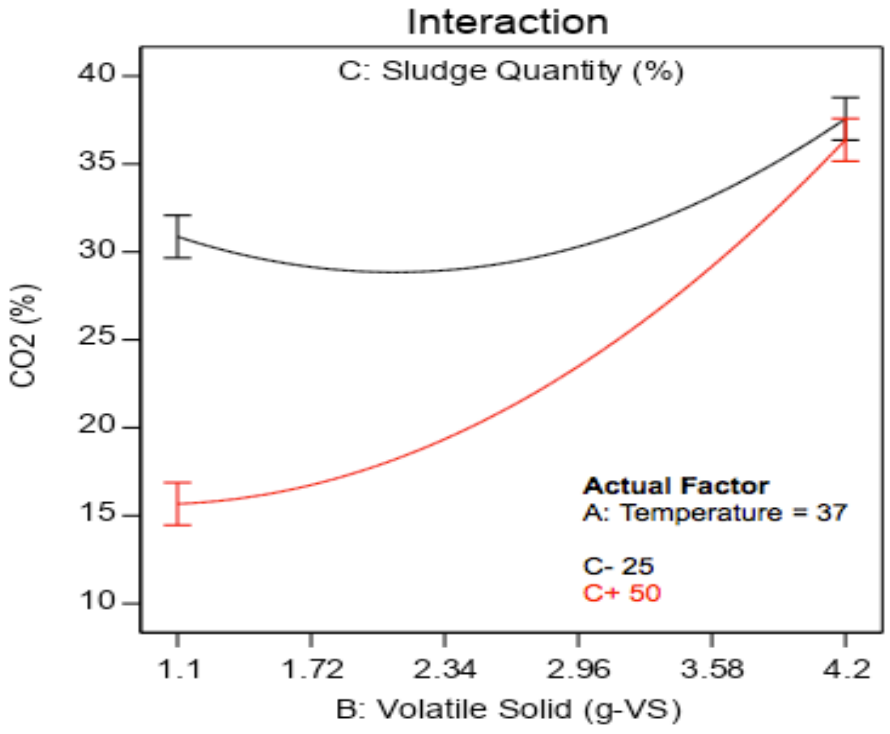

Figure 59: Interaction plot clarifies the effect of interaction between volatile solid and sludge quantity on CO_2%.

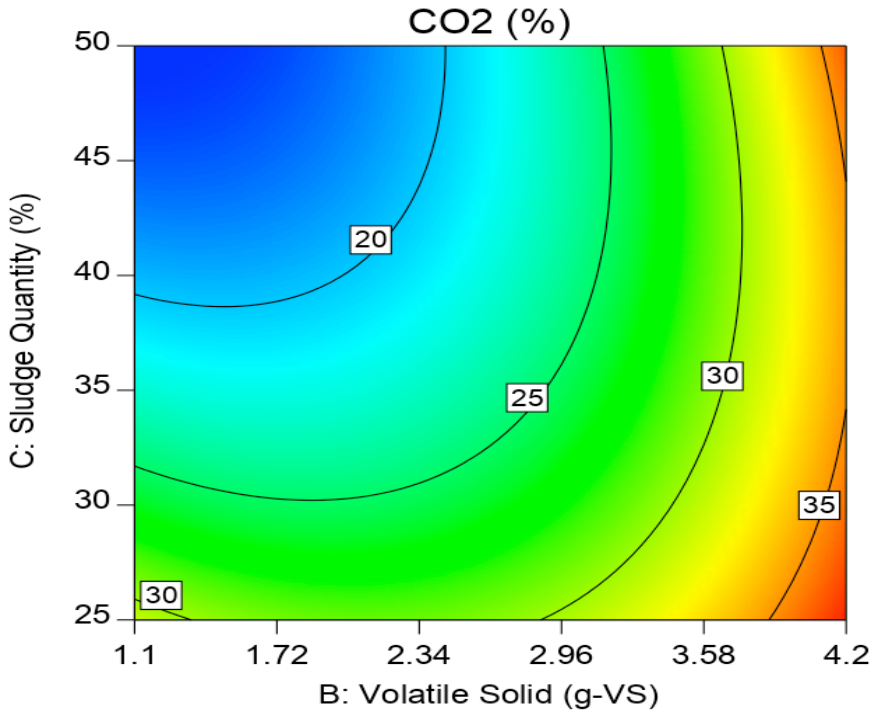

Figure 60: Contour plot views the effect of volatile solid and sludge quantity on CO_2% volume at temperature of 37°C.

4.3.6 Methane/g-VS

The direct proportion between temperature and sludge quantity on added CH_4/g-VS while the volatile solid added indirectly influenced the methane/g-VS demonstrates in Figure 61. Where at the lowest value of volatile solid of 1.1 g-VS, the highest methane/g-VS was achieved (Figure 60). The CH_4/g-VS depends on its calculation by dividing it on the volatile solid added value, so increasing the volatile solid value reduces the response value and vice versa. The influence of the interaction between the temperature and volatile solid is shown in Figure 62. The response doubled by increasing the volatile solid from 1.1 g-VS to 4.2 g-VS when the temperature was 34 °C. While it slightly rose by increasing the temperature when using the volatile solid of 1.1 g-VS and significantly increased by increasing the temperature when using the volatile solid of 4.2 g-VS. Figure 63 shows the effects of the interaction between the volatile solid added and the sludge quantity. The response doubled when the sludge quantity increased from 25% to 50% when using volatile solid of 1.1 g-VS. As shown from the same figure, the methane/g-VS for both sludge quantities was at the same value when the volatile solid value of 4.2 g-VS and this is due to the methane inhibition [389]. The 3-D surface plot shown in Figure 64 suggests the

highest CH_4/g-VS was resulted at volatile solid less than 1.5 g-VS, sludge quantity of 50% and at more than 37 °C. As it clears from the coded equation (14), the volatile solid added influence was the highest on the response:

$$CH_4/g\text{-}VS = 512.58 + 95.59*A - 167.42*B + 115.84*C - 57.98*AB - 76.13*BC - 79.6*A^2 - 49.86*C^2 \quad \text{Equation (14)}$$

The actual equation (15) for CH_4/g-VS is:

$$CH_4/g\text{-}VS = -14899.53404 + 719.50991*\text{Temperature} + 500.62903*\text{Volatile Solid} + 43.61388*\text{Sludge Quantity } 12.46774*\text{Temperature} * \text{Volatile Solid} - 3.92903*\text{Volatile Solid} * \text{Sludge Quantity} - 8.84605*\text{Temperature}^2 - 0.319133*\text{Sludge Quantity}^2 \quad \text{Equation (15)}$$

Table 31: ANOVA table for CH_4/g-VS response.

Source	Sum of Squares	df	Mean Square	F-value	p-value	
Model	4.806E+05	7	68651.47	50.86	< 0.0001	Significant
A-Temperature	73095.76	1	73095.76	54.16	< 0.0001	
B-Volatile Solid	2.242E+05	1	2.242E+05	166.14	< 0.0001	
C-Sludge Quantity	1.073E+05	1	1.073E+05	79.53	< 0.0001	
AB	13444.40	1	13444.40	9.96	0.0116	
BC	23180.06	1	23180.06	17.17	0.0025	
A^2	26762.41	1	26762.41	19.83	0.0016	
C^2	10498.41	1	10498.41	7.78	0.0211	
Residual	12147.72	9	1349.75			
Lack of Fit	9874.08	5	1974.82	3.47	0.1256	Not significant
Pure Error	2273.64	4	568.41			
Cor Total	4.927E+05	16				
Adequacy measuring tools	R^2=0.9753	Adjusted R^2=0.9562		Predicted R^2=0.8693		

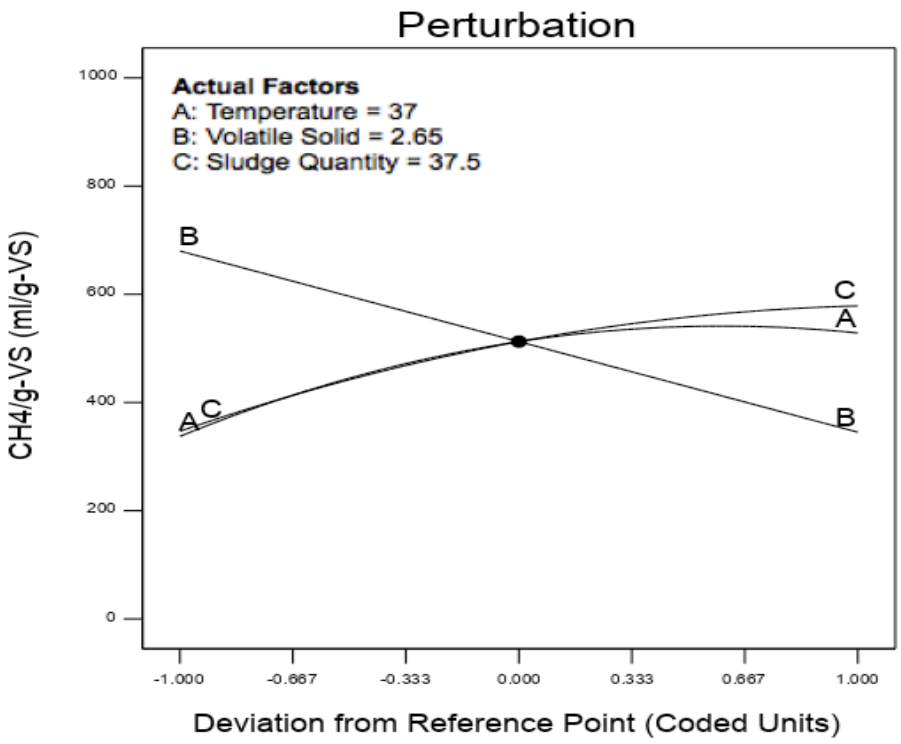

Figure 61: Perturbation plot shows the effect of all factors on CH_4/g-VS.

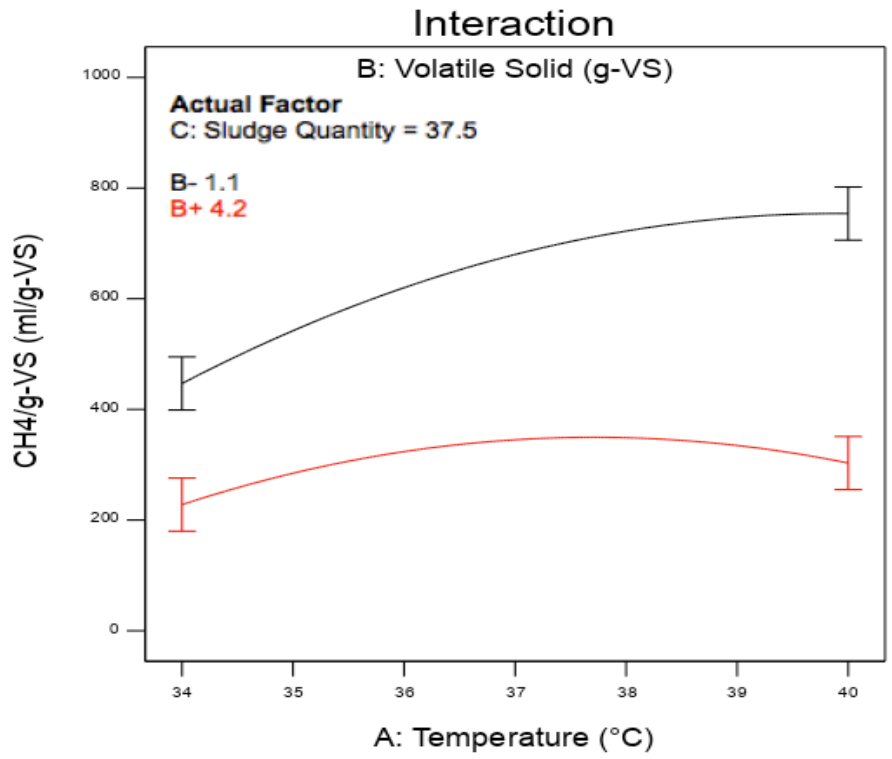

Figure 62: Interaction plot clarifies the effects of interaction between temperature and volatile solid on CH_4/g-VS.

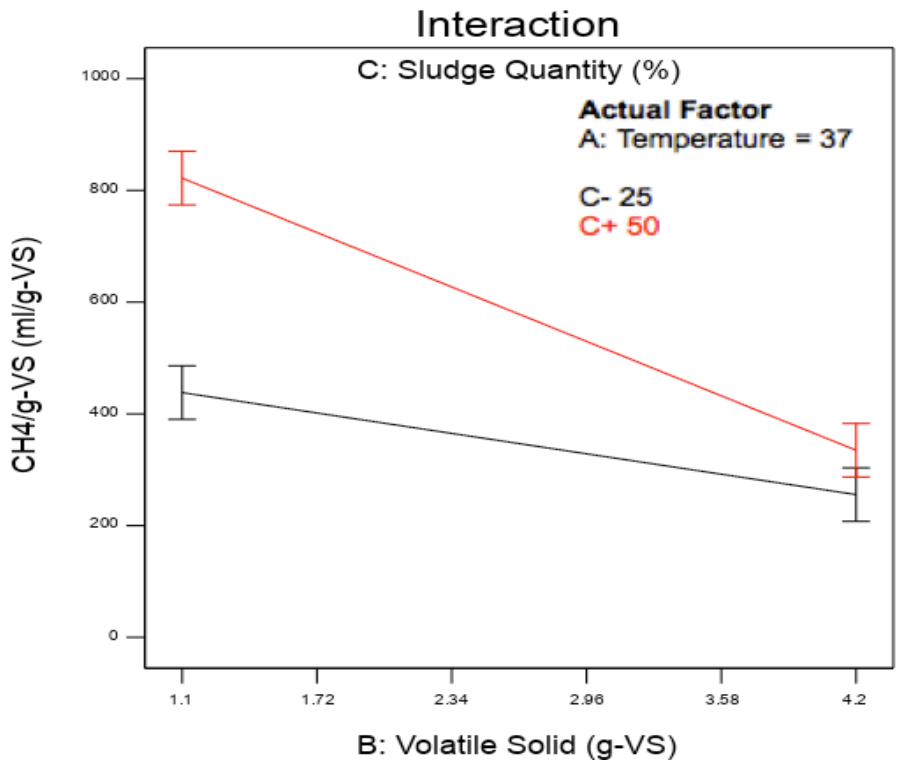

Figure 63: Interaction plot clarifies the effects of interaction between volatile solid and sludge quantity on CH_4/g-VS.

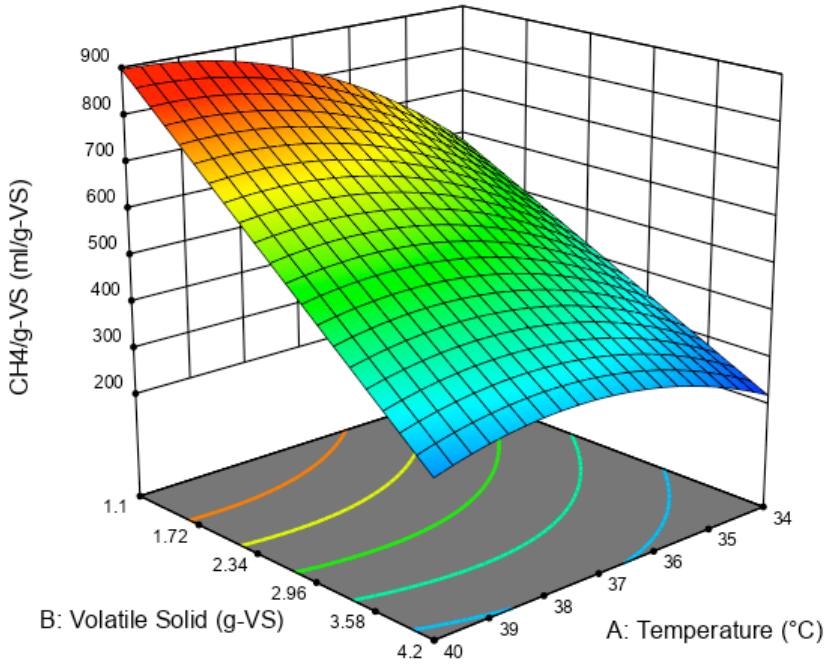

Figure 64: 3-D surface plot views the effect of volatile solid and sludge quantit on CH_4/g-VS% at 50% of sludge.

4.4 Date Seed Results

The Biogas, CH_4% and CH_4 volume produced from sludge given in Table 32 are expanded in Figures 65-67, to show the Biogas, CH_4% and CH_4 produced from sludge and after adding the date seed. The biogas yield increased due to the addition of the date seed to the sludge at all temperatures. The highest biogas was found to have increased by approximately five times at 37 °C, from around 880 ml to 4,140 ml as indicated in Figure 65. Figures 66-67 show the effect of adding date seed to sludge on the percentage and amount of methane produced. Again the highest rise in methane percentage was found at 37 °C, (from 52.9% to 71.1%). While Figure 67 shows the apparent rise due to the addition of date seeds occurred at all temperatures. The highest increase in the amount of methane was again at 37 °C from 466 ml to 2,430 ml.

Table 32: Biogas, CH_4% and methane produced from sludge.

Temperature °C	Biogas (ml)	CH_4 (%)	CH_4 (ml)
34	1103	51.7	570
37	880	52.9	466
40	801	51.3	411

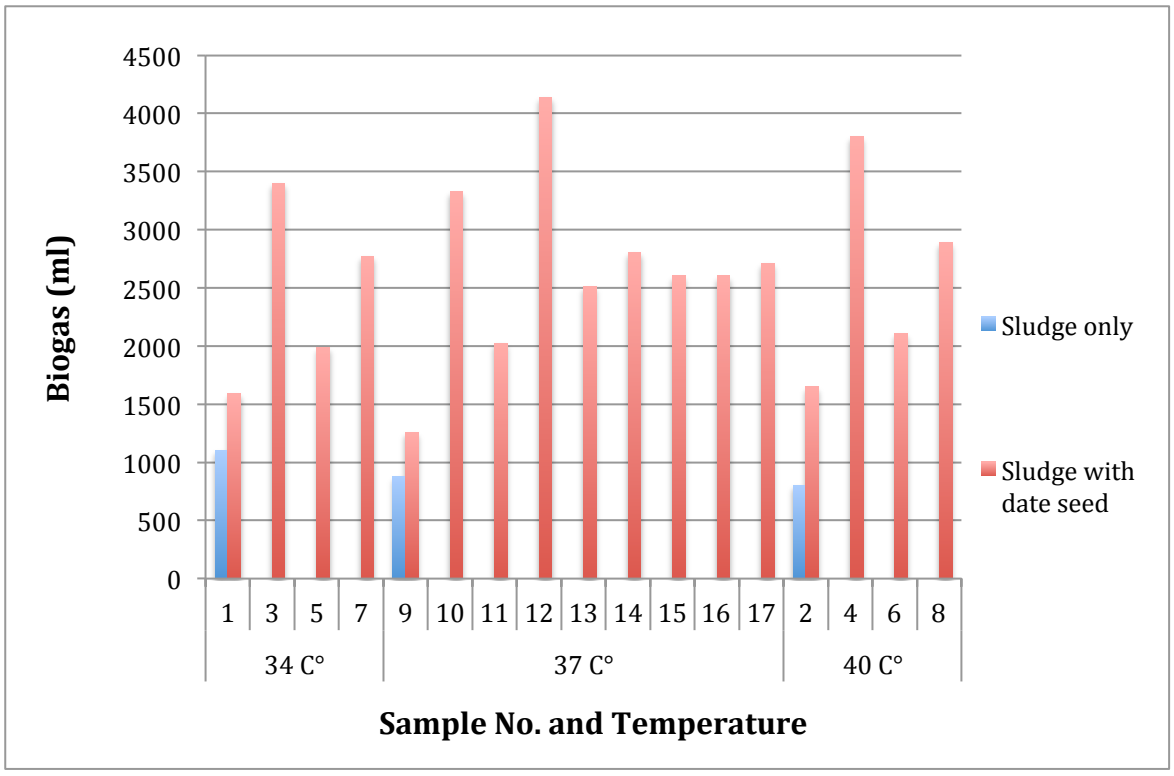

Figure 65: Biogas yield from sludge only and after adding date seed.

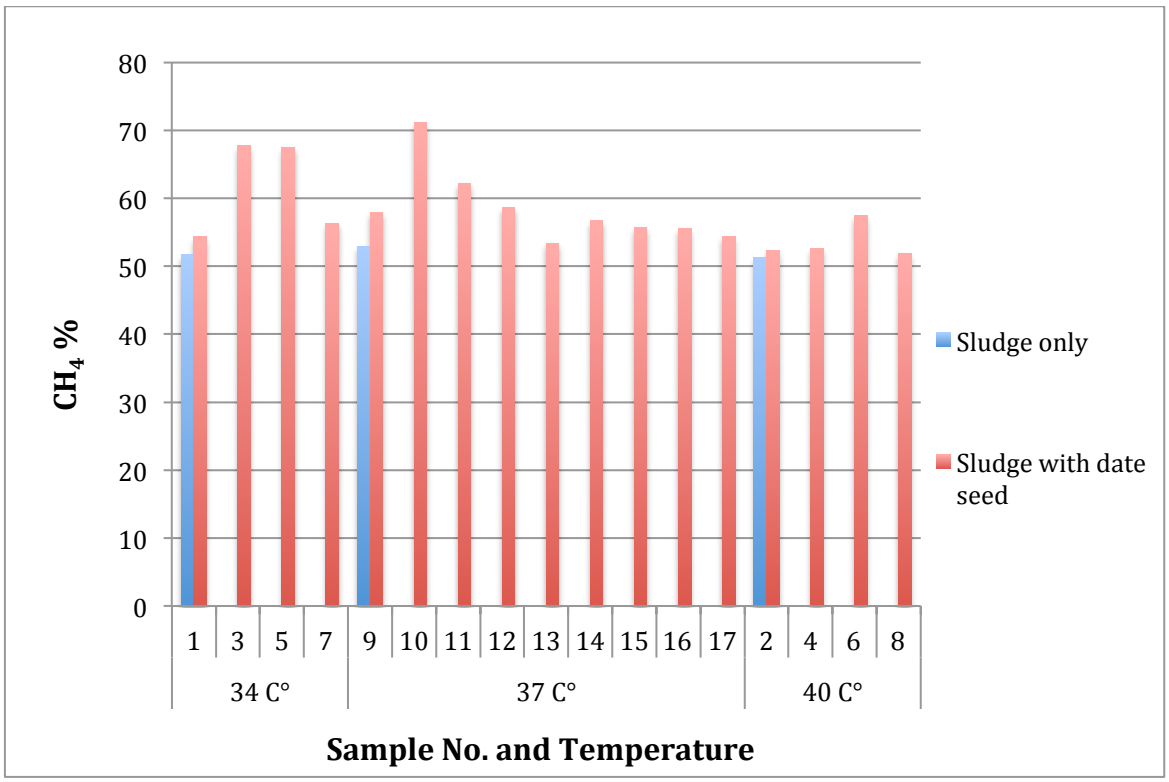

Figure 66: CH_4% variance when adding date seed to the sludge.

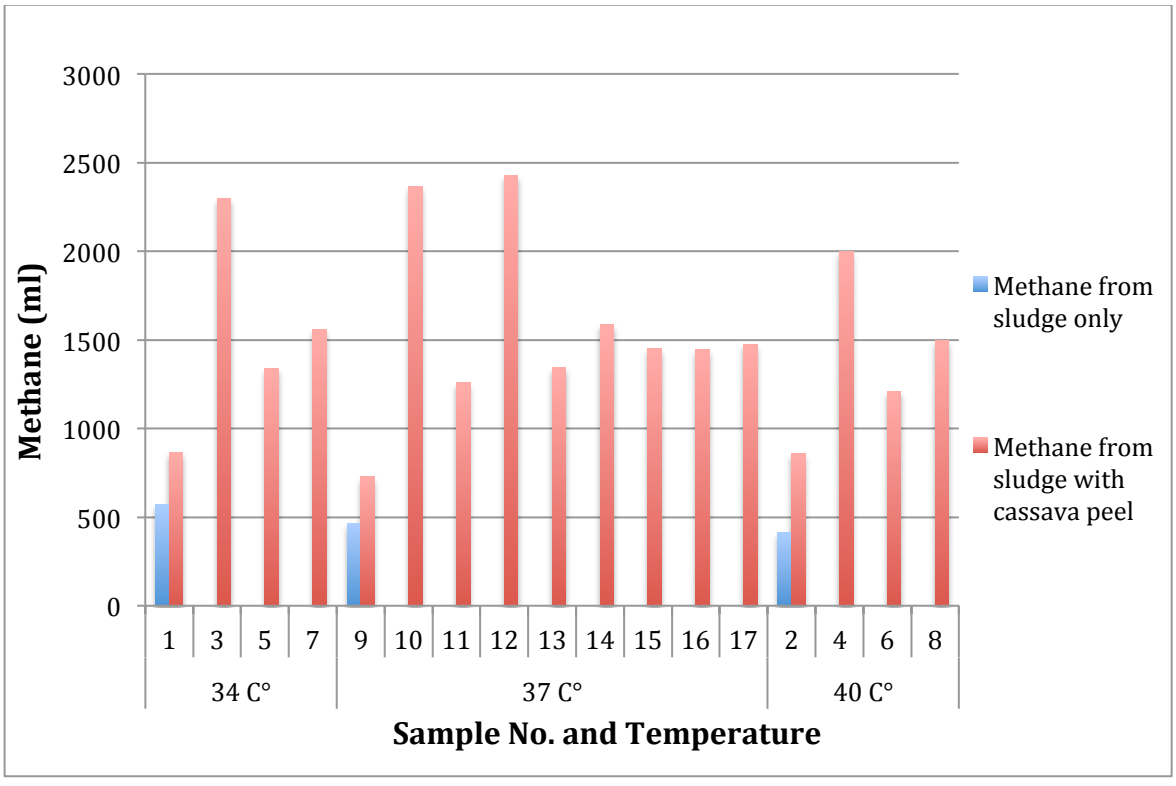

Figure 67: The changing in methane quantity following to add date seed to the sludge.

While the experiment matrix shown in Table 33 presents the conditions of each experiment run and the associated response values. It is clear from run #15 that the highest volume of biogas of 4,140 ml was achieved at 37°C, volatile solid value of 4.2 g-VS and sludge quantity of 50%. While the lowest biogas of 1,256 ml was obtained at the same temperature, volatile solid value of 1.1 g-VS and sludge amount of 25% (run #16). In both cases the CH_4 percentage was close to each other at 58.7% and 57.9%, respectively. In contrast, if the amount of CH_4 per volatile solid added is to be considered, then its value of 661 ml/g-VS (run #16) would be higher in the second case due to a lower volatile solid of 1.1 g-VS was used. However, the amount of CH_4 per volatile solid in the first case was 579 ml/g-VS (run #15), due to a higher volatile solid of 4.2 g-VS was used.

Table 33: The experiment responses results for date seed.

Std.	Run	Factor 1 A*	Factor 2 B*	Factor 3 C*	Resp. 1 Biogas	Resp. 2 Biogas/g-VS	Resp. 3 CH_4	Resp.4 CO_2	Resp. 5 CH_4/g-VS
		°C	g-VS	%	ml	ml/g-VS	%	%	ml/g-VS
1	6	34	1.10	37.5	1596	1450.5	54.3	24.0	788.1
2	14	40	1.10	37.5	1648	1497.7	52.3	22.6	783.8
3	2	34	4.20	37.5	3398	809.1	67.7	18.3	547.5
4	9	40	4.20	37.5	3801	905.0	52.6	23.9	476.0
5	12	34	2.65	25.0	1986	749.5	67.5	15.1	505.9
6	17	40	2.65	25.0	2108	795.6	57.4	19.6	456.4
7	7	34	2.65	50.0	2771	1045.8	56.3	21.2	588.4
8	1	40	2.65	50.0	2888	1089.6	51.9	24.0	565.9
9	16	37	1.10	25.0	1256	1141.6	57.9	18.2	661.0
10	8	37	4.20	25.0	3328	792.3	71.1	13.0	563.6
11	13	37	1.10	50.0	2023	1838.9	62.2	17.6	1143.8
12	15	37	4.20	50.0	4140	985.8	58.7	17.0	579.0
13	5	37	2.65	37.5	2515	949.0	53.4	24.9	506.4
14	3	37	2.65	37.5	2802	1057.3	56.7	26.2	599.2
15	11	37	2.65	37.5	2606	983.5	55.7	26.6	547.8
16	4	37	2.65	37.5	2603	982.4	55.5	25.6	545.2
17	10	37	2.65	37.5	2710	1022.7	54.4	25.5	556.4

* *A= Temperature, B= Volatile solid, C= Sludge quantity.*

However, the highest amount of Biogas per g-VS of 1,838.9 ml/g-VS was obtained at 37 °C, volatile solid value of 1.1 g-VS and at 50% sludge (run #13). At these conditions the highest CH_4/g-VS quantity of 1,143.8 ml/g-VS was recorded. On the other hand, the lowest value of Biogas/g-VS from of 749.5 ml/g-VS was reported at 34°C, 2.65 g-VS, and 25% of the sludge (run #12). The minimum CH_4/g-VS of 456.4 ml/g-VS was obtained from run #17 at 40°C, 2.65 g-VS and 25% sludge.

A methane percentage ranged between 51.9% and 71.1% was achieved which is higher than that recorded by Jaffar [183]. While the CO_2% was between 13.0% and 26.6% lower than that found in the same study [183]. Table 33 shows the relationship between CH_4% and CO_2%. It was found that as the CH_4% increased the CO_2% decreased. The highest CH_4% and lowest CO_2% was found at the following conditions: 37°C, 4.2 g-VS and 25% sludge quantity (run #8). In contrast, the lowest CH_4% of 51.9% was found from run #1 at the following conditions: 40 °C, 2.65 g-VS and 50% of the sludge. The highest CO_2% was found from run #11 at the following conditions: 37 °C, 2.65 g-VS and 37.5% of the sludge.

When comparing the amount of biogas produced in this study with previous studies [167, 183], the volume of Biogas/g-VS produced in this study was higher than the amount that recorded by Lattieff [167]. This increase is attributed to the treatment method followed in this study and inoculum used. Furthermore, it was found that the amount of biogas was two times higher than that reported in [183]. This is could be due to the treatment method used on date seed in this study as no boiling or exposing of the date seed to elevated temperatures was conducted (i.e. only grinding). Also, the difference in the inoculum used may be a reason for the change in the volume of the resulting biogas. However, due to the similarity in the components of most types of dates and their proportions, this study's results are applicable to other types of date seeds, at different times.

4.4.1 Model Estimation

Figures 68-73 illustrate the impact of temperature, volatile solids, and sludge quantity on the responses for each factor separately. Figure 68 shows that the effect of temperature on CH_4/g-VS did vary, where the highest value was found at 37 °C from sample #11. On the contrary, a decrease in the volatile solid added value caused an increase in CH_4/g-VS (Figure 69). Figure 70 shows that at 50% of the sludge, the highest amount of CH_4/g-VS was achieved.

Figures 71-73 show the effect of factors on CH_4 and CO_2 percentages. The CH_4% exceeded 71% at 37 °C, 4.2 g volatile and 25% sludge as shown from the charts. In these conditions, the lowest CO_2% was reached 13%. Also, from the same charts, the inverse relationship between CH_4% and CO_2% was evident.

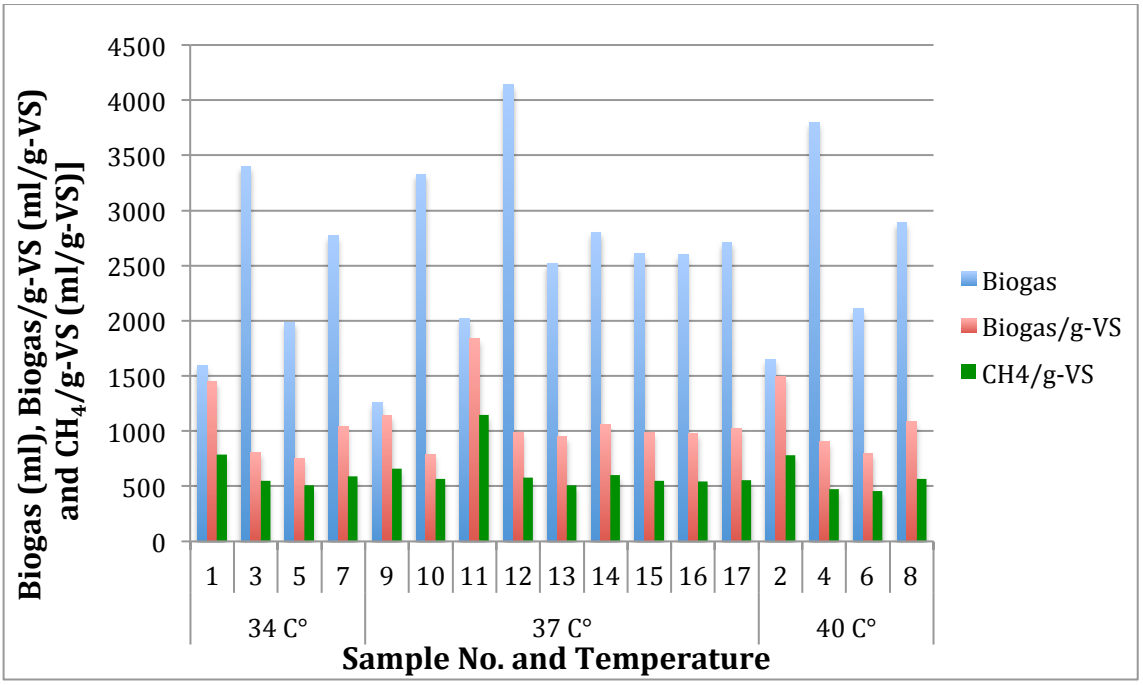

Figure 68: The impact of temperature on the Biogas, Biogas/g-VS and CH_4/g-VS.

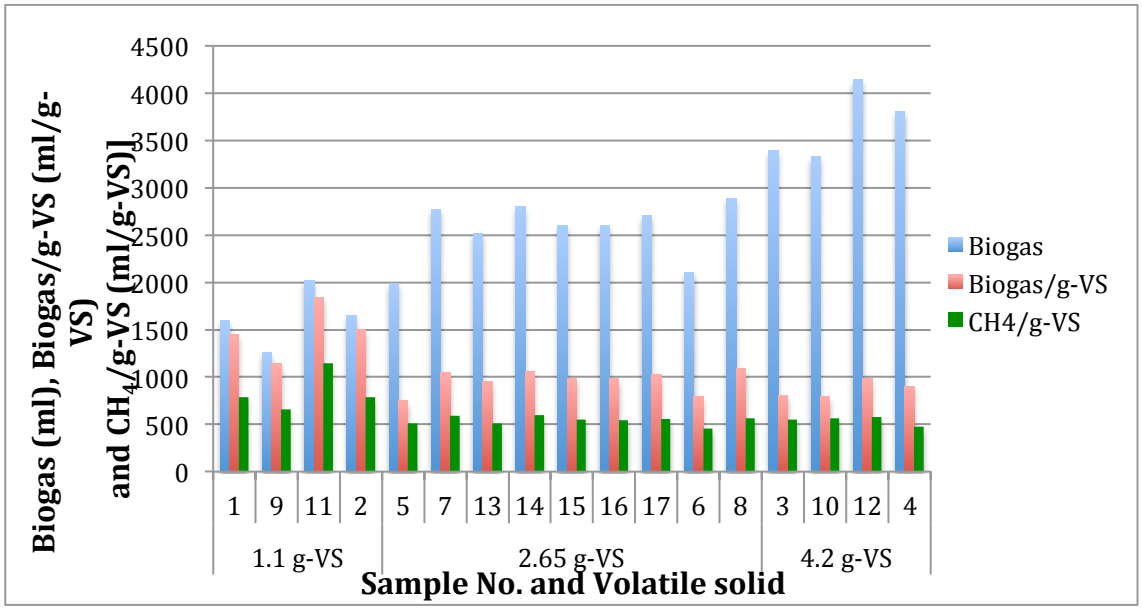

Figure 69: The infulence of volatile solid added value on the Biogas, Biogas/g-VS and CH_4/g-VS.

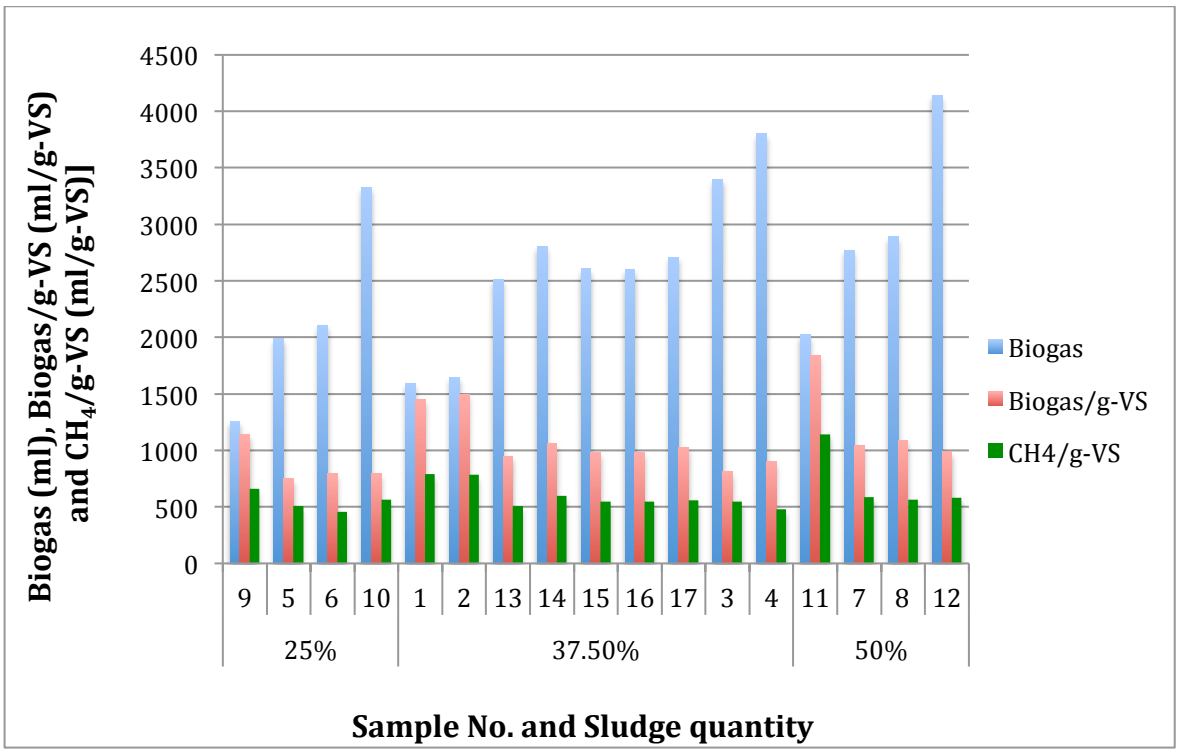

Figure 70: The effect of increasing the slaudge quantity on the Biogas, Biogas/g-VS and CH_4/g-VS.

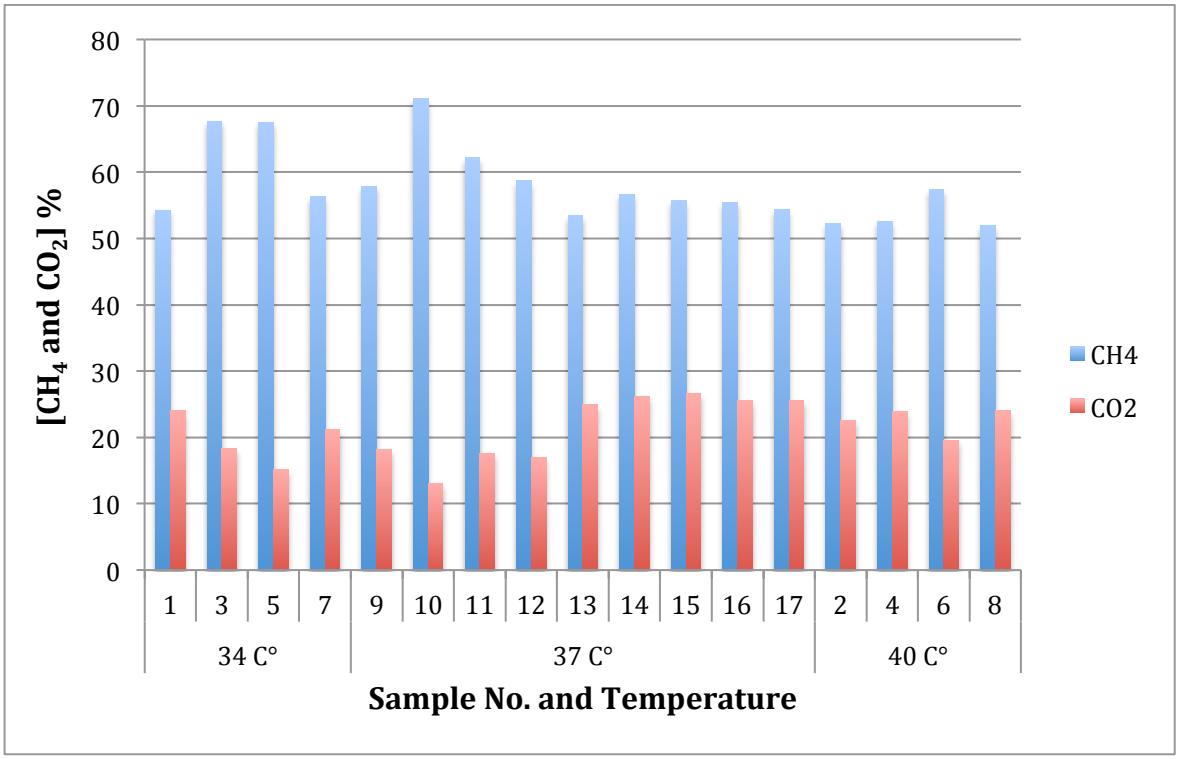

Figure 71: The alteration in biogas quality with temperature rise.

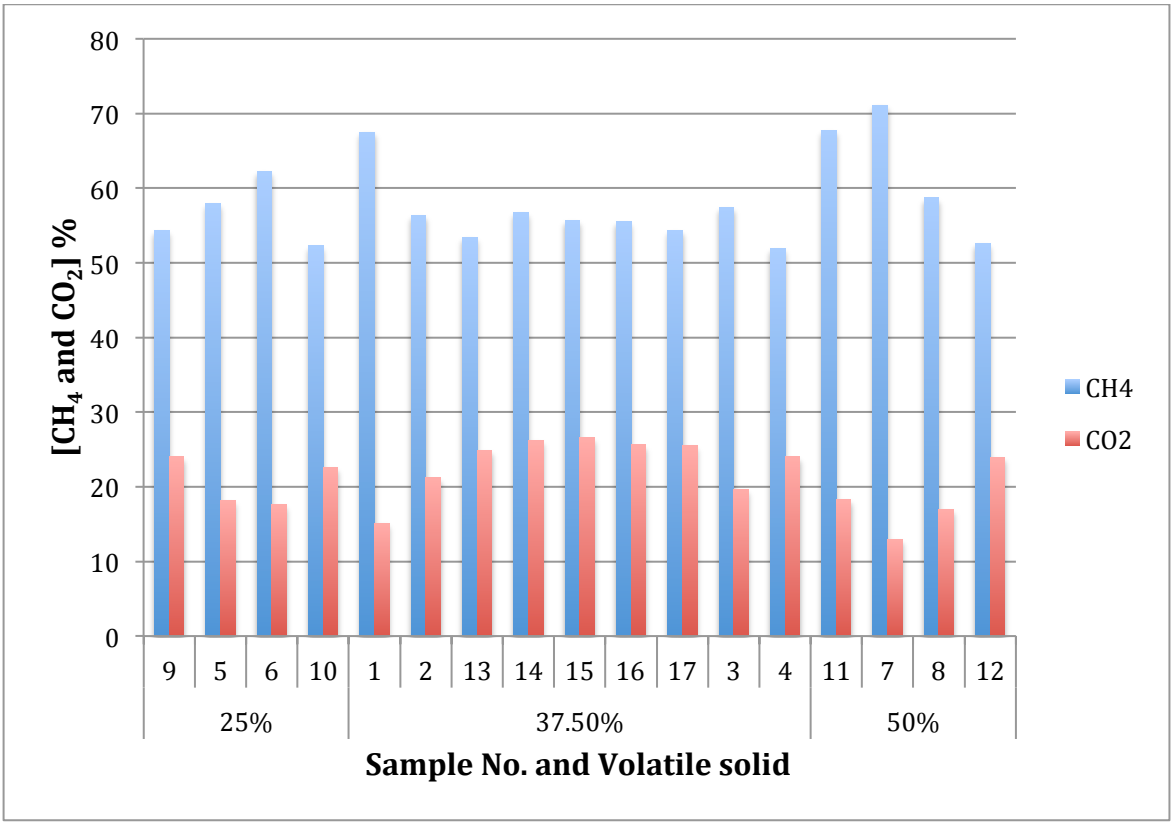

Figure 72: Shifting in biogas quality at different volatile solid values.

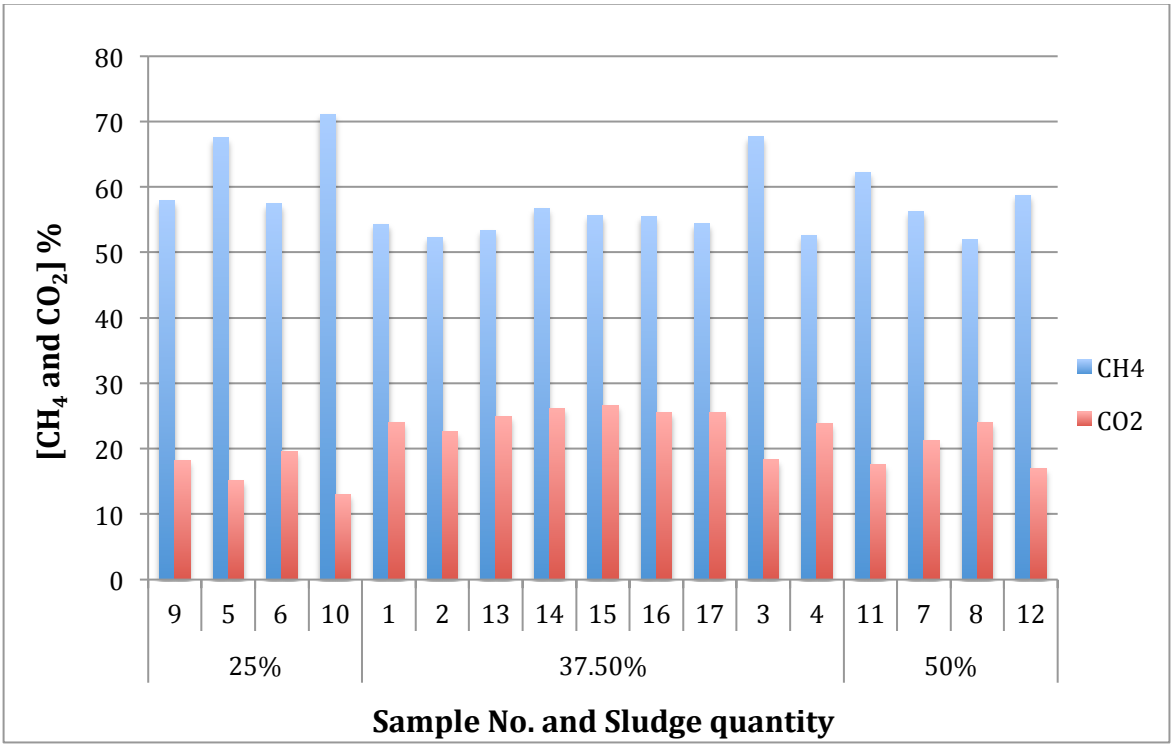

Figure 73: The impact of sludge quantity on CH_4% and CO_2%.

The ANOVA tables 34-38 show that all models were significant. The coded equations (16, 18, 20, 22 and 24) and the actual equations (17, 19, 21, 23 and 25) are shown below with each response. The influences of volatile solid (B) and sludge quantity (C) were significant for all responses, while there was no significant influence of temperature (A) on the Biogas/g-VS and CH_4/g-VS. The interaction of (BC) had a significant influence on the Biogas/g-VS, CH_4% and CH_4/g-VS responses. In contrast, the CH_4% and CO_2% were significantly affected by the interaction of temperature and volatile solid (AB). There was no significant influence for the interaction between the temperature and the amount of the sludge (AC) on all responses.

4.4.2 Biogas

As its clear from Figure 74, the highest biogas produced was found at added volatile solid of 4.2 g-VS. Also, it is clear that the biogas produced was directly proportional to the volatile solid and sludge quantity. This is in line with what Igoni et al. [390] mentioned that the volume of biogas increased with an increase in the volatile value in the batch reactor. The biogas produced was slightly affected by temperature variation as shown in Figure 74. This differs from what was stated in Lattieff [167], where the volume of biogas produced decreased by 27% when the temperature changed from 37 °C to 55 °C. This difference may be due to that the reaction changed from mesophilic to thermophilic condition and recycled digestate used. Figure 75 illustrates that the highest biogas produced was at volatile solid of 4.2 g-VS and at any temperatures. The coded equation (16) demonstrates that the most factor affect the biogas volume was the volatile solid added followed by sludge quantity and temperature. The effect of these factors on the biogas yield were a positive effect. However, this effect was on the quantity of biogas only. The effect of the factors on the quality of the biogas will be discussed later.

The coded equation (16) for Biogas is:

$$\text{Biogas} = 2619.21 + 6.75*A + 1018.00*B + 393.00*C - 145.97*A^2 + 102.53 \quad \text{Equation (16)}$$

The actual equation (17) for Biogas is:

$$\text{Biogas} = -23274.69295 + 1229.14474*\text{Temperature} + 430.59751*\text{Volatile Solid} + 31.44000*\text{Sludge Quantity} - 16.21930*\text{Temperature}^2 + 42.67485*\text{VolatileSolid}^2 \quad \text{Equation (17)}$$

Table 34: ANOVA table for the Biogas Response.

Source	Sum of Squares	df	Mean Square	F-value	p-value	
Model	9.714E+06	5	1.943E+06	191.40	< 0.0001	Significant
A-Temperature	60204.50	1	60204.50	5.93	0.0331	
B-Volatile Solid	8.291E+06	1	8.291E+06	816.77	< 0.0001	
C-Sludge Quantity	1.236E+06	1	1.236E+06	121.73	< 0.0001	
A^2	89968.45	1	89968.45	8.86	0.0126	
B^2	44382.50	1	44382.50	4.37	0.0605	
Residual	1.117E+05	11	10150.41			
Lack of Fit	62619.75	7	8945.68	0.7297	0.6648	Not significant
Pure Error	49034.80	4	12258.70			
Cor Total	9.826E+06	16				
Adequacy measuring tools	R^2= 0.9886	Adjusted R^2=0.9835			Predicted R^2= 0.9737	

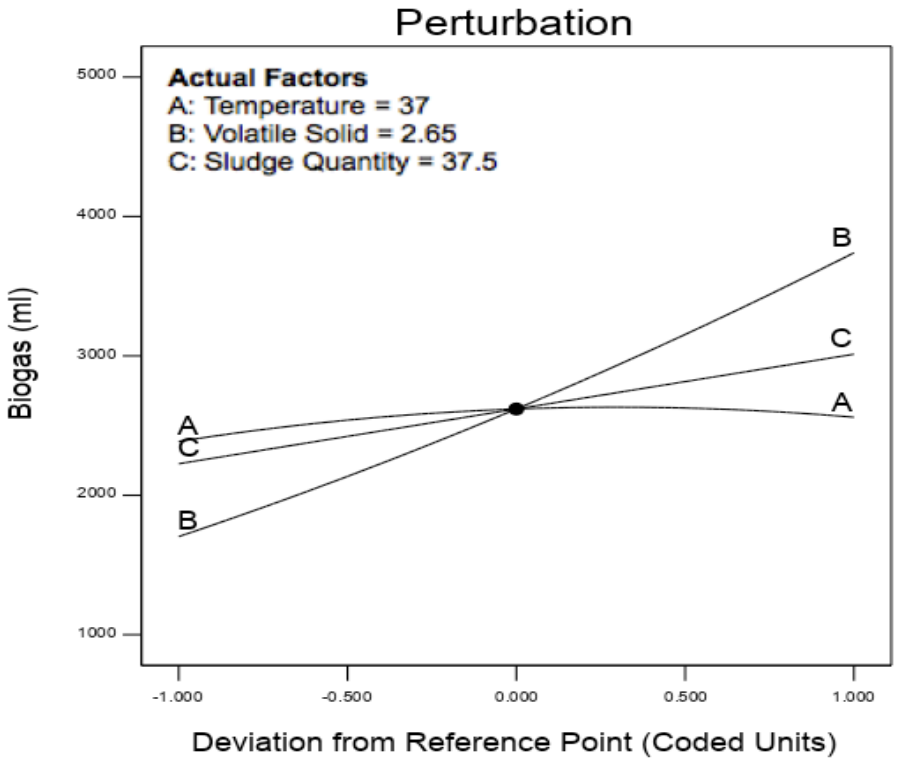

Figure 74: Perturbation plot shows the effect of all factors on Biogas volume.

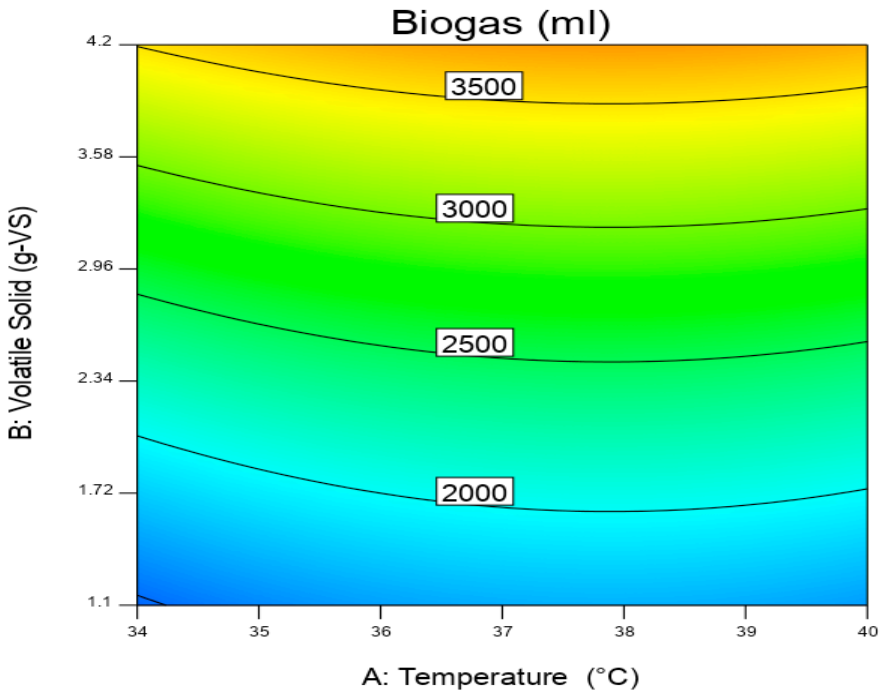

Figure 75: Contour plot views the effect of Temperature and Volatile solid on Biogas volume at sludge quantity of 37.5%.

4.4.3 Biogas/g-VS

According to Figure 76 it can be seen that, the highest amount of Biogas per gram volatile solid added produced was found at volatile solid of 1.1 g-VS. The reason for that when calculating the amount of Biogas/g-VS the biogas produced (divided by the volatile solid value). The higher the volatile solid value, the less volume of Biogas/g-VS achieved and vice versa. In contrast, direct proportion between the sludge quantity and the volume of Biogas/g-VS produced. The effect of temperature on Biogas/g-VS remained low. Figure 77 shows the interaction effect between volatile solid added and sludge quantity on the response. It is evidence from this figure that, by using volatile solid of 1.1, the maximum Biogas/g-VS of 1800 ml/g-VS could be achieved if the sludge quantity is kept at 50%. From Figure 77, using a volatile solid of 4.2 g-VS, the amount of Biogas/g-VS decreased to around 900 ml/g-VS, observing that there is no significant difference between both sludge quantities. This is due to the increase of feedstock that lead to inhibit the reaction thus the biogas produced decreased [160]. The effect of the volatile solid and the sludge quantity on the response was illustrated in Figure 78. It shows that the maximum Biogas/g-VS yield was when the volatile solid at its minimum values, sludge quantity more than 45% and 37 °C. The effect of added volatile solid was highest on Biogas/g-VS followed by sludge quantity and the interaction between them according to the coded equation (18). The effect of volatile

solid and its interaction with the sludge quantity were negative. While increasing the amount of sludge positively affected the Biogas/g-VS.

The coded equation (18) for Biogas/g-VS is:

$$\text{Biogas/g-VS} = 987.45 + 29*A - 304.56*B + 185.14*C - 125.95*BC + 216.62*B^2 \quad \text{Equation (18)}$$

The actual equation (19) for Biogas/g-VS is:

$$\text{Biogas/g-VS} = -7466.97499 + 444.71798*\text{Temperature} - 430.58564*\text{Volatile Solid} + 32.03771*\text{Sludge Quantity} - 6.50065*\text{Volatile Solid} * \text{Sludge Quantity} \; 5.87851*\text{Temperature}^2 + 90.16375*\text{Volatile Solid}^2 \quad \text{Equation (19)}$$

Table 35: ANOVA table for Biogas/g-VS Response.

Source	Sum of Squares	df	Mean Square	F-value	p-value	
Model	1.292E+06	6	2.153E+05	95.70	< 0.0001	Significant
A-Temperature	6786.12	1	6786.12	3.02	0.1131	
B-Volatile Solid	7.421E+05	1	7.421E+05	329.86	< 0.0001	
C-Sludge Quantity	2.742E+05	1	2.742E+05	121.89	< 0.0001	
BC	63453.61	1	63453.61	28.21	0.0003	
A^2	11818.45	1	11818.45	5.25	0.0449	
B^2	1.981E+05	1	1.981E+05	88.07	< 0.0001	Not significant
Residual	22496.34	10	2249.63			
Lack of Fit	15519.96	6	2586.66	1.48	0.3662	
Pure Error	6976.39	4	1744.10			
Cor Total	1.314E+06	16				
Adequacy measuring tools	R^2= 0.9829	Adjusted R^2= 0.9726			Predicted R^2= 0.9221	

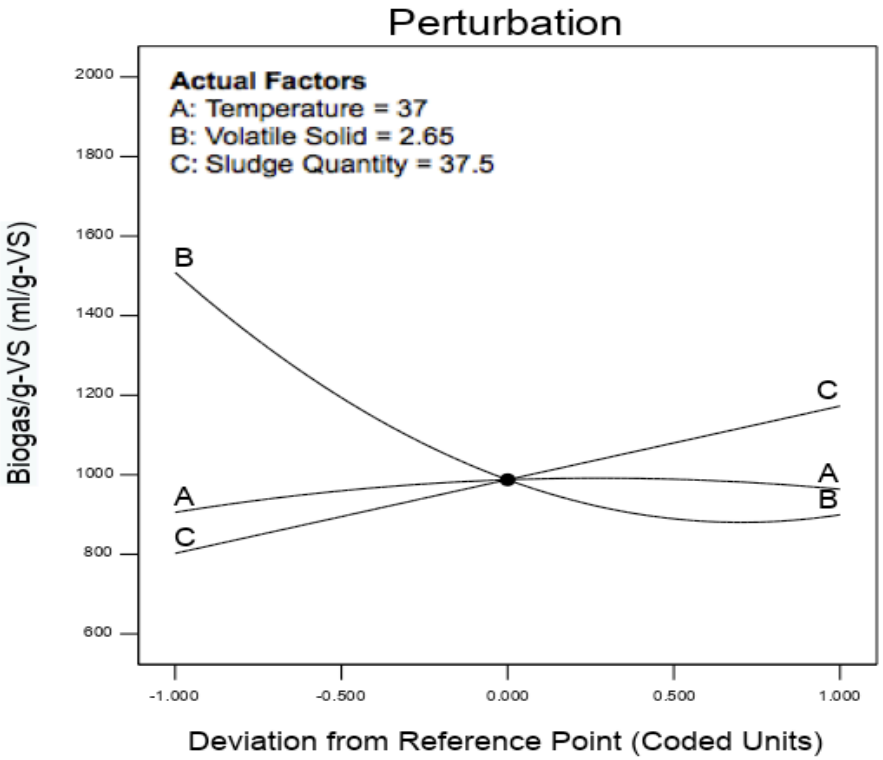

Figure 76: Perturbation plot illustrates the effect of all factors on Biogas/g-VS.

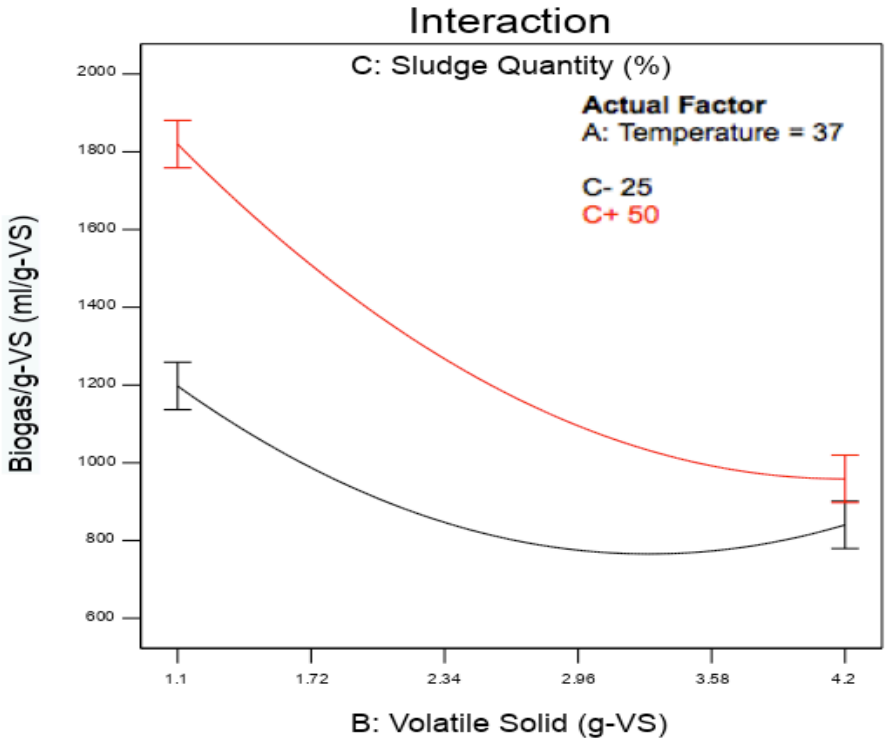

Figure 77: Interaction plot clarifies the effect of interaction between volatile solid and sludge quantity on Biogas/g-VS.

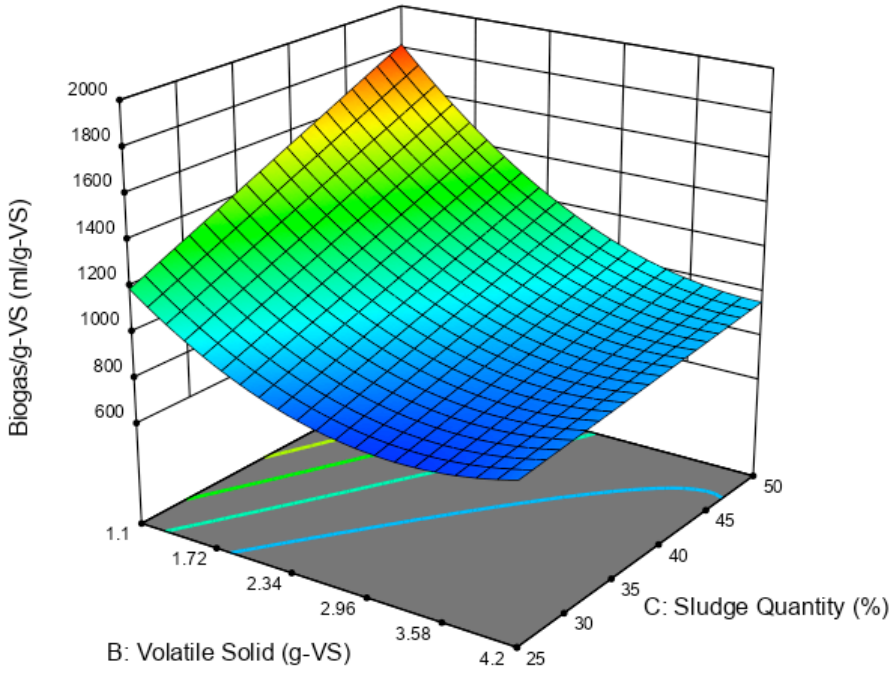

Figure 78: 3-D surface plot displays the effect of volatile solid and sludge quantity on Biogas/g-VS at 37 °C.

4.4.4 Methane Percentage

It is evident from Figure 79 that the highest amount of methane percentage (CH_4%) was achieved at 25% sludge quantity. The figure shows that the increase of temperature and sludge quantity had a negative effect on the CH_4%. An increase in temperature lead to instability in the reaction and an increase in the proportion of ammonia, thereby less methane production [167, 391]. The quantities of minerals present in the sludge influences on the methane production. Sludge containing large amounts of Ni and Mo helps in improving the digestion process. While, an increase of Al and Zn proportions in the sludge leads to inhibit the digestion process [389]. The negative effect of sludge quantity remained until it reached the centre value and then rose slightly. From Figures 80 and 81 it can be seen that the two interaction effects between volatile solid added and both temperature and sludge quantity. The more volatile solid added lead to an increase in CH_4%. The ratio of feedstock to inoculum is an important factor in the AD process [392]. Setting this ratio plays a major role in stabilising the digestion process and the biogas yield. Increasing this ratio gives high methane production in a longer incubation period. On the other hand, the intermediate ratio gives a high yield of methane over a shorter time [392]. It is

clear from Figure 80 that the methane percentage decreased as the temperature rose given that no difference in percentage of volatile solid at both settings was observed at 40 °C. Figure 81 illustrates that the CH_4% reached to its peak at value of 4.2 g-VS and sludge quantity of 25%. This percentage decreased sharply by decreasing the volatile solid value from 4.2 g-VS to 1.1 g-VS. The CH_4% was similar at a volatile solid of 1.5 g-VS for both sludge quantities (Figure 81). The coded equation (20) shows the effect of the interaction between the volatile solid added and the sludge quantity were the highest on CH_4%. These effects are related to the quality of the biogas not the quantity.

The coded equation (20) for CH_4% is:

$$CH_4\% = 54.59-3.95*A + 2.93*B - 3.10*C - 3.28*AB - 4.17*BC + 2.82*B^2 + 4.37*C^2$$ Equation (20)

The actual equation (21) for CH_4% is:

$$CH_4\% = +64.75168+ 0.549731*\text{Temperature} + 29.79773*\text{Volatile Solid} - 1.7763*\text{Sludge Quantity} - 0.704301*\text{Temperature} * \text{Volatile Solid} - 0.215484*\text{Volatile Solid} * \text{Sludge Quantity} + 1.17531*\text{Volatile Solid}^2 + 0.027992*\text{Sludge Quantity}^2$$ Equation (21)

Table 36: ANOVA table for CH_4% Response.

Source	Sum of Squares	df	Mean Square	F-value	p-value	
Model	503.37	7	71.91	19.11	0.0001	Significant
A-Temperature	124.82	1	124.82	33.17	0.0003	
B-Volatile Solid	68.45	1	68.45	18.19	0.0021	
C-Sludge Quantity	76.88	1	76.88	20.43	0.0014	
AB	42.90	1	42.90	11.40	0.0082	
BC	69.72	1	69.72	18.53	0.0020	
B^2	33.66	1	33.66	8.95	0.0152	
C^2	80.77	1	80.77	21.47	0.0012	
Residual	33.86	9	3.76			
Lack of Fit	27.41	5	5.48	3.40	0.1297	
Pure Error	6.45	4	1.61			Not significant
Cor Total	537.23	16				
Adequacy measuring tools	R^2=0.9370	Adjusted R^2=0.8879			Predicted R^2=0.6893	

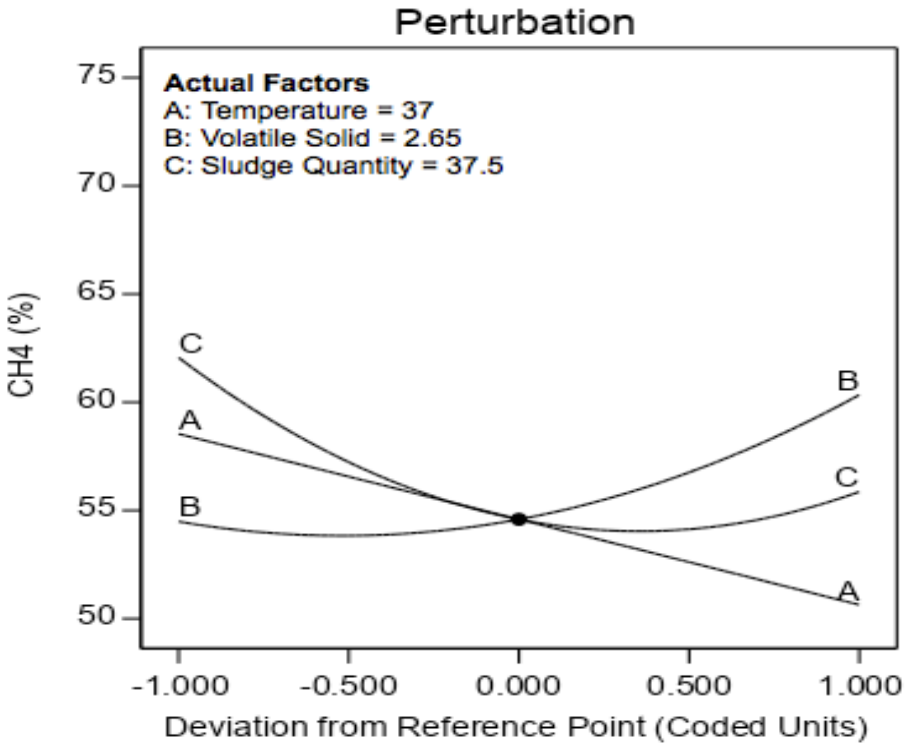

Figure 79: Perturbation plot clarifies the effect of all factors on CH_4%.

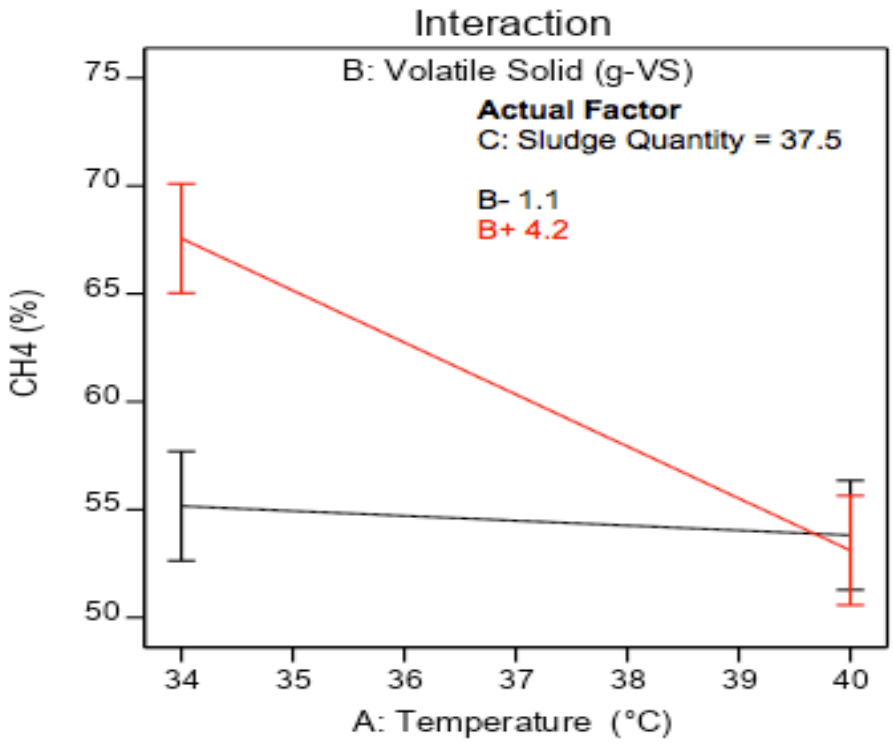

Figure 80: Interaction plot illustrates the effect of interaction between temperature and volatile solid on CH_4%.

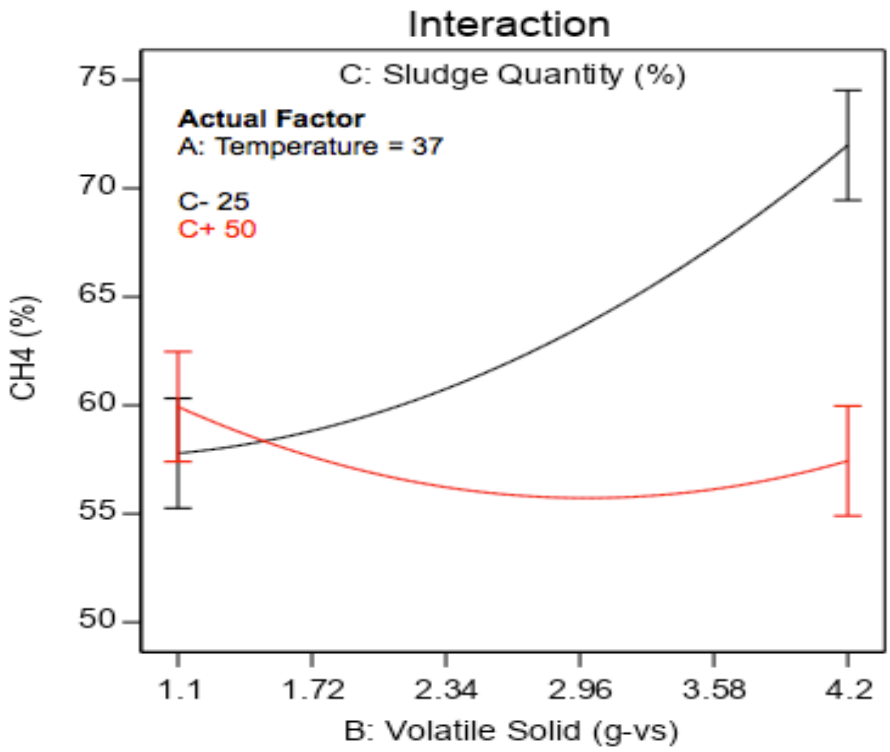

Figure 81: Interaction plot illustrates the effect of interaction between volatile solid and sludge quantity on CH_4%.

4.4.5 Carbon Dioxide Percentage

Figure 82 demonstrates that the lowest amount of CO_2% was achieved at sludge quantity of 25%, proving the inverse relationship between CH_4% and CO_2%. From the same figure it can be noticed that the CO_2% directly proportional with temperature. Furthermore, CO_2% increased by increasing the volatile solid and sludge quantity until they reach to the centre values. This was followed by a decreased in the CO_2% by increasing of the volatile solid and sludge quantity. Figure 83 shows the effect of interaction between temperature and volatile solid added on the response. It is clear from that the lowest CO_2% was found when using the volatile solid of 4.2 g-VS at 34 °C. Figure 84 illustrates the wide design space which produced the highest CO_2% at volatile solid between 1.7-3.6 g-VS, 37.5% sludge and at temperatures between 37-40 °C. The coded equation (22) shows the effect of the interaction between temperature and volatile solid added followed by the sludge quantity were the highest on carbon dioxide percentage:

$$CO_2\% = 25.75 + 1.44*A - 1.27*B + 1.74*C + 1.75*AB - 3.54*B^2 - 5.77*C^2 \qquad \text{Equation (22)}$$

The actual equation (23) for CO_2% is:

$$CO_2\% = -20.38186 - 0.518145*\text{Temperature} - 6.93040*\text{Volatile Solid} + 2.90784*\text{Sludge Quantity} + 0.376344*\text{Temperature} * \text{Volatile Solid} - 1.47489*\text{Volatile Solid}^2 - 0.036918*\text{Sludge Quantity}^2 \quad \text{Equation (23)}$$

Table 37: ANOVA table for CO_2% response.

Source	Sum of Squares	df	Mean Square	F-value	p-value	
Model	269.66	6	44.94	29.01	< 0.0001	Significant
A-Temperature	16.53	1	16.53	10.67	0.0085	
B-Volatile Solid	13.00	1	13.00	8.39	0.0159	
C-Sludge Quantity	24.15	1	24.15	15.59	0.0027	
AB	12.25	1	12.25	7.91	0.0184	
B^2	53.01	1	53.01	34.22	0.0002	
C^2	140.49	1	140.49	90.68	< 0.0001	
Residual	15.49	10	1.55			
Lack of Fit	13.76	6	2.29	5.30	0.0643	
Pure Error	1.73	4	0.4330			Not significant
Cor Total	285.16	16				
Adequacy measuring tools	R^2=0.9457	Adjusted R^2=0.9131			Predicted R^2=0.8232	

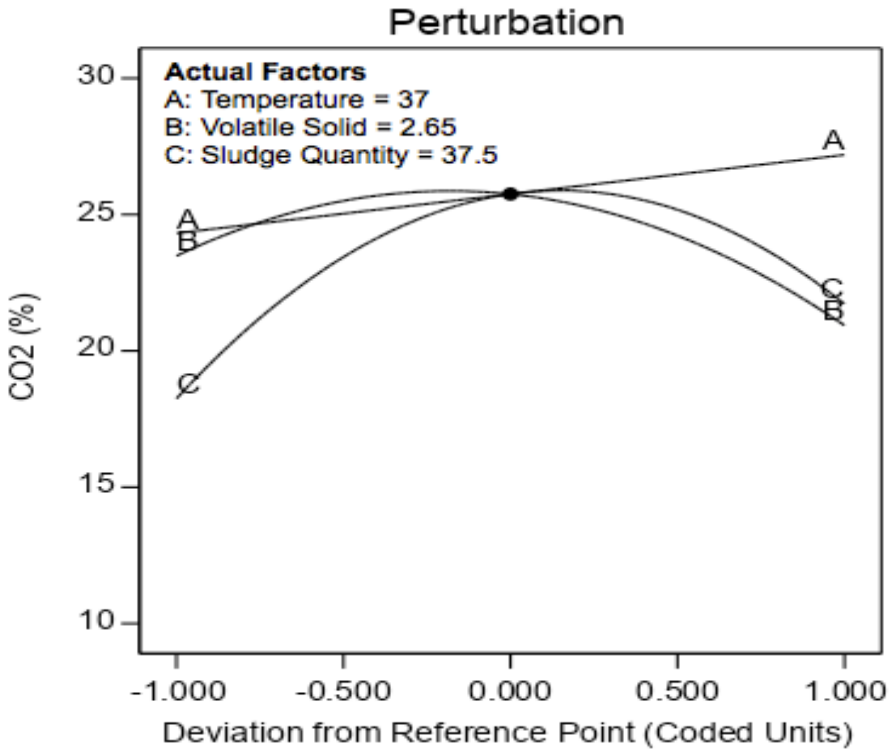

Figure 82: Perturbation plot shows the effect of all factors on CO_2%.

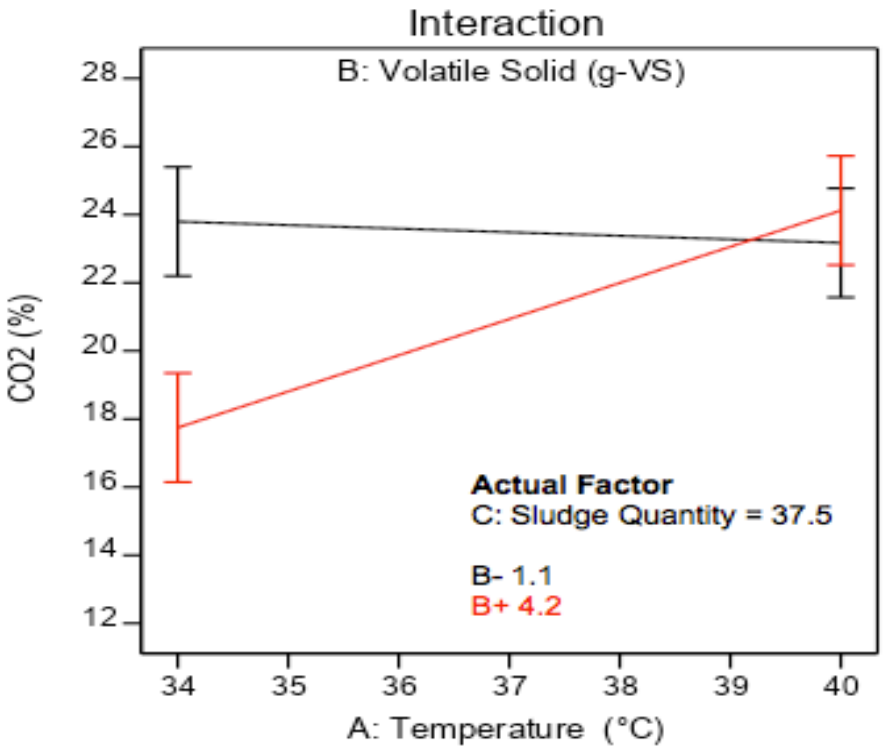

Figure 83: Interaction plot illustrates the effect of interaction between temperature and volatile solid on CO_2%.

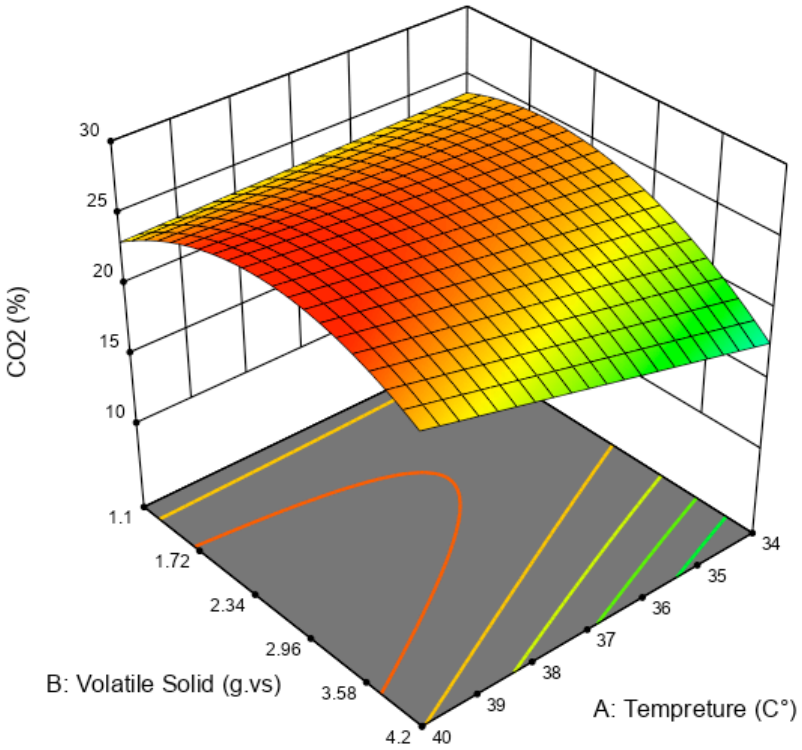

Figure 84: 3-D surface plot presents the effect of temperature and volatile solid on CO_2% at sludge quantity of 37.5%.

4.4.6 Methane/g-VS

The highest methane per gram volatile solid yield was found at the volatile solid of 1.1 g-VS. Figure 85 illustrates the indirect proportion between methane per g-VS and volatile solid added. The graph also shows that the CH_4/g-VS increased slightly by increasing the sludge quantity. Figure 86 shows the effect of the interaction between volatile solid added and sludge quantity on CH_4/g-VS. The highest methane per g-VS was found at a volatile solid of 1.1 g-VS and 50% of sludge quantity. In contrast, lower amounts of methane per g-VS were found at volatile solid of 4.0 g-VS and at both sludge quantity percentages. Although increasing the volatile solid amount increases the volume of biogas produced and the methane percentage, the highest CH_4/g-VS was found at lowest volatile solid amount. This is because when calculating the CH_4/g-VS, it was divided by amount of volatile solid. Therefore, the more volatile solid amount, the less CH_4/g-VS and vice versa. The coded equation (24) shows the highest indirect effect of volatile solid on CH_4/g-VS:

$$CH_4/g\text{-}VS = 564.93 - 18.47*A - 151.32*B + 86.28*C - 116.85*BC - 53.18*A^2 + 154.52B^2 \quad \text{Equation (24)}$$

The actual equation (25) for CH_4/g-VS is:

$$CH_4/g\text{-}VS = -7444.91102 + 431.13406*\text{Temperature} - 212.33504*\text{Volatile Solid} + 22.88406*\text{Sludge Quantity} - 6.03097*\text{Volatile Solid} * \text{Sludge Quantity} - 5.90936*\text{Temperature}^2 + 64.31458*\text{Volatile Solid}^2 \quad \text{Equation (25)}$$

Table 38: ANOVA table for CH_4/g-VS Response.

Source	Sum of Squares	df	Mean Square	F-value	p-value	
Model	4.093E+05	6	68219.69	28.85	< 0.0001	Significant
A-Temperature	2730.60	1	2730.60	1.15	0.3078	
B-Volatile Solid	1.832E+05	1	1.832E+05	77.48	< 0.0001	
C-Sludge Quantity	59547.00	1	59547.00	25.19	0.0005	
BC	54615.69	1	54615.69	23.10	0.0007	
A^2	11942.81	1	11942.81	5.05	0.0484	
B^2	1.008E+05	1	1.008E+05	42.64	< 0.0001	
Residual	23643.19	10	2364.32			Not significant
Lack of Fit	19257.75	6	3209.63	2.93	0.1589	
Pure Error	4385.44	4	1096.36			
Cor Total	4.330E+05	16				
Adequacy measuring tools	R^2=0.9454	Adjusted R^2=0.9126			Predicted R^2=0.7249	

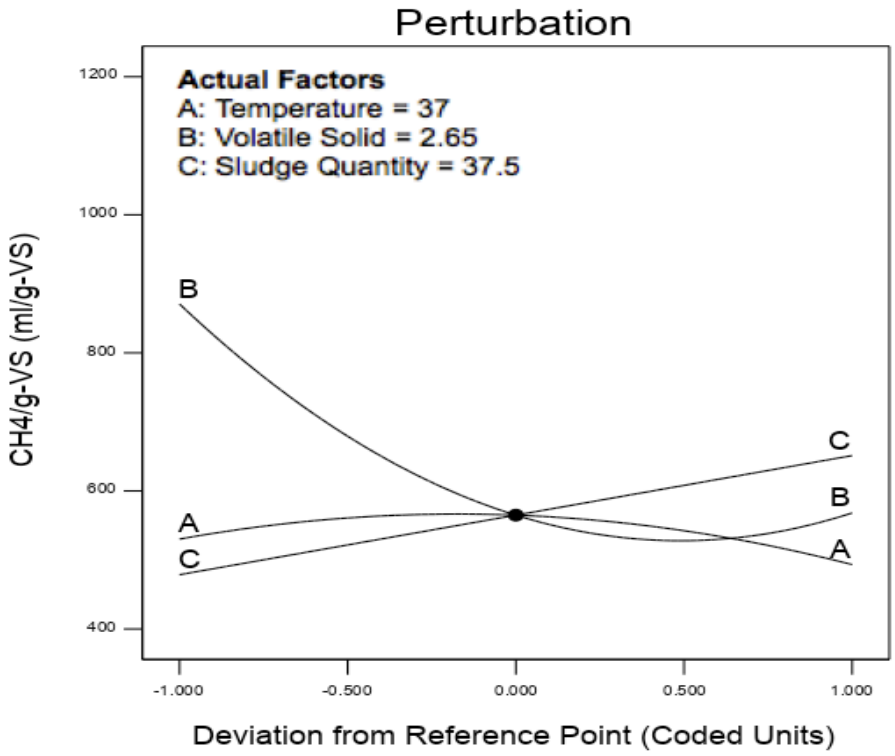

Figure 85: Perturbation plot presents the effect of all factors on CH_4/g-VS.

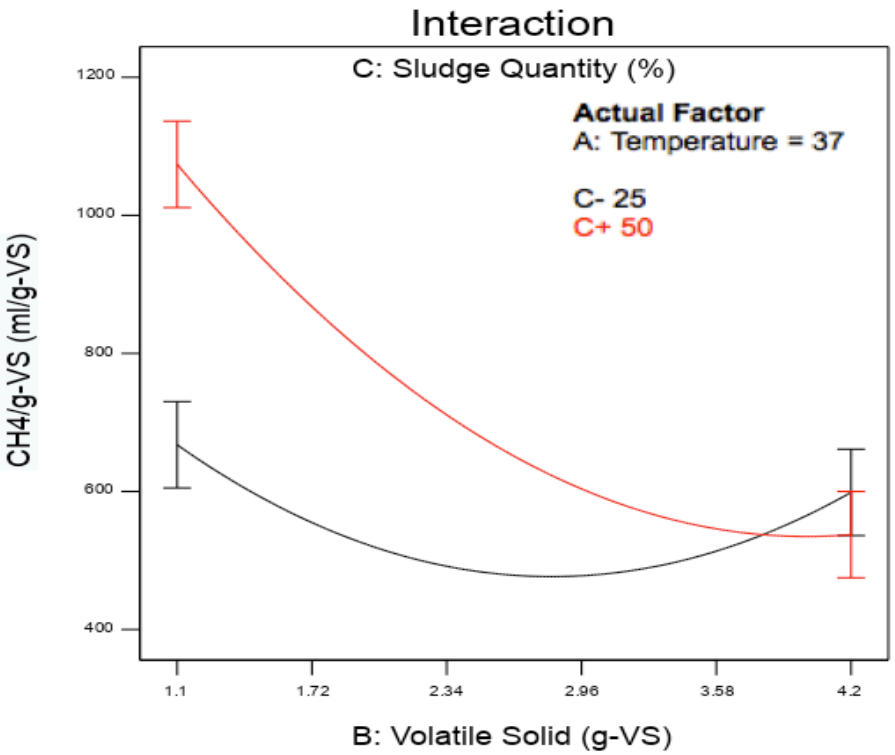

Figure 86: Interaction plot shows the effect of interaction between volatile solid and sludge quantity on CH_4/g-VS.

4.5 Extracted Oil Date Seed Results

Table 39 displays the biogas, CH_4% and methane produced from sludge only and The matrix of extracted oil date seed experiment is shown in Table 40. Figure 87 illustrates the influence of adding the extracted oil date seed on the biogas quantity. The volume of biogas reached 3,534 ml compared to 804 ml before adding date seeds at 37 °C. The same scenario also occurred at 34 °C and 40 °C however with a slightly less increase, as shown in Figure 87. It illustrates the conditions of experiment runs and the values of the responses. From Table 40 it can be seen the highest biogas yield was 3,534 ml (run #10) at 37°C, of 4.2 g-VS and 50% sludge. In contrast the lowest biogas volume was 971 ml (run #4) achieved at 37°C, 1.1 g-VS and 25% sludge. The difference in CH_4% in both cases was quite small at 56.5% and 54.6% respectively. The CH_4/g-VS was 482.5 ml/g-VS (run #4) at the lowest biogas yield, which is a little higher than the first case 475.7 ml/g-VS (run #10). That is due to a lower volatile solid of 1.1 g-VS was used in the second case and the higher volatile solid value (4.2 g-VS) was used in the first case.

Table 39: Biogas, CH_4% and methane obtained from sludge.

Temperature °C	Biogas (ml)	CH_4 (%)	CH_4 (ml)
34	1129	54.1	611
37	804	52.3	420
40	763	49.7	379

Table 40: The Experiment matrix.

Std.	Run	Factor 1	Factor 2	Factor 3	Resp. 1	Resp. 2	Resp. 3	Resp. 4	Resp. 5
		A*	B*	C*	Biogas	Biogas/g-VS	CH_4	CO_2	CH_4/g-VS
		°C	g-VS	%	ml	ml/g-VS	%	%	ml/g-VS
1	12	34	1.10	37.5	1407	1279.0	53.1	24.6	679.2
2	13	40	1.10	37.5	1479	1344.2	50.8	23.2	682.8
3	17	34	4.20	37.5	2933	698.4	65.4	19.3	457.0
4	3	40	4.20	37.5	3232	769.5	51.3	24.7	394.5
5	15	34	2.65	25.0	1699	641.1	66.2	16.6	424.7
6	11	40	2.65	25.0	1786	674.0	51.1	20.5	344.4
7	14	34	2.65	50.0	2579	973.2	53.9	22.7	524.5
8	1	40	2.65	50.0	2706	1021.1	50.7	24.8	517.3
9	4	37	1.10	25.0	971	883.1	54.6	19.4	482.5
10	5	37	4.20	25.0	2795	665.5	69.3	15.6	461.0
11	9	37	1.10	50.0	1711	1555.1	61.1	19.0	949.6
12	10	37	4.20	50.0	3534	841.4	56.5	18.8	475.7
13	16	37	2.65	37.5	2224	839.4	52.8	26.5	443.5
14	8	37	2.65	37.5	2346	885.2	51.2	27.4	453.2
15	7	37	2.65	37.5	2198	829.5	53.4	25.5	442.9
16	6	37	2.65	37.5	2048	772.9	52.4	26.6	405.2
17	2	37	2.65	37.5	2249	848.6	53.4	26.8	453.5

* *A= Temperature, B= Volatile solid, C= Sludge quantity.*

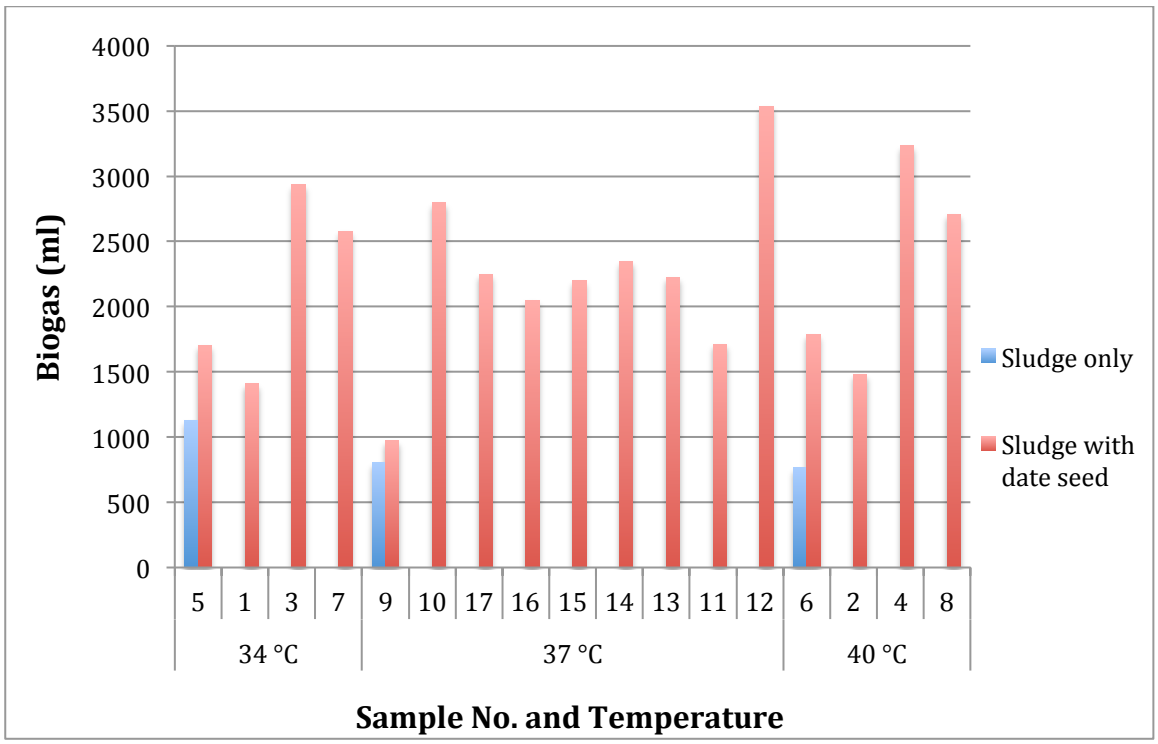

Figure 87: The considerable increase in biogas yield by adding extracted oil date seed.

Furthermore, the highest amount of biogas/g-VS was 1,555.1 ml/g-VS and the highest value of CH_4/g-VS was 949.6 ml/g-VS (run #9) were achieved at 37 °C, 1.1 g-VS and 50% sludge. On the other hand, the lowest value of biogas/g-VS was 641.1 ml/g-VS reported at 34°C, 2.65 g-VS, and 25% of the sludge (run #15). The minimum CH_4/g-VS was 344.4 ml/g-VS (run #11) was found at 40°C, 2.65 g-VS, and 25% sludge.

Methane percentage ranged between 50.7% and 69.3%, while CO_2% was between 15.6% and 27.4%. Table 40 illustrates the indirect relationship between CH_4% and CO_2%. The highest CH_4% and lowest CO_2% values were 37°C, 4.2 g-VS and 25% sludge (run #5). In contrast, the lowest CH_4% was found at the following conditions: 40 °C, 2.65 g-VS and 50% of the sludge (run #1). The highest CO_2% (run #8) was found at 37 °C, 2.65 g-VS and 37.5% of the sludge.

Figures 88 and 89 display the effect of added extracted oil date seeds on the quality of the resulting biogas. It is evident from Figure 88 that the CH_4% reached 69.3% when the date seeds were added compared to approximately 52.3% of sludge only at 37 °C and a little lower values of CH_4% at 34 °C. In contrast, at 40 °C, the effect of adding date seeds on CH_4% was insignificant. Figure 89 shows the effect of adding date seeds on the methane yield which increased more than five times at 37 °C from 379 ml to 1,997 ml.

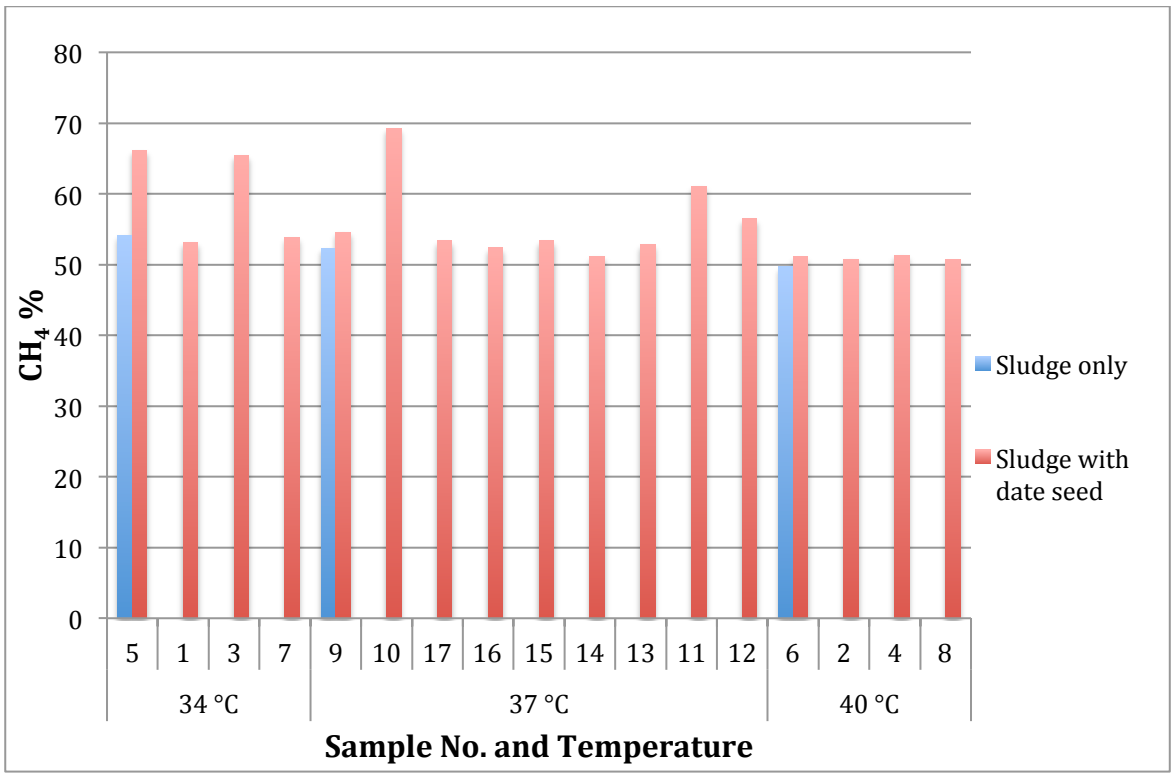

Figure 88: Different CH_4% after adding date seed.

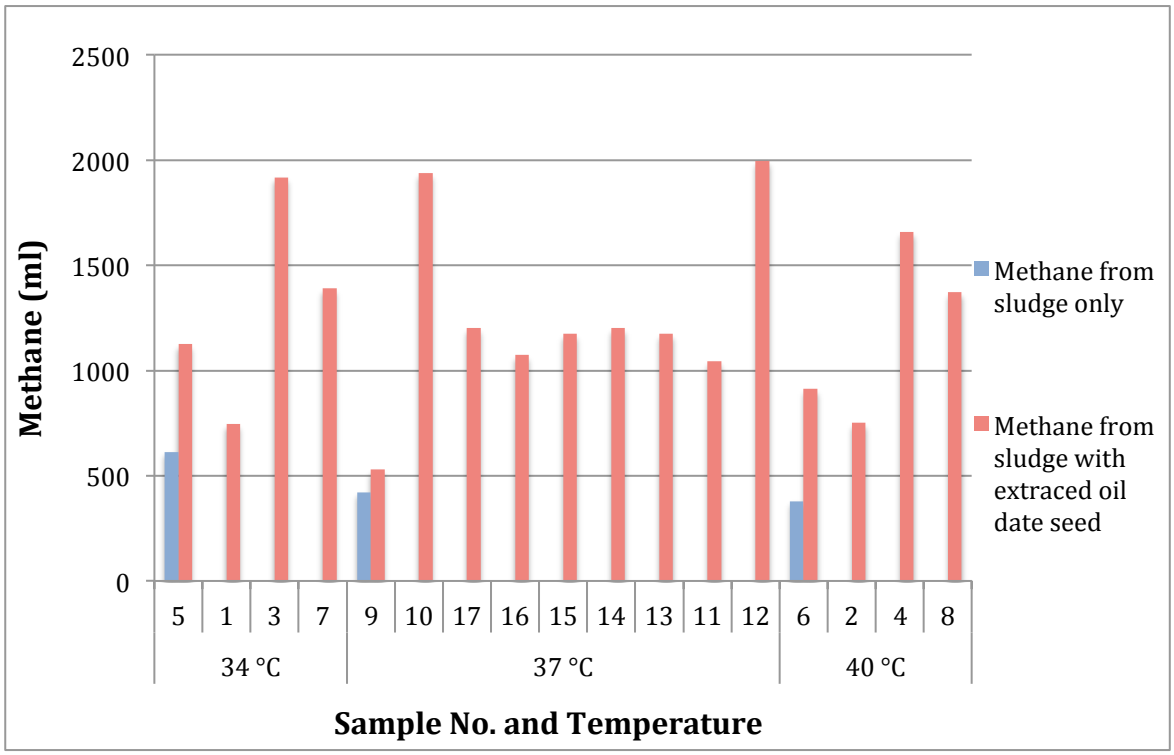

Figure 89: The effect of adding extracted oil date seed on methane volume

Comparing the amount of biogas/g-VS that was resulted from this study with the findings of Shanableh and Radeef (2017) [181], it can be seen that the biogas produced from this study was much higher, almost four times, noticing that the prepared samples were much lower than this study (30 ml of date seed/sludge mixtures). Furthermore, the methane yield from this study was higher approximately by the same proportion. The reason for this may be due to several factors; including the exposure of the date seeds to drying in the oven at 50 °C for 24 hours, crushing the date seeds by a steel hammer and different solvent used in the oil extraction process (mixture of methanol, chloroform and water). Also, the grinding process using a blender did not grind the core of the date seed so it was excluded [181]. The study found no significant difference between the quantities of biogas before and after oil extraction, which is corresponded with this study. The use of small quantities of date seed/sludge mixtures (30 ml) may be the reason for the differences in biogas quantities been somewhat similar, especially during the three-week retention time [181].

4.5.1 Model Estimation

Figures 90-92 display the effects of factors on Biogas, Biogas/g-VS and CH_4/g-VS quantities, while Figures 93-95 demonstrates their effect on CH_4% and CO_2%. It is evident from the Figures 90-92 that at 37 °C, 1.1 g-VS and 50% of sludge, produced the highest biogas/g-VS and CH_4/g-VS but not the highest biogas yield. The highest biogas yield was 3,534 ml at 37 °C, 4.2 g-VS and 50% sludge.

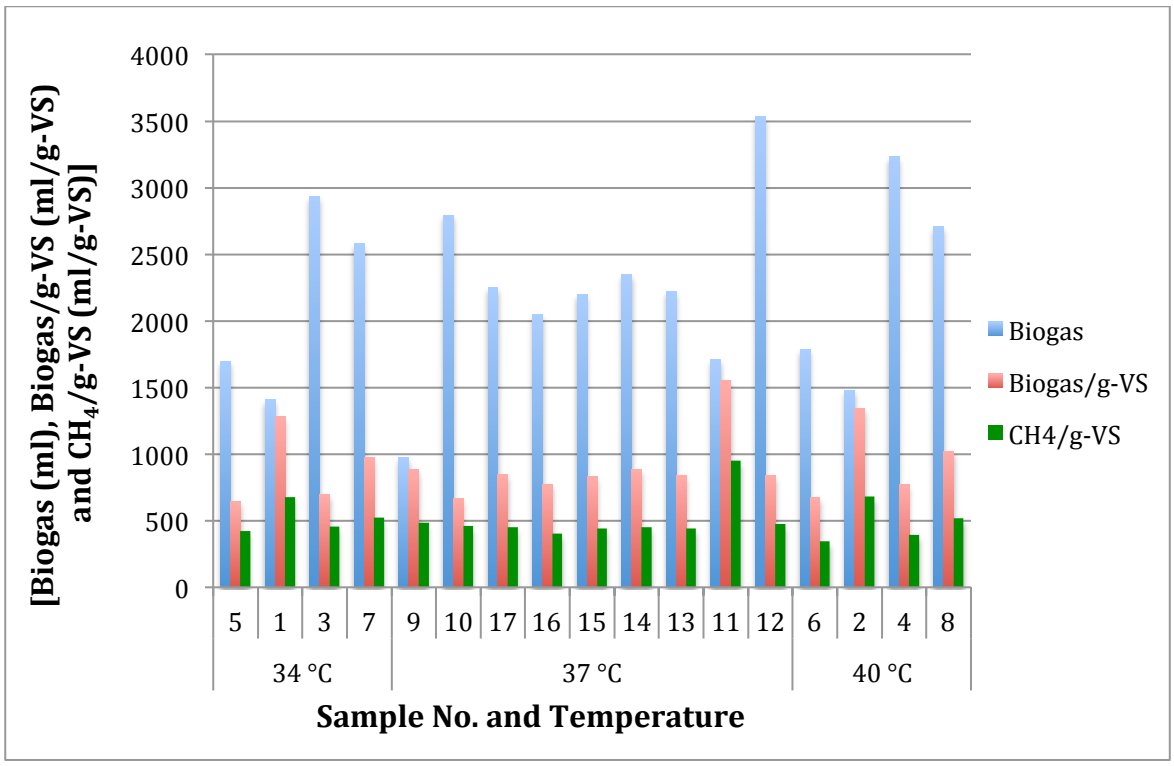

Figure 90: The effect of temperature alteration on Biogas, Biogas/g-VS and CH_4/g-VS yields.

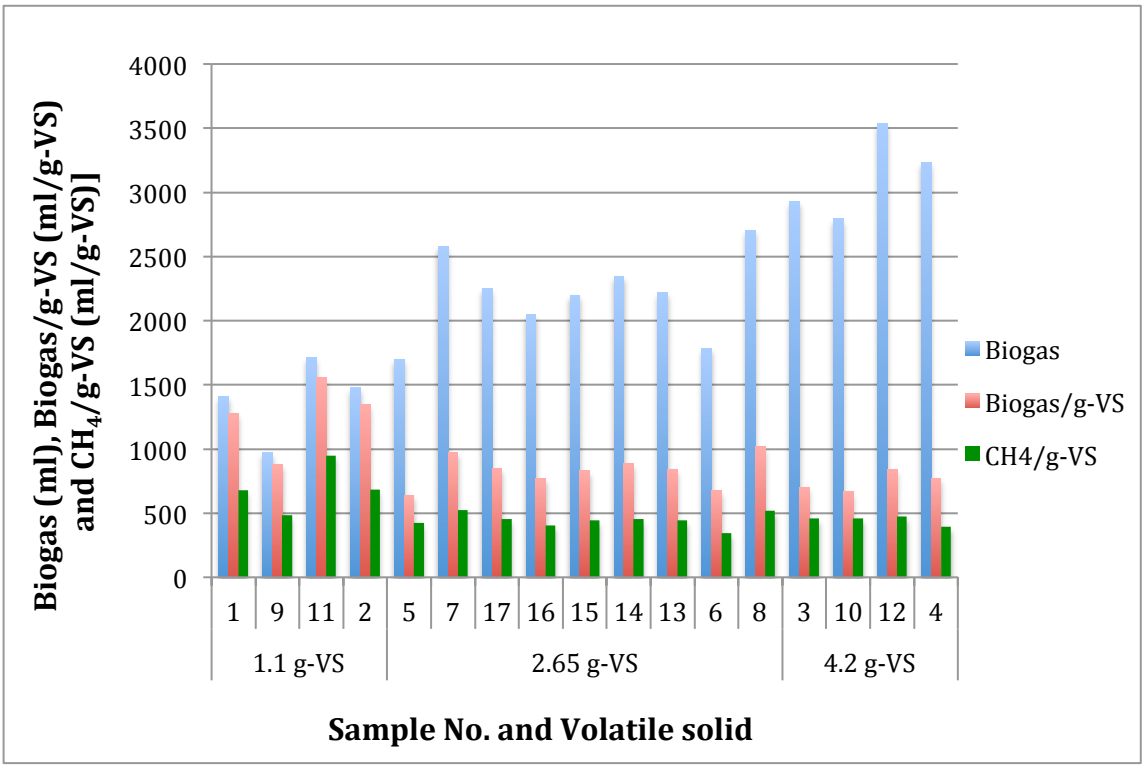

Figure 91: The increase in Biogas, Biogas/g-VS and CH_4/g-VS volumes with volatile solid values increase.

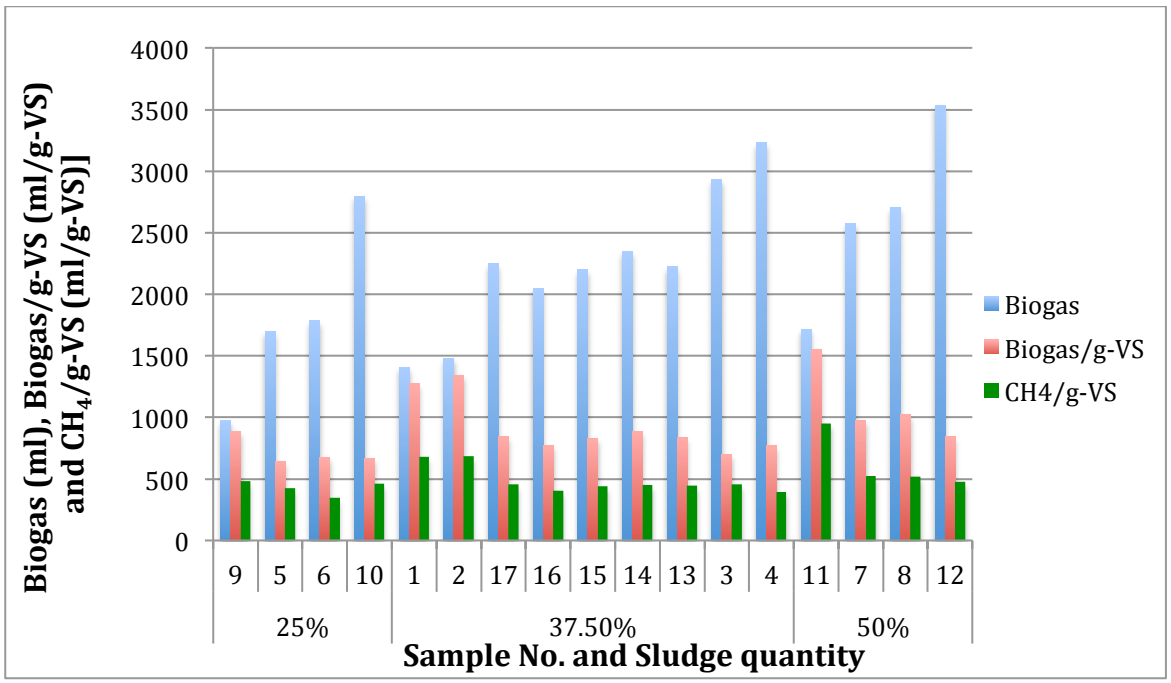

Figure 92: The influence of sludge quantity on the Biogas, Biogas/g-VS and CH_4/g-VS quantities.

The factors had different effects on CH_4% and CO_2%, as shown in Figures 93-95. The highest CH_4% and the lowest CO_2% were 69% and 13% at 37 °C. The values of volatile solid and sludge were 4.2 g-VS and 25%.

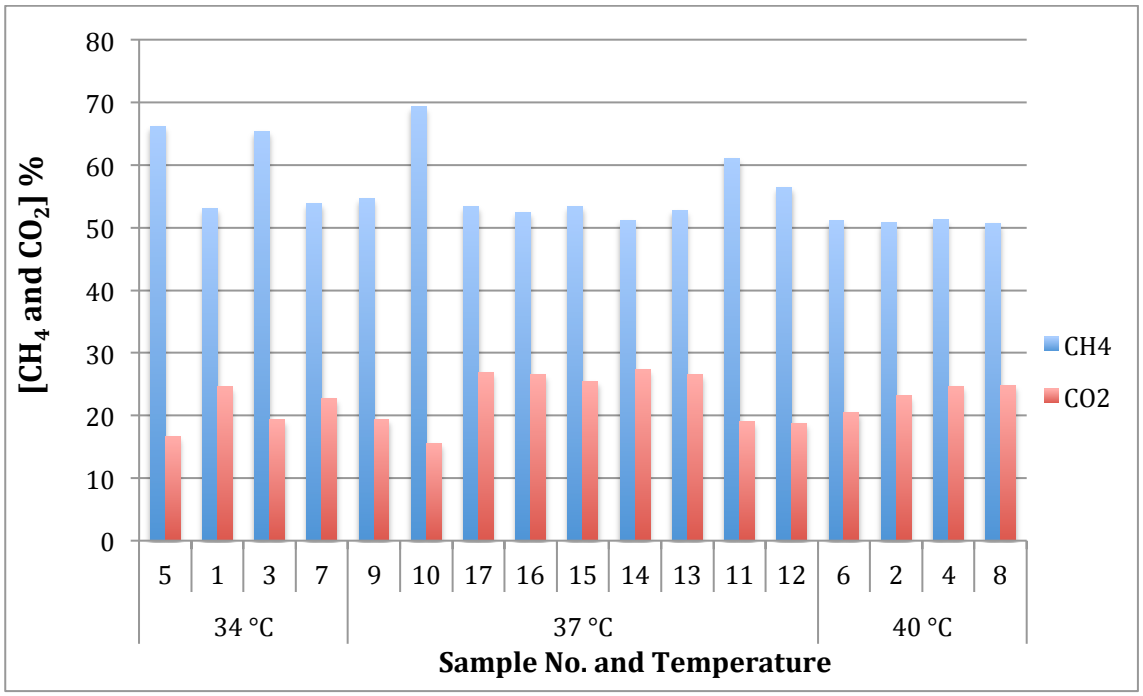

Figure 93: The impact of temperature on the biogas quality.

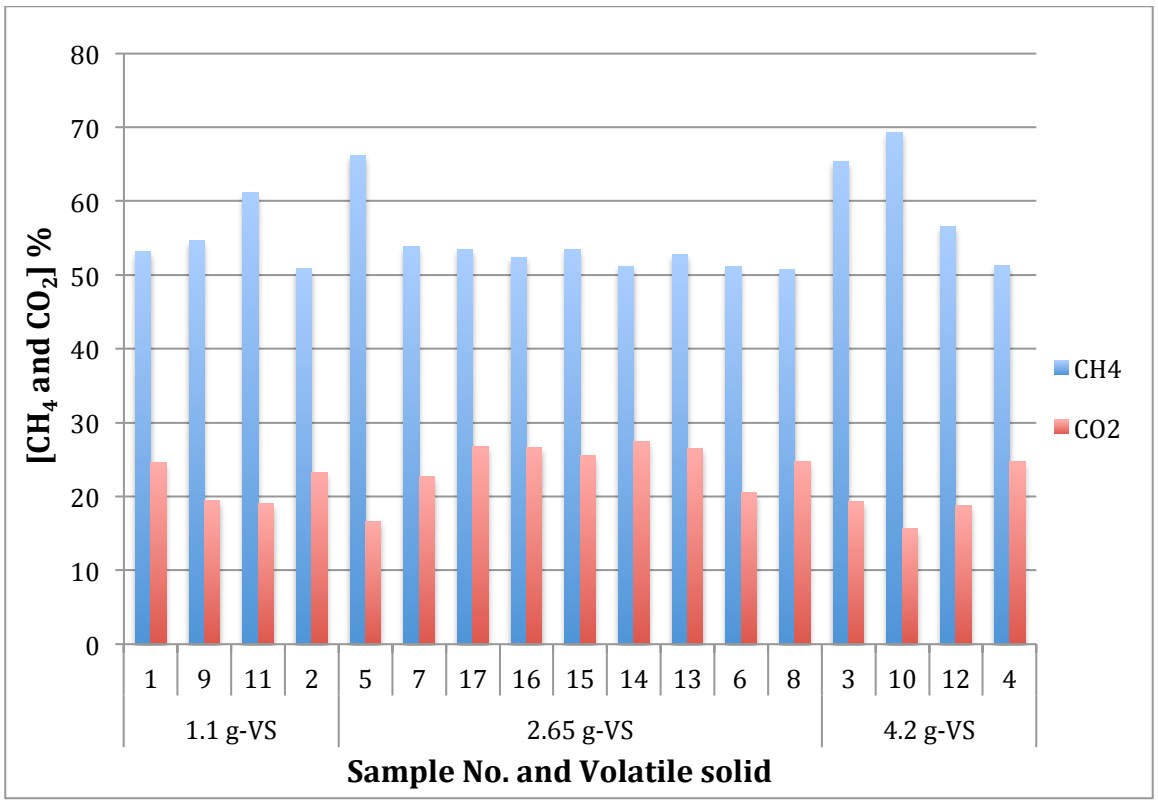

Figure 94: The volatile solid value effect on CH_4% and CO_2%.

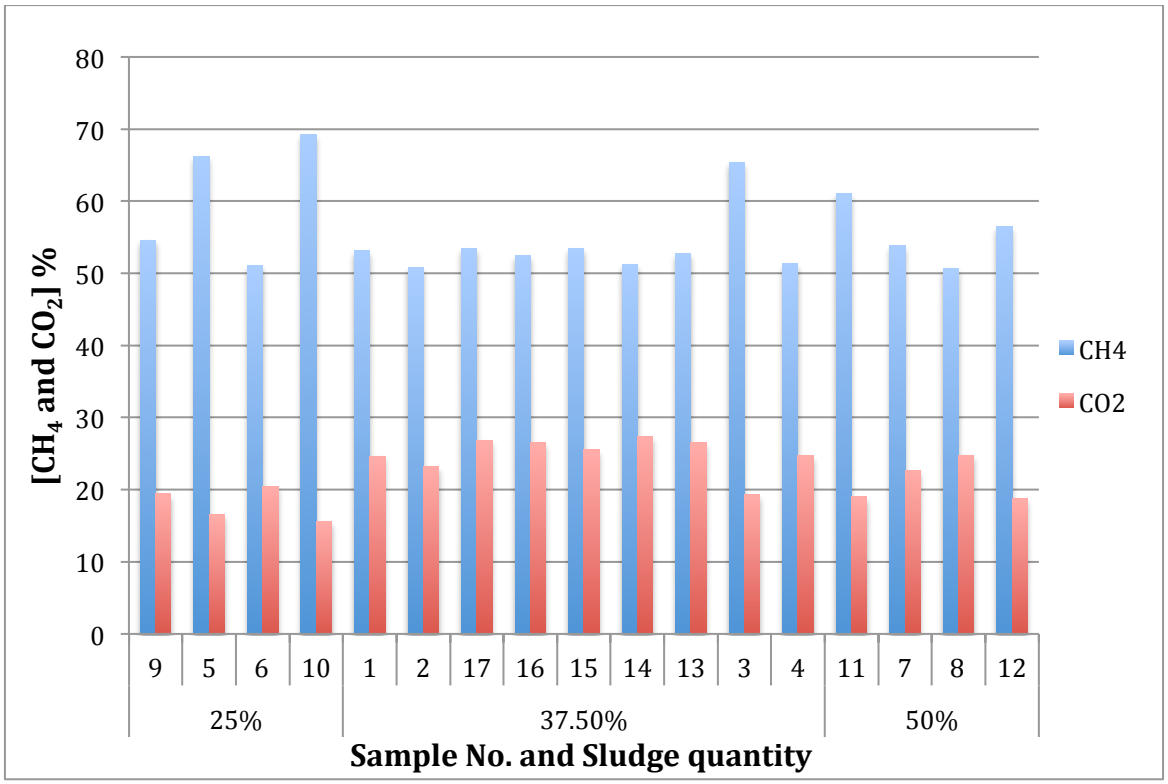

Figure 95: The influence of different sludge quantities on the CH_4% and CO_2%.

The ANOVA Tables 41-45 show that all models were significant. The coded equations (26, 28, 30, 32 and 34) and the actual equations (27, 29, 31, 33 and 35) are shown below with each response. The influences of volatile solid (B) and sludge quantity (C) were significant on all responses, while there was no significant influence of temperature (A) on the biogas/g-VS and CH_4/g-VS. The interaction of (BC) had a significant influence on the biogas/g-VS, CH_4% and CH_4/g-VS responses. In contrast, the CO_2% were significantly affected by the interaction of temperature and volatile solid (AB). There was significant influence for the interaction between the temperature and the amount of the sludge (AC) only on CH_4%.

4.5.2 Biogas

From Figure 96, it can be seen that the highest biogas achieved was found at 4.2 g-VS of volatile solid. The same figure shows that the biogas yield is directly proportional to the volatile solid added and sludge quantity. This corresponds to what was stated in Shanableh and Radeef study [181]. At the incubation period of 3 weeks, when the date seeds/inoculum ratio increased, the biogas produced increased. Moreover, the study found that the inhibition decreased at 20% and 40% ratios due to the oil extraction from date seed which inhibits acid formation but not affected the microorganisms that forming the biogas. Also the figure shows the slight effect of temperature increased on the amount of biogas produced. Figure 97 demonstrates that the highest biogas was found at more than 3.7 g-VS of volatile solid, 50% of the sludge, and at all temperatures. The coded Equation (26) shows that the highest effect on the biogas volume was the volatile solid added followed by sludge quantity. These factors affected positively on the biogas yield and their effect was on the quantity of biogas only. The effect of the factors on the biogas in quality terms will be discussed later in this section.

The coded equation (26) for Biogas is:

$$\text{Biogas} = +2213.00 + 73.13*A + 865.75*B + 409.88*C + 56.75*AB + 10.00*AC - 0.2500*BC - 5.25*A^2 + 55.00*B^2 - 15.25*C^2 \quad \text{Equation (26)}$$

The actual equation (27) for Biogas is:

$$\text{Biogas} = -608.37227 + 25.20027*\text{Temperature} - 13.85883*\text{Volatile Solid} + 30.27753*\text{Sludge Quantity} + 12.20430*\text{Temperature} * \text{Volatile Solid} + 0.266667*\text{Temperature} * \text{Sludge Quantity} - 0.012903*\text{Volatile Solid} * \text{Sludge Quantity} - 0.583333*\text{Temperature}^2 + 22.89282*\text{Volatile Solid}^2 - 0.097600*\text{Sludge Quantity}^2 \quad \text{Equation (27)}$$

Table 41: ANOVA Table for the Biogas Response.

Source	Sum of Squares	df	Mean Square	F-value	p-value	
Model	7.410E+06	9	8.233E+05	72.54	< 0.0001	Significant
A-Temperature	42778.12	1	42778.12	3.77	0.0933	
B-Volatile Solid	5.996E+06	1	5.996E+06	528.33	< 0.0001	
C-Sludge Quantity	1.344E+06	1	1.344E+06	118.42	< 0.0001	
AB	12882.25	1	12882.25	1.14	0.3221	
AC	400.00	1	400.00	0.0352	0.8564	
BC	0.2500	1	0.2500	0.0000	0.9964	
A^2	116.05	1	116.05	0.0102	0.9223	
B^2	12736.84	1	12736.84	1.12	0.3246	
C^2	979.21	1	979.21	0.0863	0.7775	
Residual	79445.25	7	11349.32			
Lack of Fit	32889.25	3	10963.08	0.9419	0.4995	Not significant
Pure Error	46556.00	4	11639.00			
Cor Total	7.489E+06	16				
Adequacy measuring tools	R^2= 0.9894	Adjusted R^2=0.9758			Predicted R^2= 0.9200	

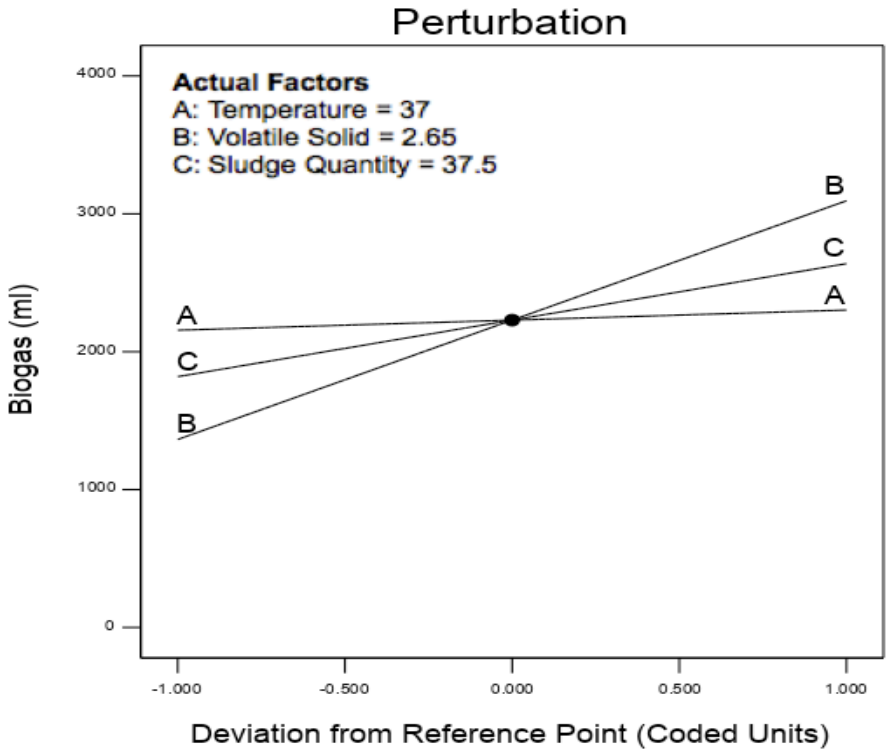

Figure 96: Perturbation plot views the effect of all factors on the biogas volume.

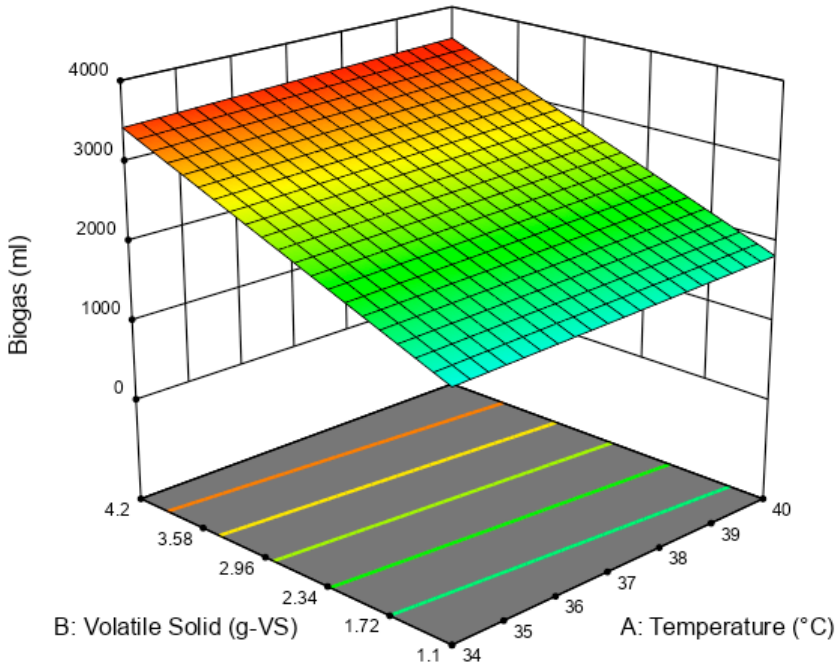

Figure 97: 3-D surface Plot shows the effect of Temperature and Volatile solid on the Biogas yield at sludge quantity of 50%.

4.5.3 Biogas/g-VS

According to Figure 98, it can be seen that the highest biogas/g-VS was achieved at a volatile solid of 1.1 g-VS, because when calculating the biogas/g-VS, the biogas produced was divided by the volatile solid added value. The biogas/g-VS is indirectly proportion with the volatile solid value, so the highest volume of biogas was achieved at the lowest volatile solid value. While the sludge quantity and temperature are directly proportion to the volume of biogas/g-VS produced, the interaction effect between volatile solid added and sludge quantity on the biogas/g-VS is illustrated in Figure 99. From that figure it can be seen that by using the lowest amount of volatile solid, the maximum biogas/g-VS of 1,600 ml/g-VS was achieved when the sludge quantity was 50%. Figure 99 also shows that at a volatile solid of 4.2 g-VS, the amount of biogas/g-VS drop sharply to around 800 ml/g-VS. It can be noted that there was no significant difference between biogas/g-VS values at 4.2 g-VS, 37 °C and both sludge quantities due to the inhibition of the reaction resulting from increased the volatile solid [160]. Figure 100 shows the effect of the volatile solid added and the sludge quantity on the biogas/g-VS. The highest biogas/g-VS produced was at a volatile solid of 1.1 g-VS and sludge quantity more than 45%.

The coded Equation (28) illustrates that the negative effect of volatile solid (B) was highest on biogas/g-VS followed by the positive effect of sludge quantity (C), the positive effect of the square of volatile solid (B^2) and the negative interaction (BC) between them (volatile solid and sludge quantity).

The coded equation (28) for Biogas/g-VS is:

$$\text{Biogas/g-VS} = +831.67 + 27.14*A - 260.82*B + 190.89*C - 124.02*BC + 172.86*B^2 \quad \text{Equation (28)}$$

The actual equation (29) for Biogas/g-VS is:

$$\text{Biogas/g-VS} = +239.37109 + 9.04583*\text{Temperature} - 309.55741*\text{Volatile Solid} + 32.23442*\text{Sludge Quantity} - 6.40129*\text{Volatile Solid} * \text{Sludge Quantity} + 71.94936*\text{Volatile Solid}^2 \quad \text{Equation (29)}$$

Table 42: ANOVA Table for Biogas/g-VS Response.

Source	Sum of Squares	df	Mean Square	F-value	p-value	
Model	1.030E+06	5	2.059E+05	115.06	< 0.0001	Significant
A-Temperature	5891.55	1	5891.55	3.29	0.0970	
B-Volatile Solid	5.442E+05	1	5.442E+05	304.06	< 0.0001	
C-Sludge Quantity	2.915E+05	1	2.915E+05	162.86	< 0.0001	
BC	61528.80	1	61528.80	34.38	0.0001	
B^2	1.266E+05	1	1.266E+05	70.70	< 0.0001	
Residual	19689.05	11	1789.91			
Lack of Fit	13078.11	7	1868.30	1.13	0.4805	Not significant
Pure Error	6610.95	4	1652.74			
Cor Total	1.049E+05	16				
Adequacy measuring tools	R^2= 0.9812	Adjusted R^2= 0.9727			Predicted R^2= 0.9333	

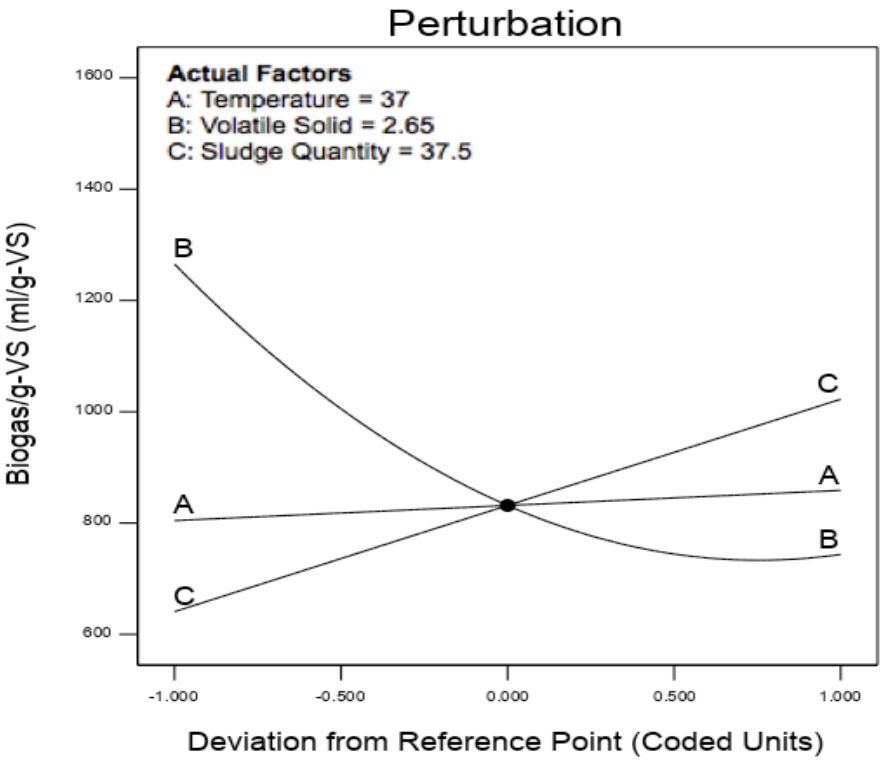

Figure 98: Perturbation plot illustrates the effect of all factors on the biogas/g-VS.

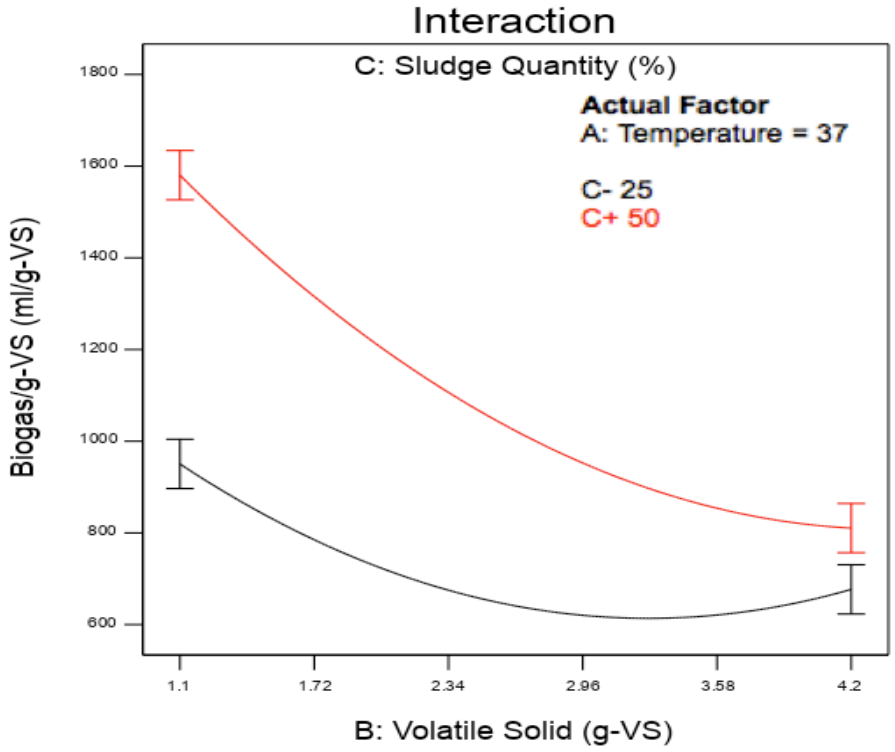

Figure 99: Interaction Plot clarifies the effect of interaction between volatile solid and sludge quantity on biogas/g-VS.

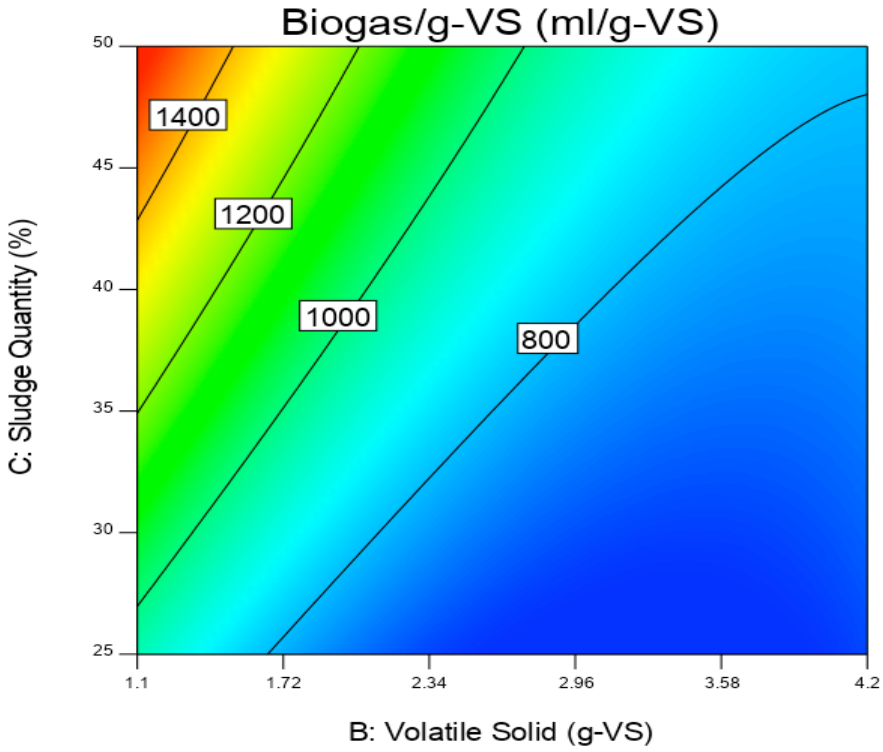

Figure 100: Contour Plot displays the effect of volatile solid and sludge quantity on the Biogas/g-VS at 37 °C.

4.5.4 Methane Percentage

The highest methane percentage was formed at 25% of sludge quantity as shown in Figure 101. The figure also illustrates the negative effect on the CH_4% when the temperature and the sludge quantity was increased. The amount of ammonia increases with increasing reaction temperature due to the degradation of proteins and amino acids, which leads to a reduction in biogas and methane produced [393]. Likewise, some minerals in the sludge such as Al and Zn inhibit the digestion process. In contrast, the presence of minerals like Ni and Mo activate the digestion process [389]. The increase in the volatile solid value did not effect on the methane percentage until it reached the centre value, then the methane percentage increased with the increase in the volatile solid added value. The negative effect of sludge quantity on the methane percentage remained until it reached centre value and rose slightly. The importance of the date seed/ inoculum ratio in controlling the reaction clearly affects the amount of biogas produced. An increase in this ratio leads to higher methane production at a longer incubation time. Setting this ratio at an average value yields high methane production over a shorter incubation time [392]. The interaction effects between all factors are demonstrated in Figures 102-104. From Figure

102, it can be seen that the methane percentage decreased with temperature increase, noticing that no difference in this percentage was found at both volatile solid values at 40 °C. Figure 103 shows the impact of low temperature on the CH_4% as a methane percentage of 65% was found at 34 °C and 25% of sludge quantity. The CH_4% readily decreased by increasing the temperature, noticing, when CH_4% reached its lowest value at the highest temperature of 40 °C and at both sludge quantities values. It can also be seen from Figure 104 that the highest CH_4% was formed at a volatile solid value of 4.2 g-VS and sludge quantity of 25%. The CH_4% clearly declined sharply when the volatile solid added value shifted from 4.2 g-VS to 1.1 g-VS. When the volatile solid value was 1.75 g-VS and at both sludge quantities (25% or 50%), the CH_4% was 56%, as shown in the same Figure. The 3-D surface plot in Figure 105 shows that the highest methane percentage were achieved at a volatile solid values of 3.7-4.2 g-VS, sludge quantities of 25-27% and at 37 °C. The effect of the interaction between the volatile solid added and the sludge quantity was followed by the effect of the temperature were the highest on CH_4%, as clarified in the coded equation (30). These negatively effected the quality of the biogas, rather than the quantity.

The coded equation (30) for CH_4% is:

$$CH_4\% = + 52.14 - 4.34*A + 2.86*B - 2.38*C - 2.95*AB + 2.98*AC - 4.83*BC + 3.64*B^2 + 3.97*C^2 \quad \text{Equation (30)}$$

The actual equation (31) for CH_4% is:

$$CH_4\% = + 177.33719 - 2.73965*\text{Temperature} + 26.62399*\text{Volatile Solid} - 4.36961*\text{Sludge Quantity} - 0.634409*\text{Temperature} * \text{Volatile Solid} + 0.079333*\text{Temperature} * \text{Sludge Quantity} - 0.249032*\text{Volatile Solid} * \text{Sludge Quantity} + 1.51596*\text{Volatile Solid}^2 + 0.025389*\text{Sludge Quantity}^2 \quad \text{Equation (31)}$$

Table 43: ANOVA Table for CH_4% Response.

Source	Sum of Squares	df	Mean Square	F-value	p-value	
Model	554.16	8	69.27	35.06	< 0.0001	Significant
A-Temperature	150.51	1	150.51	76.17	< 0.0001	
B-Volatile Solid	65.55	1	65.55	33.18	0.0004	
C-Sludge Quantity	45.12	1	45.12	22.84	0.0014	
AB	34.81	1	34.81	17.62	0.0030	
AC	35.40	1	35.40	17.92	0.0029	
BC	93.12	1	93.12	47.13	0.0001	
B^2	56.01	1	56.01	28.35	0.0007	
C^2	66.45	1	66.45	33.63	0.0004	
Residual	15.81	8	1.98			
Lack of Fit	12.50	4	3.12	3.77	0.1133	Not significant
Pure Error	3.31	4	0.8280			
Cor Total	569.96	16				
Adequacy measuring tools	R^2=0.9723	Adjusted R^2=0.9445			Predicted R^2=0.7911	

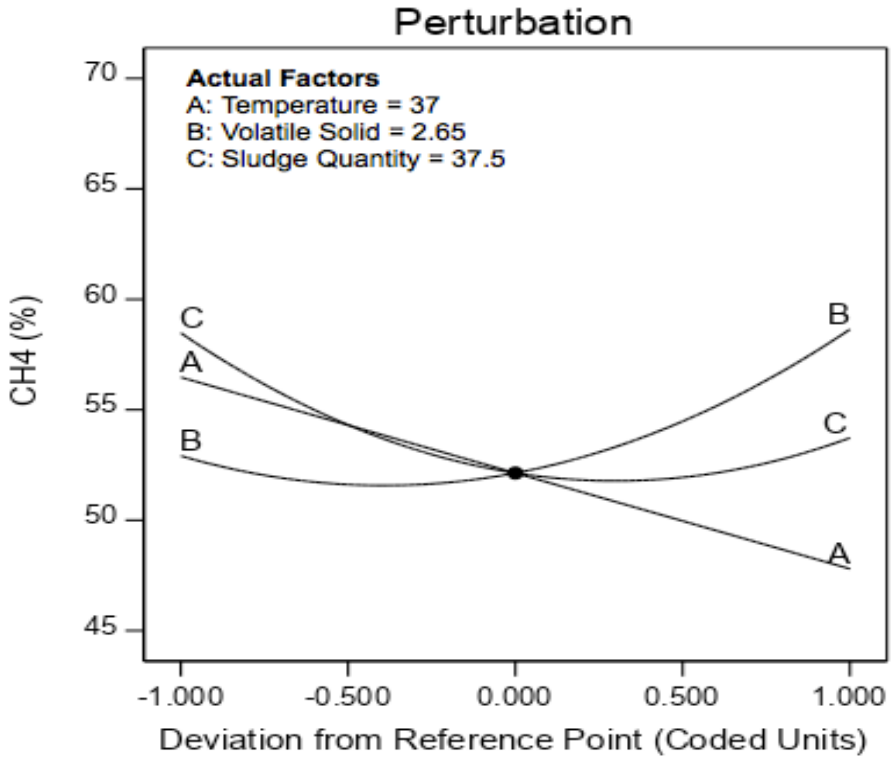

Figure 101: Perturbation plot clarifies the effect of all factors on CH_4%.

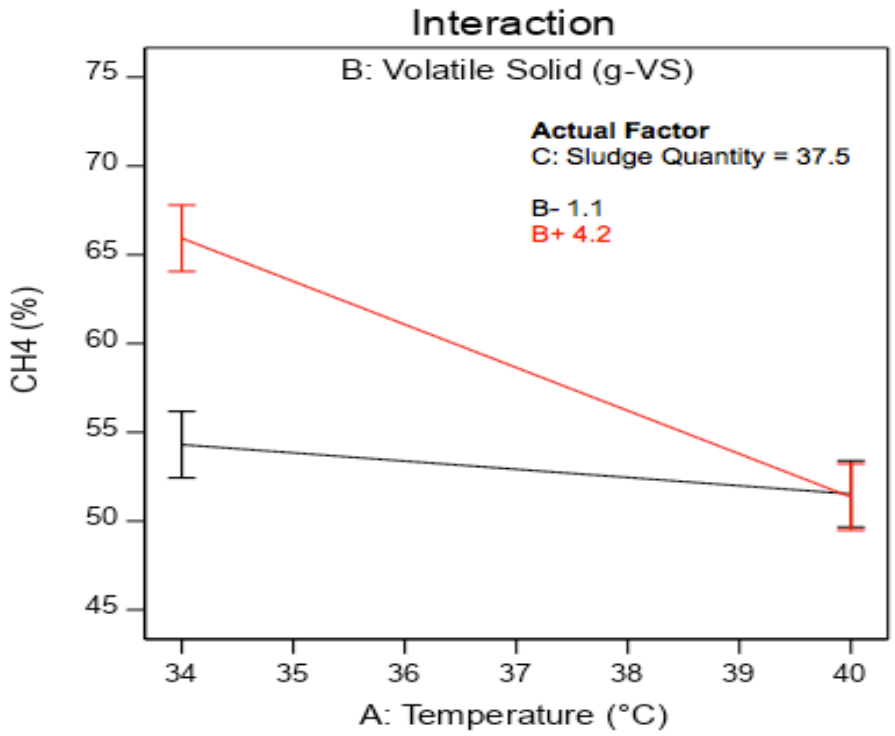

Figure 102: Interaction Plot shows the effect of interaction between temperature and volatile solid.

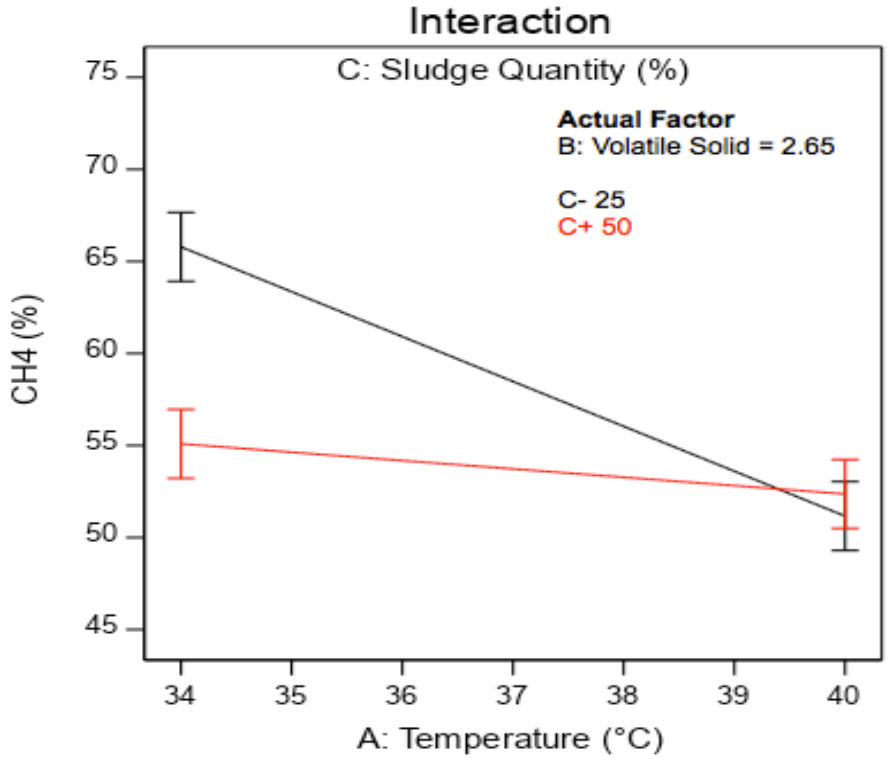

Figure 103: Interaction Plot views the effect of interaction between temperature and sludge quantity on CH_4 percentage.

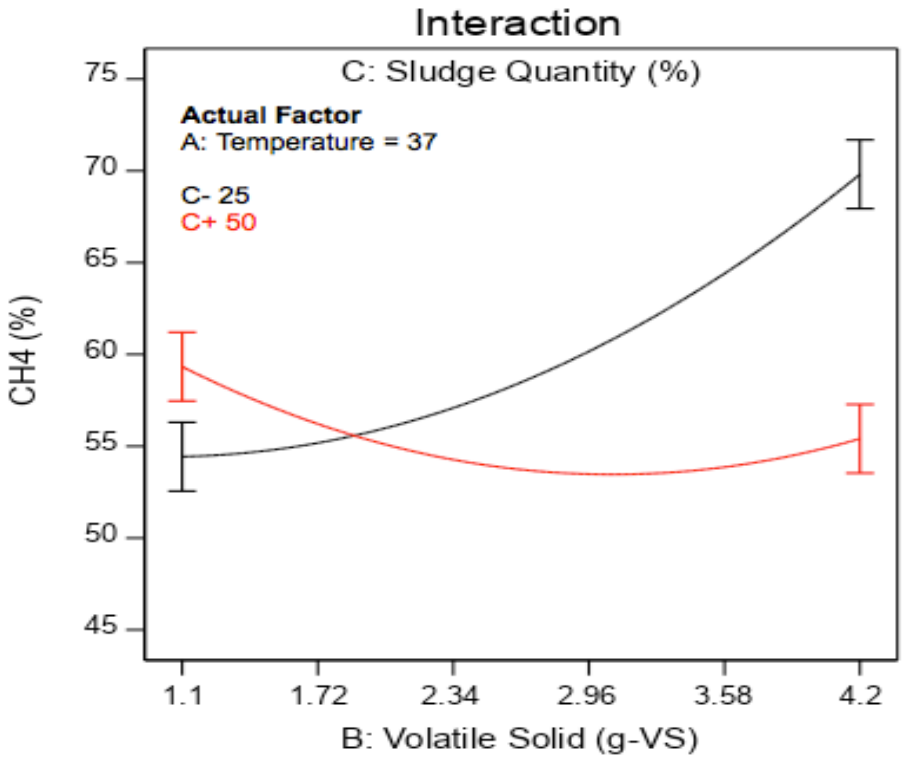

Figure 104: Interaction Plot illustrates the effect of interaction between volatile solid and sludge quantity on CH_4 percentage.

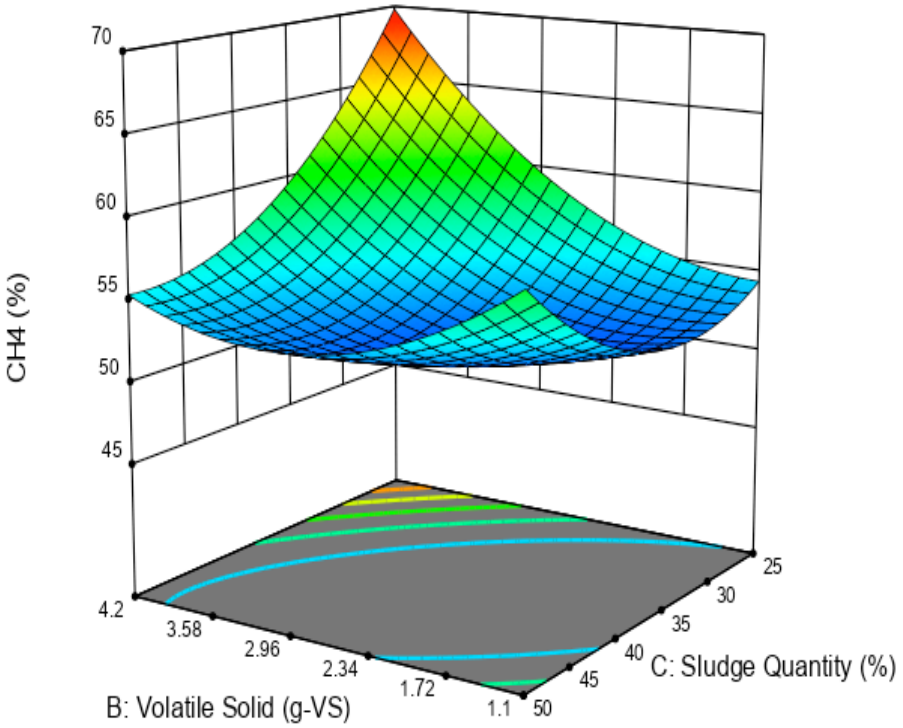

Figure 105: 3-D surface Plot shows the effect of volatile solid and sludge quantity on the CH_4% at 37 °C.

4.5.5 Carbon Dioxide Percentage

As evidenced by Figure 106, a sludge quantity of 25% produced the lowest amount of CO_2% proving the inverse relationship between CH_4% and CO_2%. The figure shows a direct relationship between the CO_2% and temperature. The increase in the volatile solid added and sludge quantity led to an increase in the CO_2% until they both reached their centre values. The CO_2% decreased after the centre values, as in at increasing values of volatile solid added and sludge quantity. The effect of the interaction between temperature and volatile solid on the CO_2% is demonstrated in Figure 107 which shows, that using a volatile solid of 4.2 g-VS at 34 °C, produced the lowest CO_2% achieved. Moreover, the contour plot in Figure 108, shows that when a temperature greater than 36 °C was used and volatile solid added values between (1.72-3.5) g-VS, the highest CO_2% can produced. The coded equation (32) illustrates the highest positive effect of the interaction between temperature and volatile solid followed by the sludge quantity on CO_2%:

$$CO_2\% = +26.42 + 1.25*A - 0.9750*B + 1.65*C + 1.70*AB - 3.30*B^2 - 5.10*C^2 \quad \text{Equation (32)}$$

The actual equation (33) for CO_2% is:

$$CO_2\% = -11.94696 - 0.552151*\text{Temperature} - 6.88180*\text{Volatile Solid} + 2.57874*\text{Sludge Quantity} + 0.36559*\text{Temperature} * \text{Volatile Solid} - 1.37247*\text{Volatile Solid}^2 - 0.032623*\text{Sludge Quantity}^2 \quad \text{Equation (33)}$$

Table 44: ANOVA table for CO_2% response.

Source	Sum of Squares	df	Mean Square	F-value	p-value	
Model	217.45	6	36.24	25.66	< 0.0001	Significant
A-Temperature	12.50	1	12.50	8.85	0.0139	
B-Volatile Solid	7.60	1	7.60	5.38	0.0427	
C-Sludge Quantity	21.78	1	21.78	15.42	0.0028	
AB	11.56	1	11.56	8.18	0.0169	
B^2	45.91	1	45.91	32.50	0.0002	
C^2	109.71	1	109.71	77.67	< 0.0001	
Residual	14.13	10	1.41			
Lack of Fit	12.23	6	2.04	4.31	0.0894	Not significant
Pure Error	1.89	4	0.4730			
Cor Total	231.58	16				
Adequacy measuring tools	R^2=0.9390	Adjusted R^2=0.9024			Predicted R^2=0.8130	

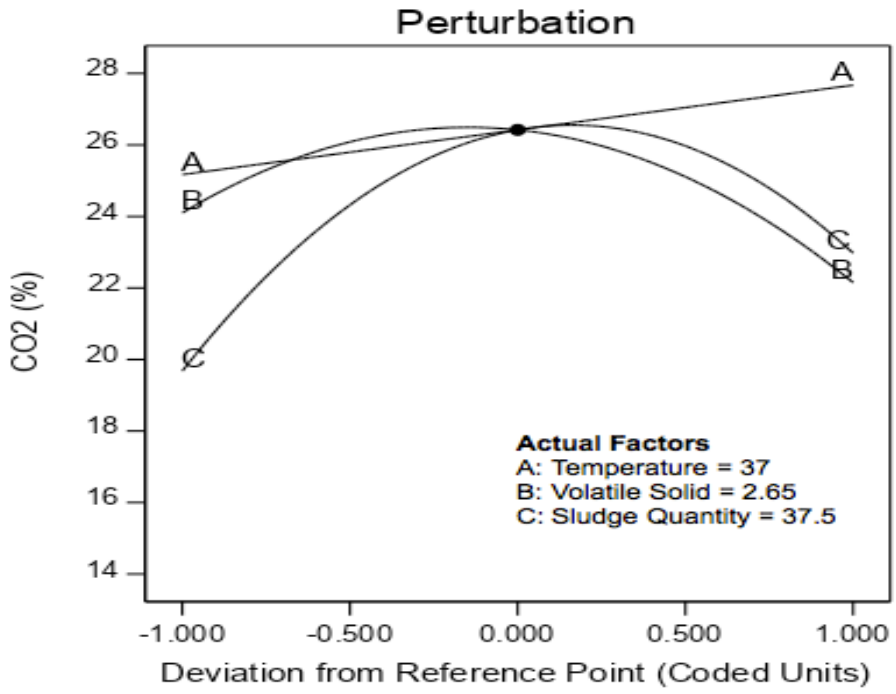

Figure 106: Perturbation plot shows the effect of all factors on CO_2%.

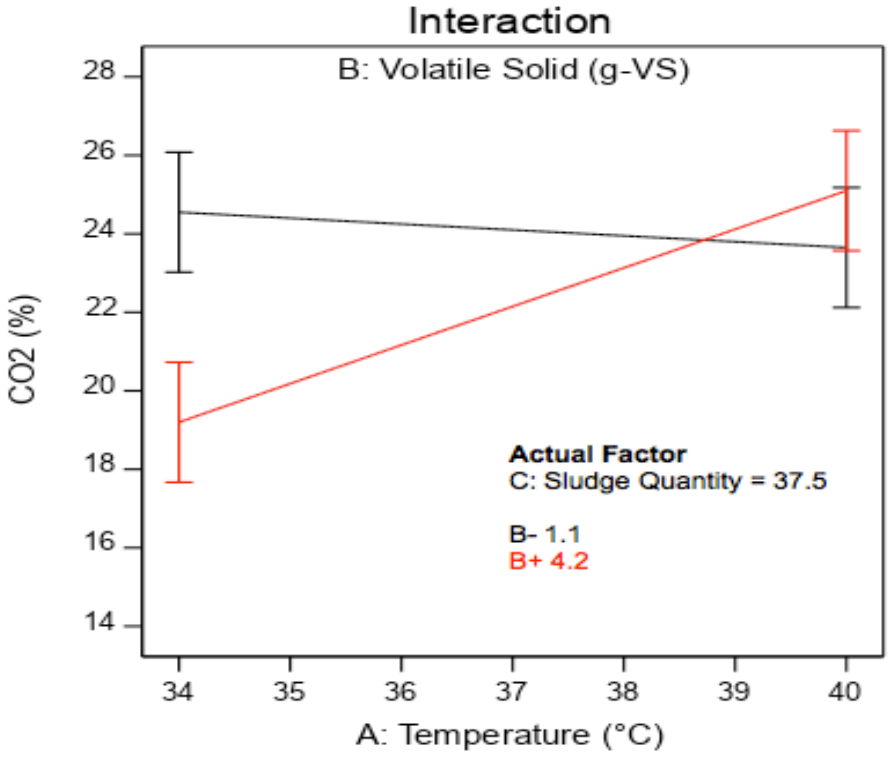

Figure 107: Interaction Plot views the effect of interaction between temperature and volatile solid on CO_2%.

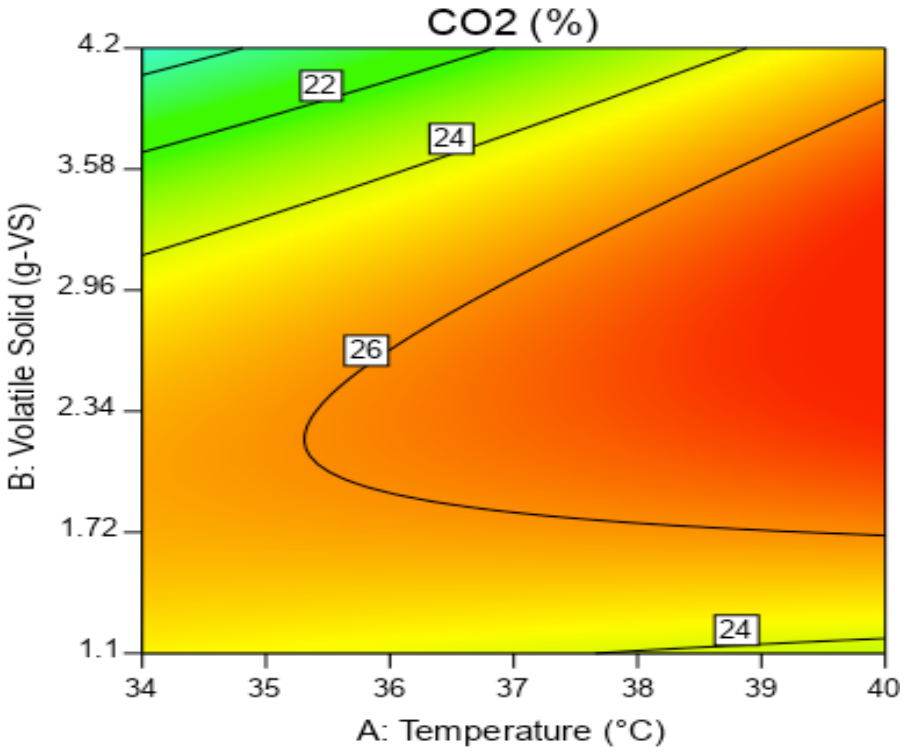

Figure 108: Contour Plot presents the effect of temperature and volatile solid on CO_2% at sludge quantity of 37.5%.

4.5.6 Methane/g-VS

It can be seen that from Figure 109 that at the volatile solid of 1.1 g-VS, the highest methane per gram volatile solid added volume was obtained. The graph also shows that the CH_4/g-VS decreased slightly with temperature decrease. The same Figure also shows the indirect proportion between methane per g-VS and volatile solid and the direct relation with that of sludge quantity. The interaction between volatile solid added and sludge quantity on CH_4/g-VS is illustrated in Figure 110. The highest CH_4/g-VS was gained at a volatile solid of 1.1 g-VS and 50% of sludge quantity. In contrast, the lowest amounts of methane per g-VS were found at a volatile solid of 4.2 g-VS for both sludge quantities. The highest yield of methane per gram volatile solid was obtained at the lowest volatile solid value due to the division by the volatile solid added value when calculating the methane per gram volatile solid. Figure 111 shows the highest CH_4/g-VS can be achieved at 1.1 g-VS, greater than 45% sludge and at 37 °C. The highest indirect effect of volatile solid on CH_4/g-VS is clear from the coded Equation (34):

$$CH_4/g\text{-}VS = + 445.47 - 18.30*A - 125.74*B + 94.31*C - 113.10*BC + 127.32*B^2$$

Equation (34)

The actual equation (35) for CH_4/g-VS is:

CH_4/g-VS = + 395.26458 - 6.10000*Temperature - 143.09200*Volatile Solid+ 23.01416*Sludge Quantity - 5.83742*Volatile Solid * Sludge Quantity + 52.99514*Volatile Solid²

Equation (35)

Table 45: ANOVA Table for CH_4/g-VS Response.

Source	Sum of Squares	df	Mean Square	F-value	p-value	
Model	3.201E+05	5	64028.07	54.15	< 0.0001	Significant
A-Temperature	2679.12	1	2679.12	2.27	0.1604	
B-Volatile Solid	1.265E+05	1	1.265E+05	106.97	< 0.0001	
C-Sludge Quantity	71158.78	1	71158.78	60.18	< 0.0001	
BC	51166.44	1	51166.44	43.27	< 0.0001	
B²	68656.64	1	68656.64	58.07	< 0.0001	
Residual	13006.00	11	1182.36			
Lack of Fit	11418.38	7	1631.20	4.11	0.0951	Not significant
Pure Error	1587.61	4	396.90			
Cor Total	3.331E+05	16				
Adequacy measuring tools	R^2= 0.9610	Adjusted R^2=0.9432			Predicted R^2= 0.8502	

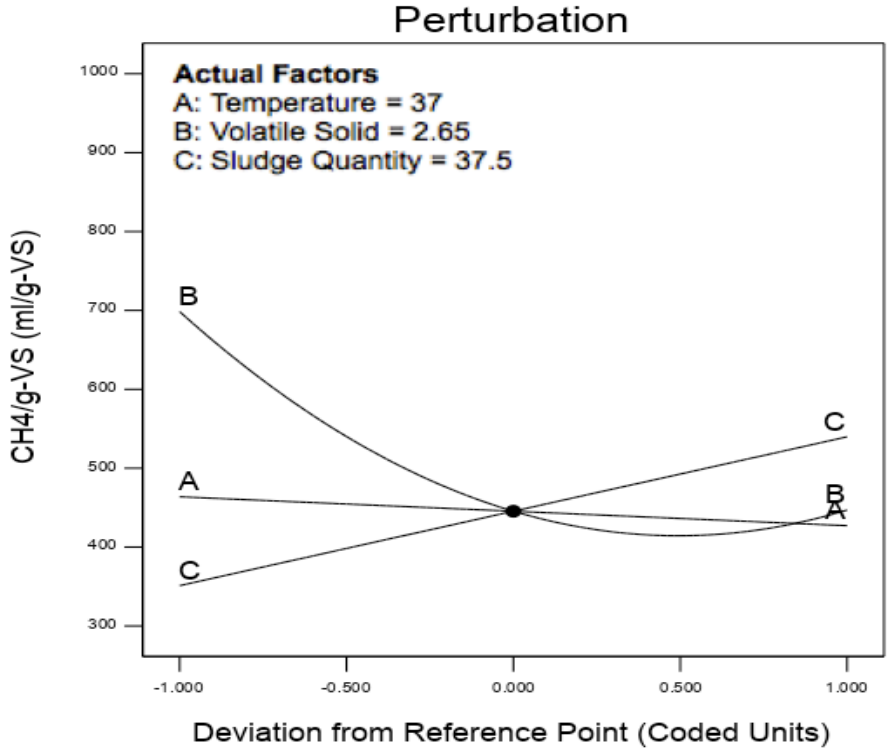

Figure 109: Perturbation plot presents the effect of all factors on CH_4/g-VS.

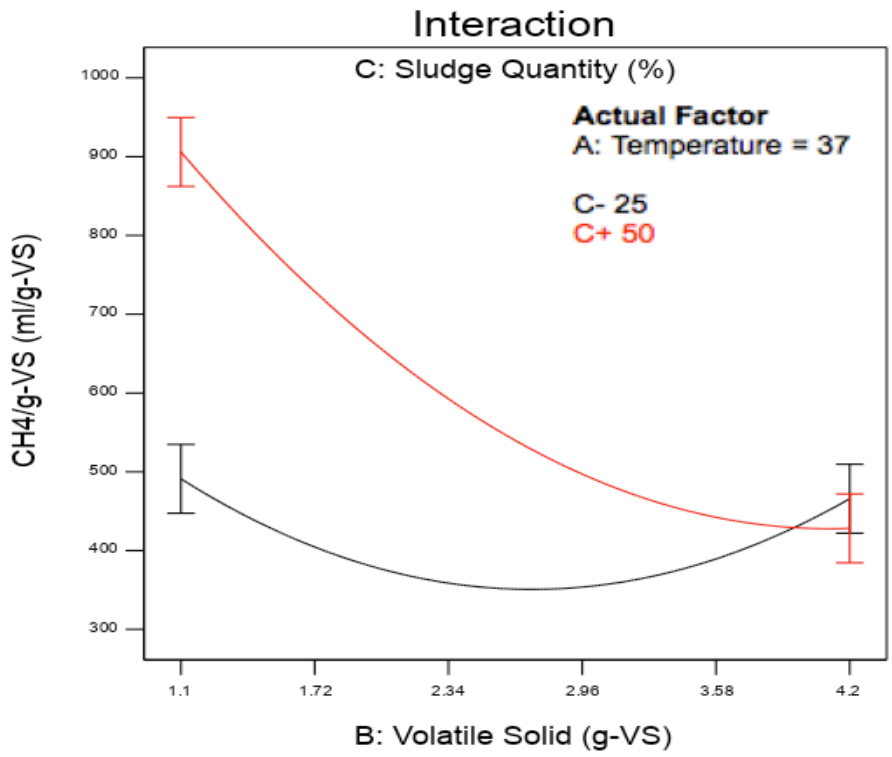

Figure 110: Interaction Plot illustrates the effect of interaction between volatile solid and sludge quantity on CH_4/g-VS.

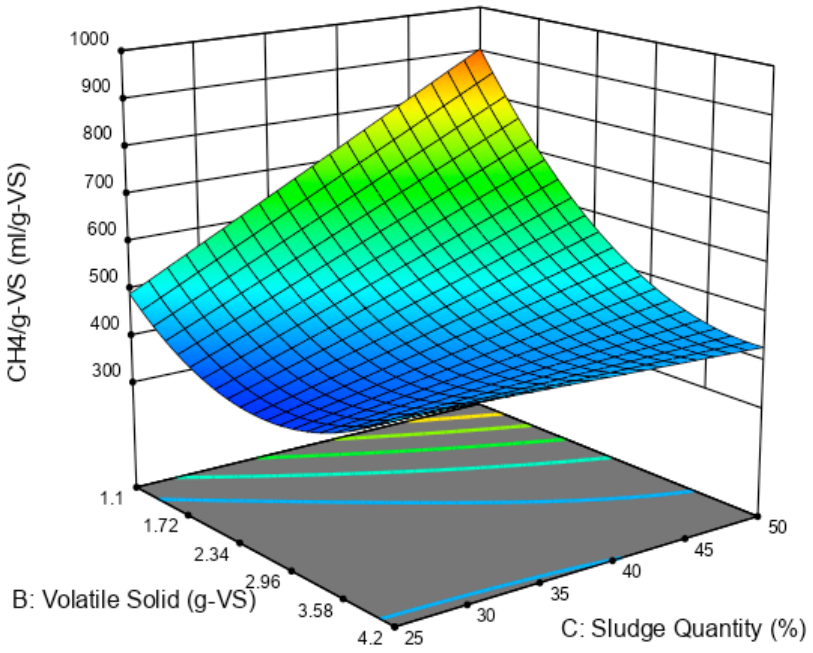

Figure 111: 3-D surface Plot illustrates the effect of volatile solid and sludge quantity on CH_4/g-VS% at 37 °C.

4.6 Date Seed Vs. Extracted Oil Date Seed

The differences between the responses of date seeds before and after oil extraction illustrate in Figures 112-116. The figures show the impact of oil extraction on all responses, particularly those concerning the resulting biogas quality. Figure 112 displays the difference in biogas before and after oil extraction, where the largest decrease in biogas volume was 22.7% from sample #9, while the smallest decrease was 6.3%. The highest amount of biogas produced from date seeds (sample #12) before oil extraction was 4,140 ml, while it decreased to 3,534 ml after oil extraction. Furthermore, the variance in biogas/g-VS was similar to the difference in the biogas, as shown in Figure 113.

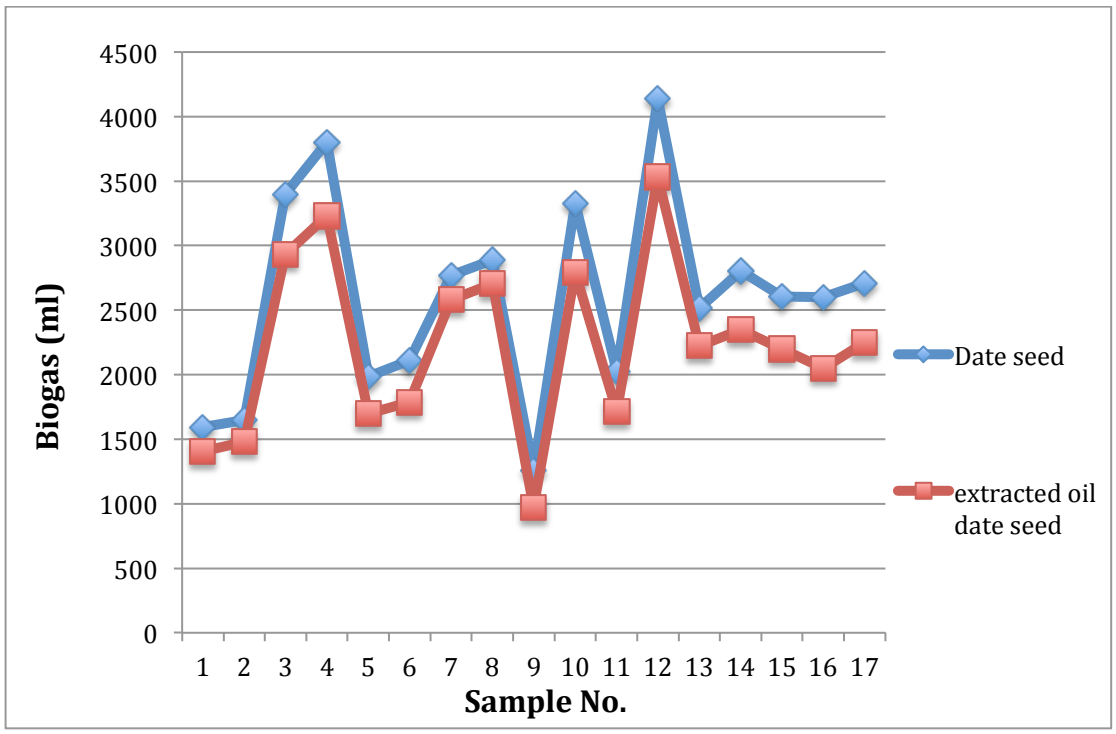

Figure 112: The difference in the biogas volume produced before and after oil extraction from the date seeds.

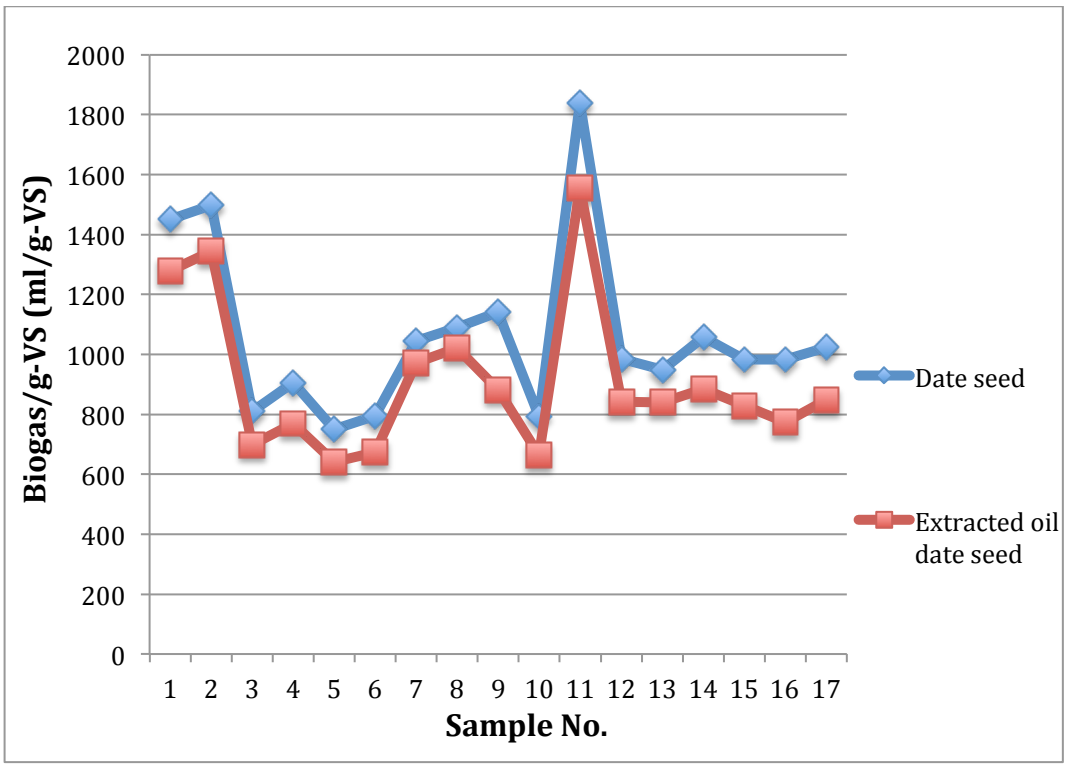

Figure 113: The variation in the Biogas/g-VS quantity of date seed and extracted oil date seed.

Figure 114 shows the highest and lowest differences in CH_4% were 10.98% (sample #6) and 1.12% (sample #13), respectively, while the highest and lowest differences in CO_2% were 4.14% (sample #15) and -20% (sample #10), respectively, as shown in Figure 115. The highest percentage of methane before and after oil extraction from sample #10 was 71.1% and 69.3%, a decrease of 2.53%. On the other hand, the lowest amount of CO_2% reached before oil extraction from sample #10 was 13% and after oil extraction, it rose to 15.6%, by an increase of 16.7%. This indicates the effect of oil removal on biogas quality.

The difference in the amount of CH_4/g-VS can be seen in Figure 116, where it found that extracting the oil from date seed led to a decrease in the amount of CH_4/g-VS for all sample, with varying percentages ranging from 8.59% to 27%. The highest amount of CH_4/g-VS before oil extraction was 1,143.8 ml and after oil extraction, this amount decreased to 949.6 ml. The decrease in the highest amounts of CH_4/g-VS from date seed to extracted oil date seed was 16.98%, according to sample #11.

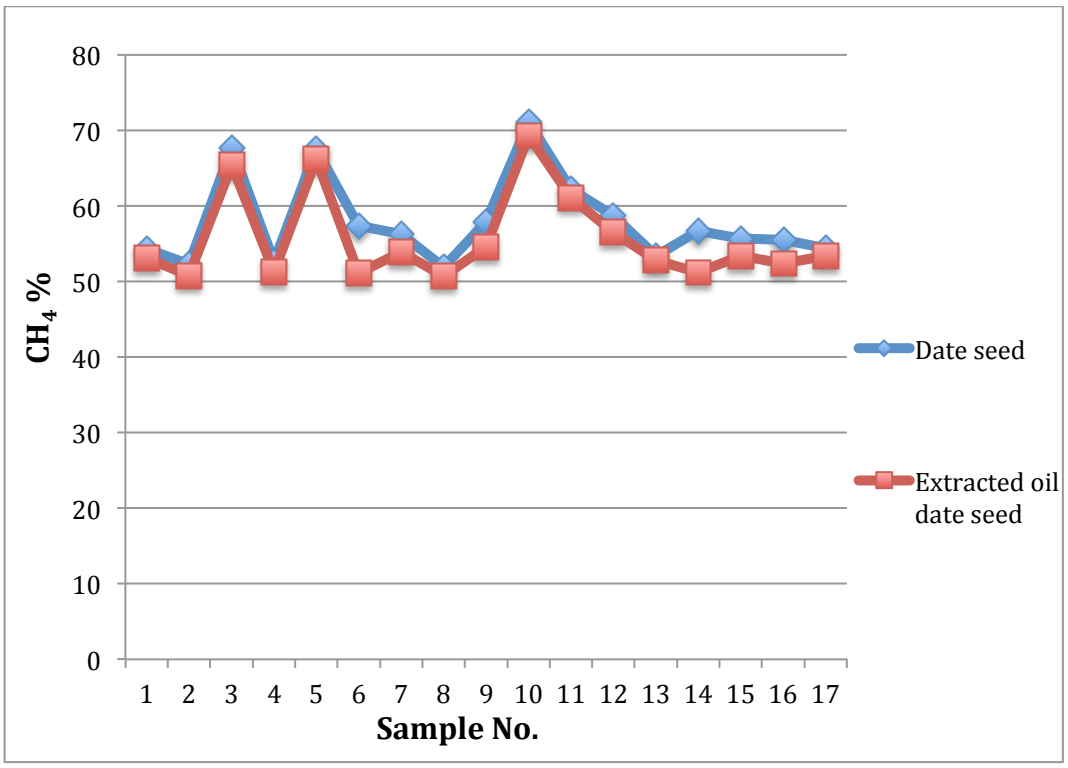

Figure 114: CH_4% of date seed and extracted oil date seed.

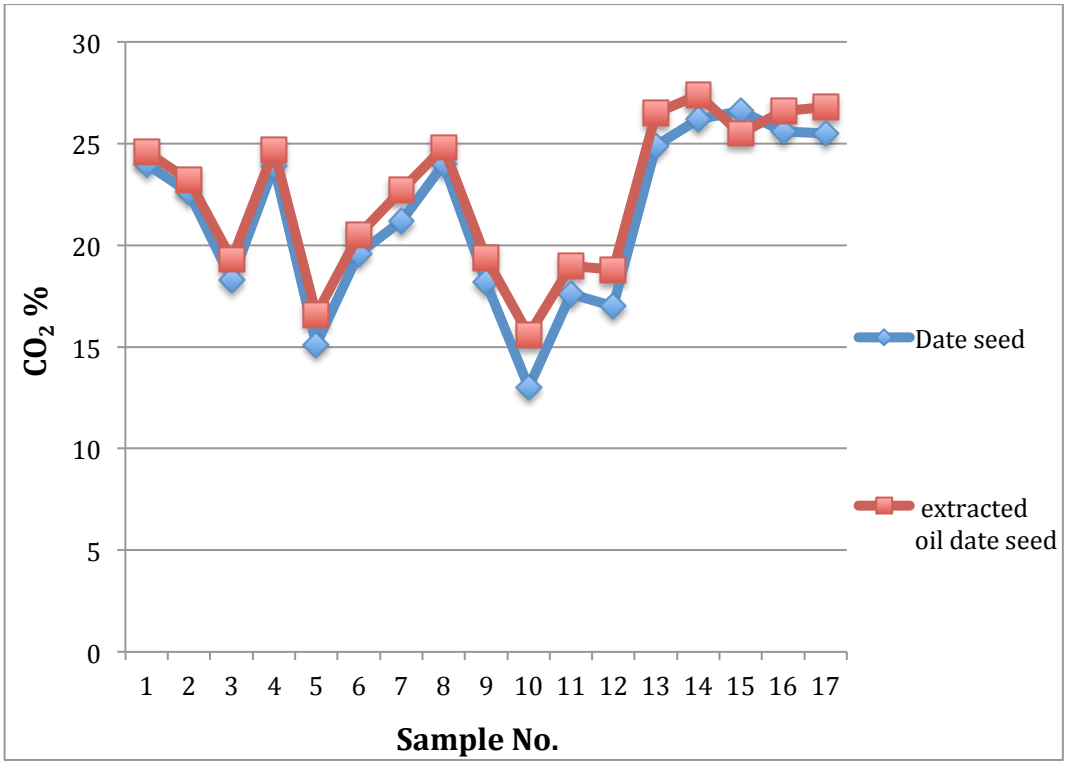

Figure 115: The alteration in CO_2% between date seed and extracted oil date seed.

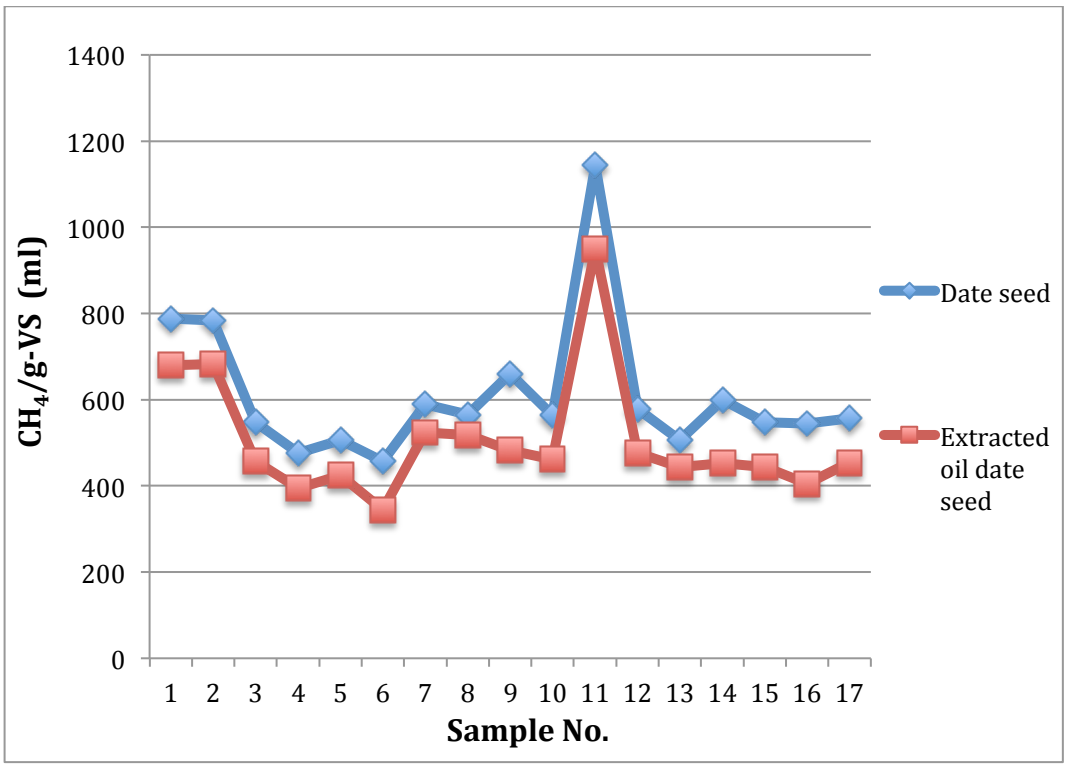

Figure 116: CH_4/g-VS yields before and after date seed oil extraction.

4.7 Digestate

Table 46 shows the test result of the digestates (Appendix B) produced from the cassava peel, date seed and extracted oil date seed which confirmed its content of the three main nutrients of conventional fertilisers (N, P and K) and its dry matter (DM). These amounts of nutrients match with what is recommended which were mentioned in Chapter 2 (section 2.11) [272]. Although potassium content was less than what was mentioned, this is not considered not ideal for all plants and types of soils. It was mentioned in the literature that it is difficult to determine the optimum ratios due to the difference in plants diet [102, 272]. The presence of these elements in the resulting digestate enhances the possibility of its usage in different areas such as agriculture, whether in its liquid form or after it has been dried [394-396]. The same table shows different N:P:K ratios obtained from each substance. Extracting the oil from the date seed increased the N content and decreased the P and K contents in the digestate.

Table 46: The test results of the produced digestates.

Components	Unit	Cassava peel	Date seed	Extracted oil date seed
Total nitrogen	mg/kg	3886	2322	4038
Total phosphorous	mg/kg	632	347	263
Potassium	mg/kg	526	382	292
Dry matter	g/100g	2.7	1.7	2.4
N: P: K ratio	-	1.0: 0.16: 0.14	1.0: 0.15: 0.16	1.0: 0.07: 0.07

4.8 Biodiesel

The oil samples before and after removing the n-hexane are shown in Figure 117. The percentage of oil produced from the date seeds was approximately 16.0 wt.% of the date seed used in the extraction process. The percentage was determined from the mass of extracted oil divided by the mass of the powder date seed used. In other words, each gram of ground date seed gave approximately 0.202 ml (0.16 g) of oil. This percentage is within the values obtained by Jamil et al. (2016) [293], but it is slightly less than the optimal value obtained, which was 16.5%. This may be due to the use of more reaction time (7 hour) [293].

(a) (b)

Figure 117: The extracted oil (a) before separating n-hexane (b) after separating n-hexane.

The resulting biodiesel accounted for approximately 79 wt.% of the date seed oil. The separating the biodiesel and glycerine was implemented by placing them in a separating funnel as shown in Figure 118. The biodiesel sample (not the total amount produced) before and after the washing process is shown in Figure 119. The properties of the biodiesel produced from the extraction process and the comparison with ASTM D6751 and EN 14214 standard are given in Table 47 [397-399]. The resulting biodiesel was yellowish in colour and had a hazy liquid look. The acid value was measured at 0.01 mg KOH/g, which is in range of the ASTM and EN standard value of maximum 0.5 mgKOH/g. This low acid value indicates that the produced biodiesel is suitable for use in engines. An increase in the acid value of the fuel leads to engine corrosion. Moreover, high acid values impact the low temperature properties of biodiesel due to the high melting points [400]. Also, the high acid value indicates the inability of biodiesel to store and may cause tank corrosion [158]. The cetane number was calculated at 47.6, which is lies in the range of the ASTM and EN standards as shown in Table 47. The importance of the cetane number refers to the quality of the fuel in terms of ignition. It depends on the composition of the biodiesel, so it directly affects the engine [401]. The cetane number depends on the chemical compound of the fuel, and it varies from one substance to another. It can effect the engines starting ability, noise level and exhaust emissions [292]. The sulphur content was 0.005 %mass which is a bit higher than the ASTM standard of 0.002 %mass, but lower than the EN standard of 0.02 %mass. Compared with fossil fuels, one of the most important advantages of biodiesel is its low emissions of sulphur compounds into the atmosphere [402].

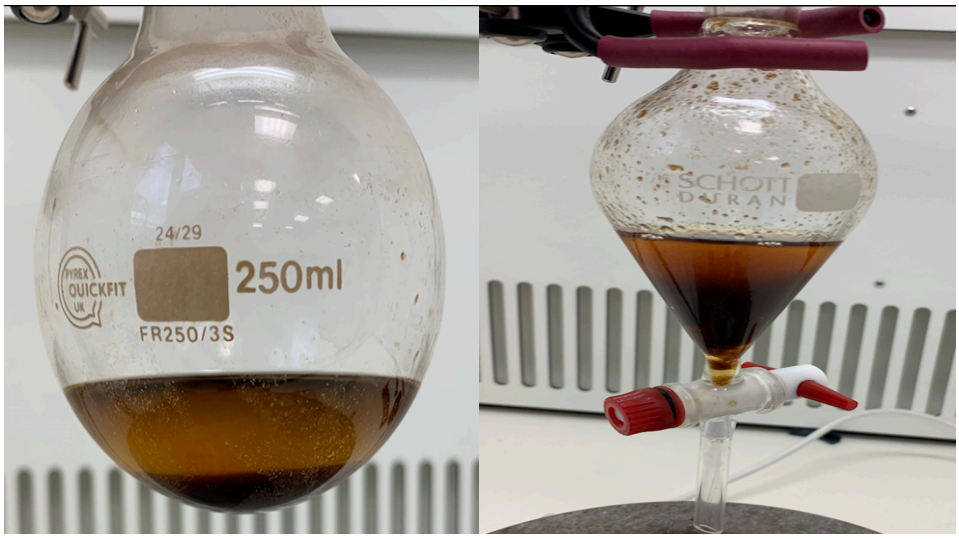

Figure 118: Density difference between biodiesel and glycerin.

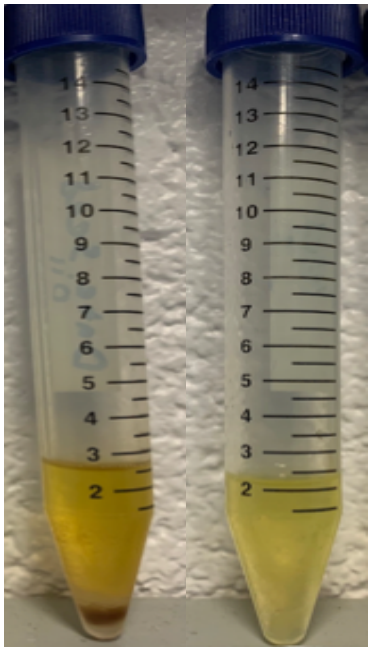

(a) (b)

Figure 119: Samples from produced biodiesel (a) Before and (b) After purification.

Table 47: Biodiesel produced properties compared to ASTM and EN standards [397-399].

Test	Result	Unit	ASTM D6751	EN14214
Colour	Yellowish	Visual	N/A	N/A
Appearance	Hazy Liquid	Visual	N/A	N/A
Acid Number	0.01	mgKOH/g	0.5 max	0.5 max
Cetane Index	47.6	Calculated	47 min	51 min
Sulphur content	0.005	%Mass	0.002	0.02 max
Final Boiling Point	439	°C	100-615	N/A
Cloud Point	0	°C	-3 to -12	N/A
Density at 15 °C	890	kg/m^3	880	860-900
Flash Point	147	°C	130 min	101 min
Pour point	-2.0	°C	-15 to -16	N/A
Viscosity Kinematic at 40 °C	4.11	mm^2/s	1.9-6.0	3.5-5.0

The cloud point was measured to be 0 °C which is less than the ASTM standard of -3 to -12 °C, while the pour point of the biodiesel from the study was -2 °C compared to the ASTM standard of -15 to -16 °C. The values of the cloud and pour points as indicated are higher than the standards, which is a disadvantage for the resulting biodiesel. All biodiesels from various sources have high cloud and pour points [292]. The reason for that is because the fatty acids directly affect the cold flow properties of biodiesel. Increasing the carbon atoms in the carbon chain increases the freezing point of the biodiesel, while it decreases with the double bonds [403].

Based on the standard density values of biodiesel for the ASTM and EN standards at 880 kg/m^3 and 860-900 kg/m^3 respectively, the density of the biodiesel produced from the date seed oil was 890 kg/m^3, which is within the ranges of the two standards. The density of biodiesel prevents it from breaking up in the engine upon combustion [404]. The mass of injected fuel increases with increasing fuel density. Also the injection timing and the injection spray pattern are directly affected by the density [405]. The penetration of fuel droplets will increase in the combustion chamber with the rise in density. As the density increases, it causes an increase in the fuel droplets diameter [406]. The importance of viscosity lies in its effect on injection in the engine and its spray atomisation after injection. Therefore, the viscosity of biodiesel is high, at 4.11 mm^2/s. The viscosity value in the ASTM standard is 1.9-6 mm^2/s and 3.5-5 mm^2/s in EN standard [407, 408]. Moreover, increasing the viscosity value of biodiesel leads to early injection that moves fuel ignition near the top dead centre, which causes an increase in the pressure and temperature in the combustion chamber [405, 406].

The temperature at which biodiesel will ignite in contact with air is called the flash point [400]. A low flash point makes the fuel highly volatile, while high flash point leads to carbon deposits in the combustion chambers [401]. The flash point of biodiesel is an important consideration for safety measures in transportation and storage [293]. The flash point is related to the volatility, low volatility with high viscosity leads to misfire, delay in the ignition and poor cold engine starting up [409]. Therefore, the flash point must be at least 130 min according to ASTM D6751 standard or 101 min or more based on EN 14214 standard [397]. As the flash point in this study was 147 min, it was within range. The biodiesel produced a boiling point of 439 °C which is in the range of the ASTM boiling point between 100-615 °C. The boiling point is related to the volatility of the fatty substances and thus is related to the flash point. Volatility decreases with increasing carbon chain, thus low volatility of flammable materials means higher flash points [410-412].

4.9 Glycerine

Glycerine was produced as a brownish and gelatinous at room temperature as a by-product from the biodiesel production process as shown in Figure 120. The dark colour of the crude glycerin produced was due to it containing ash, water, and other organic matter other than glycerin [413]. The amount of glycerine obtained was estimated at 9 wt.% of the date seed oil. This percentage

is in line with the previous studies [308-312]. The physical properties of glycerine are shown in Table 48. The density of glycerine at 15 °C was 1.047 g/ml, with a flash point of 149.5 °C and a glycerine pH of 9.16 which is in the range of the crude glycerol mentioned in the previous studies [306, 413]. The glycerine contained 38% water.

Figure 120: Glycerine.

Table 48: Glycerine produced properties.

Test	Result	Unit
Colour	Brownish	Visual
Appearance at room T	Gelatinous	Visual
Density @ 15 °C	1.047	g/ml
Flash Point	149.5	°C
pH value @ 20°C	9.16	
Water Content	38	%

4.10 Starch-Based Bio Adhesive

This section presents the statistical results of the adhesive substance resulting from the base and acid gelatinisation. Figures 121 and 122 show the adhesives produced from the two gelatinisation types and the specimens of plywood, plastic and paperboard after applying the adherent with the adhesive. The checked probabilities of all models are presented in the ANOVA Tables 51-60. The convergence of R^2, predicted R^2 and adjusted R^2 to 1 value indicates that the models were

adequate. The difference between Predicted R^2 and Adjusted R^2 was less than 0.2 for all models, so they were in reasonable agreement. As it is clear from the normal probability graphs (Figures 123-127) for the adhesive from the NaOH gelatinisation and (Figures 128-132) for the adhesive from the HCl gelatinisation, the distribution was normal, as in all of the points were close to the distribution line. The adaptation of the model was adequate, which shows the normal probability and predicted of all responses. The agreement between the actual and predicted response was excellent, as the majority of the points did not deviate from the line.

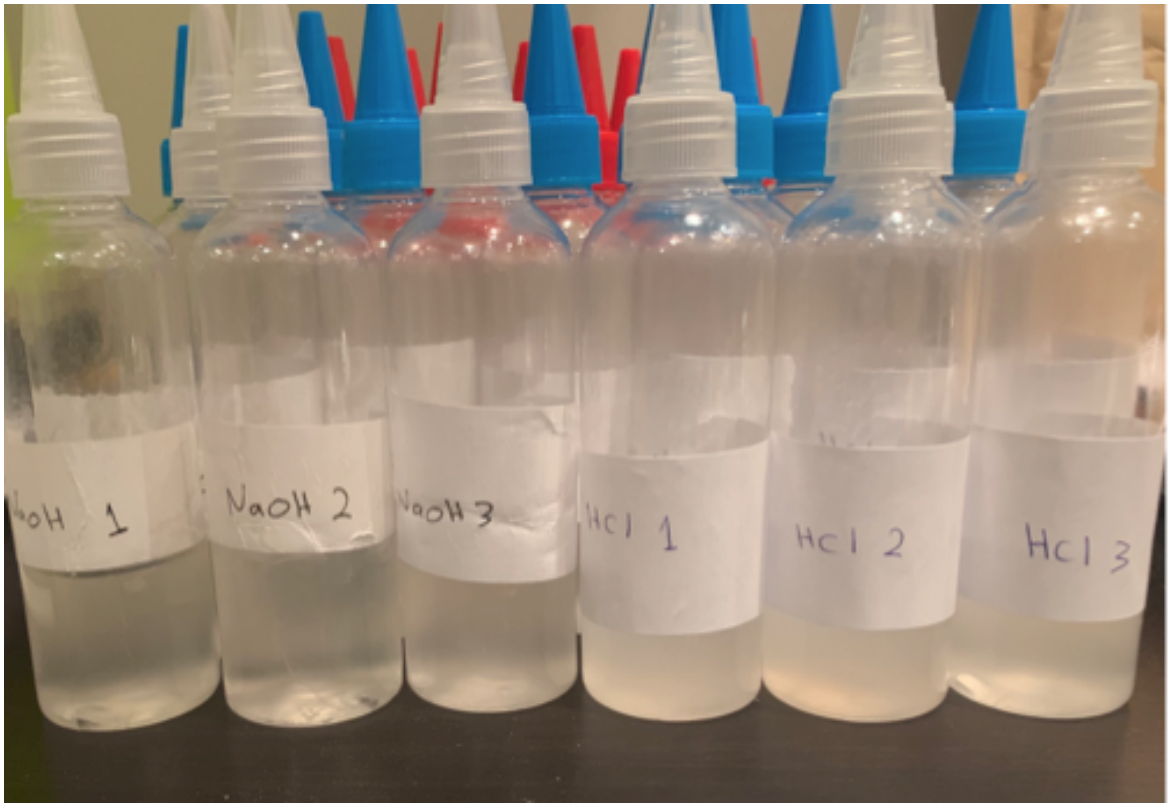

Figure 121: Starch-based adhesive from NaOH and HCl gelatinisation.

(a) (b) (c)

Figure 122: (a) plywood, (b) plastic and (c) paperboard prepared glued samples.

A) NaOH Gelatinisation

The experimental matrix and results of the adhesive produced are present in Table 49. It can be seen that from the table, the highest shear strength of plywood and paperboard at 3.59 MPa (run #21) and 0.848 MPa (run #26) respectively were achieved at the following conditions: 40 ml of gelatinisation, 0.2 g of borax and 85 °C for plywood shear strength and 45 ml of gelatinisation, 0.3 g of borax and 85 °C for paperboard shear strength. The adhesive viscosities at these conditions were 1,337.16 mPa.s and 2,820.50 mPa.s while the density was 1.045 g/cm^3 and 1.037 g/cm^3 respectively. However, at a higher gelatinisation quantity of 50 ml, 0.2 g of borax and 65 °C, the lowest shear strength values were found for plywood at 2.33 MPa (run #33) and for paperboard it was 0.617 MPa (run #7) at 50 ml of gelatinisation, 0.1 g of borax and 75 °C. The viscosity values ranged between 815.27 to 3,953.00 mPa.s, while the resulting adhesive densities were from 1.005 to 1,064 g/cm^3. All of the failures that occurred for the plywood were cohesive failures, while the failures of paperboard samples were in the substrates except for one sample that failed due to cohesive failure. Although the surface was treated with sandpaper (100 grit) to increase its roughness, the adhesive failure persisted. Further investigations are required of other types of gelatinisation and surfaces treatment methods to be applied in order to address the plastic adhesion issue.

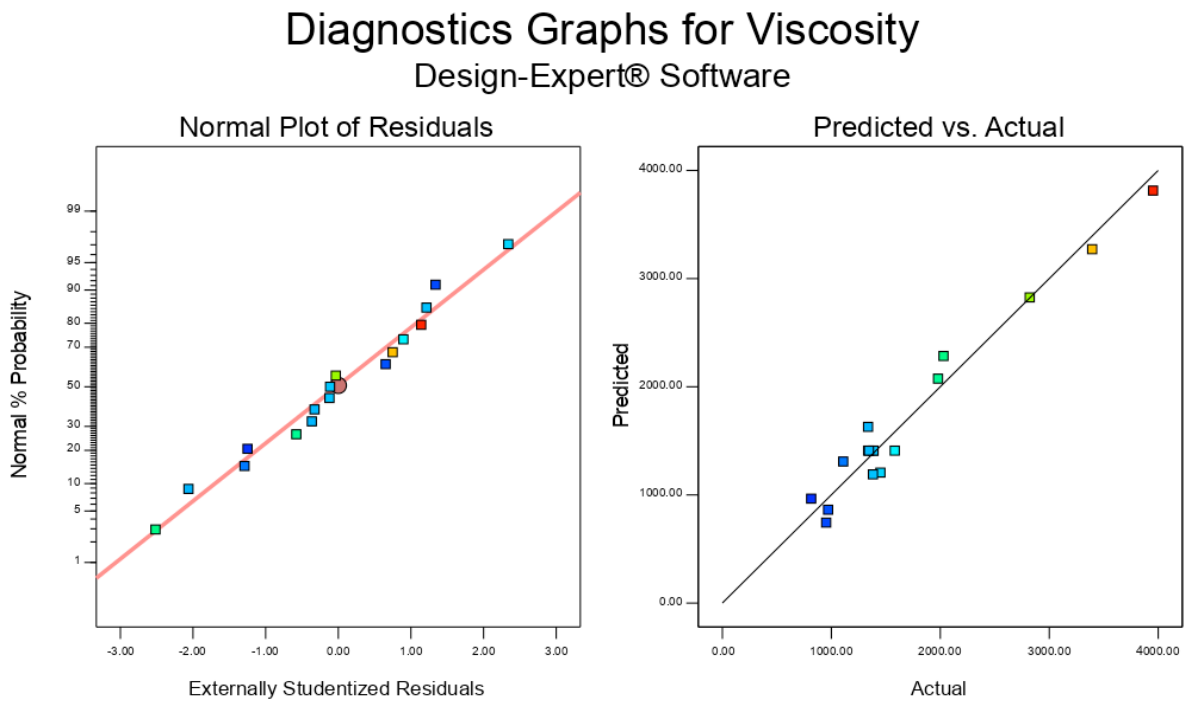

Figure 123: Normal probability and predicted versus actual residuals plot of viscosity.

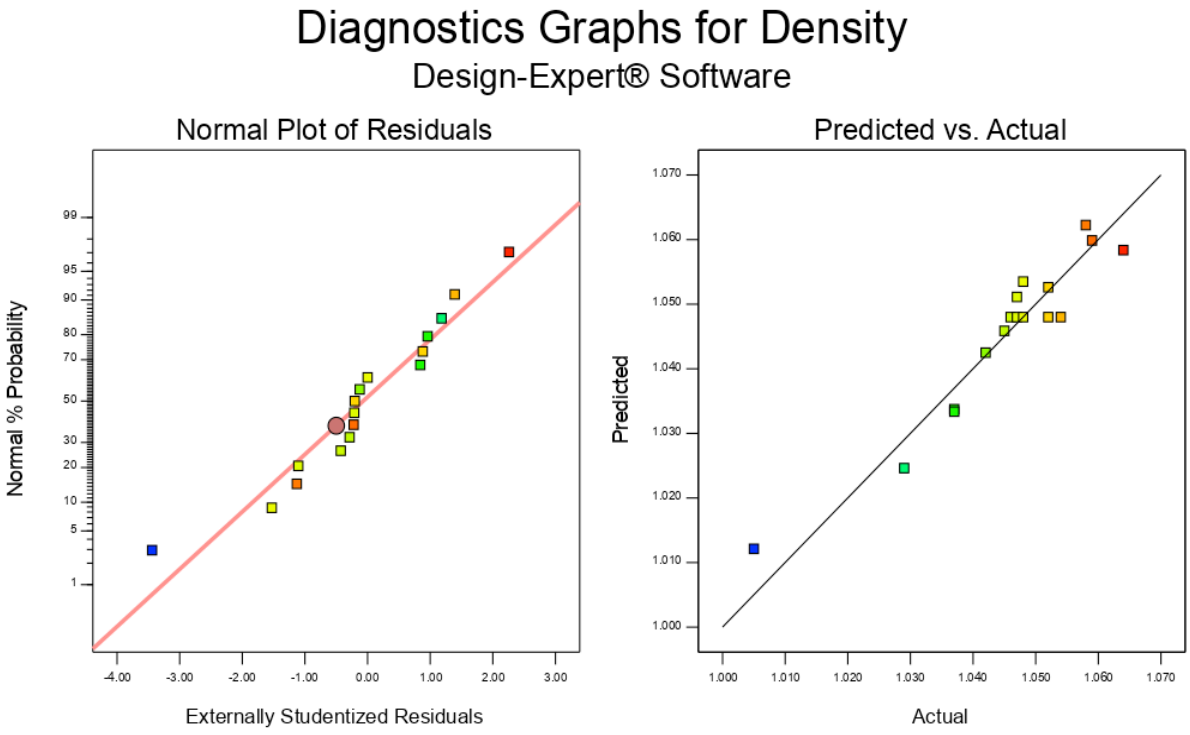

Figure 124: Normal probability and predicted versus actual residuals plot of density.

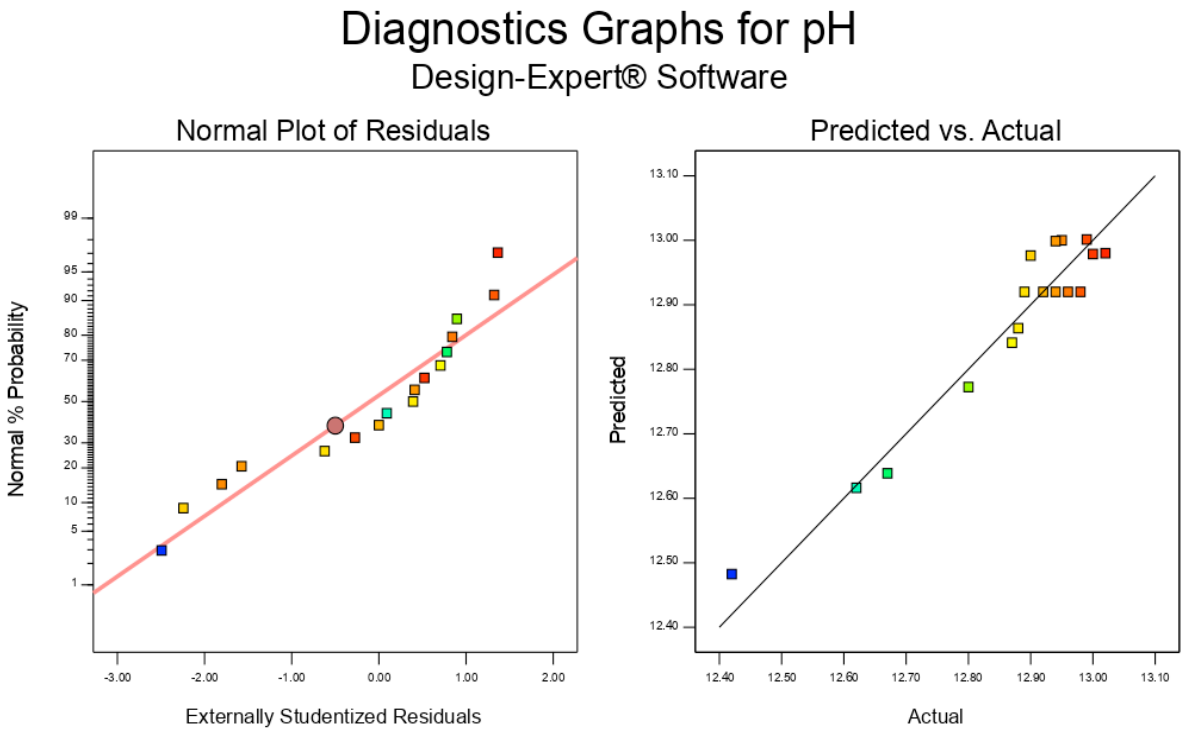

Figure 125: Normal probability and predicted versus actual residuals plot of pH.

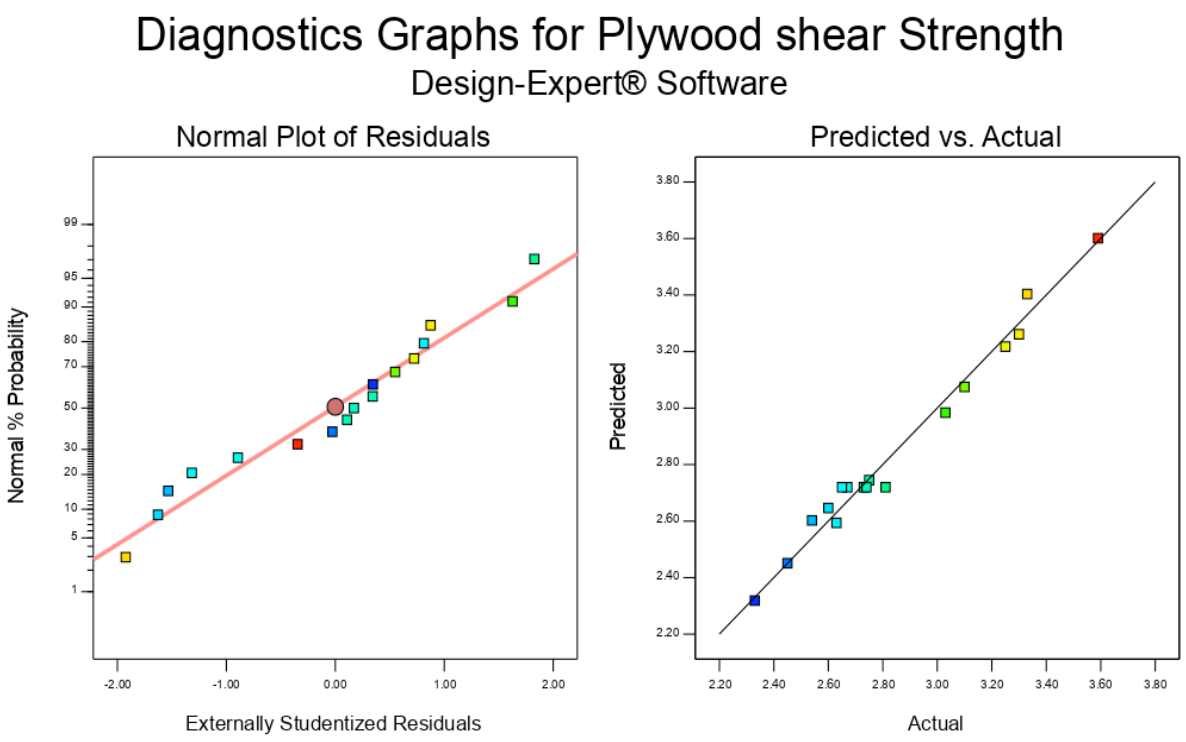

Figure 126: Normal probability and predicted versus actual residuals plot of Plywood Shear strength.

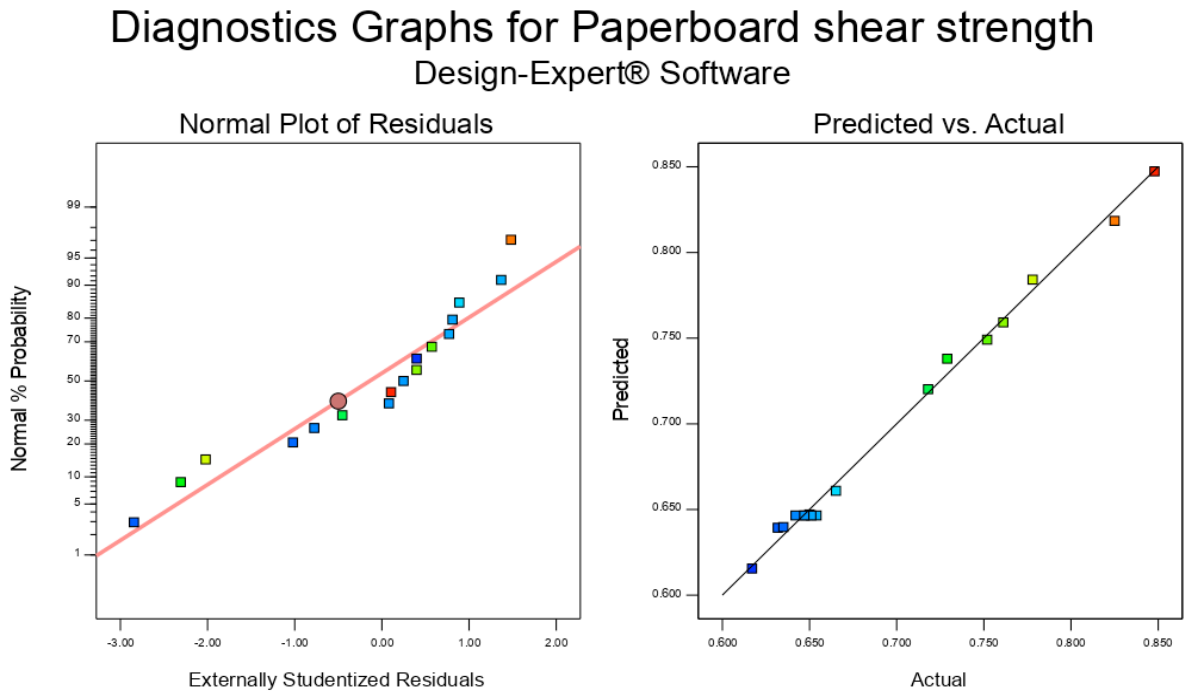

Figure 127: Normal probability and predicted versus actual residuals plot of Paperboard shear strength.

Table 49: The experiment responses results for adhesive production from NaOH gelatinisation

		Factor 1	Factor 2	Factor 3	Resp. 1	Resp. 2	Resp. 3	Resp. 4	Material	Failure locus
Std.	Run	A: NaOH	B: Borax	C: Temperature	Viscosity	Density	pH	Shear Strength		
		ml	g	°C	mPa.s	g/cm^3		MPa		
1	2	40	0.1	75	1450.47	1.048	12.95	3.30		CF
2	20	50	0.1	75	815.27	1.037	13.02	2.45		CF
3	13	40	0.3	75	3953.00	1.058	12.42	3.33		CF
4	34	50	0.3	75	2029.35	1.042	12.80	2.63		CF
5	10	40	0.2	65	1979.09	1.064	12.87	3.03		CF
6	33	50	0.2	65	1381.93	1.052	12.90	2.33		CF
7	21	40	0.2	85	1337.16	1.045	12.88	3.59		CF
8	16	50	0.2	85	953.02	1.005	12.94	2.60	Plywood	CF
9	12	45	0.1	65	1109.18	1.047	13.00	2.54		CF
10	8	45	0.3	65	3394.07	1.059	12.62	2.75		CF
11	24	45	0.1	85	970.17	1.029	12.99	3.10		CF
12	19	45	0.3	85	2820.50	1.037	12.67	3.25		CF
13	6	45	0.2	75	1337.60	1.046	12.92	2.73		CF
14	18	45	0.2	75	1385.62	1.052	12.89	2.74		CF
15	25	45	0.2	75	1581.95	1.054	12.94	2.67		CF
16	3	45	0.2	75	1387.32	1.047	12.96	2.81		CF
17	15	45	0.2	75	1344.95	1.048	12.98	2.65		CF

18	32	40	0.1	75	1450.47	1.048	12.95	0.632		SF
19	7	50	0.1	75	815.27	1.037	13.02	0.617		SF
20	17	40	0.3	75	3953.00	1.058	12.42	0.778		SF
21	22	50	0.3	75	2029.35	1.042	12.80	0.650		SF
22	30	40	0.2	65	1979.09	1.064	12.87	0.718		SF
23	14	50	0.2	65	1381.93	1.052	12.90	0.635		CF
24	28	40	0.2	85	1337.16	1.045	12.88	0.825		SF
25	9	50	0.2	85	953.02	1.005	12.94	0.729		SF
26	31	45	0.1	65	1109.18	1.047	13.00	0.665		SF
27	27	45	0.3	65	3394.07	1.059	12.62	0.752		SF
28	5	45	0.1	85	970.17	1.029	12.99	0.761		SF
29	26	45	0.3	85	2820.50	1.037	12.67	0.848		SF
30	4	45	0.2	75	1337.60	1.046	12.92	0.648		SF
31	23	45	0.2	75	1385.62	1.052	12.89	0.642		SF
32	29	45	0.2	75	1581.95	1.054	12.94	0.654		SF
33	11	45	0.2	75	1387.32	1.047	12.96	0.651		SF
34	1	45	0.2	75	1344.95	1.048	12.98	0.647		SF

SF: Substrate failure, CF: Cohesive Failure, AF: Adhesive Failure

B) HCl Gelatinisation

Table 50 illustrates the experiment matrix and results of the adhesive produced. The highest plywood shear strength was 3.12 MPa for run #20 at 40 ml gelatinisation, 0.2 g borax and 85 °C. At these conditions, the adhesive viscosity was 351.63 mPa.s and the density was 1.018 g/cm^3. While at 45 ml of gelatinisation, 0.3 g borax and 85 °C, the highest paperboard shear strength was achieved of 0.832 MPa from run #8. The viscosity of adhesives was 446.13 mPa.s and the density was 1.013 g/cm^3. The least shear strength value for plywood was found at 2.47 MPa (run #5) at 50 ml of gelatinisation, 0.2 g borax, and at low temperature of 65 °C. In contrast, at 50 ml of gelatinisation, 0.1 g of borax and 75 °C, the lowest paperboard shear strength of 0.581 MPa (run #12) was obtained. The viscosity values ranged between 223.19 to 1,035.05 mPa.s, while the densities were from 1.003 to 1.029 g/cm^3. Cohesive failure occurred for all plywood samples, while adhesive failure occurred for all plastic samples, even with surface treatment by sandpaper. The failure of paperboard samples took place in the substrates or cohesive failure for some samples.

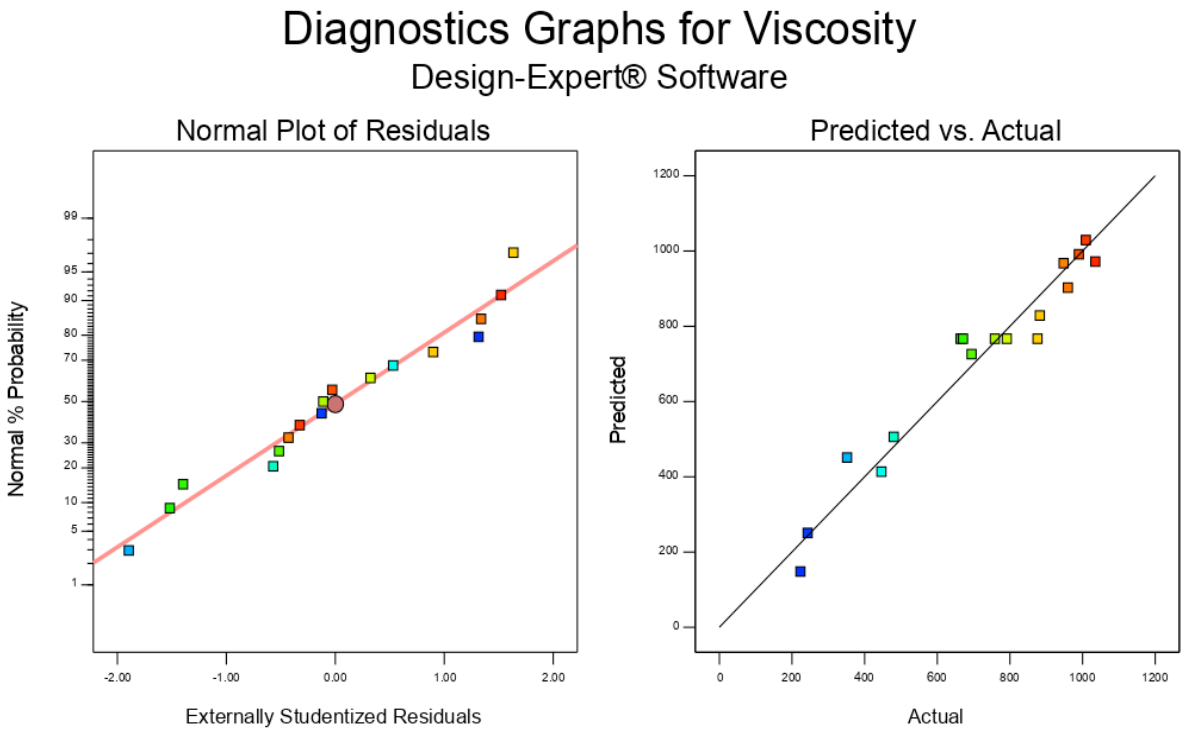

Figure 128: Normal probability and predicted versus actual residuals plot of viscosity.

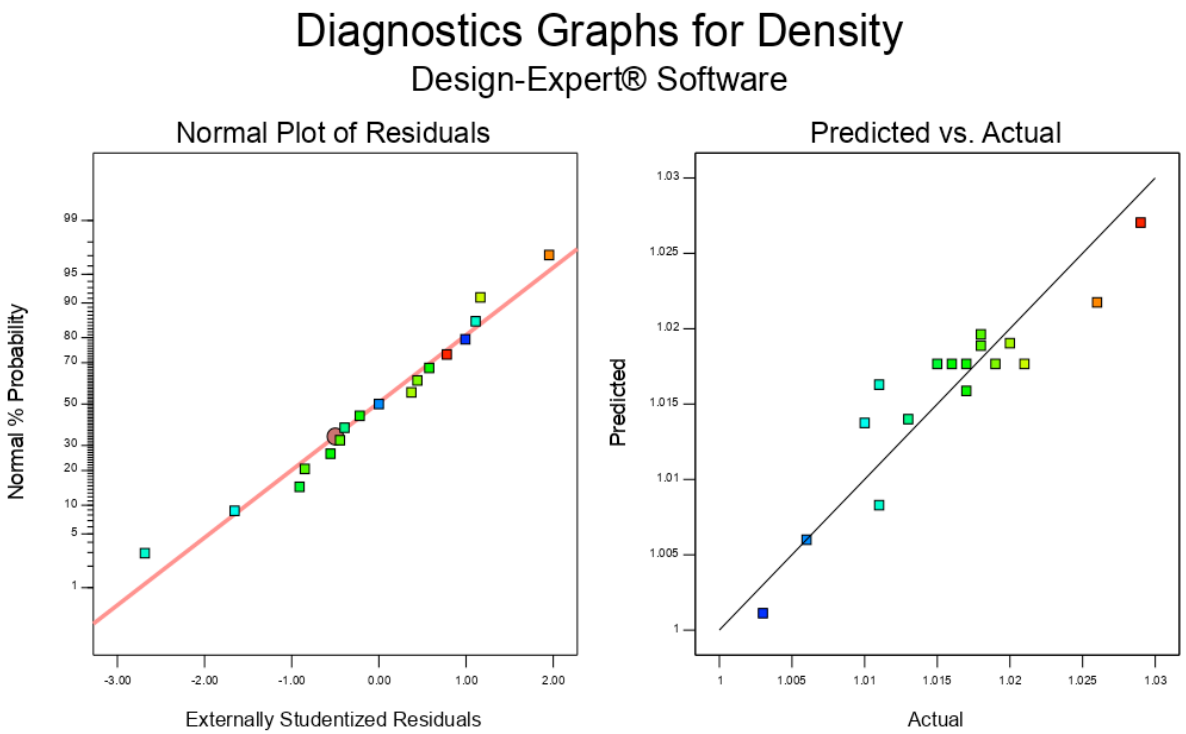

Figure 129: Normal probability and predicted versus actual residuals plot of density.

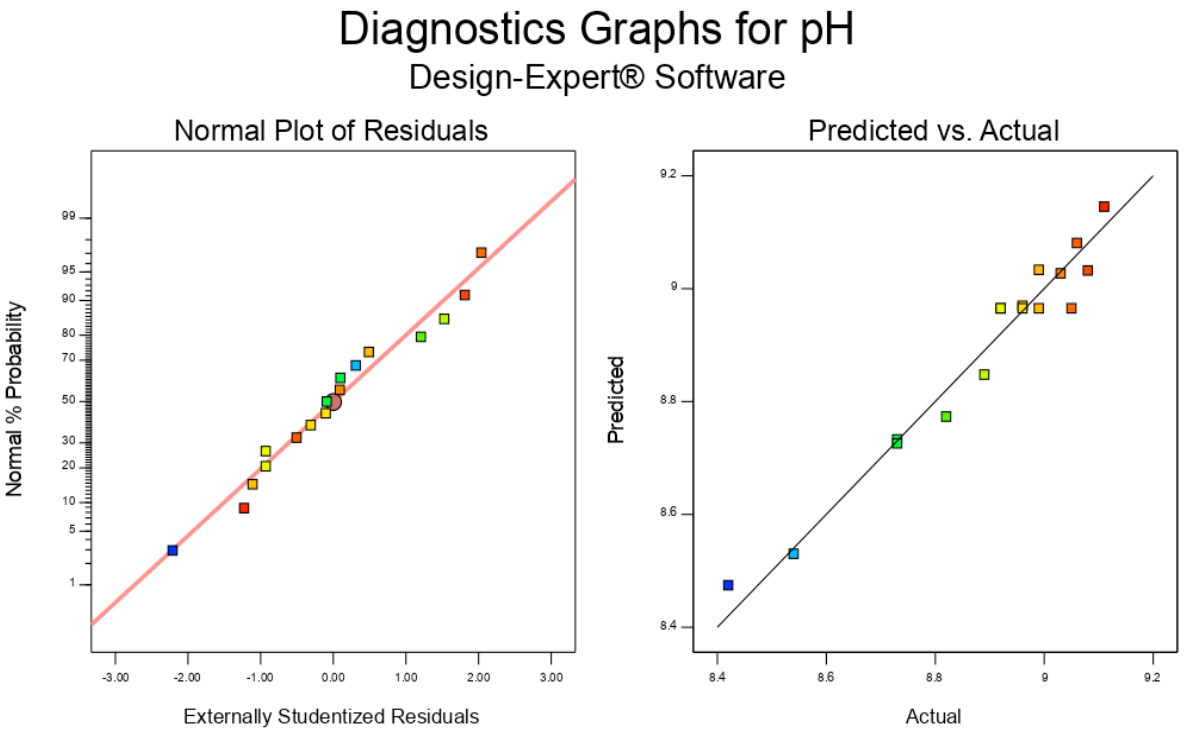

Figure 130: Normal probability and predicted versus actual residuals plot of pH.

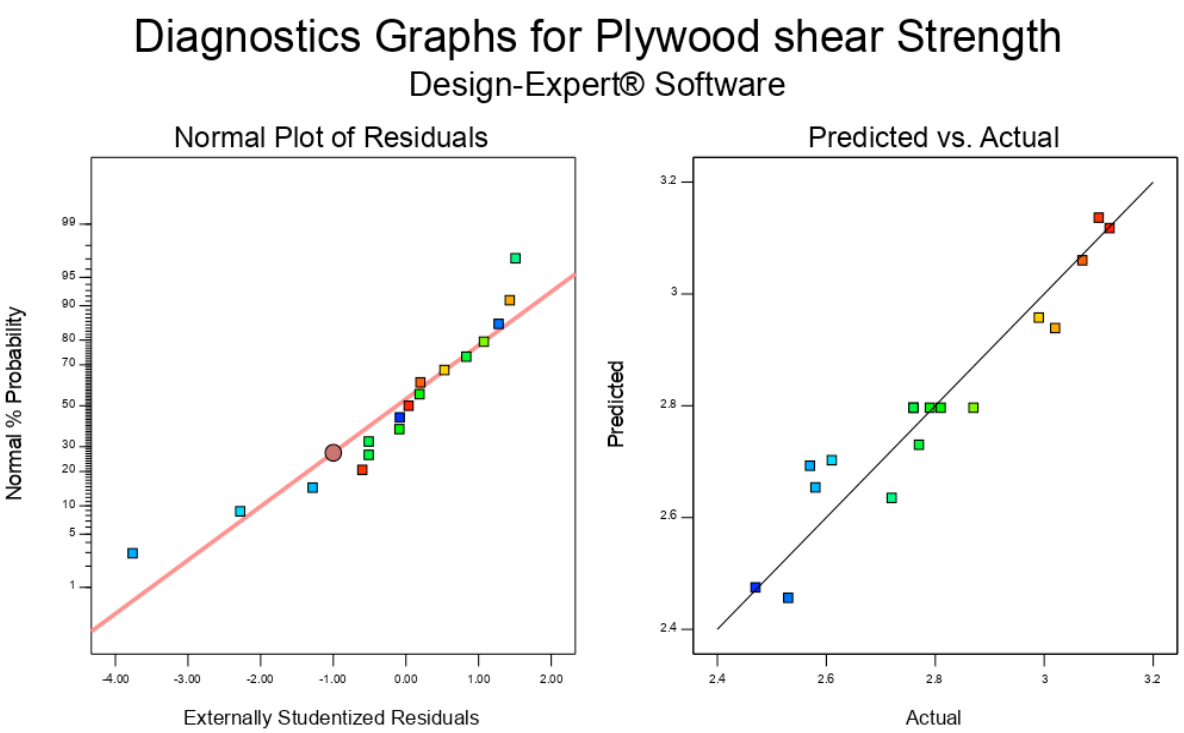

Figure 131: Normal probability and predicted versus actual residuals plot of Plywood shear strength.

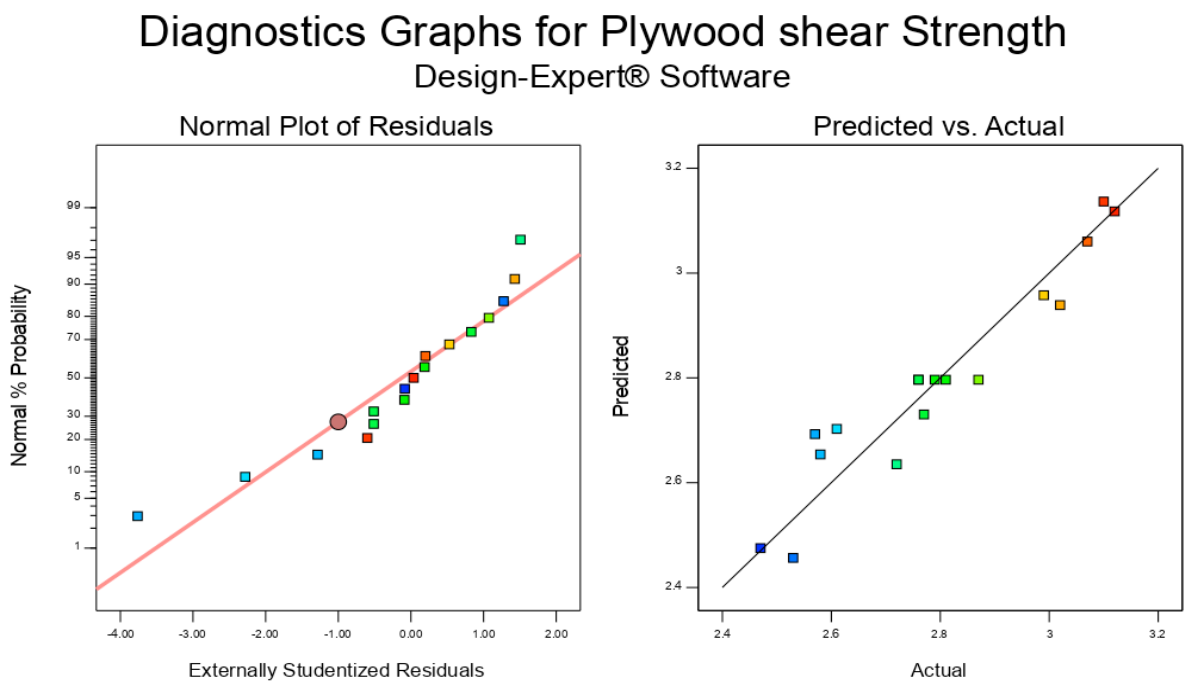

Figure 132: Normal probability and predicted versus actual residuals plot of Paperboard shear strength.

Table 50: The experiment responses results for adhesive production from HCl gelatinisation

		Factor 1	Factor 2	Factor 3	Resp. 1	Resp. 2	Resp. 3	Resp. 4	Material	Failure locus
Std.	Run	A: HCl	B: Borax	C: Temperature	Viscosity	Density	pH	Shear Strength		
		ml	g	°C	mPa.s	g/cm^3		MPa		
1	19	40	0.1	75	959.52	1.020	8.42	2.57		CF
2	2	50	0.1	75	480.15	1.011	8.96	2.61		CF
3	17	40	0.3	75	1035.05	1.029	9.03	3.07		CF
4	7	50	0.3	75	947.84	1.011	9.08	2.77		CF
5	22	40	0.2	65	1008.99	1.018	8.54	2.72		CF
6	5	50	0.2	65	882.27	1.017	9.11	2.47		CF
7	20	40	0.2	85	351.63	1.018	8.89	3.12		CF
8	4	50	0.2	85	243.09	1.003	8.73	2.99		CF
9	13	45	0.1	65	694.44	1.010	8.82	2.53		CF
10	27	45	0.3	65	989.73	1.026	9.06	2.58		CF
11	16	45	0.1	85	223.19	1.006	8.73	3.02		CF
12	25	45	0.3	85	446.13	1.013	8.99	3.10		CF
13	28	45	0.2	75	758.53	1.015	8.96	2.76		CF
14	6	45	0.2	75	664.13	1.021	9.05	2.87		CF
15	18	45	0.2	75	670.82	1.019	8.92	2.76		CF
16	15	45	0.2	75	875.89	1.017	8.99	2.79		CF
17	30	45	0.2	75	791.33	1.016	8.92	2.81		CF

18	3	40	0.1	75	959.52	1.020	8.42	0.599	Paperboard	SF
19	12	50	0.1	75	480.15	1.011	8.96	0.581		SF
20	24	40	0.3	75	1035.05	1.029	9.03	0.744		SF
21	14	50	0.3	75	947.84	1.011	9.08	0.627		SF
22	34	40	0.2	65	1008.99	1.018	8.54	0.652		CF
23	9	50	0.2	65	882.27	1.017	9.11	0.621		CF
24	33	40	0.2	85	351.63	1.018	8.89	0.784		CF
25	21	50	0.2	85	243.09	1.003	8.73	0.689		SF
26	26	45	0.1	65	694.44	1.010	8.82	0.627		CF
27	23	45	0.3	65	989.73	1.026	9.06	0.694		SF
28	31	45	0.1	85	223.19	1.006	8.73	0.715		SF
29	8	45	0.3	85	446.13	1.013	8.99	0.832		SF
30	1	45	0.2	75	758.53	1.015	8.96	0.622		SF
31	11	45	0.2	75	664.13	1.021	9.05	0.636		SF
32	29	45	0.2	75	670.82	1.019	8.92	0.629		SF
33	32	45	0.2	75	875.89	1.017	8.99	0.635		SF
34	10	45	0.2	75	791.33	1.016	8.92	0.626		SF

SF: Substrate failure, CF: Cohesive Failure, AF: Adhesive Failure

4.10.1 Model Estimation of NaOH Gelatinisation

The ANOVA Tables 51-55 illustrates that all responses were significant. The coded (36, 38, 40, 42 and 44) and actual equations (37, 39, 41, 43 and 45) are clarified below for each response. The impact of gelatinisation (A), borax (B) and temperature (C) were significant for all responses except the pH which was not significantly affected by temperature. The interaction effect of gelatinisation and borax (AB) was significant on the viscosity, pH and plywood' and paperboard' shear strengths. While the effect of starch and temperature (AC) was significant on the density, pH and paperboard shear strength and there was significant effect for the interaction of borax and temperature (BC) on paperboard shear strength only.

4.10.2 Viscosity

It can be seen from Figure 133 that there was a linear relationship between viscosity and all factors. It decreased by increasing the gelatinisation quantity and temperature while it increased with an increase of borax. The lowest viscosity value of adhesive was found at the highest value of gelatinisation and lowest value of borax and 75 °C. The adhesive viscosity decreased sharply with an increasing the amount of gelatinisation at 0.3 g of borax and 75 °C. In comparison, the viscosity decreased slightly due to an increase in gelatinisation, at 0.1 g of borax and 75 °C as shown in Figure 134. Figure 135 describes the highest viscosity values obtained when the gelatinisation was 42 ml and less, the amount of borax was more than 0.27 g and at 75 °C. The

highest positive effect of borax, was followed by an inverse effect of gelatinisation quantity as seen in coded Equation 36:

$$\text{Viscosity} = + 1409.85 - 442.52*A + 981.48*B - 222.93*C - 322.11*AB + 657.90*B^2 \quad \text{Equation (36)}$$

The actual equation (37) for Viscosity is:

$$\text{Viscosity} = + 1935.10083 + 40.34125*\text{NaOH} + 12488.81806*\text{Borax} - 22.29275*\text{Temperature} - 644.2250*\text{NaOH} * \text{Borax} + 65790.23611*\text{Borax}^2 \quad \text{Equation (37)}$$

Table 51: ANOVA table for viscosity response.

Source	Sum of Squares	df	Mean Square	F-value	p-value	
Model	1.192E+07	5	2.384E+06	58.53	< 0.0001	Significant
A-NaOH	1.567E+06	1	1.567E+06	38.46	< 0.0001	
B-Borax	7.706E+06	1	7.706E+06	189.21	< 0.0001	
C-Temperature	3.976E+05	1	3.976E+05	9.76	0.0097	
AB	4.150E+05	1	4.150E+05	10.19	0.0086	
B^2	1.833E+06	1	1.833E+06	45.01	< 0.0001	
Residual	4.480E+05	11	40729.87			
Lack of Fit	4.079E+05	7	58273.04	5.81	0.0542	Not significant
Pure Error	40117.28	4	10029.32			
Cor Total	1.237E+07	16				
Adequacy measuring tools	R^2= 0.9638	Adjusted R^2= 0.9473		Predicted R^2= 0.8517		

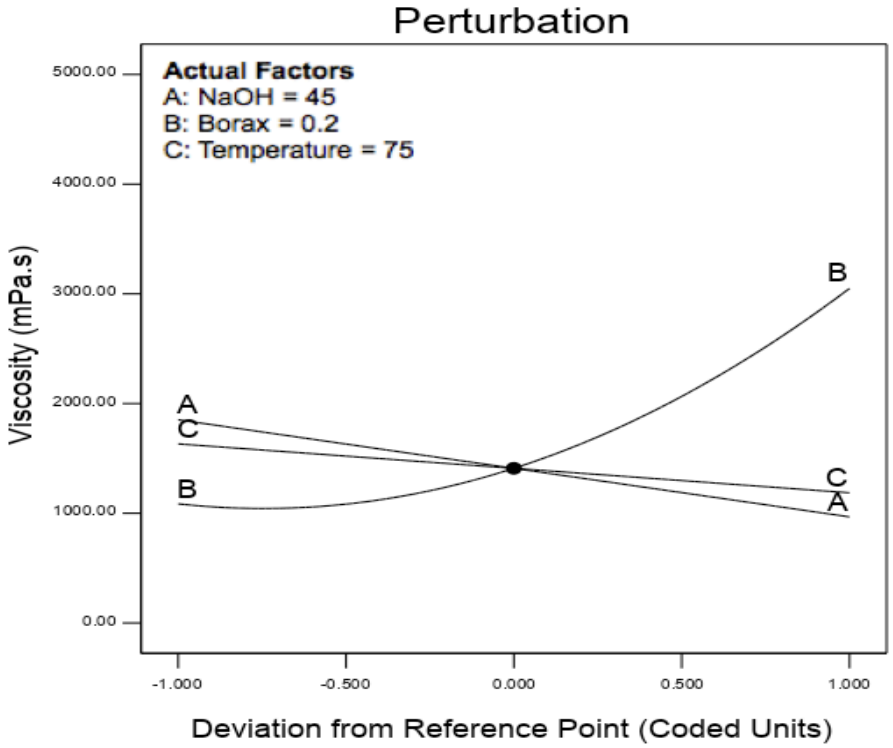

Figure 133: Perturbation plot shows the effect of all factors on viscosity.

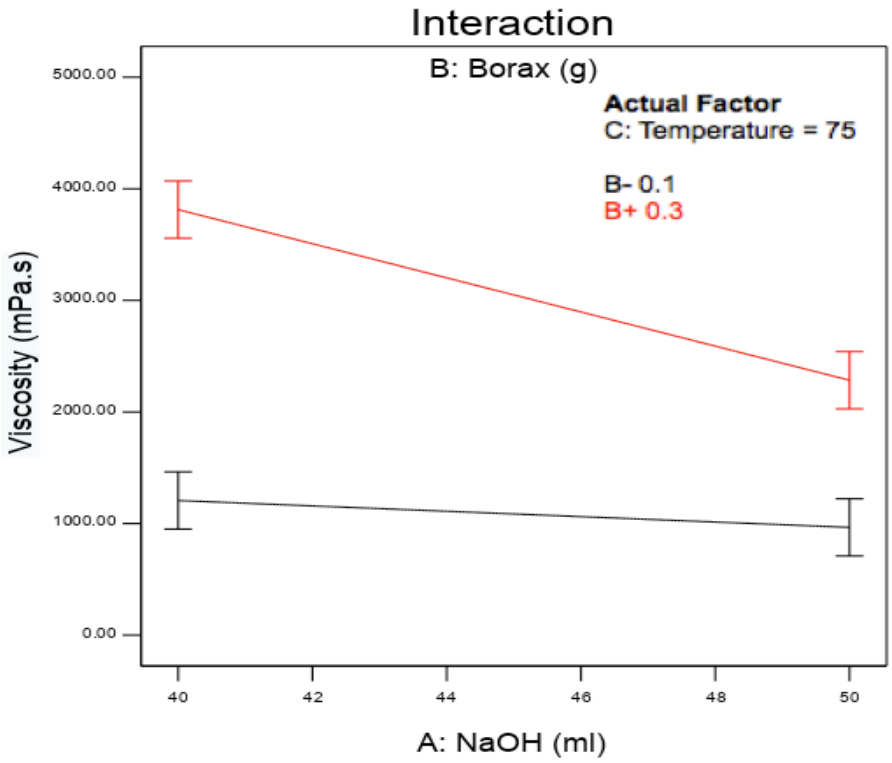

Figure 134: Interaction plot describes the effect of the interaction between gelatinisation and borax on viscosity.

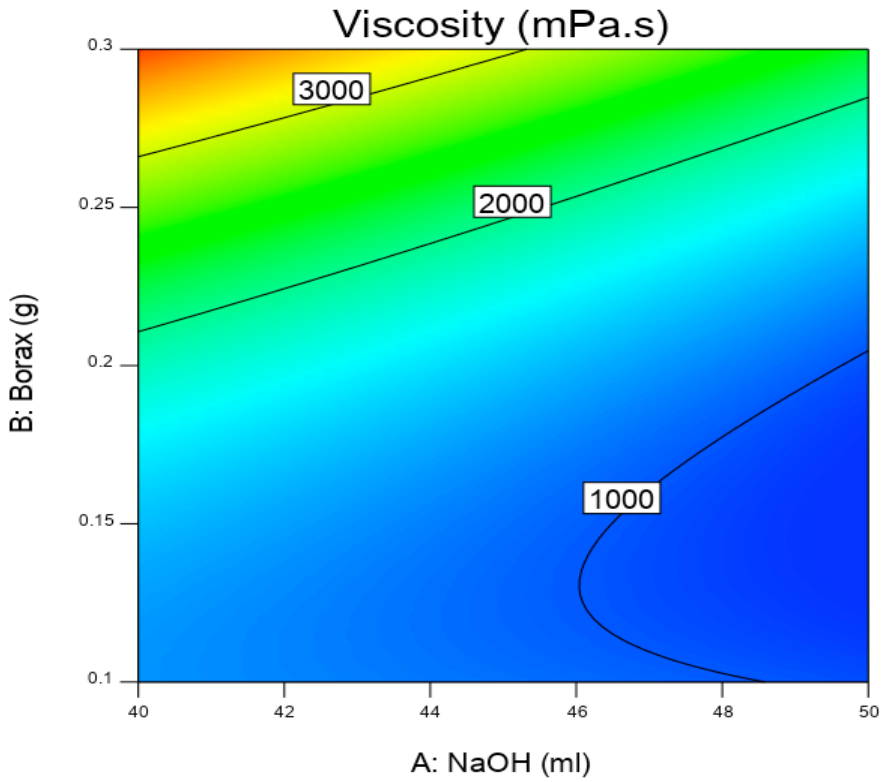

Figure 135: Contour plot views of the effect of gelatinisation and borax on viscosity at 75 °C.

4.10.3 Density

Figure 136 shows the effect of factors on adhesive density. It shows a similar trend to the effect of factors on density with viscosity. The density decreased with the increase of gelatinisation and temperature and increased with an increase of borax. Figure 137 demonstrates that the density was significantly decreased with the increasing of gelatinisation quantity at 0.2 g of borax and 85 °C while it decreased slightly when the borax was 0.2 g and at 65 °C. The density was at its highest level when the gelatinisation was less than 44 ml, at 0.2 g of borax and the temperature was less than 72 °C as illustrated in Figure 138. Equation (38) shows that the temperature (C) had greatest influence of on the adhesive density:

$$\text{Density} = +1.05 - 0.0099*A + 0.0044*B - 0.0133*C - 0.0070*AC - 0.0058*C^2 \quad \text{Equation (38)}$$

The actual equation (39) for Density is:

$$\text{Density} = + 0.431562 + 0.008525*\text{NaOH} + 0.043750*\text{Borax} + 0.013600*\text{Temperature} - 0.000140*\text{NaOH} * \text{Temperature} - 0.000058*\text{Temperature}^2 \quad \text{Equation (39)}$$

Table 52: ANOVA table for density response.

Source	Sum of Squares	df	Mean Square	F-value	p-value	
Model	0.0027	5	0.0005	23.55	< 0.0001	Significant
A-NaOH	0.0008	1	0.0008	34.36	0.0001	
B-Borax	0.0002	1	0.0002	6.74	0.0248	
C-Temperature	0.0014	1	0.0014	61.86	< 0.0001	
AC	0.0002	1	0.0002	8.63	0.0135	
C^2	0.0001	1	0.0001	6.17	0.0304	
Residual	0.0002	11	0.0000			
Lack of Fit	0.0002	7	0.0000	2.45	0.2019	Not significant
Pure Error	0.0000	4	0.0000			
Cor Total	0.0029	16				
Adequacy measuring tools	R^2= 0.9146	Adjusted R^2= 0.8757		Predicted R^2= 0.6787		

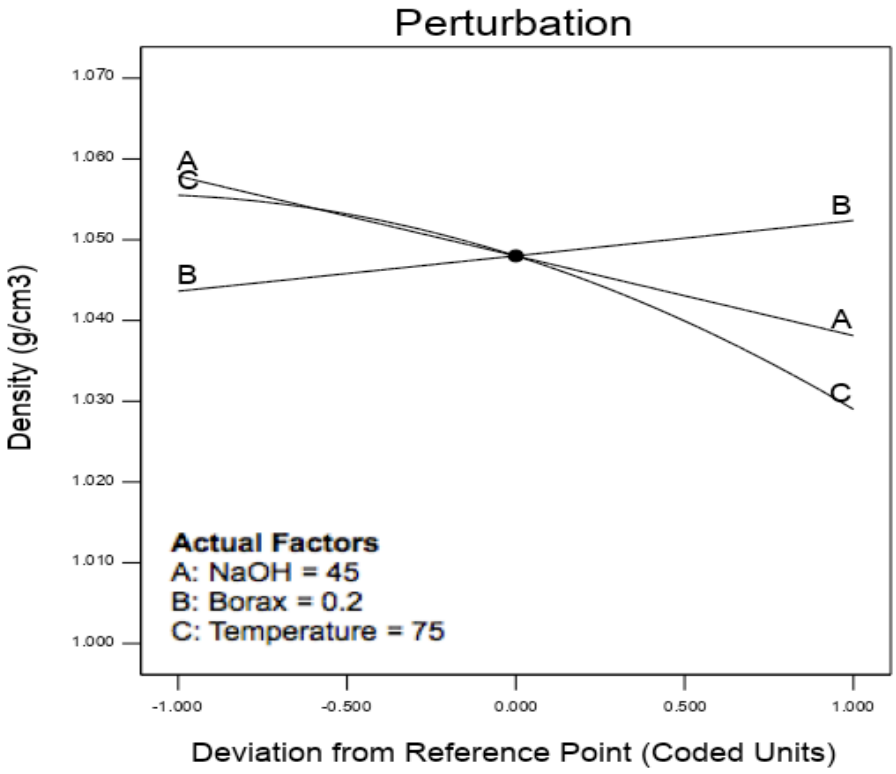

Figure 136: Perturbation plot illustrates the effect of all factors on density.

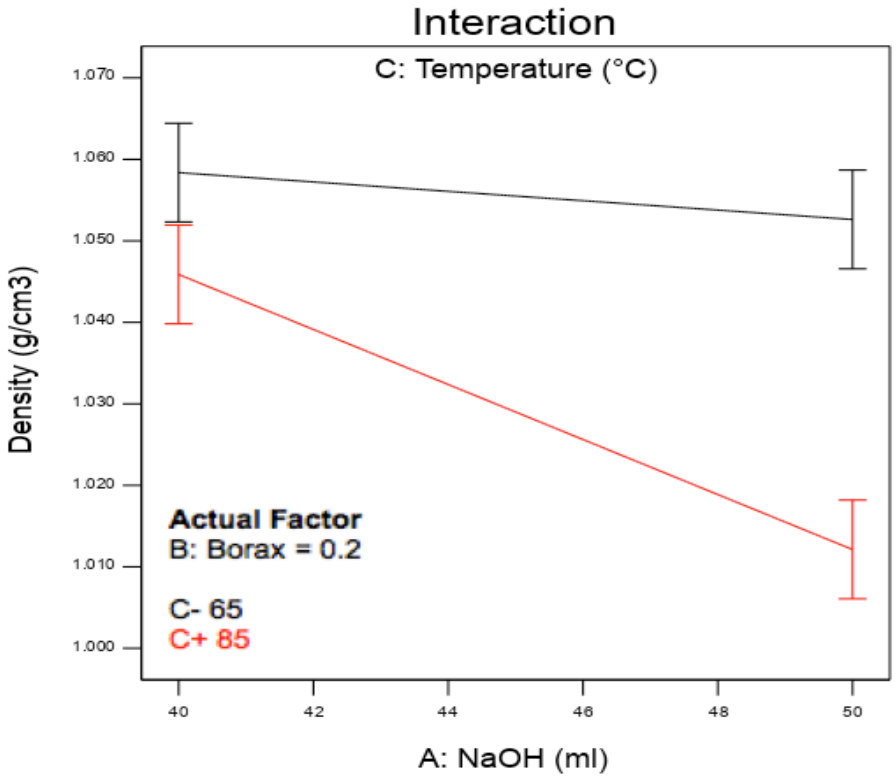

Figure 137: Interaction plot shows the effect of interaction between gelatinisation and temperature on density.

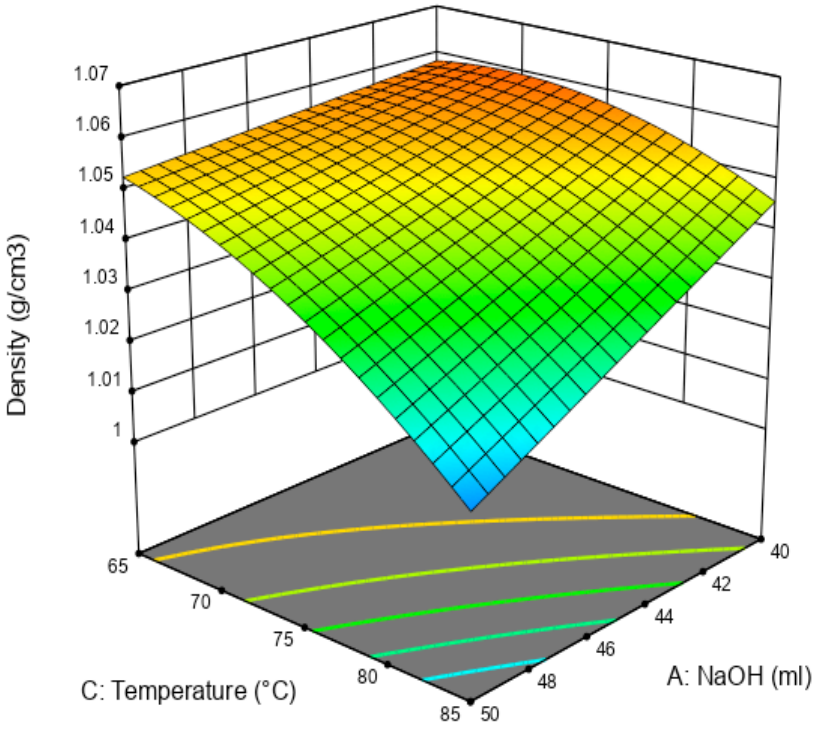

Figure 138: 3-D surface plot demonstrating the effect of gelatinisation and temperature on density at 0.2 g of borax.

4.10.4 pH

The pH was significantly affected by the amount of gelatinisation and borax, whereas the temperature did not significantly affect it, as shown in Figure 139. From the same figure, the pH increased slightly with increasing the amount of gelatinisation and it decreased significantly with an increase in borax. Figure 140 shows that the pH remained almost constant with increasing gelatinisation when using 0.1 g of borax and at 75 °C. In contrast, it increased with increasing gelatinisation, at 0.3 g of borax and at 75 °C. Figure 141 shows the highest pH values were in the bounded area between any amount of gelatinisation, borax less than 0.17 g and at 75 ° C. The coded equation (40) illustrates that the highest impact was for borax on the pH value:

$$pH = + 12.92 + 0.0675*A - 0.1813*B + 0.0113*C + 0.0775*AB - 0.1112*B^2 \quad \text{Equation (40)}$$

The actual equation (41) for pH is:

$$pH = + 13.54063 - 0.017500*NaOH - 4.33750*Borax + 0.001125*Temperature + 0.155000*NaOH * Borax -11.12500*Borax^2 \quad \text{Equation (41)}$$

Table 53: ANOVA table for density response.

Source	Sum of Squares	df	Mean Square	F-value	p-value	
Model	0.3767	5	0.0753	30.48	< 0.0001	Significant
A-NaOH	0.0364	1	0.0364	14.75	0.0027	
B-Borax	0.2628	1	0.2628	106.33	< 0.0001	
C-Temperature	0.0010	1	0.0010	0.4097	0.5352	
AB	0.0240	1	0.0240	9.72	0.0098	
B^2	0.0524	1	0.0524	21.21	0.0008	
Residual	0.0272	11	0.0025			
Lack of Fit	0.0223	7	0.0032	2.61	0.1853	Not significant
Pure Error	0.0049	4	0.0012			
Cor Total	0.4039	16				
Adequacy measuring tools	R^2= 0.9327	Adjusted R^2= 0.9021			Predicted R^2= 0.7526	

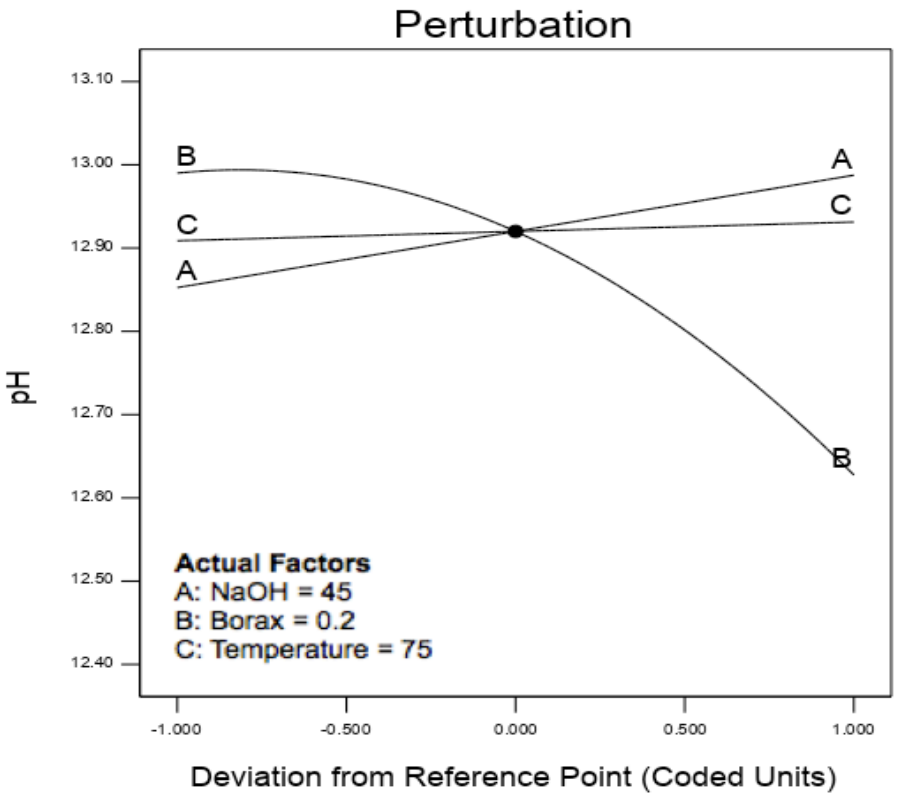

Figure 139: Perturbation plot illustrating the effect of all factors on pH.

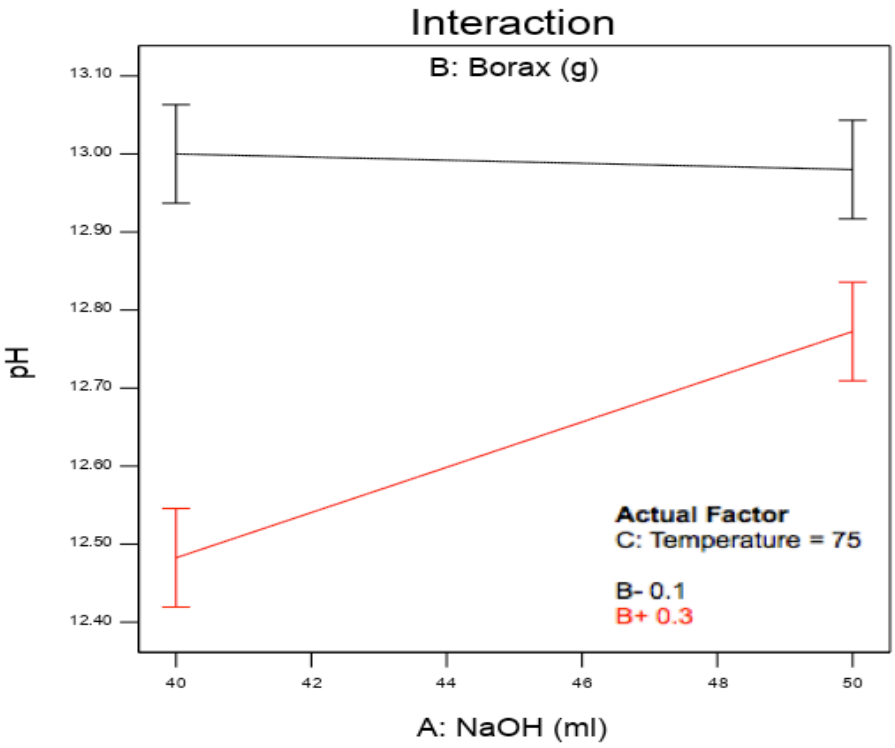

Figure 140: Interaction plot shows the effect of interaction between gelatinisation and borax on pH.

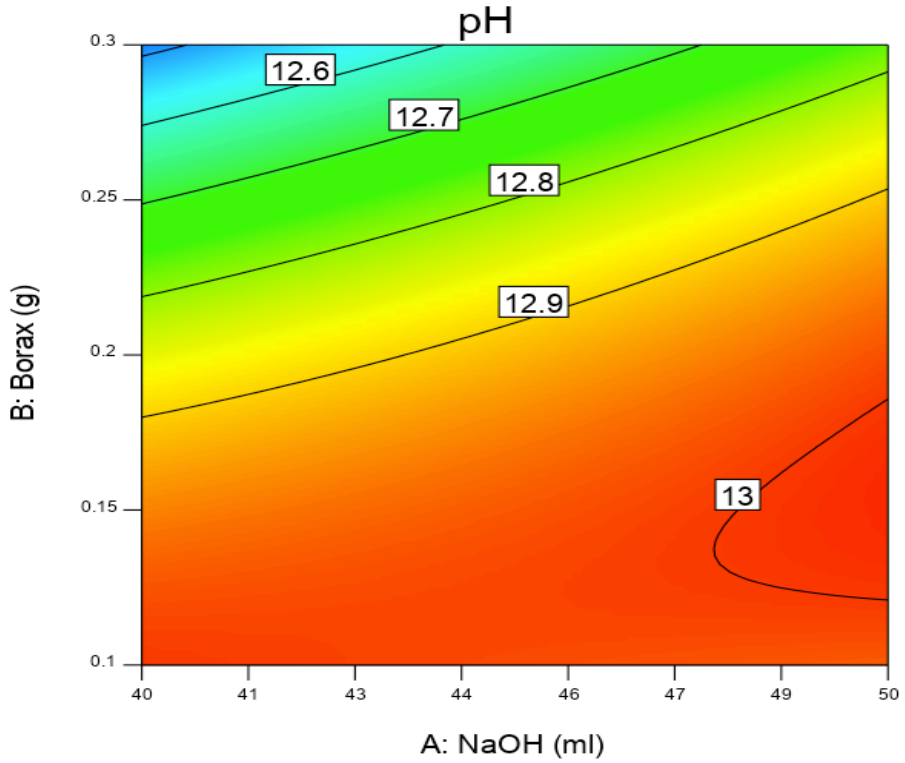

Figure 141: Contour plot demonstrating the effect of gelatinisation and borax on density at 75 °C.

4.10.5 Shear Strength of Plywood

The shear strength value of plywood specimens decreased with an increase of gelatinisation, but increased as both borax and temperature increased as shown in Figure 142. The shear strength decreased significantly with increasing the gelatinisation amount, at 0.2 g of borax and 65 °C and 85 °C as shown in Figure 143. The shear strength was at its lowest value when the gelatinisation was 50 ml, 0.2 g of borax and 65 °C. In contrast, highest shear strength of plywood specimens was achieved at 40-41 ml of gelatinisation, 0.2 g of borax and 80-85 °C as shown in Figure 144. The effects of gelatinisation quantity, followed by temperature, had the largest effect on plywood shear strength as describes by Equation (42):

$$\text{Plywood shear Strength} = + 2.72 - 0.4050*A + 0.0713*B + 0.2363*C - 0.0725*AC + 0.0925*A^2 + 0.1150*B^2 + 0.0750*C^2 \quad \text{Equation (42)}$$

The actual equation (43) for Plywood shear strength is:

$$\text{Plywood shear Strength} = + 11.72813 - 0.305250*\text{NaOH} - 3.88750*\text{Borax} - 0.023625*\text{Temperature} - 0.001450*\text{NaOH} * \text{Temperature} + 0.003700*\text{NaOH}^2 + 11.50000*\text{Borax}^2 + 0.000750*\text{Temperature}^2 \quad \text{Equation (43)}$$

Table 54: ANOVA table for plywood shear strength response.

Source	Sum of Squares	df	Mean Square	F-value	p-value	
Model	1.95	7	0.2784	72.84	< 0.0001	Significant
A-NaOH	1.31	1	1.31	343.31	< 0.0001	
B-Borax	0.0406	1	0.0406	10.63	0.0098	
C-Temperature	0.4465	1	0.4465	116.82	< 0.0001	
AC	0.0210	1	0.0210	5.50	0.0436	
A^2	0.0360	1	0.0360	9.43	0.0134	
B^2	0.0557	1	0.0557	14.57	0.0041	
C^2	0.0237	1	0.0237	6.20	0.0345	
Residual	0.0344	9	0.0038			
Lack of Fit	0.0184	5	0.0037	0.9200	0.5475	Not significant
Pure Error	0.0160	4	0.0040			
Cor Total	1.98	16				
Adequacy measuring tools	R^2= 0.9827	Adjusted R^2= 0.9692		Predicted R^2= 0.9229		

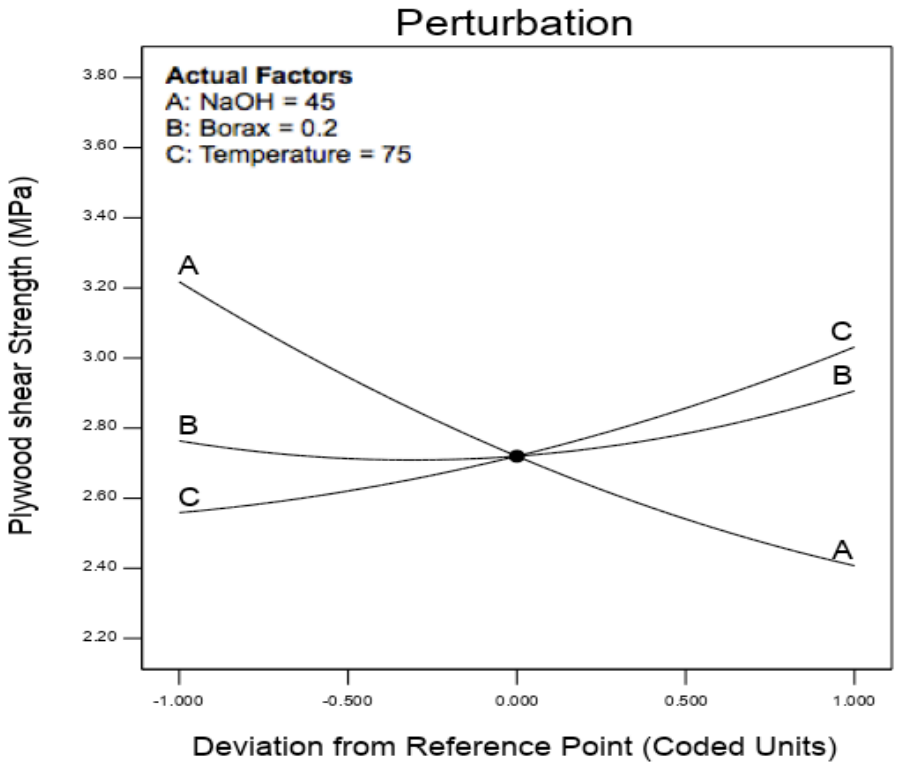

Figure 142: Perturbation plot demonstrating the effect of all factors on plywood shear strength.

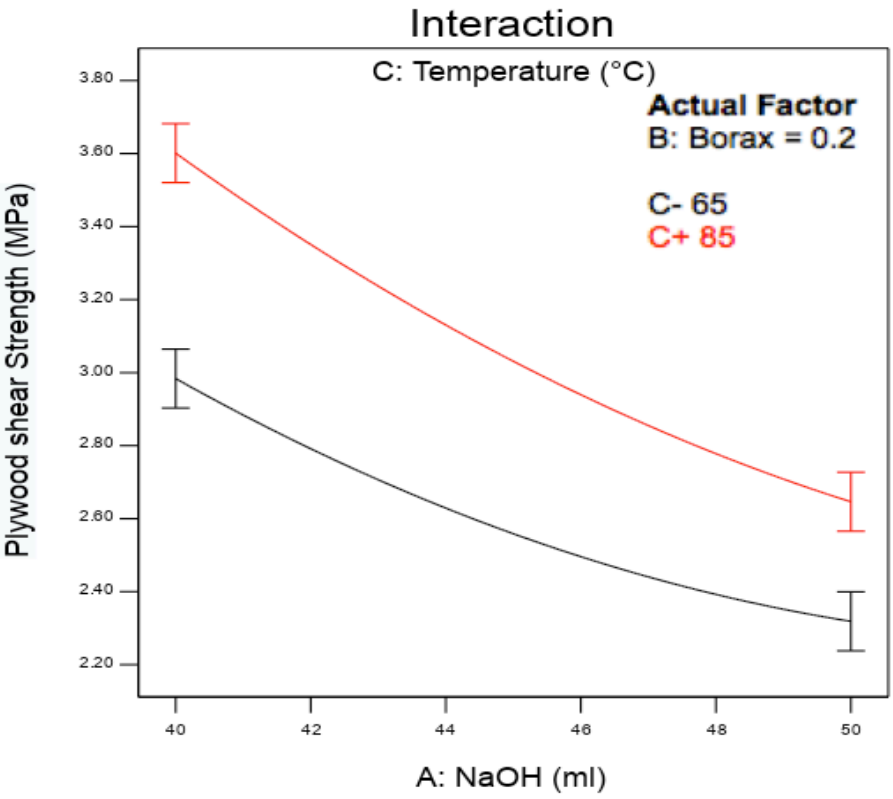

Figure 143: Interaction plot illustrating the effect of the interaction between gelatinisation and temperature on paperboard shear strength.

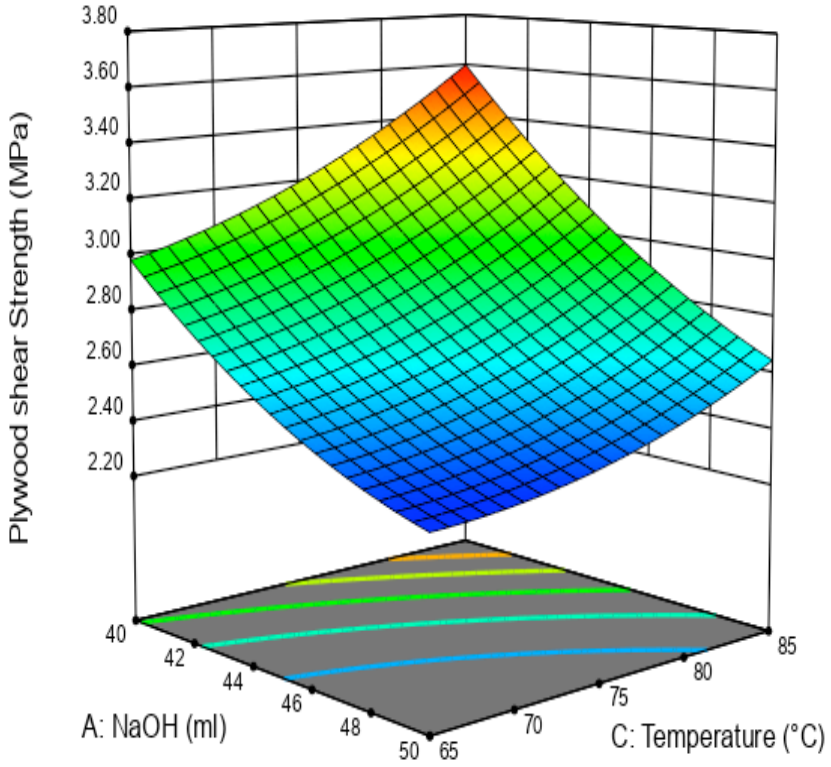

Figure 144: Contour plot shows the effect of gelatinisation and temperature on plywood shear strength at 0.2 g of borax.

4.10.6 Shear Strength of Paperboard

The indirect proportional relationship of gelatinisation quantity, on plywood shear strength continued with the paperboard shear strength as shown in Figure 145. The figure also shows the direct relationship between borax and the paperboard shear strength. The temperature had an inverse influence on the paperboard shear strength until it reached the centre level value where it then rose. Figure 146 shows the impact of gelatinisation and borax quantities on the paperboard shear strength. The shear strength decreased significantly when the gelatinisation was increased, at 0.3 g of borax and decreased slightly, at 0.1 g of borax when the temperature was 75 °C. It reached its highest values when the gelatinisation was less than 44 ml, for samples with more than 0.22 g of borax at 85 °C (Figure 147). The coded Equation (44) shows the effects of such factors on the response:

$$\text{Paperboard shear strength} = + 0.6465 - 0.0402*A + 0.0441*B + 0.0491*C - 0.0283*AB + 0.0250*B^2 + 0.082*C^2 \quad \text{Equation (44)}$$

The actual equation (45) for Paperboard shear strength is:

$$\text{Paperboard shear strength} = + 4.78861 + 0.003275*\text{NaOH} + 1.98608*\text{Borax} - 0.118978*\text{Temperature} - 0.056599*\text{NaOH} * \text{Borax} + 2.50440*\text{Borax}^2 + 0.000826*\text{Temperature}^2 \quad \text{Equation (45)}$$

Table 55: ANOVA table for paperboard shear strength response.

Source	Sum of Squares	df	Mean Square	F-value	p-value	
Model	0.0835	6	0.0139	360.72	< 0.0001	Significant
A-NaOH	0.0129	1	0.0129	335.42	< 0.0001	
B-Borax	0.0155	1	0.0155	402.92	< 0.0001	
C-Temperature	0.0193	1	0.0193	500.27	< 0.0001	
AB	0.0032	1	0.0032	83.01	< 0.0001	
B^2	0.0026	1	0.0026	68.62	< 0.0001	
C^2	0.0288	1	0.0288	746.35	< 0.0001	
Residual	0.0004	10	0.0000			
Lack of Fit	0.0003	6	0.0001	2.50	0.1970	Not significant
Pure Error	0.0001	4	0.0000			
Cor Total	0.0839	16				
Adequacy measuring tools	R^2= 0.9954	Adjusted R^2= 0.9926		Predicted R^2= 0.9789		

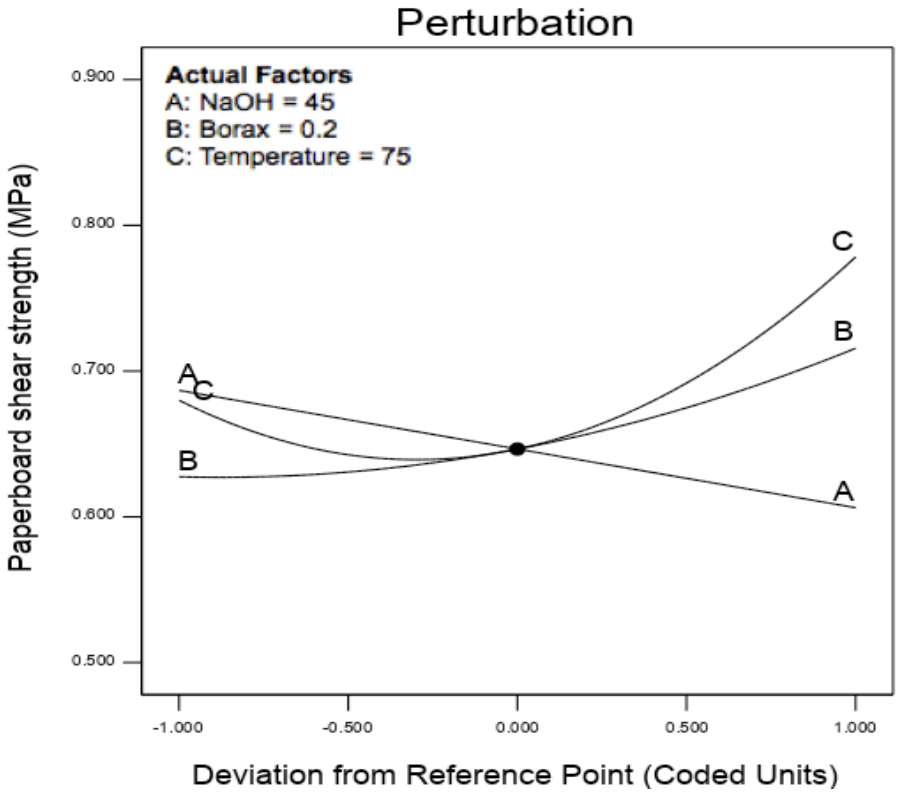

Figure 145: Perturbation plot shows the effect of all factors on paperboard shear strength.

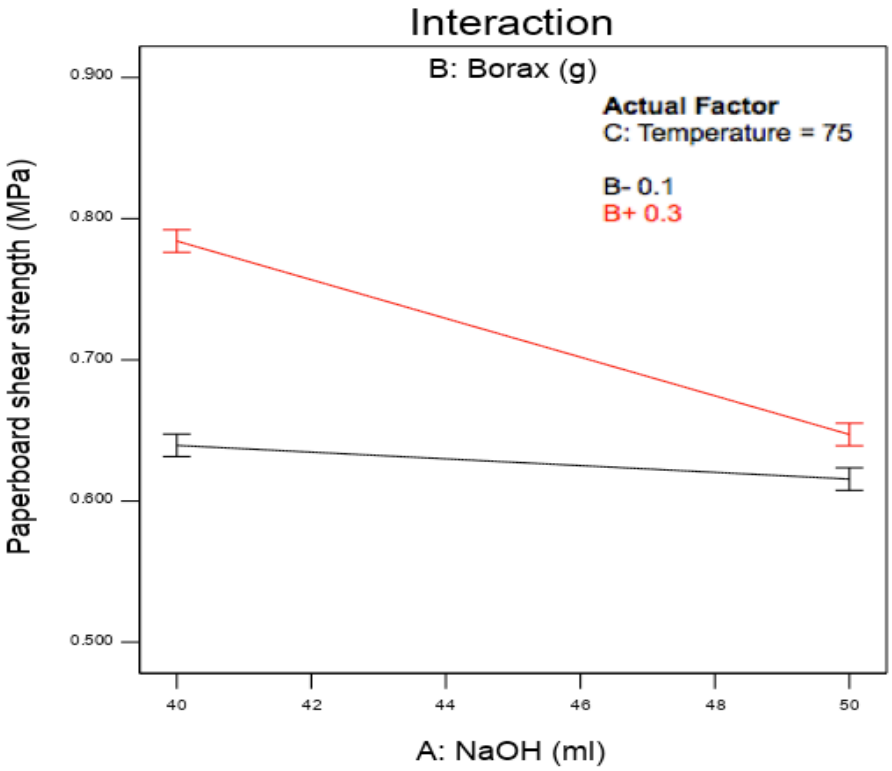

Figure 146: Interaction plot displaying the effect of the interaction between gelatinisation and borax on paperboard shear strength.

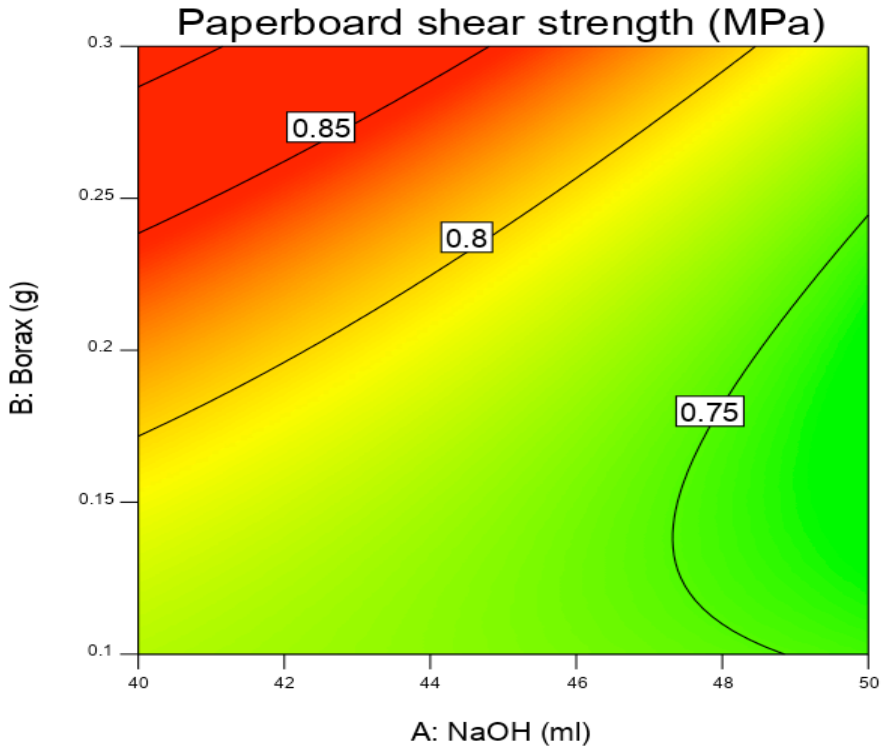

Figure 147: Contour plot illustrating the effect of gelatinisation and borax on paberboard shear strength at 85 °C.

4.10.7 Model Estimation of HCl Gelatinisation

The significance of all responses is seen in ANOVA Tables 56-60, while the coded equations (46, 48, 50, 52 and 54) and actual equations (47, 49, 51, 53 and 55) are illustrated below for all the responses. The impact of gelatinisation (A), borax (B) and temperature (C) was significant for all responses except the pH, which was not significantly affected by temperature. The interaction effect of gelatinisation and borax (AB) was significant on the viscosity and plywood shear strength. The effect of starch and temperature (AC) was significant on the density, pH and paperboard' shear strength. The interaction of borax and temperature (BC) only affected the paperboard shear strength.

4.10.8 Viscosity

Figure 148 displays the relationships between the factors and the adhesive viscosity. The interaction impacts of gelatinisation and borax on the viscosity is shown in Figure 149. The lowest viscosity was obtained at 50 ml of gelatinisation, 0.1 g of borax and 75 °C. The viscosity was at its highest value a 40 ml of gelatinisation, both for 0.1 and 0.3 g of borax and 75 °C as shown in the same figure. Simultaneously, the viscosity decreased significantly with the increase of gelatinisation at 0.1 g of borax and 75 °C. While it decreased slightly by increasing gelatinisation at 0.3 g of borax and 75 °C until the centre value, it rose slightly. The highest viscosity values of adhesive were obtained at 40 ml of gelatinisation, all amounts of borax and 75 °C as shown from the 3D surfaces plot (Figure 150). From the same figure, it can be noticed that, at any gelatinisation quantity, 0.3 g of borax and 75 °C, achieved the highest viscosity values. The coded Equation (46) illustrated the highest negative impact of temperature on the viscosity followed by the positive impact of borax:

$$\text{Viscosity} = +766.96 - 100.23*A + 132.68*B - 288.92*C + 98.04*AB + 70.16*A^2 - 197.10*C^2 \quad \text{Equation (46)}$$

The actual equation (47) for Viscosity is:

$$\text{Viscosity} = -68.53788 - 311.84899*HCl - 7496.68125*Borax + 266.76226*Temperature + 196.07750*HCl * Borax + 2.80653*HCl^2 - 1.97103*Temperature^2 \quad \text{Equation (47)}$$

Table 56: ANOVA table for viscosity response.

Source	Sum of Squares	df	Mean Square	F-value	p-value	
Model	1.106E+06	6	1.844E+05	29.95	< 0.0001	Significant
A-HCl	80369.43	1	80369.43	13.05	0.0047	
B-Borax	1.408E+05	1	1.408E+05	22.87	0.0007	
C-Temperature	6.678E+05	1	6.678E+05	108.46	< 0.0001	
AB	38446.39	1	38446.39	6.24	0.0315	
A^2	20785.45	1	20785.45	3.38	0.0960	
C^2	1.640E+05	1	1.640E+05	26.64	0.0004	
Residual	61572.12	10	6157.21			
Lack of Fit	30323.62	6	5053.94	0.6469	0.6987	Not significant
Pure Error	31248.50	4	7812.13			
Cor Total	1.168E+06	16				
Adequacy measuring tools	R^2= 0.9473	Adjusted R^2= 0.9156			Predicted R^2= 0.8339	

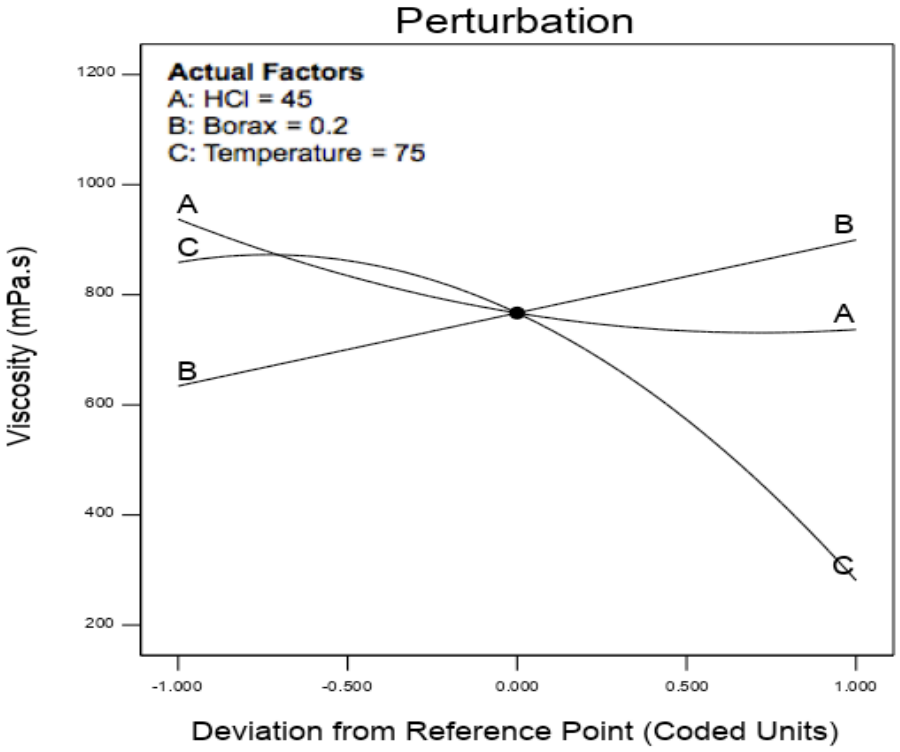

Figure 148: Perturbation plot shows the effect of all factors on the viscosity.

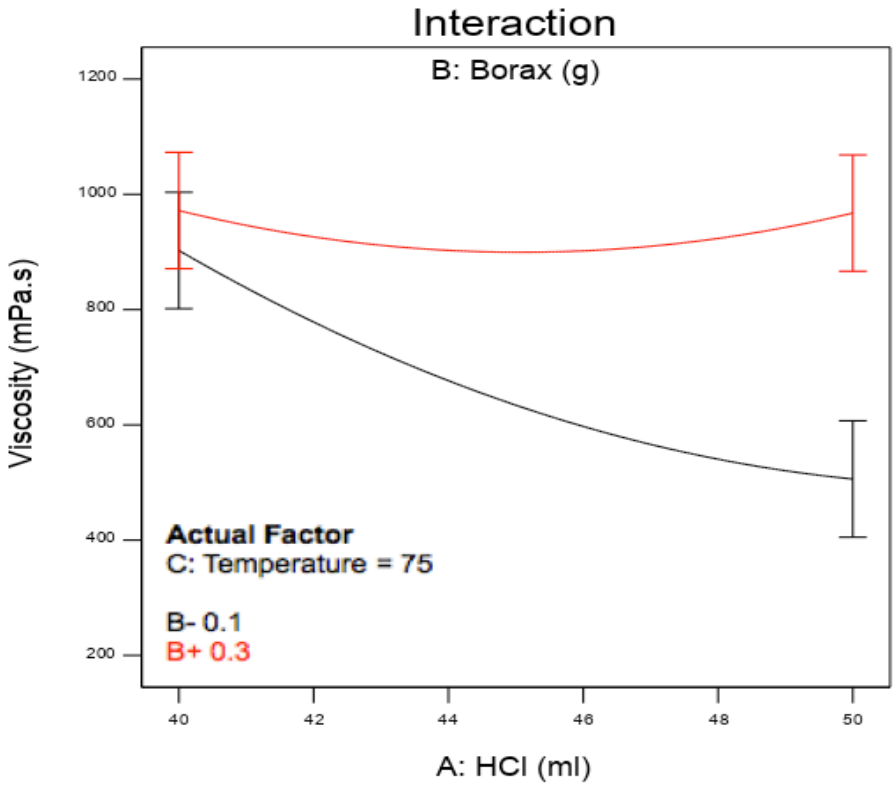

Figure 149: Interaction plot illustrates the effect of interaction between gelatinisation and borax on the viscosity.

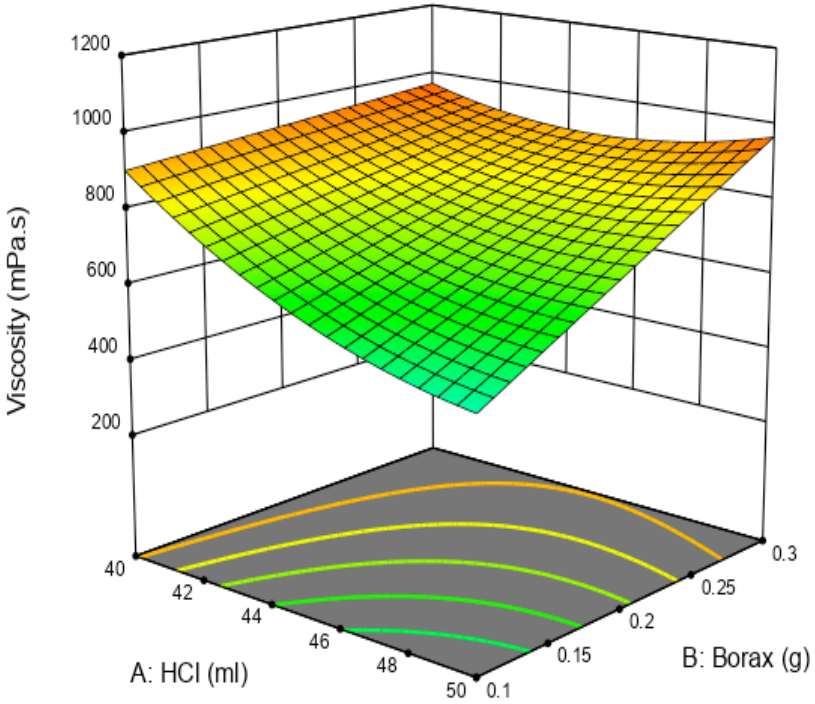

Figure 150: Contour plot shows the effect of gelatinisation and borax on the viscosity at 75 °C.

4.10.9 Density

The linear relationships between gelatinisation, borax and density are shown in Figure 151. The density of the adhesive decreased with the increase of gelatinisation amount and increased with an increase of borax. Figure 152 shows that the density decreased slightly by increasing the gelatinisation, at 0.2 g of borax and 65 °C while it dropped significantly by increasing the gelatinisation at 0.2 g of borax and 85 °C. At 40 ml of gelatinisation, 0.2 g of borax and both temperatures 65 and 85 °C, the highest adhesive density was achieved. The highest adhesive density resulted when the gelatinisation was less than 41 ml, 0.3 g of borax and temperatures between 67 and 81°C as clarifying in Figure 153. The gelatinisation had the highest effect on density as indicated by coded Equation (48):

$$\text{Density} = + 1.02 - 0.0054*A + 0.0040*B - 0.0039*C - 0.0035*AC - 0.0038*C^2 \quad \text{Equation (48)}$$

The actual equation (49) for Density is:

$$\text{Density} = + 0.637573 + 0.004175*\text{HCl} + 0.040000*\text{Borax} + 0.008450*\text{Temperature} - 0.000070*\text{HCl} * \text{Temperature} - 0.000038*\text{Temperature}^2 \quad \text{Equation (49)}$$

Table 57: ANOVA table for density response.

Source	Sum of Squares	df	Mean Square	F-value	p-value	
Model	0.0006	5	0.0001	12.39	0.0003	Significant
A-HCl	0.0002	1	0.0002	24.30	0.0005	
B-Borax	0.0001	1	0.0001	13.46	0.0037	
C-Temperature	0.0001	1	0.0001	12.63	0.0045	
AC	0.0000	1	0.0000	5.15	0.0443	
C^2	0.0001	1	0.0001	6.40	0.0280	
Residual	0.0001	11	9.511E-06			
Lack of Fit	0.0001	7	0.0000	2.01	0.2614	Not significant
Pure Error	0.0000	4	5.800E-06			
Cor Total	0.0007	16				
Adequacy measuring tools	R^2= 0.8492	Adjusted R^2= 0.7806			Predicted R^2= 0.6099	

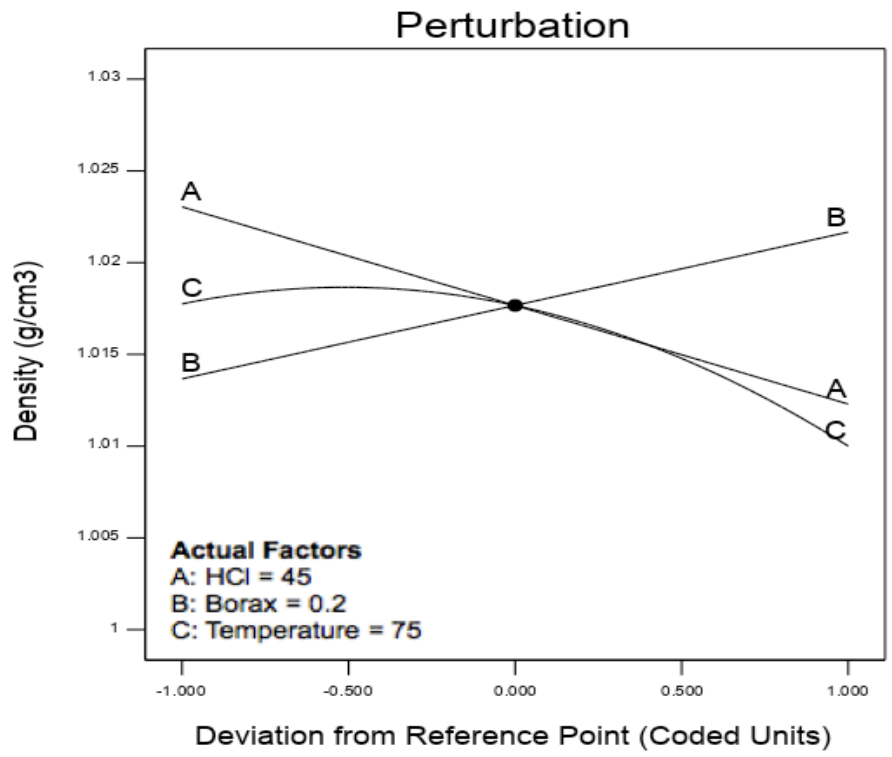

Figure 151: Perturbation plot illustrates the effect of all factors on the dinsety.

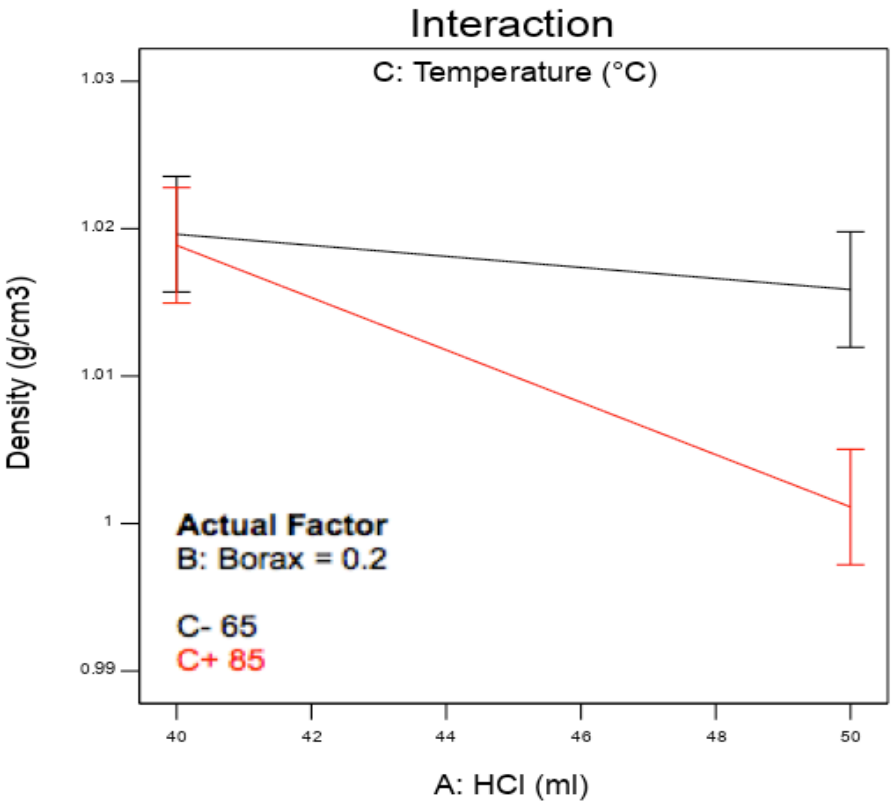

Figure 152: Interaction plot shows the effect of interaction between gelatinisation and temperature on the density.

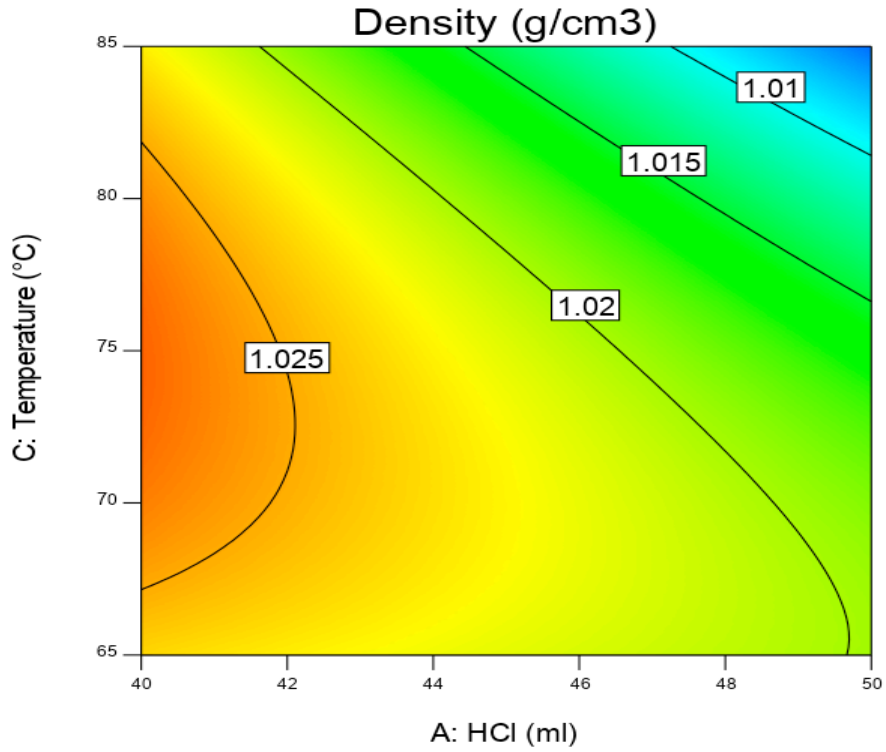

Figure 153: Contour plot display of the effect of gelatinisation and temperature on the density at 0.3 g of borax.

4.10.10 pH

Figure 154 shows that the pH value increased with increasing amounts of gelatinisation and borax, while the temperature did not significantly affect it. The pH value was approximately 9 at 50 ml of gelatinisation, at both of the borax values of 0.1 and 0.3 g and 75 °C, as shown in Figure 155. The pH value increased significantly with the increasing the gelatinisation, at 0.1 g of borax and 75 ° C, as shown in Figure 155. Moreover, the pH increased from 8.5 to approximately 9.2 with an increase in gelatinisation, at 0.2 g of borax and 65 °C, while it decreases slightly over the same conditions, but at 85 °C as shown in Figure 156. The pH has the same value (approximately 8.83) at 44 ml of gelatinisation, at 0.2 g of borax at both temperatures 65 and 85 °C. The highest pH values were obtained at any gelatinisation value, once borax was more than 0.27 g and at 75 °C as seen in Figure 157. The factors influences are shown in coded Equation (50):

$$pH = + 8.97 + 0.1250*A + 0.1538*B - 0.0237*C - 0.1225*AB - 0.1825\ AC - 0.0893*A^2 - 0.0618*C^2 \quad \text{Equation (50)}$$

The actual equation (51) for pH is:

$$pH = -17.52819 + 0.669382*HCl + 12.56250*Borax + 0.254638*Temperature - 0.245000*HCl * Borax - 0.003650*HCl * Temperature - 0.003574*HCl^2 - 0.000618*Temperature^2$$

Equation (51)

Table 58: ANOVA table for density response.

Source	Sum of Squares	df	Mean Square	F-value	p-value	
Model	0.5645	7	0.0806	29.11	< 0.0001	Significant
A-HCl	0.1250	1	0.1250	45.12	< 0.0001	
B-Borax	0.1891	1	0.1891	68.26	< 0.0001	
C-Temperature	0.0045	1	0.0045	1.63	0.2338	
AB	0.0600	1	0.0600	21.67	0.0012	
AC	0.1332	1	0.1332	48.09	< 0.0001	
A^2	0.0337	1	0.0337	12.17	0.0069	
C^2	0.0161	1	0.0161	5.83	0.0390	
Residual	0.0249	9	0.0028			
Lack of Fit	0.0131	5	0.0026	0.8790	0.5655	Not significant
Pure Error	0.0119	4	0.0030			
Cor Total	0.5894	16				
Adequacy measuring tools	R^2= 0.9577	Adjusted R^2= 0.9248			Predicted R^2= 0.8029	

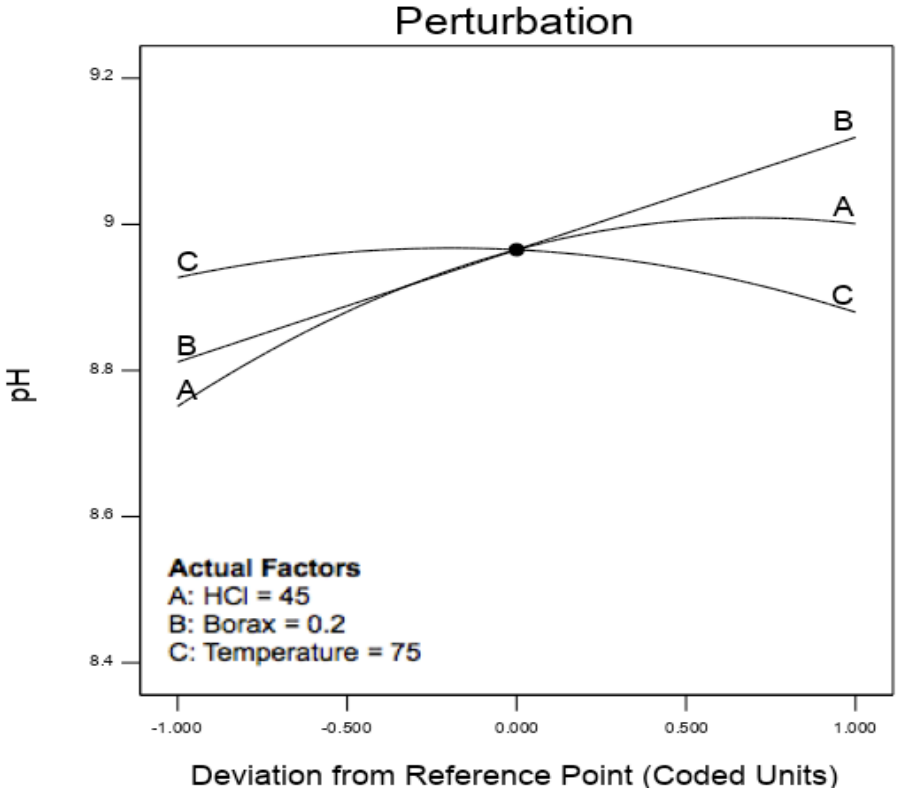

Figure 154: Perturbation plot illustrating the effect of all factors on the pH.

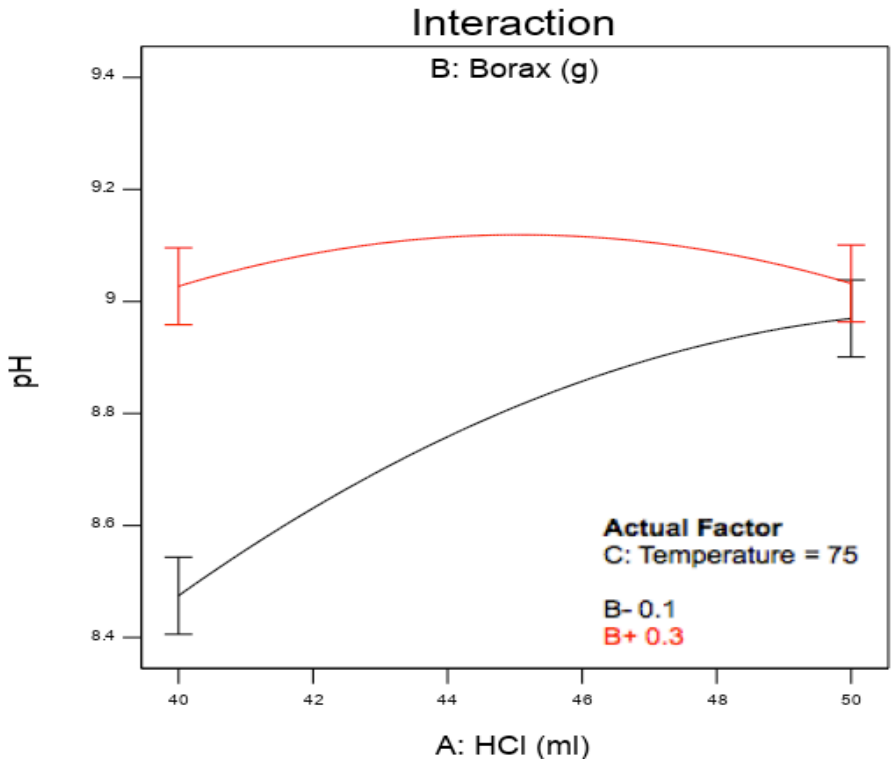

Figure 155: Interaction plot showing the effect of the interaction between gelatinisation and borax on the pH.

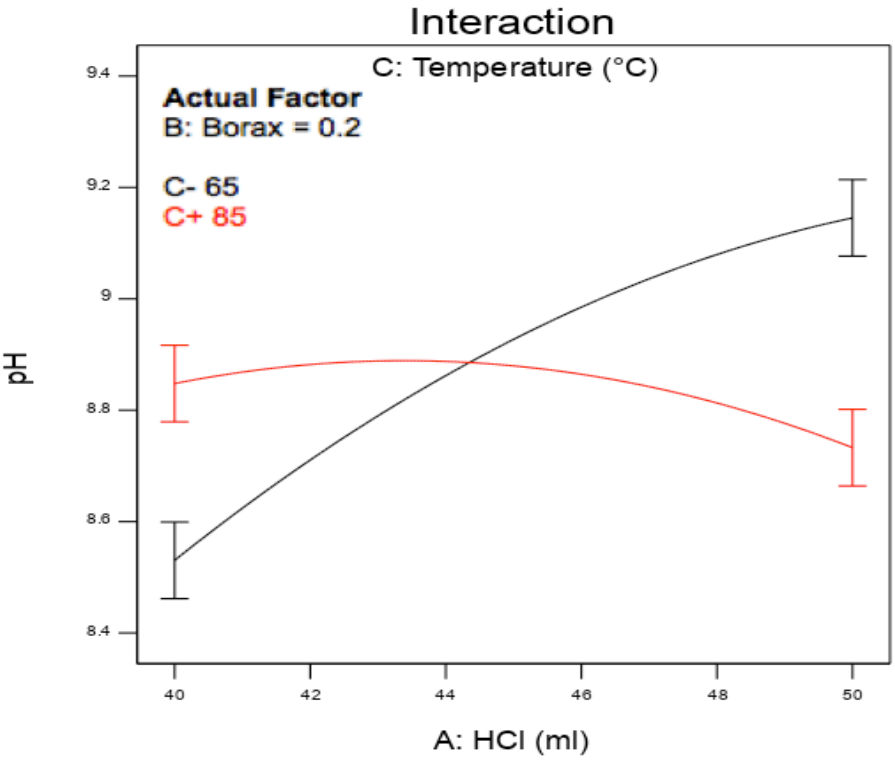

Figure 156: Interaction plot showing the effect of the interaction between gelatinisation and temperature on the pH.

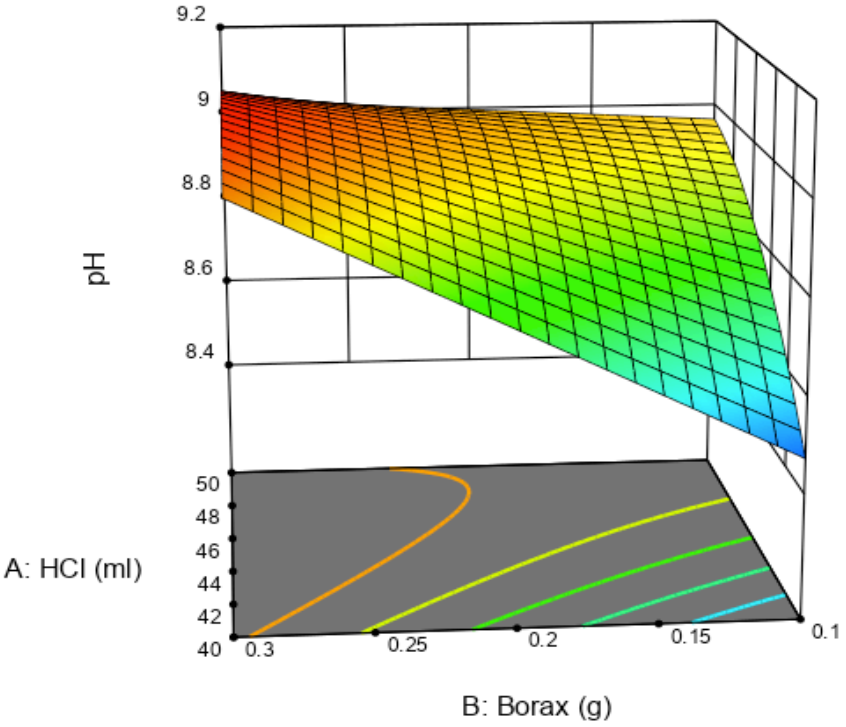

Figure 157: 3-D surface plot displaying the effect of gelatinisation and borax on the pH at 75 °C.

4.10.11 Shear Strength of Plywood

From Table 59, although the Predicted and Actual R^2 values were not as close to 1 as found for the other responses, their difference was still less than 0.2, plus the model was significant and the lack of fit was insignificant, given as none of the p-values were greater than 0.05. The linear relationship between all factors and the plywood shear strength is described in Figure 158. The shear strength of the plywood decreased with an increase of gelatinisation and increased with increasing borax and temperature. The plywood shear strength decreased with an increase of gelatinisation, at 0.3 g borax and 75 °C. In comparison, it was almost constant when increasing the amount of gelatinisation, at 0.1 g of borax and 75 °C, as shown in Figure 159. From the same figure, it can be found that at 50 ml of gelatinisation and 75 °C, the same shear strength value of 2.7 MPa was obtained for both borax quantities. The highest shear strength at 85 °C was attained when less than 45 ml of gelatinisation and more than 0.2 g of borax was used and 85 °C as shown in Figure 160. The coded Equation (52) illustrates the influence of factors on shear strength and the impact of the gelatinisation and borax (AB) interaction:

$$\text{Plywood shear Strength} = + 2.80 - 0.0800*A + 0.0988*B + 0.2413*C - 0.0850*AB \quad \text{Equation (52)}$$

The actual Equation (53) for Plywood shear strength is:

Plywood shear Strength = - 0.020404 + 0.018000*HCl + 8.63750*Borax + 0.024125*Temperature - 0.170000*HCl * Borax Equation (53)

Table 59: ANOVA table for plywood shear strength response.

Source	Sum of Squares	df	Mean Square	F-value	p-value	
Model	0.6237	4	0.1559	30.85	< 0.0001	Significant
A-HCl	0.0512	1	0.0512	10.13	0.0079	
B-Borax	0.0780	1	0.0780	15.43	0.0020	
C-Temperature	0.4656	1	0.4656	92.10	< 0.0001	
AB	0.0289	1	0.0289	5.72	0.0341	
Residual	0.0607	12	0.0051			
Lack of Fit	0.0524	8	0.0065	3.16	0.1405	Not significant
Pure Error	0.0083	4	0.0021			
Cor Total	0.6844	16				
Adequacy measuring tools	R^2= 0.9114	Adjusted R^2= 0.8818			Predicted R^2= 0.7134	

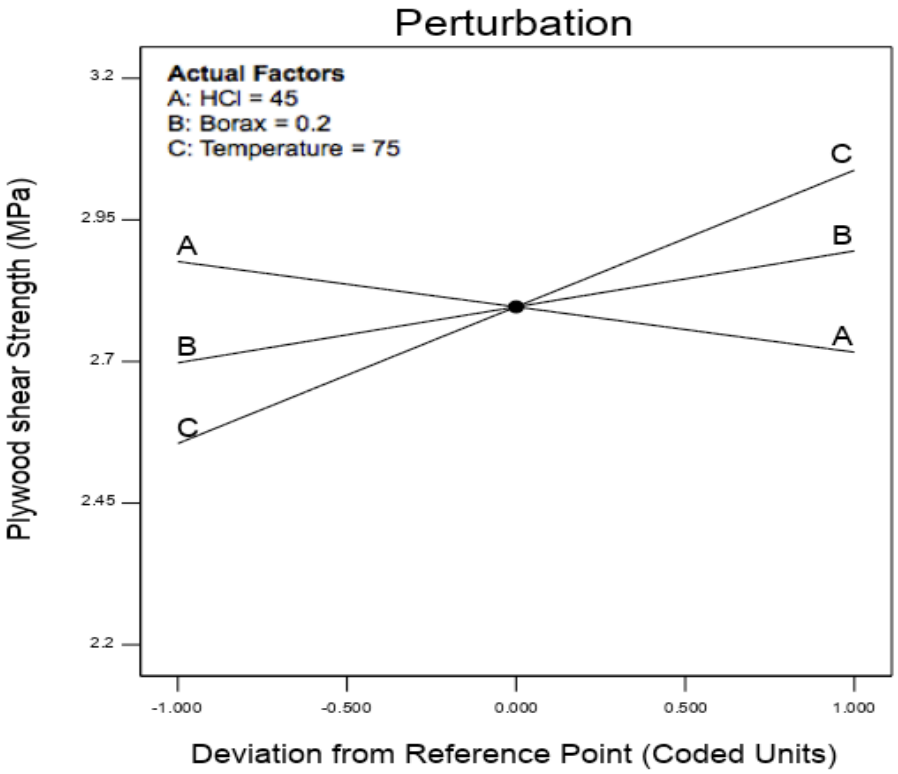

Figure 158: Perturbation plot demonstrates the effect of all factors on the plywood shear strength.

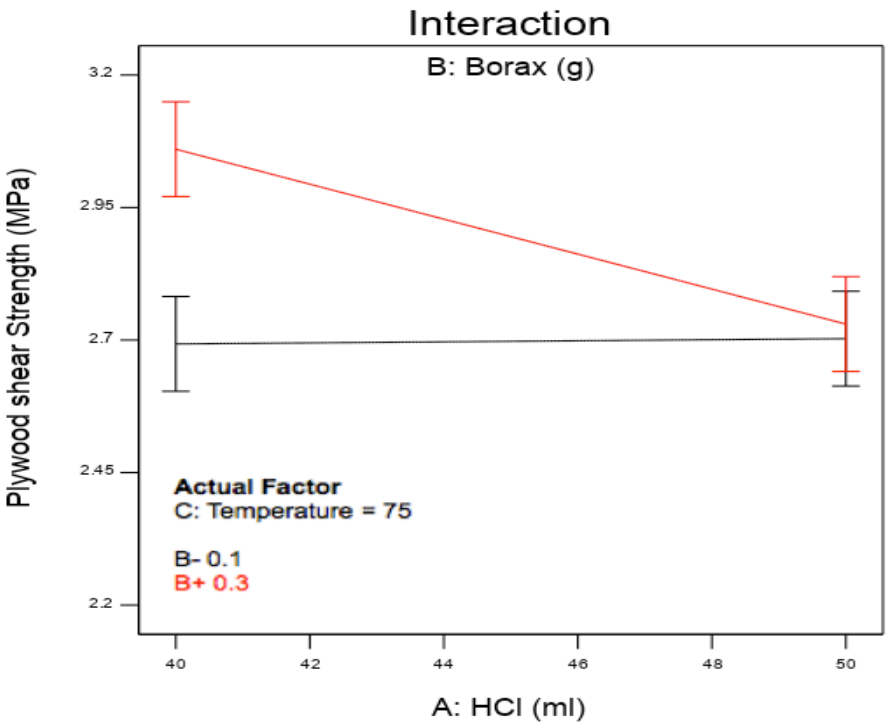

Figure 159: Interaction plot displays the effect of interaction between gelatinisation and borax on the plywood shear strength.

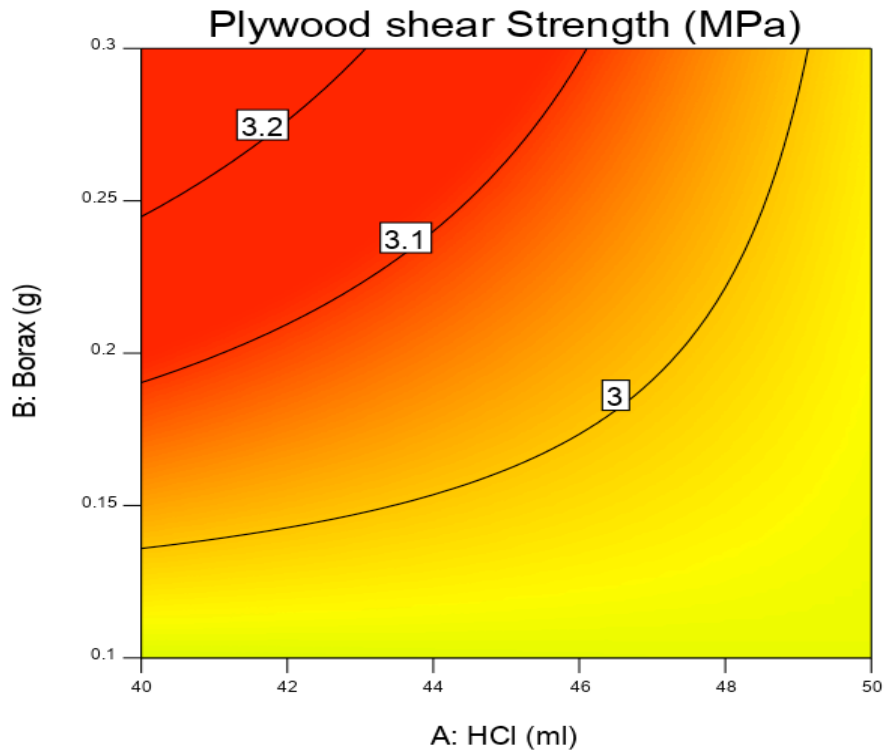

Figure 160: Contour plot clarifies the effect of gelatinisation and borax on plywood shear strength at 85 °C.

4.10.12 Shear Strength of Paperboard

Figure 161 illustrates the indirect proportional of the paperboard shear strength with gelatinisation, while the shear strength increased with increasing the borax. Figures 162 and 163 show the effect of the interactions of gelatinisation with borax and temperature on the paperboard shear strength. The shear strength decreased with increasing gelatinisation, at 0.3 g of borax and 75 °C, while it was almost at the same value for all gelatinisation values, at 0.1 g of borax and 75 °C (Figure 162). In contrast, the decrease in shear strength was noticeable by increasing the amount of gelatinisation, at 0.2 g of borax and 85 °C, while the decrease in shear strength was slight, at 0.2 g of borax and 65 °C (Figure 163). The interaction trend between borax and temperature was approximately similar at 45 ml of gelatinisation and temperatures of 65 and 85 °C (Figure 164), nevertheless, the increase in shear strength, at 85 °C was slightly higher than at 65 °C. The highest paperboard shear strength at 85 °C was found when the gelatinisation was less than 45 ml and the borax was greater than 0.25 g as shown in Figure 165. Equation (54) demonstrates the effect of factors on the response:

$$\text{Paperboard shear strength} = + 0.6296 - 0.0326*A + 0.0469*B + 0.0533*C - 0.0248*AB - 0.0160*AC + 0.0125*BC - 0.0112*A^2 + 0.0193*B^2 + 0.0681*C^2 \quad \text{Equation (54)}$$

The actual Equation (55) for Paperboard shear strength is:

$$\text{Paperboard shear strength} = + 2.09344 + 0.067605*HCl + 0.985750*Borax - 0.084888*Temperature - 0.049500*HCl * Borax - 0.000320*HCl * Temperature + 0.012500*Borax * Temperature - 0.000447*HCl^2 + 1.93250*Borax^2 + 0.000681*Temperature^2 \quad \text{Equation (55)}$$

Table 60: ANOVA table for paperboard shear strength response.

Source	Sum of Squares	df	Mean Square	F-value	p-value	
Model	0.0748	9	0.0083	240.37	< 0.0001	Significant
A-HCl	0.0085	1	0.0085	246.36	< 0.0001	
B-Borax	0.0176	1	0.0176	508.56	< 0.0001	
C-Temperature	0.0227	1	0.0227	656.30	< 0.0001	
AB	0.0025	1	0.0025	70.89	< 0.0001	
AC	0.0010	1	0.0010	29.63	0.0010	
BC	0.0006	1	0.0006	18.08	0.0038	
A^2	0.0005	1	0.0005	15.21	0.0059	
B^2	0.0016	1	0.0016	45.49	0.0003	
C^2	0.0195	1	0.0195	564.53	< 0.0001	
Residual	0.0002	7	0.0000			
Lack of Fit	0.0001	3	0.0000	0.9514	0.4961	
Pure Error	0.0001	4	0.0000			Not significant
Cor Total	0.0750	16				
Adequacy measuring tools	R^2= 0.9968	Adjusted R^2= 0.9926		Predicted R^2= 0.9756		

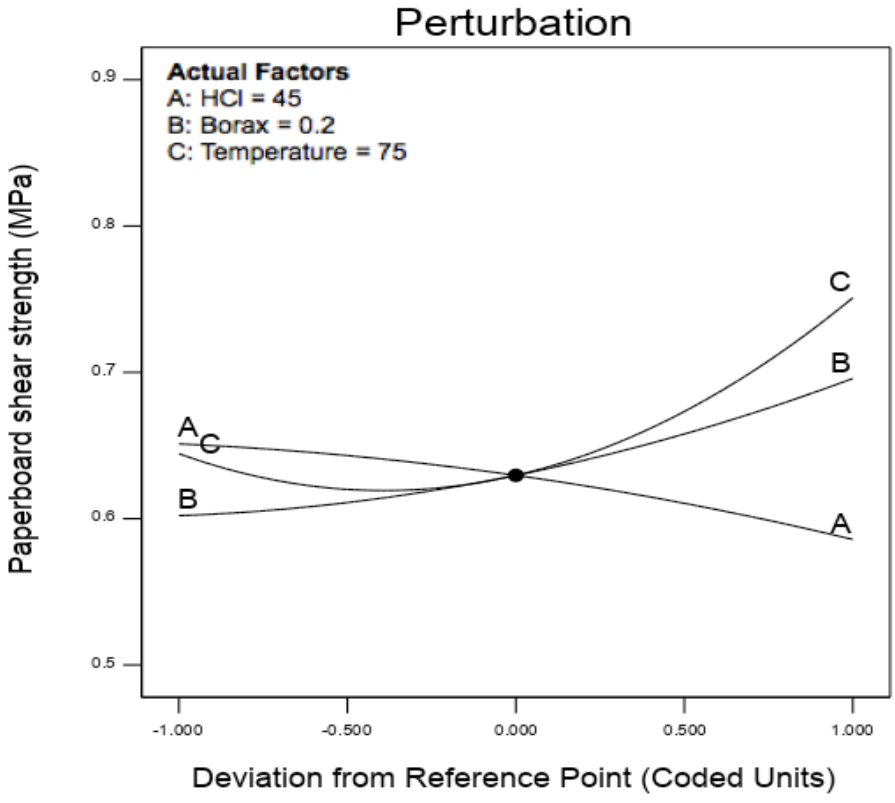

Figure 161: Perturbation plot describing the effect of all factors on paperwood shear strength.

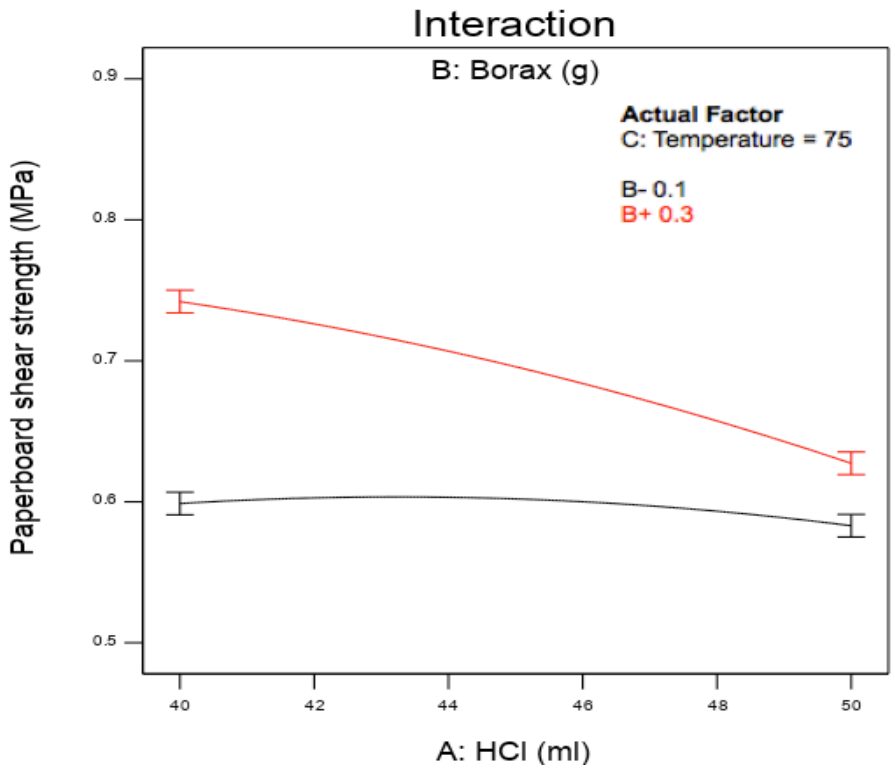

Figure 162: Interaction plot describing the effect of the interaction between gelatinisation and borax on the paperboard shear strength.

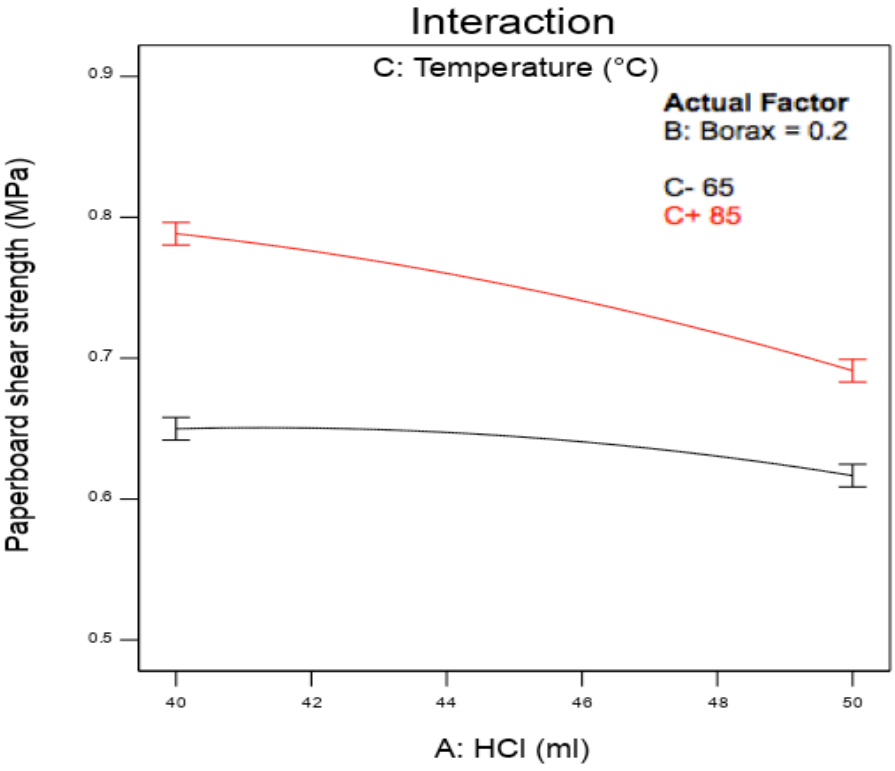

Figure 163: Interaction plot illustrating the effect of the interaction between gelatinisation and temperature on the paperboard shear strength.

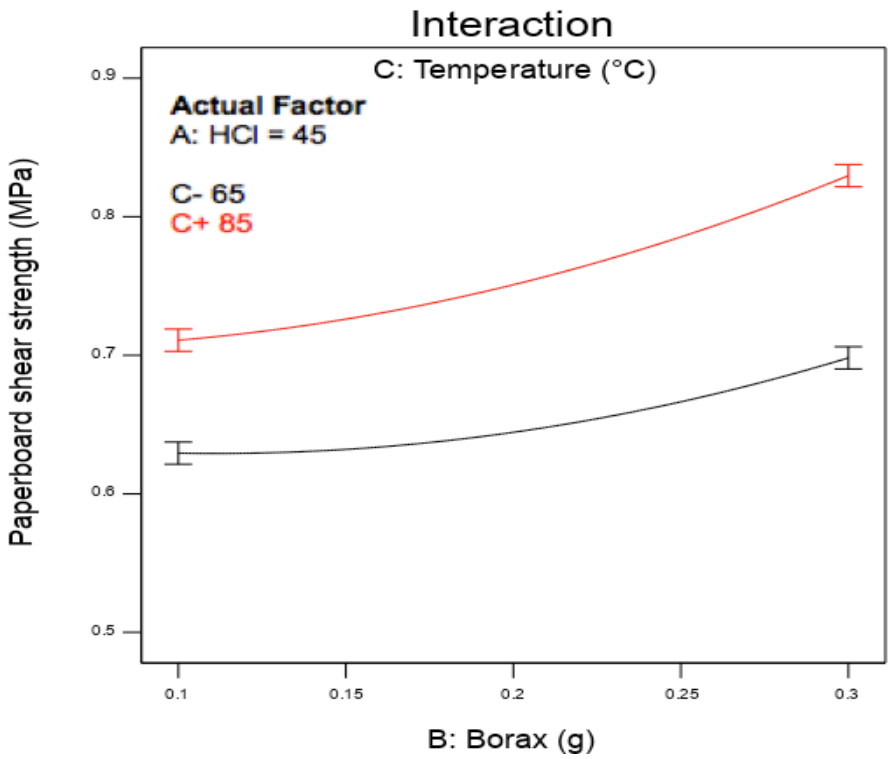

Figure 164: Interaction plot presenting the effect of the interaction between borax and temperature on the paperboard shear strength.

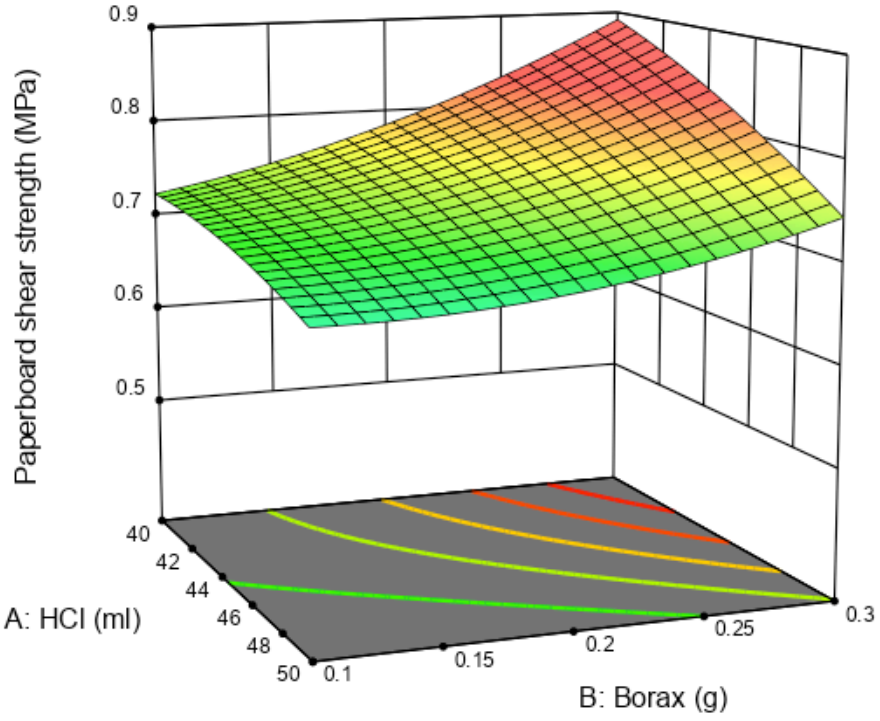

Figure 165: 3-D surface plot demonstrating the effect of gelatinisation and borax on paperboard shear strength at 85 °C.

4.10.13 Adhesives Performance on Plywood and Paperboard

Figures 166 and 167 show the variance in plywood shear strength value compared to paperboard at the centre values of factors using NaOH and HCl gelatinisation. This difference was due to the different nature and properties of each substance. It is evident from the same figures that the shear strength of both plywood and paperboard adhered by NaOH gelatinisation adhesive was higher than that adhered by HCl gelatinisation adhesive. The substrates surfaces were not treated before adhesion. Plywood and paperboard adhered successfully, while the adhesive failed to adhere the plastic samples as a result of inappropriate surface roughness of plastic samples. To remedy this failure, the surface roughness of the plastic specimens was treated with sandpaper. This treatment did not lead to the adhesion of the plastic samples, therefore the adhesion failure continued. Further investigations are required of other techniques for preparing plastic surfaces such as sandblasting and mechanical polishing to ahere the plastic samples [342, 349].

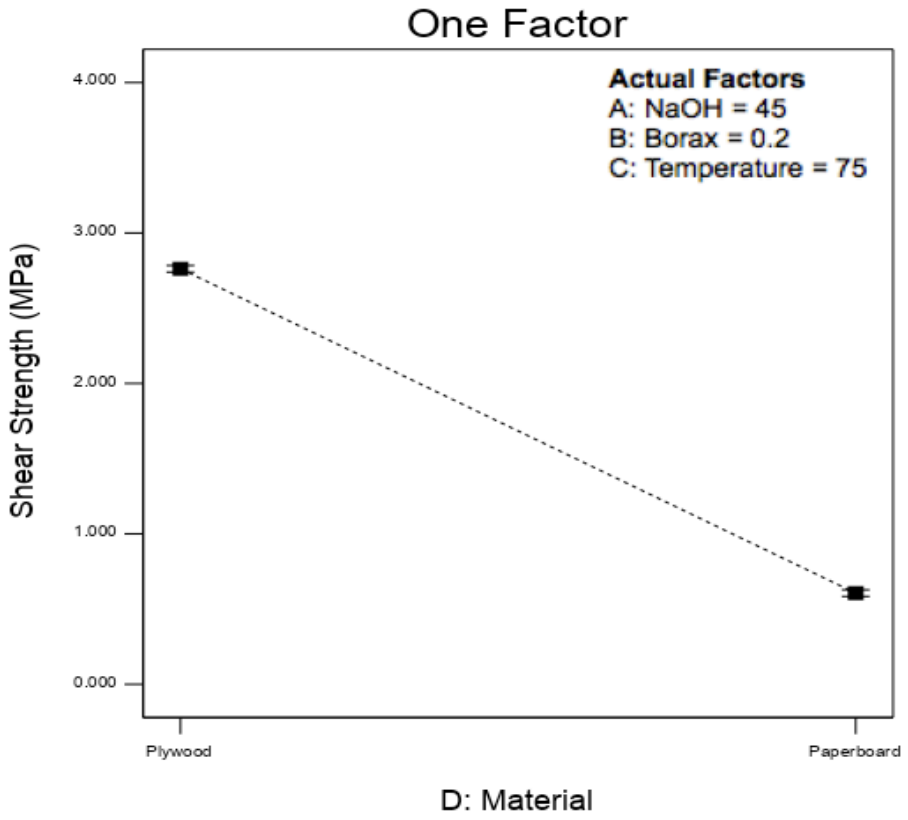

Figure 166: The variance in shear strength between plywood and paperboard when using NaOH gelatinisation.

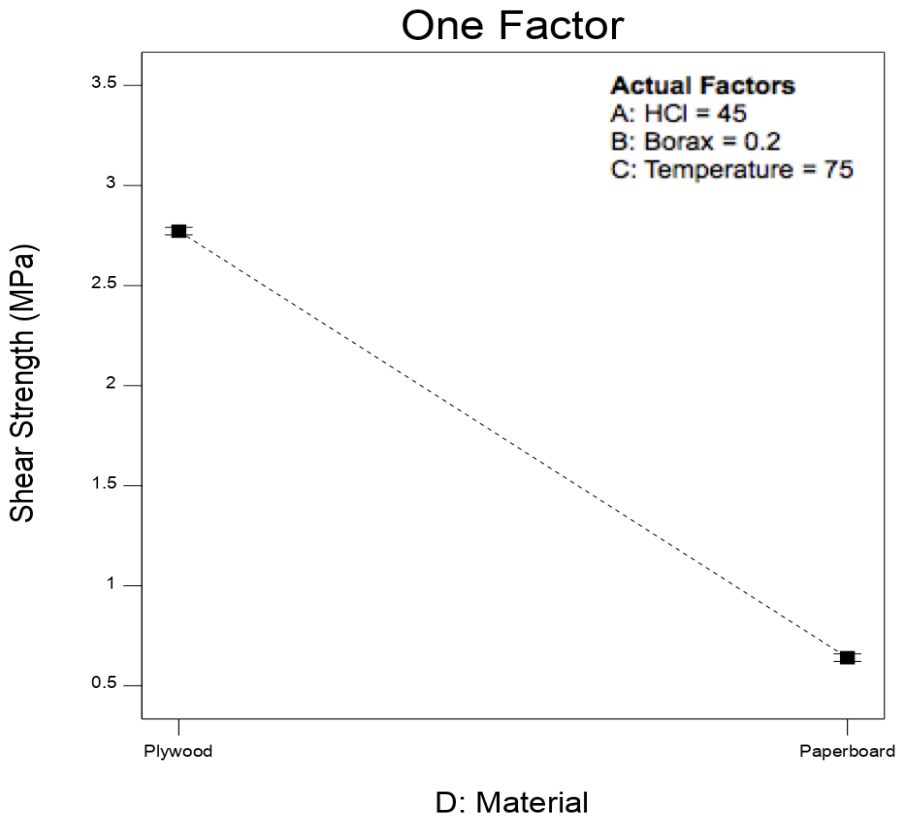

Figure 167: The variance in shear strength between plywood and paperboard when using HCl gelatinisation.

(A) NaOH Gelatinisation

The effect of gelatinisation and temperature on the adhesive production process, using NaOH gelatinisation affected the plywood shear strength as shown in Figures 168 and 169. In contrast, this effect was quite low on the paperboard shear strength. The gelatinisation quantity increased contributing to a decrease in plywood shear strength. It decreased with gelatinisation increasing from 40 ml to 50 ml, 0.2 g of borax and 75 °C, from 3.2 MPa to around 2.62 MPa (Figure 168). Moreover, the plywood shear strength increased as temperature increased at 45 ml of gelatinisation and 0.2 g of borax as seen in Figure 169.

The shift in paperboard shear strength was slight when gelatinisation quantity increased from 40 ml to 50 ml, at 0.2 g of borax and 75 °C as illustrated in Figure 168. On the other hand, the shear strength of the paperboard increased slightly by increasing the temperature from 65 °C to 85 °C, and when the gelatinisation was 45 ml and the borax was 0.2 g as clear from Figure 169.

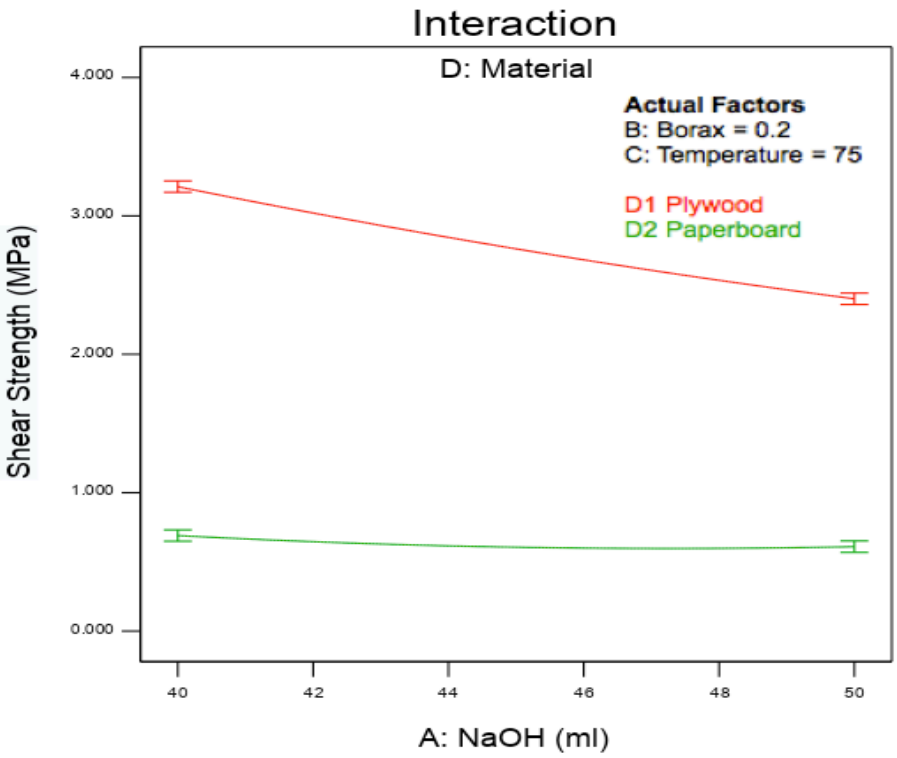

Figure 168: Interaction plot demonstrates the effect of starch on plywood and paperboard shear strength when using NaOH gelatinisation.

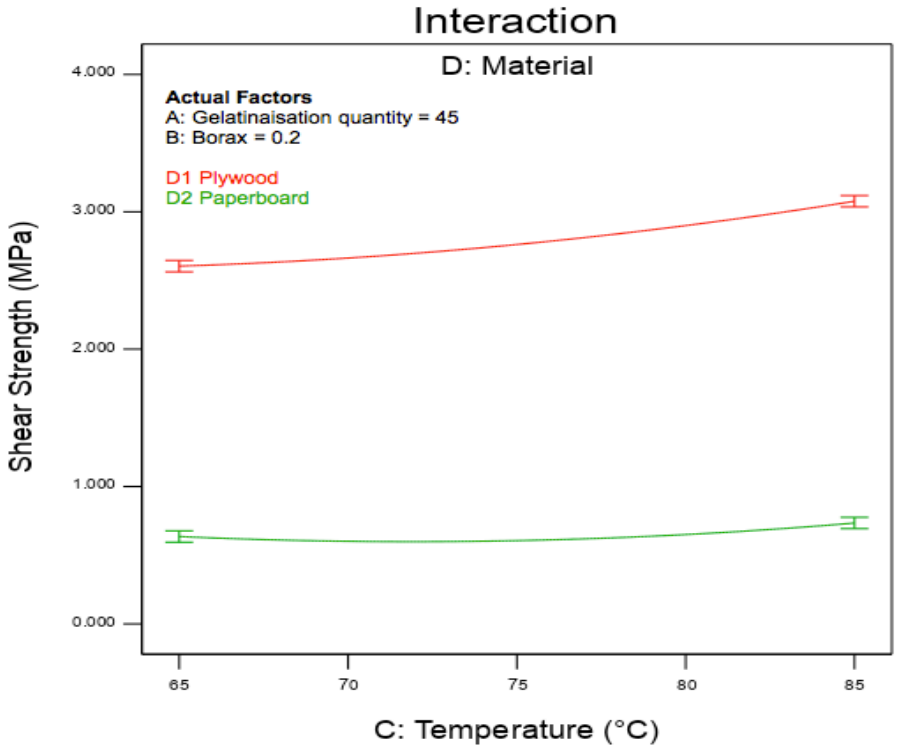

Figure 169: Interaction plot presents the effect of tempreature on plywood and paperboard shear strength when using NaOH gelatinisation.

(B) HCl Gelatinisation

The same applies to the adhesive produced from HCl gelatinisation, in addition to the effect of borax on the plywood shear strength, as presented in Figures 170-172. The increased in the amounts of gelatinisation had a negative effect on the shear strength of the plywood, as the shear strength decreased slightly when increasing the gelatinisation quantity at 0.2 g of borax and 75 °C, as shown in Figures 170. The borax and temperature positively impacted the plywood shear strength, as shown in figures 171 and 172. The increase in shear strength was obvious from 2.55 MPa to approximately 3 MPa when the temperature increased from 65 °C to 85 °C, 45 ml of gelatinisation and 0.2 g of borax as shown in Figure 172.

Figure 170 illustrates the effect of gelatinisation on the shear strength of paperboard, as the shear strength decreased slightly with an increase in the gelatinisation amount. In contrast, the paperboard shear strength increased slightly with increasing of borax and temperature as demonstrated in Figures 171 and 172.

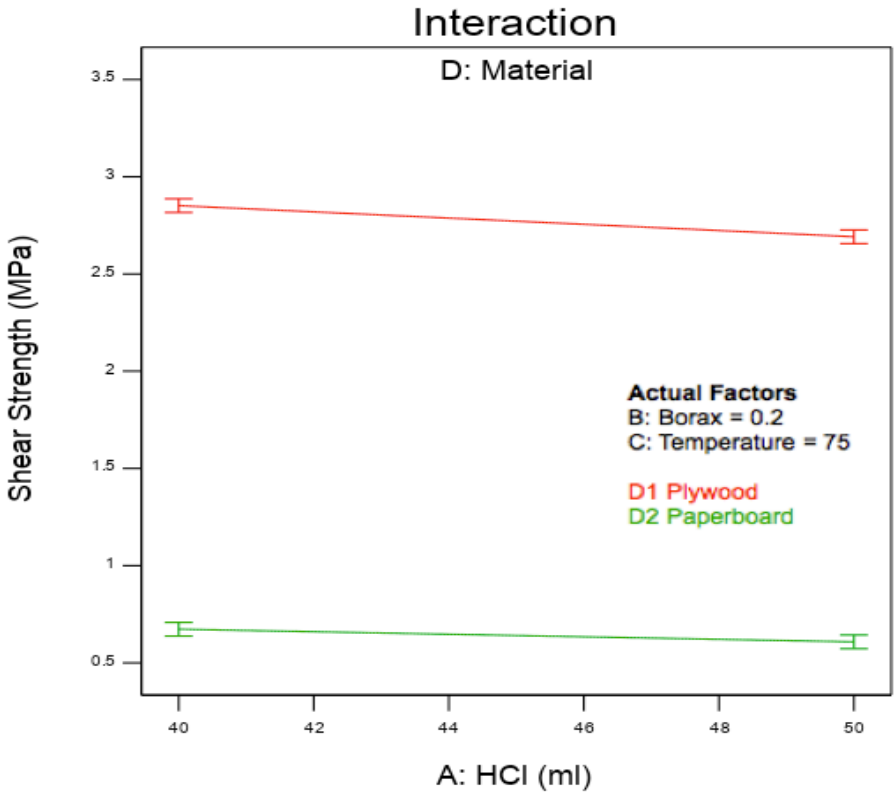

Figure 170: Interaction plot demonstrates the effect of gelatinisation on plywood and paperboard shear strength when using HCl gelatinisation.

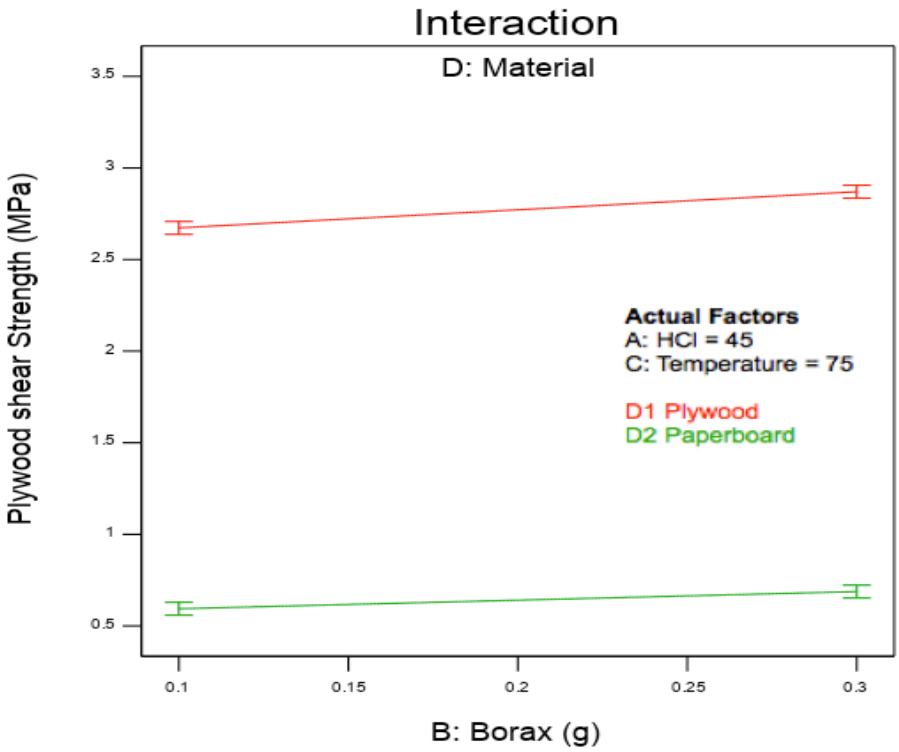

Figure 171: Interaction plot demonstrates the effect of borax on plywood and paperboard shear strength when using HCl gelatinisation.

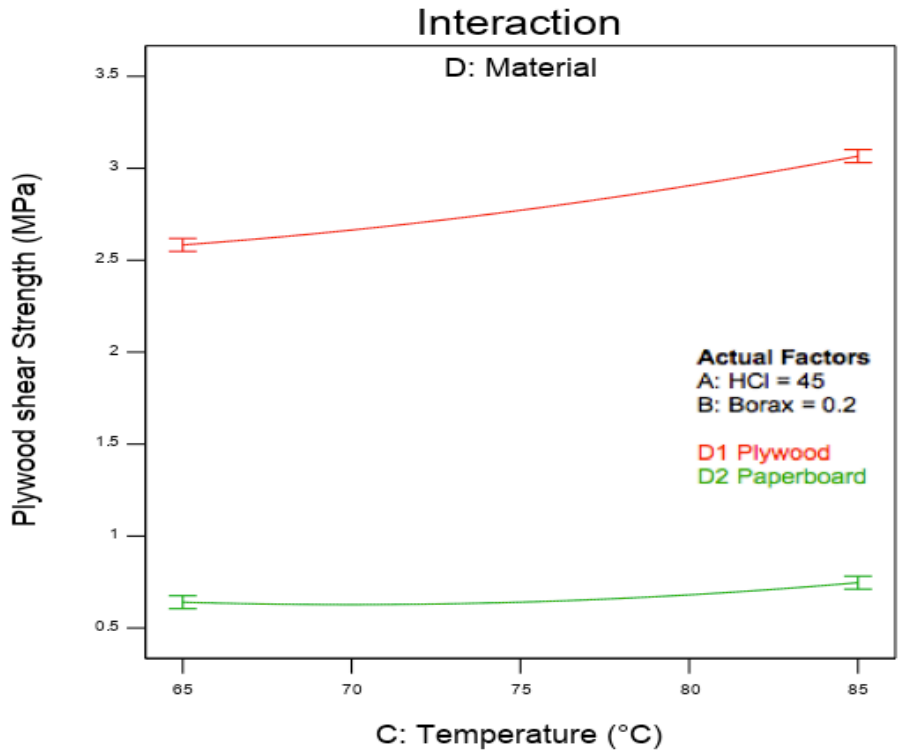

Figure 172: Interaction plot demonstrates the effect of temperature on plywood and paperboard shear strength when using HCl gelatinisation.

4.10.14 Effect of Gelatinisation Type on Adhesive Performance

Figures 173 to 177 illustrate the effect of NaOH and HCl gelatinisation on responses. Figure 173 shows a slight difference in viscosity at the centre values of the factors. The viscosity was slightly higher with NaOH. The difference remains approximately at the same rate for the density and pH of the adhesive when using both types of gelatinisation, with a slightly higher density of the adhesive produced from NaOH and quite higher pH of NaOH than HCl gelatinisation as presented in Figures 174-175.

At 45 ml of gelatinisation, 0.2 g of borax and 75 °C, the plywood shear strength with NaOH (2.82 MPa) was almost similar to what achieved with HCl (2.77 MPa) gelatinisation, as shows in Figure 176. In contrast, the paperboard shear strength decreased by 4.9% with HCl, reaching 0.623 MPa compared to 0.655 MPa when NaOH was used (Figure 177), which shows the paperboard shear strength at 45 ml of HCl, 0.2 g of borax and 75 °C.

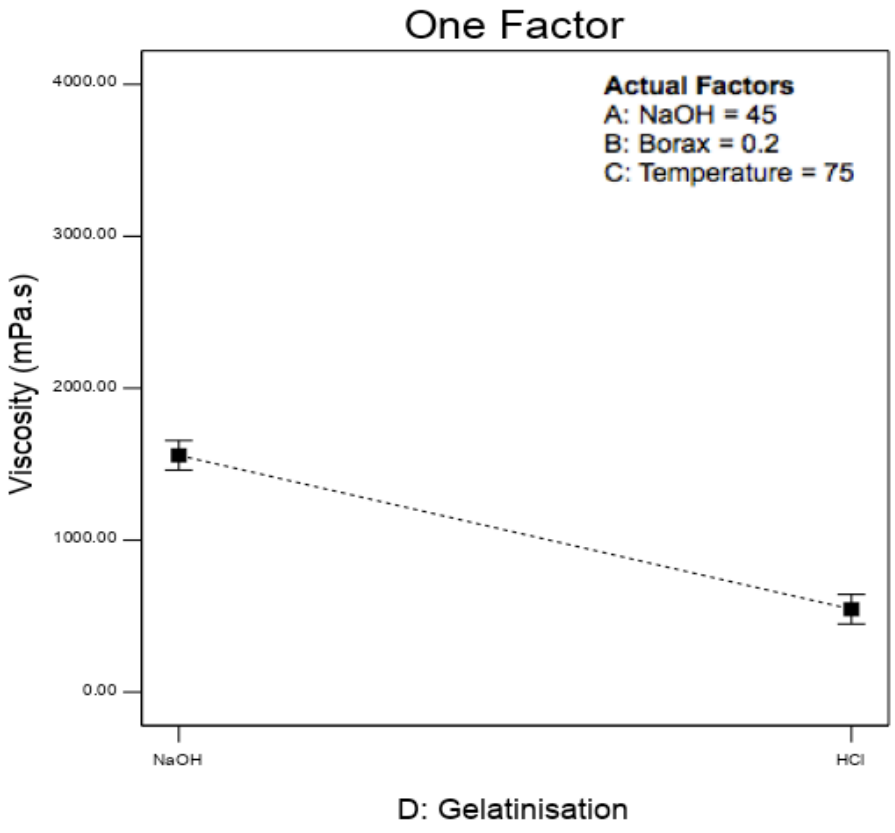

Figure 173: The variance in adhesive viscosity between NaOH and HCl gelatinisation.

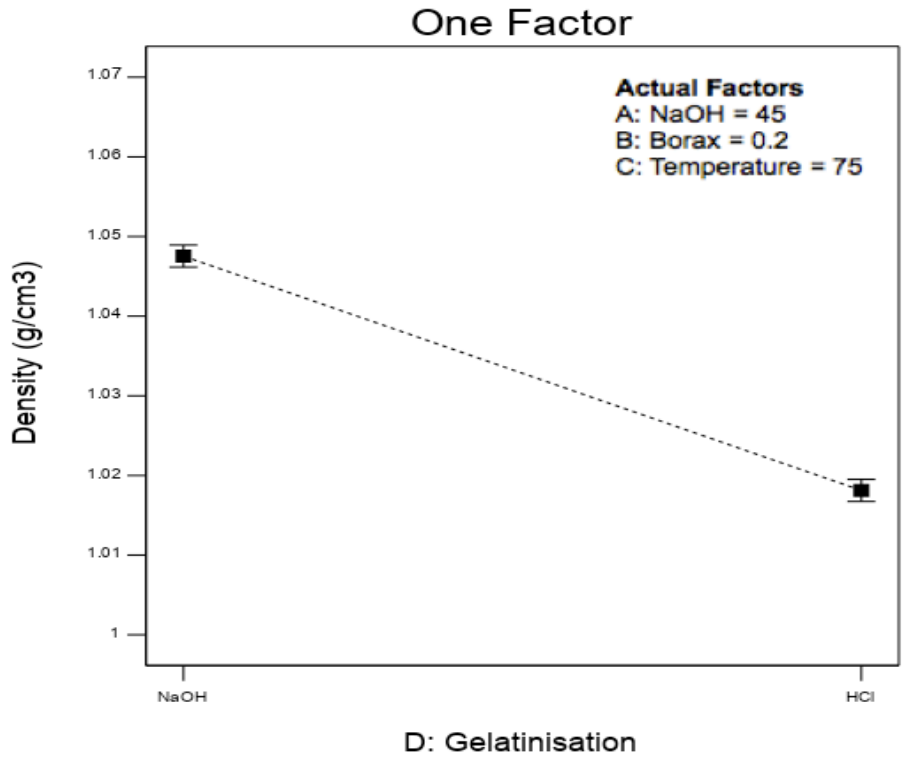

Figure 174: The variance in adhesive density between NaOH and HCl gelatinisation.

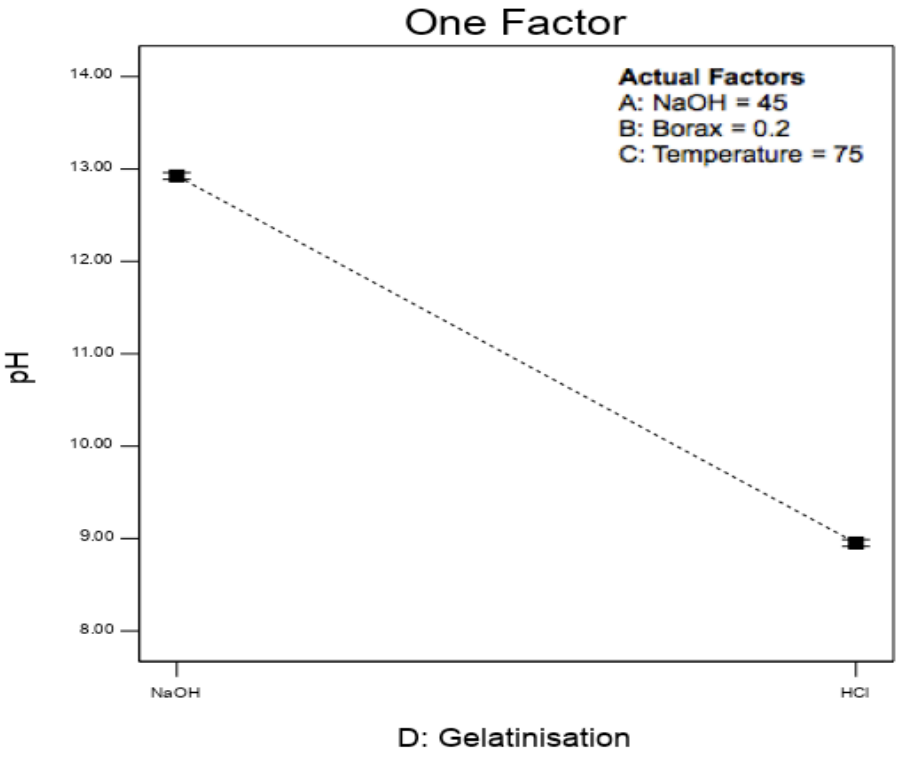

Figure 175: The variance in pH between NaOH and HCl gelatinisation.

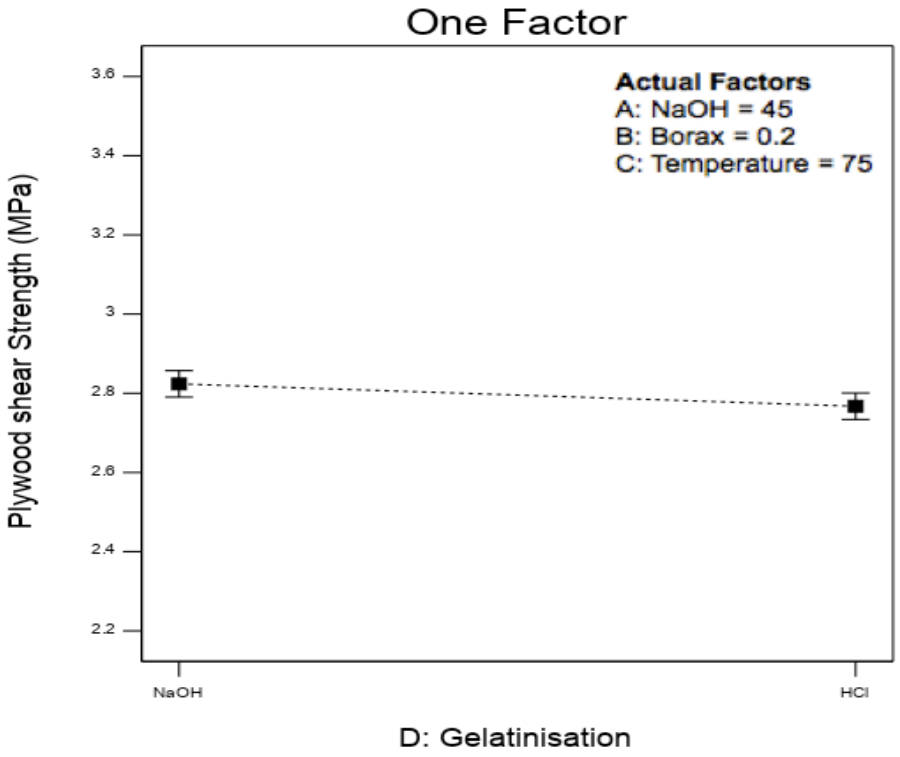

Figure 176: The variance in plywood shear strength between NaOH and HCl gelatinisation.

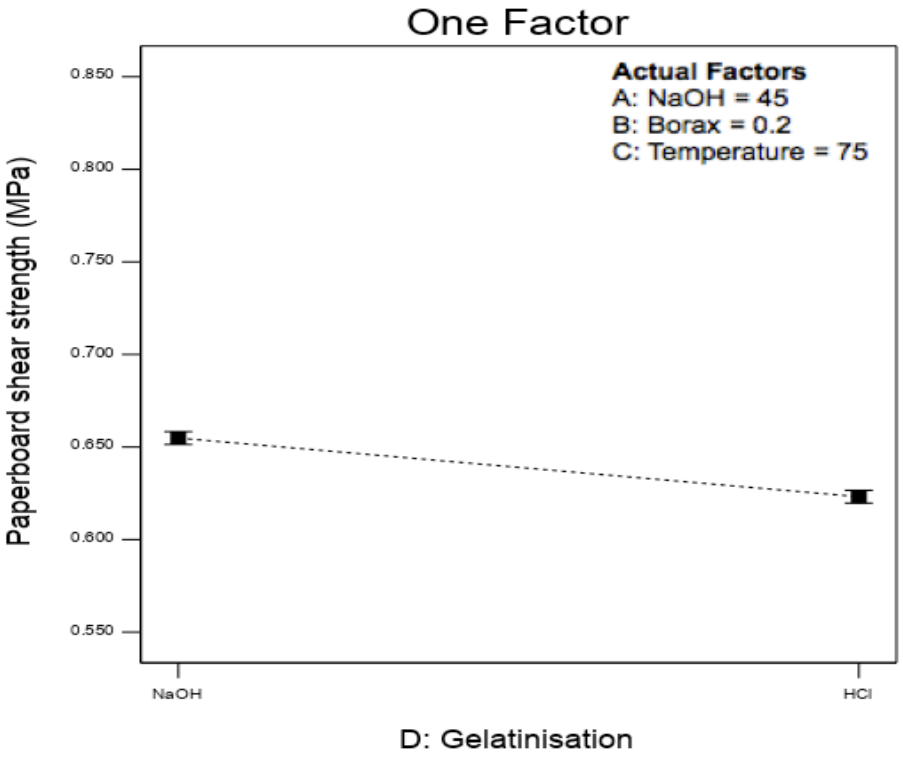

Figure 177: The variance in paperboard shear strength between NaOH and HCl gelatinisation.

Figures 178 to 182 show the effects of factors on responses of both NaOH and HCL gelatinisation. Figure 178 illustrates the effect of gelatinisation on the viscosity of the adhesive for both gelatinisations. The viscosity of the adhesives obtained from NaOH gelatinisation, at 0.2 g of borax and 75 °C decreased by increasing gelatinisation quantity. In contrast, the viscosity approximately remained at the same value when using HCl gelatinisation and at the same conditions. The lowest viscosities of both gelatinisation were achieved, when the gelatinisation was 50 ml, 0.2 g of borax and at 75 °C. The effect of borax on both gelatinisations adhesive is shown in Figure 179. At 45 ml of gelatinisation, 0.1 g of borax and 75 °C, the lowest viscosities values achieved for both gelatinisations. The viscosity of NaOH gelatinisation adhesive increased sharply as borax increased. In contrast, the viscosity of HCl gelatinisation adhesive decreased slightly, with increasing borax quantity until the centre values and rose slightly thereafter.

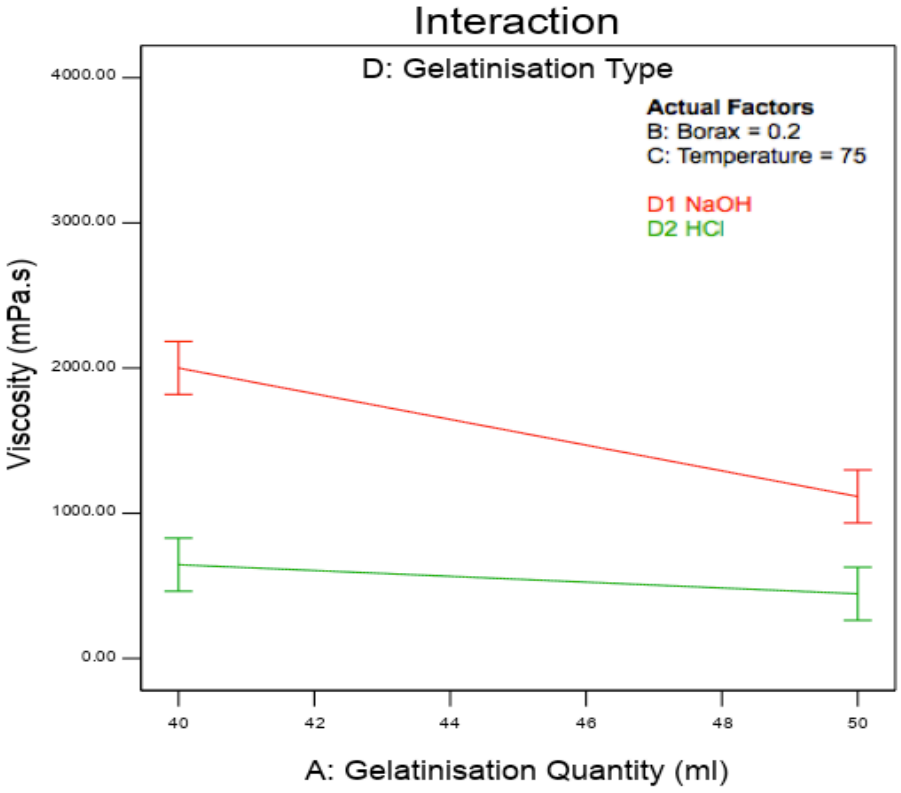

Figure 178: Interaction plot shows the effect of gelatinisation on viscosity when using NaOH and HCl gelatinisation.

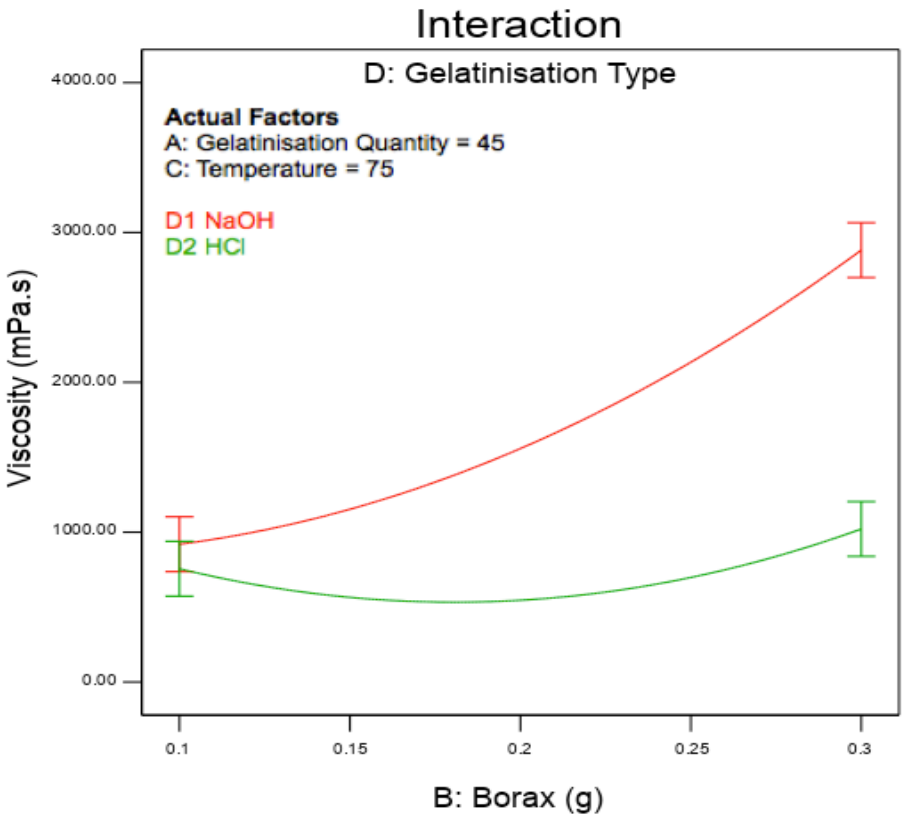

Figure 179: Interaction plot shows the effect of borax on viscosity when using NaOH and HCl gelatinisation.

The adhesives density of both gelatinisations decreased with increasing gelatinisation and temperature. Figure 180 shows the density decreased with increasing gelatinisation, at 0.2 g of borax and 75 °C, while Figure 181 highlights that density decreased with increasing temperature, at 45 ml of gelatinisation and 0.2 g of borax. However, Figure 181 shows the density remained steady with increasing temperature until the centre values and then it decreased slightly when using HCl gelatinisation. The pH showed a different behaviour for both gelatinisation, it decreased slightly with increasing borax quantity at 45 ml of gelatinisation and 75 °C when using NaOH gelatinisation, and increased slightly with increasing borax when using HCl gelatinisation as illustrated in Figure 182.

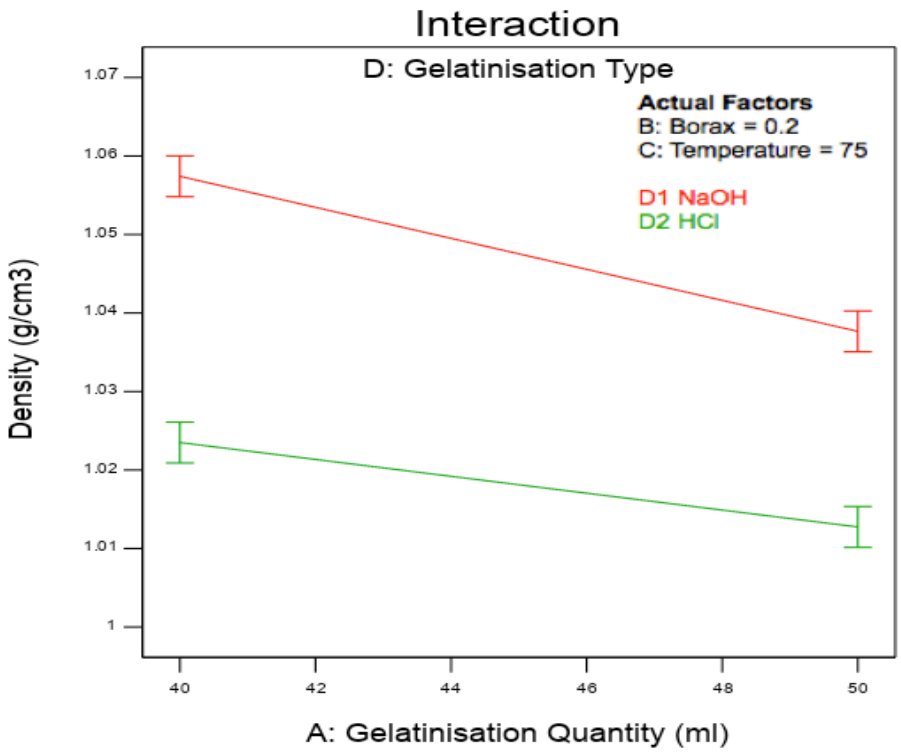

Figure 180: Interaction plot displays the effect of gelatinisation quantity on density when using NaOH or HCl gelatinisation.

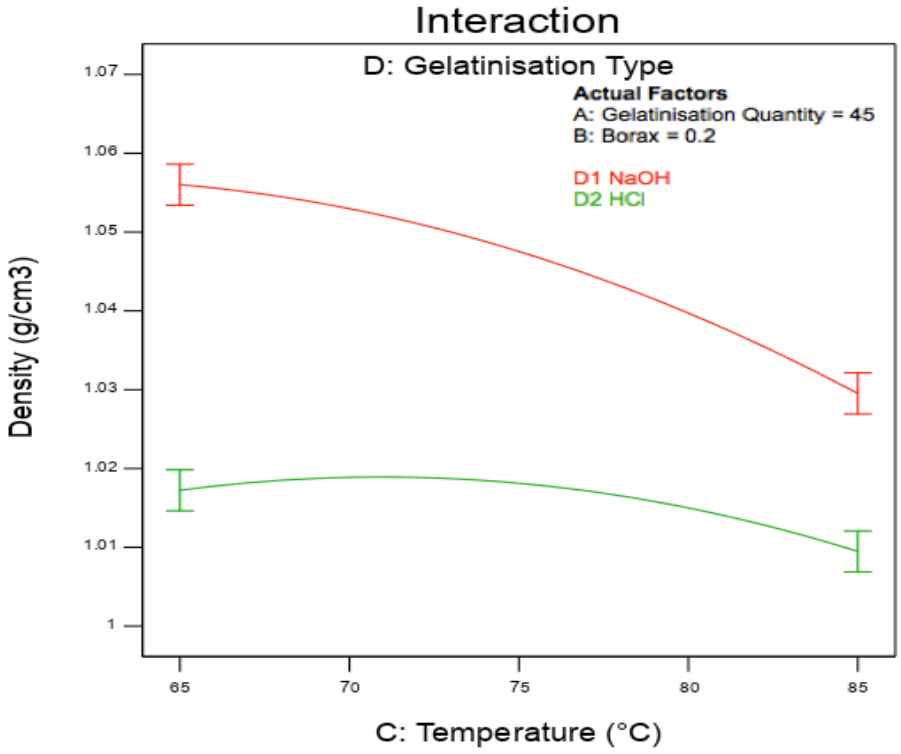

Figure 181: Interaction plot describes the effect of temperature on density when using NaOH or HCl gelatinisation.

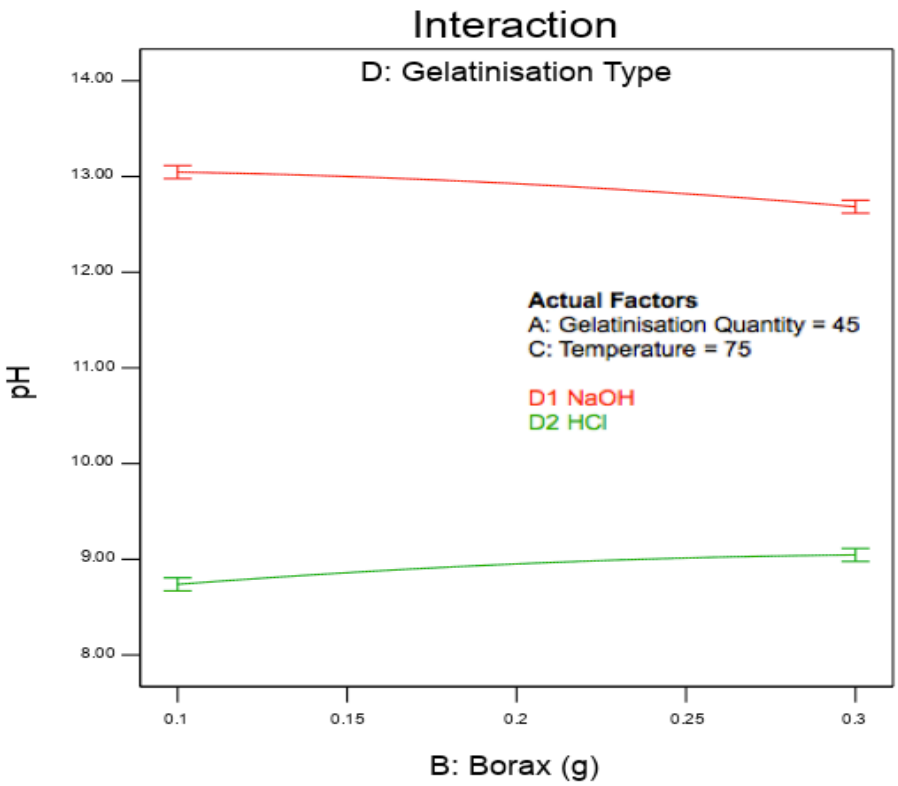

Figure 182: Interaction plot clarifies the effect of borax on pH when using NaOH or HCl gelatinisation.

The shear strength of the plywood decreased dramatically with an increase of gelatinisation quantity for the NaOH gelatinisation, and decreased slightly with HCl gelatinisation as shown in Figure 183. The same figure shows both gelatinisations have the same plywood shear strength value at 46 ml of gelatinisation, 0.2 g of borax and 75 °C at approximately 2.8 MPa.

Figure 184 shows the effect of gelatinisation quantity on the shear strength of paperboard with NaOH and HCl gelatinisation. The shear strength of the paperboard decreased with increasing the amount of gelatinisation, at 0.2 g of borax and 75 °C. In contrast, Figure 185 shows the paperboard shear strength value of both gelatinisations increased when the amount of borax increased, at 45 ml of borax and 75 °C.

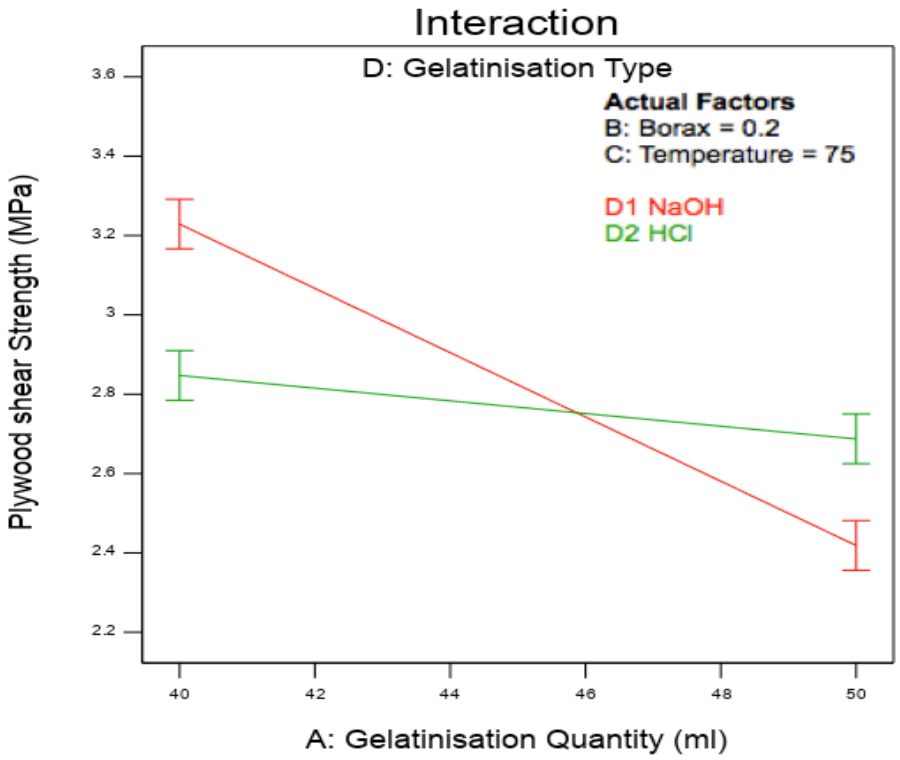

Figure 183: Interaction plot demonstrates the effect of gelatinisation quantity on plywood shear strength when using NaOH or HCl gelatinisation.

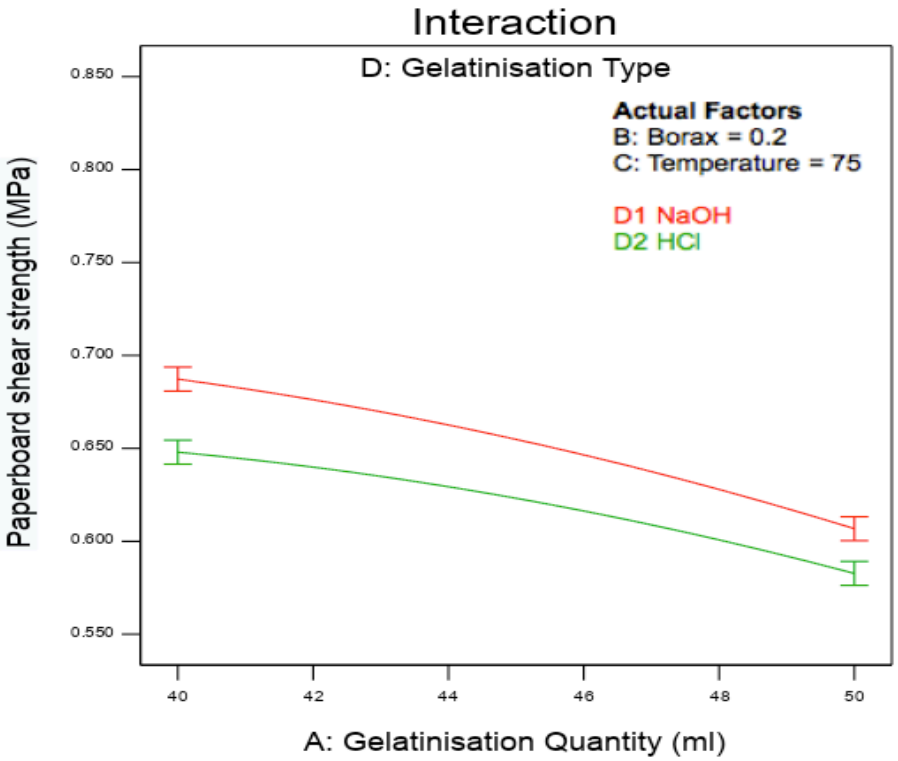

Figure 184: Interaction plot illustrates the effect of gelatinisation quantity on paperboard shear strength when using NaOH or HCl gelatinisation.

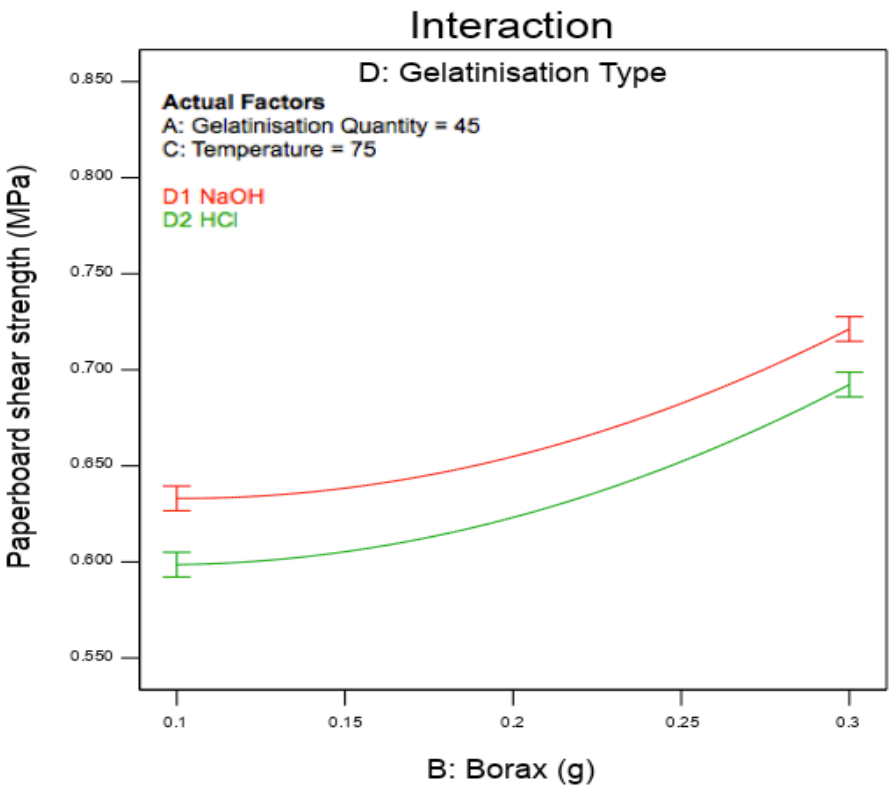

Figure 185: Interaction plot illustrates the effect of borax on paperboard shear strength when using NaOH or HCl gelatinisation.

4.10.15 Discussion

The viscosity of the liquid is the resistance to flow which inversely proportional to temperature. As the temperature increases, the liquid became lighter and had a lower flow resistance [333]. Besides, higher temperatures reduce the friction between starch molecules, which leads to a decrease in the viscosity [414]. On the contrary, borax is used as a thickener and thus works to make the adhesive material more cohesive, increasing the liquid's resistance to flow and its viscosity [333]. Although the increase in the viscosity of the starch-based adhesive contributes to an increase of the adhesive bonding strength, a large increase in the viscosity reduces the penetration of the adhesive into the cavities of the material, thus reduces the possibility of adhesion of the materials [337]. Moreover, the viscosity affects the mechanical properties of the adhesive, such as tensile and shear strength. The viscosity of the adhesive depends on the dispersion of the starch particles, thus increasing the adhesion strength [414]. Since the density of a substance refers to its mass per unit volume, it basically depends on these two factors. Higher temperatures lead to the swelling of the adhesive material, thus increasing its volume

[415, 416]. Furthermore, it decreases the water content, which leads to a decrease in the adhesive weight. In contrast, borax increases water retention in the adhesive, which leads to an increase in its mass. In other words, increasing the amount of borax in the adhesive material increases its density [333, 417]. Increasing the quantities of gelatinisation solutions in the adhesive increases its pH, as the pH is the negative logarithm of base 10 for the concentration of the solution [333]. Temperature does not have much effect on the pH. It was found that increasing borax concentrations and rising temperatures did not affect pH value [333].

Increasing or decreasing basic gelatinisation (NaOH) quantity in starch-based adhesive leads to weakness in its adhesive properties. This is because reducing the amount of gelatinisation increases the viscosity, leading to the starch breakdown. Also, the high viscosity of the adhesive does prevent it from penetrating the substrate surfaces, thus weakening the adhesive strength. On the other hand, an increase in gelatinisation amount leads to insufficient gelatine formation, thus changing the adhesive properties [418]. In producing the adhesive from starch by adding acid gelatinisation (HCl), it was found that the viscosity and density decreased with increasing temperature and increased with increasing the amount of borax. The temperature and borax have the same effect on HCl gelatinisation, which reduces the resistance to the flow of the liquid. In contrast, increasing the amount of borax increases the adhesive volume at the constant mass [334]. The viscosity of the adhesive increases with increasing the amount of acid gelatinisation and then decreases again when it reaches certain concentrations. The high concentrations of acid gelatinisation reduce the molecular size of the starch, leading to its solubility rather than swelling during temperature increase, thus causes a reduction in the adhesive's viscosity [419]. Acid gelatinisation breaks down the hydrogen bonds between the starch molecules. Increasing the amount of acid gelatinisation to certain values leads to an increased in the free hydroxyl groups, thus increasing the bond strength. Then the free hydroxyl groups begin to decrease, as well as the bond strength. The crystalline structure of starch changes with the addition of acid; as the amount of acid increases, the starch crystallinity decreases [420].

The viscosity of the adhesive material obtained from NaOH gelatinisation ranged between 815.27 mPa.s to 3953 mPa.s. The adhesive viscosities from HCl gelatinisation were less than from NaOH gelatinisation. The lowest viscosity was 223.19 mPa.s and the highest viscosity was 1,035.05 mPa.s. The difference in viscosity values between both gelatinisations may because the

acid gelatinisation reduces the molecular size of starch and its solubility in water, leading to a decrease in its viscosity [419]. The viscosity values obtained from this study are similar to the values obtained from the study that produced the adhesive from cassava starch with an esterification modifier [337]. The higher viscosity values of NaOH gelatinisation were a bit lower than those obtained from cassava starch when adding the bio-oil in different proportions [421]. Simultaneously, the highest viscosity of corn starch was approximately 450 mPa.s at the highest concentration of carboxymethyl cellulose [338] which is quite low compared to than the viscosity of NaOH gelatinisation and approximately half of the higher viscosity achieved from HCl gelatinisation.

The highest shear strength of plywood using NaOH and HCl gelatinisation was 3.59 and 3.12 MPa, respectively. These values are 27.3% and 16.3% higher than the highest shear value found from the Sun et al. [337] study. These values are in line with the values obtained from the adhesive produced from corn starch [338] and the adhesive produced from palm oil polyester with PMDI, but less than adhesive produced from bio oil polyester with TDI [422]. The highest shear strength value of the paperboard resulted from this study were approximately the same for both gelatinisation (slightly higher at 1.9% for the NaOH gelatinisation). These values are within the range of the values obtained from the paperboard adhesion study by Wu et al. (2020) [261], which were 1.07 MPa at 20% humidity and 0.33 MPa at 100% humidity. At 60% humidity the shear strength was about 0.9 MPa, which was a little higher than the shear strength achieved in this study. The difference in value may be due to the difference in humidity [261].

4.11 Summary of Results

This study explored several results and added more knowledge to the science in solving some of the AD process issues and filling the previously mentioned gaps in the first and second chapters. The study sought to utilise food waste to produce multiple bio-products to enhance the viability of AD process. The main findings that were reached can be summarised as follows:

1- Cassava peel represents 17-20% of the cassava weight, which means its use in energy production provides a solution to the accumulation of waste.
2- In terms of its highest effect, adding cassava peel to the sludge increased the yield of the resulting biogas. The methane percentage also increased from 62% after adding the

cassava peel, while it was below 55% for sludge only. The starch extracting from the cassava peel did not significantly affect the volume and quality of the resulting biogas.

3- Exposing date seeds to additional pre-treatment processes before grinding pre-treatment process leads to a loss of weight and change in their properties. This study proved that grinding the dates seed directly led to an increase in the biogas yield.
4- Adding date seeds to the sludge increased the biogas volume by nearly five times. The rise in methane percentage was also noticeable, from about 53% to 71%. So it is worth using them for energy production rather than sending them to waste.
5- Extracting the oil from the date seeds reduced the amount of biogas by 6.3% to 22.7% (from 4,140 ml to 3,534 ml at the highest biogas values). The drop in the methane percentage at its highest values was slight, from 71.1% to 69.3%. The highest CH_4/g-VS from extracted oil date seeds was 949.6 ml compared to 1,143.8 ml before extracting process, by approximately 17%.
6- The effect of the factors did differ on each response during the AD process. The volatile solid added value had the highest effect on all responses, either alone or interacting with another factor.
7- The loss from date seed oil was compensated in the production of biodiesel and crude glycerine from date seed oil. The percentage of oil produced from date seeds was 16 wt.% of the date seed mass. The percentage of biodiesel in date seed oil reached 79% compared to 9% of glycerine.
8- The adhesive performed well with plywood and paperboard, while it failed to adhere the plastic specimens. The shear strength of the adhesive obtained from NaOH gelatinisation was higher than the shear strength of the HCl gelatinisation for plywood and paperboard.
9- Digestate properties and its elements produced from cassava peels were not significantly affected by starch and oil extraction. Whereas, the amount of N in the digestate from the AD of date seed after oil extraction increased from 2,322 to 4,038 mg/kg, while the amounts of phosphorous and potassium decreased slightly. In contrast, the quantities of elements in the digestate resulting from AD of cassava peel were higher than that of date seed except for the N which was quite similar to the extracted oil date seed value.

Chapter 5

5 BIOREFINARY EVALUATION

5.1 Introduction

In this chapter, optimal results of anaerobic digestion of cassava peel and date seeds before and after oil extraction will be discussed and the energy evaluations based on these optimal results. The producing biodiesel, glycerol and starch-based adhesive material costs and the preliminary analysis of process boundary assessments will be mentioned later in this chapter.

5.2 Biogas Production

The optimisation process is the process of defining a combination of factors to achieve a specific goal using numerical and graphical optimisation. The optimisation process was carried out in the study to calculate the energy balance at the optimal results. The results of the energy balance may at a later time allow the investigation of the economic effect of the incorporation of the production process of starch-based products on the economic feasibility of the AD plant. The optimisation process was carried out in the study based on three criteria. The first criterion was set to enhance the quality with no limitation on the factors. However, the other two criteria were set to reduce the operating cost. In all the three criteria, the goals of the responses were fixed as follows; maximise the Biogas/g-VS, CH_4%, CH_4/g-VS and minimising the CO_2%. Due to the major influence of the concentration of the CH_4 on the value of the energy gained from one gram of volatile solid (Ep), the importance of the CH_4% response was set to 5 (the highest), while, the importance of the other responses was set to 3.

Furthermore, the gate fee is one of the main revenues of some AD plants [423]. Food processing industries are the second largest generator of wastes to the environment [424]. In addition to all of that, the maximisation of the volatile solid added allows for benefiting from as much amount of starch and oil as possible and increases the contribution of the AD of cassava peel and date seed in waste management. Therefore, all goals of the volatile solid factor were set to “maximise” in the 2nd and 3rd criteria.

According to Cré -Composting and Anaerobic Digestion Association of Ireland [425], sludge usually contain high proportions of water. The preservation of the digestate negatively influences the economic aspects of the AD plants [426, 427]. As long as the AD plants are producing biogas, digestate will be generated. On one hand, the generation of the digestate in large amounts has a negative impact on the environment and could lead to major issues [428]. On other hand, storing, transporting and maintaining the digestate in large amounts, is costly as the TS of the digestate is usually low and its MS is high [427]. As a result, the sludge quantity has a significant influence on the quantity and quality of the biogas produced from the AD of cassava peel and date seed, its goal was set to "minimise" in the 2nd criterion. In the setting of the 3rd criterion, all these factors were taken into accounts in addition to the revenue of the AD Plants from the sales of the bio-fertiliser and the goal of the sludge quantity was set to "in range".

In terms of temperature, it was set to "minimise" in the 2nd and 3rd criteria in order to reduce the cost of the energy consumed in the digestion process. Note, however, the digestion process is a major expense for AD plants, whereas the energy consumed in the beating and grinding pre-treatment was quite low and thus neglected. Table 61 shows the three criteria, their goals and importance. DOE provides the optimal results numerically and graphically.

Table 61: The optimisation criterion and goals.

Factors and responses	1st criteria		2nd criteria		3rd criteria	
	Goal	Importance	Goal	Importance	Goal	Importance
A: Temperature	In range	3	Minimise	3	Minimise	3
B: Volatile Solid	In range	3	Maximise	3	Maximise	3
C: Sludge Quantity	In range	3	Minimise	3	In range	3
Biogas	In range	3	In range	3	In range	3
Biogas/g-VS	Maximise	3	Maximise	3	Maximise	3
CH_4	Maximise	5	Maximise	5	Maximise	5
CO_2	Minimise	3	Minimise	3	Minimise	3
CH_4/g-VS	Maximise	3	Maximise	3	Maximise	3

5.2.1 Optimisation and Energy Evaluation of Cassava Peel

The insignificant influence of the starch on the biogas produced from the AD of the cassava peel supports exploiting the starch as a raw material in the production of bio-products simultaneously with the biogas and bio-slurry. The production of starch-based products simultaneously with biogas and bio-slurry could enhance the economic feasibility of AD plants.

Table 62 illustrates the optimal results based on the three criteria numerically. Figures 186-188, show the optimal results at the optimal set of factors in over-lay figures based on each of the criteria. As shown in Table 62, the CH_4% resulting from the three results were closer to each other. In terms of the biogas volume produced from one gram of volatile solid, the highest volume was a result of the quality criteria (1st criterion) while, the lowest was based on the second criterion. The average electric energy consumed by the water baths at a temperature of 34, 37, 40 °C were 50.54, 61.51 and 79.61 kWh respectively.

Table 62: The optimal results of the three criterions for cassava peel.

Criterion	A: °C	B: g-VS	C: %	Biogas ml	Biogas/g-VS ml/g-VS	CH_4 %	CO_2 %	CH_4/g-VS ml/g-VS
1st	38.6	1.2	50.0	1831	1448.1	59.8	15.9	871.5
2nd	36.8	2.1	39.4	2012	939.7	61.4	20.6	578.9
3rd	36.5	2.0	50.0	2195.4	1053.2	60.9	17.9	652.4

Table 63 shows the energy gain/loss based on the optimal results. In the calculation of the energy balance, the optimal results which were selected by the software as the highest in desirability were only the ones considered. From Table 63, it can be noted that, the highest loss was attributed to the quality criterion, while, the highest energy gain was based on the 3rd criterion. As it is clear from that table, the changing of the goal of the sludge quantity from “minimise” to “in range” led to a 40% increase in the energy gain. On the other hand, the changing of the goals of the temperature and volatile solid added concentration in the 1st and 3rd criterion to “minimise” and “maximise” respectively resulted in a large increase in the energy balance. This finding enhances the economic feasibility of the AD plants by reducing the energy consumed in the digestion process and

applying gate fees for accepting wastes. The finding also supports increasing the contribution of the AD of cassava peel in waste management.

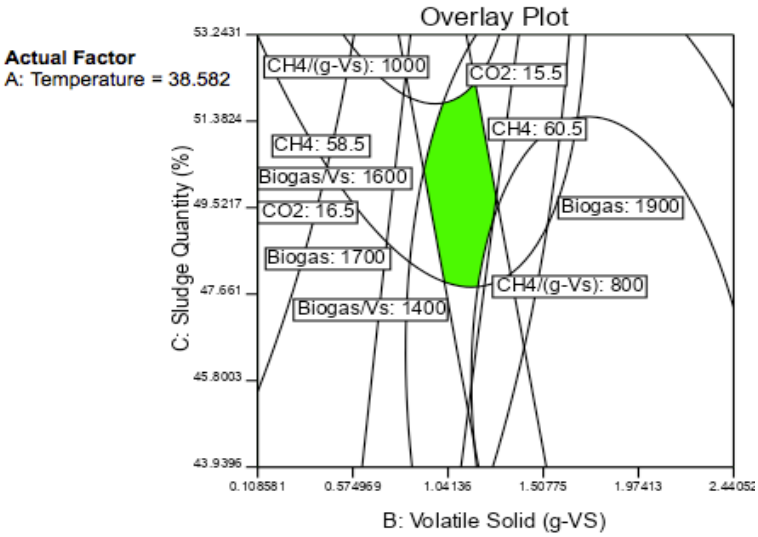

Figure 186: Overlay plot based on the first criterion for cassava peel.

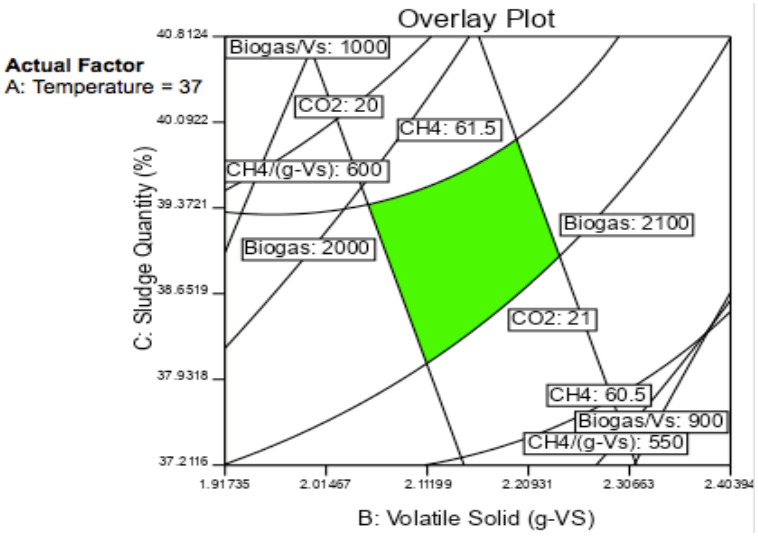

Figure 187: Overlay plot based on the second criterion for cassava peel.

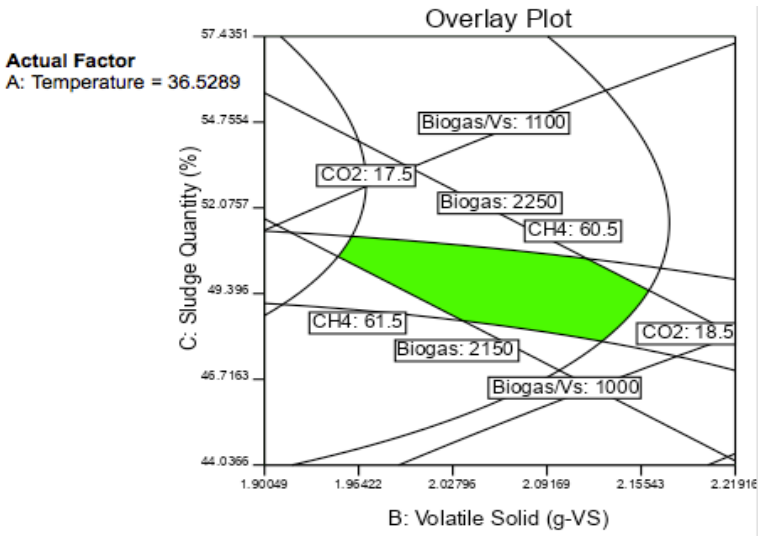

Figure 188: Overlay plot based on the third criterion for cassava peel.

Table 63: Energy evaluation of optimisation criterion for cassava peel.

Criterion	Energy consumed, kWh	Volatile solid weight, g	B_s, kWh/m^3	E_p, kWh/ g-VS	E_c, kWh/g-VS	Net E_p, kWh/g-VS	Energy balance, %
1st	70.6	1.15	5.78	0.62	0.82	-0.20	-23.27
2nd	56.2	2.13	5.93	0.41	0.35	0.07	18.93
3rd	56.2	2.05	5.89	0.47	0.37	0.10	27.26

5.2.2 Optimisation and Energy Evaluation of Date Seed

Three optimisation criteria were implemented in the study of date seed as the second and third criteria have the same energy balance value so that the third criterion removed. The average electric energy consumed by the water baths at the temperature of 34, 37, 40°C were 50.54, 61.51 and 79.61 kWh respectively. Table 64 and Figures 189-190 describe the numerical and graphical optimal results based on the two criteria. The desired optimal solution by the software only considered in the energy balance calculations. It is clear from the Table 64 that the quantity of Biogas/g-VS produced by the quality criterion was more than double that of the cost criterion. In contrast, methane in the cost criterion was 73.4%, which is 18% higher than the quality criterion.

Table 64: The optimal results of the two criterions for date seed.

Criterion	A °C	B g-VS	C %	Biogas ml	Biogas/g-VS ml/g-VS	CH_4 %	CO_2 %	CH_4/g-VS ml/g-VS
1st	36.0	1.10	50.0	2049.2	1803.3	60.2	19.6	1073.9
2nd	36.2	4.20	25.4	3325.5	830.5	73.4	13.0	598.8

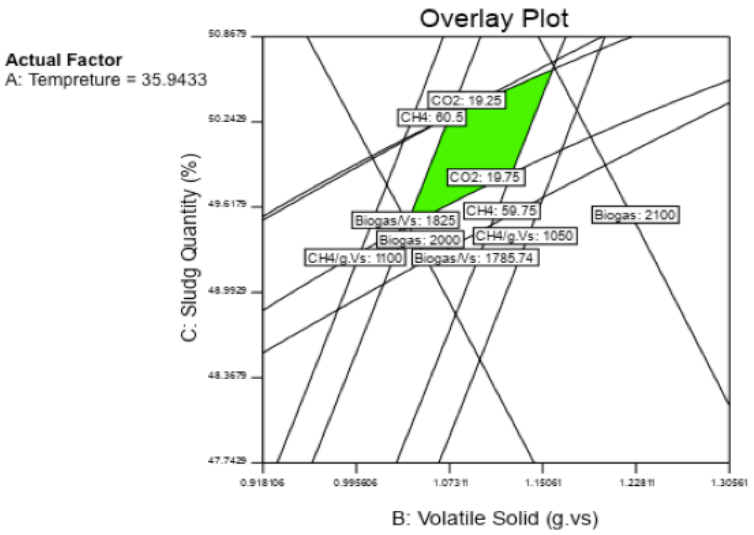

Figure 189: Overlay plot based on the first criterion for date seed.

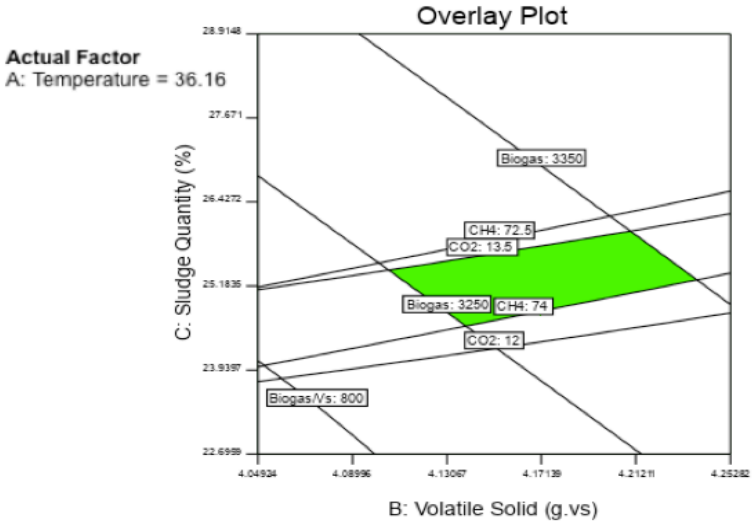

Figure 190: Overlay plot based on the second criterion for date seed.

As shown in Table 65, the highest energy gain was based on the cost criterion (131.6%) while the energy gain based on the quality criteria was 11.3%. When comparing the two criteria, changing the temperature and sludge quantity goals to “minimise” and the volatile solid to “maximise” resulted in a dramatic rise in energy balance of almost 12 times higher.

Table 65: Energy evaluation of optimisation criterion for date seed.

Criterion	Energy consumed, kWh	Volatile solid weight, g	B_s, kWh/m^3	E_p, kWh/g-VS	E_c, kWh/g-VS	Net E_p, kWh/g-VS	Energy balance, %
1st	58.3	1.10	5.82	0.79	0.71	0.08	11.3
2nd	58.7	4.20	7.10	0.44	0.19	0.25	131.6

5.2.3 Optimisation and Energy Evaluation of Extracted Oil Date Seed

Three optimisation criteria were implemented in this study as shown previously in Table 61. The first criterion was the quality criterion to maximise CH_4% with no restrictions on the AD process factors. The second and third criteria were the cost criterion to maximise CH_4% with restrictions on the AD process factors to reduce the AD process cost. The second and third criteria had the same results, so the third criterion was excluded. Table 61 shows the goals and importance set for each criterion. The responses were identified as follows; maximising the biogas/g-VS, CH_4%, CH_4/g-VS and minimising the CO_2% for each criterion. The importance of the CH_4% response was set to the highest value (5) due to its beneficial effect on energy balance calculations. The importance of the rest of the responses were set to 3.

In addition, temperatures were minimised in the second and third criterion to reduce the energy costs used in the biogas production process. The volatile solid added was set to maximum to take advantage of the largest quantity of date seed. The purpose of that is to contribute to the waste management process, waste disposal without dumping it to landfill and to reduce food waste, which is the second highest source of waste [424]. The sludge contains high portions of water as mentioned by Cré -Composting & Anaerobic Digestion Association of Ireland [425], thus negatively affects the economic aspects of the AD process due to the increase in costs related to digestate [426, 427]. The high MS and TS make the storage, transportation and maintenance processes of the digestate costly particularly with the large quantities resulting from the AD process [427]. For these reasons the sludge quantity goal was set to “minimise” in the second criterion and “in range” in the third criterion. The purpose of changes the goal of the sludge quantity in the third criterion to consider the gain of the AD Plants from the sales of the bio fertiliser.

Furthermore, applying the gate fees can be used to enhance the AD process [427]. Gate fees are the costs that the provider pays to AD plants for disposing of waste. These costs are lower than the costs of other options of disposing wastes, which provide a profit for both parties [429]. The energy consumed in the grinding process was quite low (0.21 kWh in 10 min) and thus neglected. Although the grinding machine capacity is 250-350 Kg/h, it needs further investigation when it is applied on a large scale. The average electric energy consumed by the water baths at the temperature of 34, 37, 40°C were 50.54, 61.51 and 79.61 kWh respectively. Table 66 and Figures 191-192 describe the numerical and graphical optimal results based on the two criteria. The optimal solution with the highest desirability that determined by the software was selected in the energy balance calculations. It is clear from Table 66 that the quantity of biogas/g-VS produced by the quality criterion was more than double that of the cost criterion. In contrast, methane in the cost criterion was 71.2%, which was 14.5% higher than the quality criterion.

Table 66: The optimal results of the two criterions for extracted oil date seed.

Criterion	A °C	B g-VS	C %	Biogas ml	Biogas/g-VS ml/g-VS	CH_4 %	CO_2 %	CH_4/g-VS ml/g-VS
1st	40.0	1.10	49.99	1818.2	1607.4	60.9	20.2	887.6
2nd	34.0	4.20	31.97	2818.7	686.9	71.2	17.5	473.7

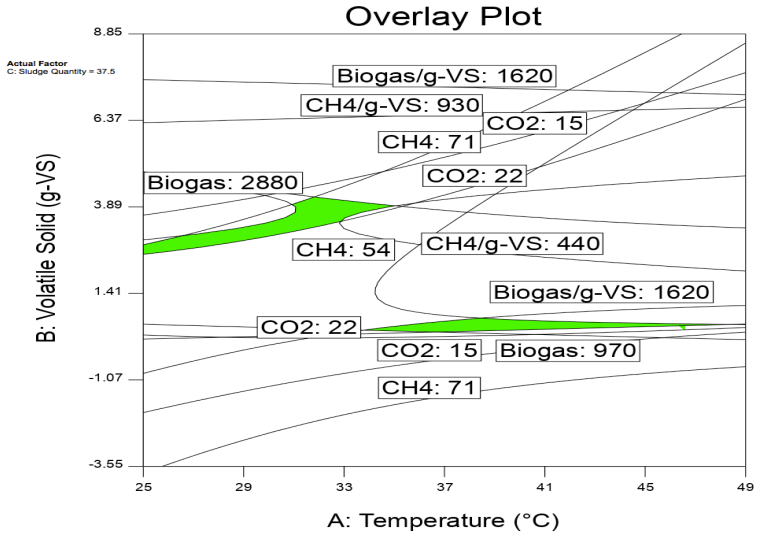

Figure 191: Overlay plot based on the first criterion for extracted oil date seed.

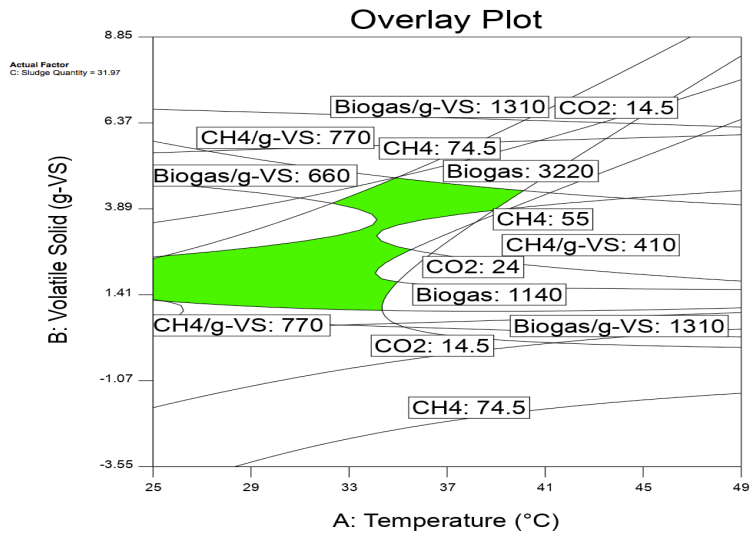

Figure 192: Overlay plot based on the second criterion for extracted oil date seed.

As shown in Table 67, the highest energy gains were based on the cost criterion at 121.5%, while an energy loss resulted based on the quality criteria at -27.1%. When comparing the criteria, changing the temperature to "minimise", sludge quantity goals to "minimise" or "in range" and the volatile solid to "maximise" resulted in a dramatic rise in energy balance.

Table 67: Energy evaluation of optimisation criterion for extracted oil date seed.

Criterion	Energy consumed, kWh	Volatile solid weight, g	Bs, kWh/m^3	Ep, kWh/g-VS	Ec, kWh/g-VS	Net Ep, kWh/g-VS	Energy balance, %
1st	79.61	1.10	5.88	0.71	0.96	-0.25	-27.1
2nd	50.54	4.20	6.88	0.35	0.16	0.19	121.5

5.3 Starch-based Adhesive Optimisation

The optimisation process was implemented to calculate the energy balance using optimal results in the adhesive production process. The purpose of this was to investigate the economic impact of producing additional bio-product from the food wastes. Three criteria were set during the optimisation process. The first and second were set to improve the adhesive quality, while the third criterion was set to reduce the production costs. The first criterion was set without any restrictions and the second criterion was set as follows: minimising the gelatinisation quantity and maximising borax and temperature. In the third criterion, restrictions were placed to minimise all factors. Responses goals were set

for all responses without restrictions on viscosity, density, pH, and maximising plywood and paperboard shear strength. The importance of shear strength was set at 5 due to its importance in this study, while the importance of the remaining responses were set at 3. Table 68 illustrates the goals and restrictions of the optimisation process for all criteria. The energy consumed in extracting starch from cassava peels was neglected because it was quite low (0.15 kwh in 5 min). This value requires re-evaluation on an industrial scale.

Table 68: The optimisation criterion and goals.

Factors and responses	1st criteria		2nd criteria		3rd criteria	
	Goal	Importance	Goal	Importance	Goal	Importance
A: Gelatinisation	In range	3	Minimise	3	Minimise	3
B: Borax	In range	3	Maximise	3	Minimise	3
C: Temperature	In range	3	Maximise	3	Minimise	3
Viscosity	In range	3	In range	3	In range	3
Density	In range	3	In range	3	In range	3
pH	In range	3	In range	3	In range	3
Plywood shear strength	Maximise	5	Maximise	5	Maximise	5
Paperboard shear strength	Maximise	5	Maximise	5	Maximise	5

5.3.1 NaOH Gelatinisation

The viscosity of the adhesive at the optimum values was varied slightly while its density and pH were close to each other as shown in Table 69. The same table displays the difference in shear strength of plywood and paperboard. The highest shear strength was achieved using the second criterion (quality criteria), with an increase by 3.17% and 3.71% for plywood and paperboard, respectively compared to the first criterion. When changing the restrictions from "in range" to "minimise" for all factors in the cost criterion the shear strength decreased by 20.1% and 18.4%, respectively. Figures 193-195 display the optimum graphical results.

Table 69: The optimal results of the three criterions for NaOH gelatinisation.

Criterion	A ml	B g	C °C	Viscosity mPa.s	Density g/ml	pH %	Plywood shear strength MPa	Paperboard shear strength MPa
1st	40.5	0.28	84.8	3037.6	1.048	12.6	3.66	0.882
2nd	40.0	0.30	85	3590.91	1.050	12.5	3.78	0.916
3rd	40.0	0.23	65	2578.29	1.060	12.7	3.02	0.747

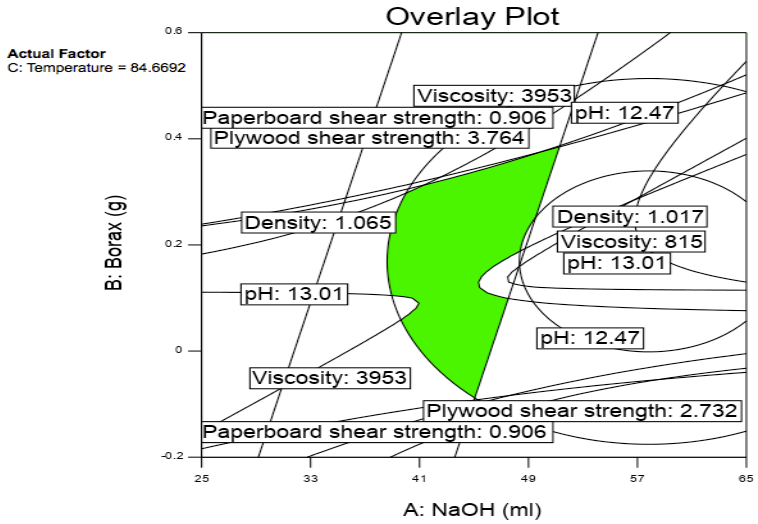

Figure 193: The first criterion overlay figure for NaOH gelatinisation.

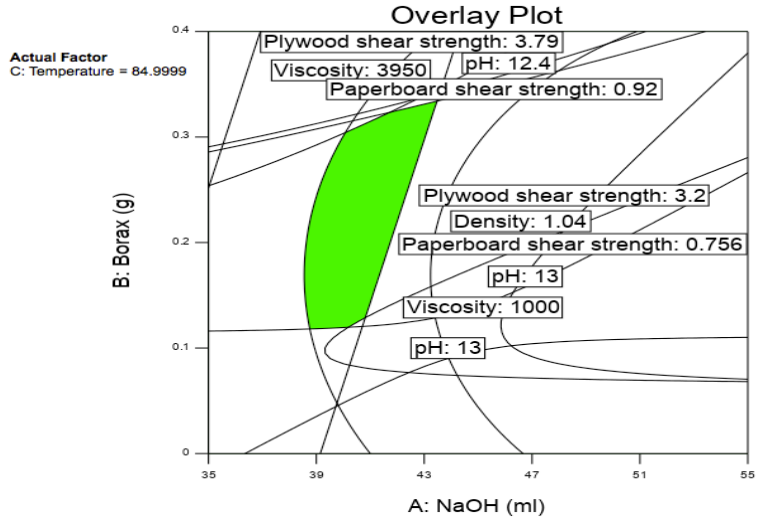

Figure 194: The second criterion overlay figure for NaOH gelatinisation.

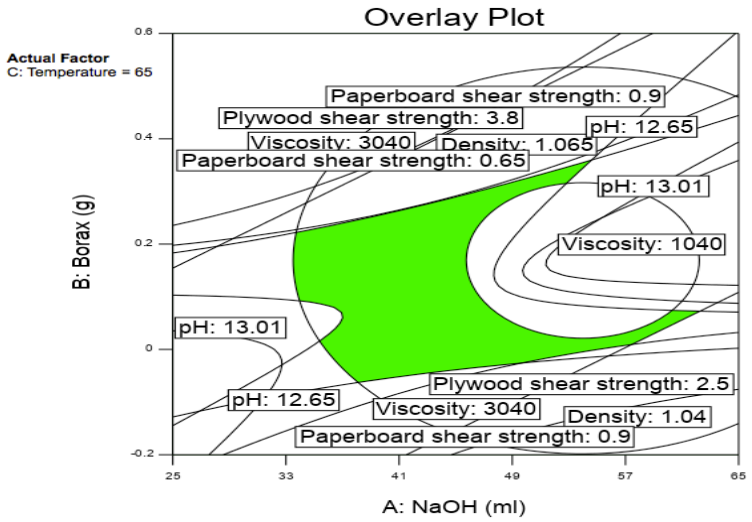

Figure 195: The third criterion overlay figure for NaOH gelatinisation.

5.3.2 HCl Gelatinisation

Table 70 shows the optimal response values and Figures 196-198 illustrate the optimum graphical results for the HCl gelatinisation. In the quality criterion, the viscosity of the adhesive was almost equal, while for the cost criteria it increased significantly. The difference in adhesive density and pH were quite low. The table also illustrates the difference between the plywood and paperboard shear strength, using the quality criterion at 2.7% and 3.9%, respectively. The decrease in shear strength in the third criterion compared to the second criterion was 6.7% for plywood shear strength and 16.7% for paperboard shear strength.

Table 70: The optimal results of the three criterions for HCl gelatinisation.

Criterion	A ml	B g	C °C	Viscosity mPa.s	Density g/ml	pH %	Plywood shear strength MPa	Paperboard shear strength MPa
1st	42.7	0.29	84.8	441.334	1.018	9.09	3.20	0.851
2nd	40	0.29	85.0	484.20	1.023	9.11	3.29	0.886
3rd	40	0.23	80.6	727.14	1.023	8.91	3.07	0.738

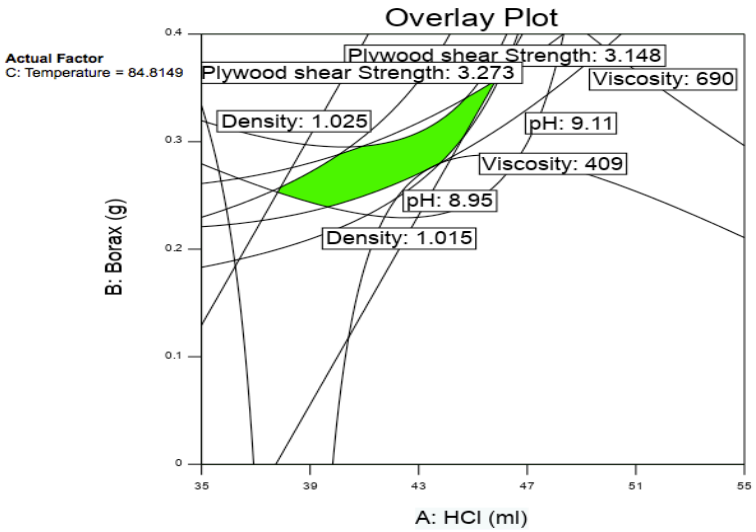

Figure 196: The first criterion overlay figure for HCl gelatinisation.

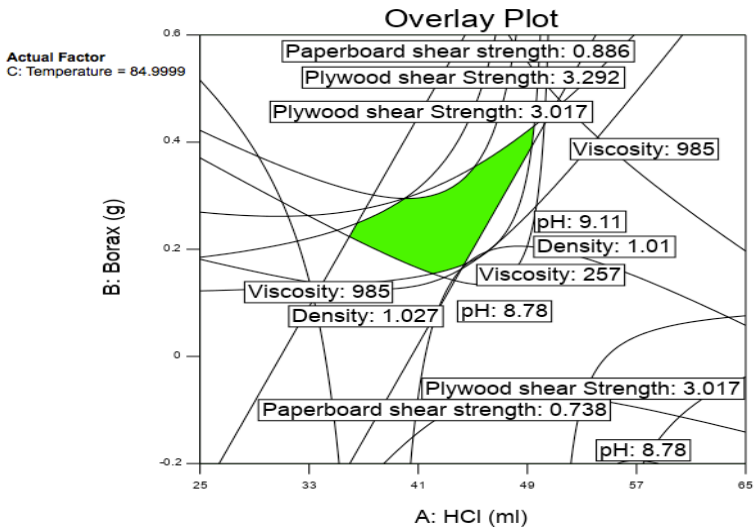

Figure 197: The second criterion overlay figure for HCl gelatinisation.

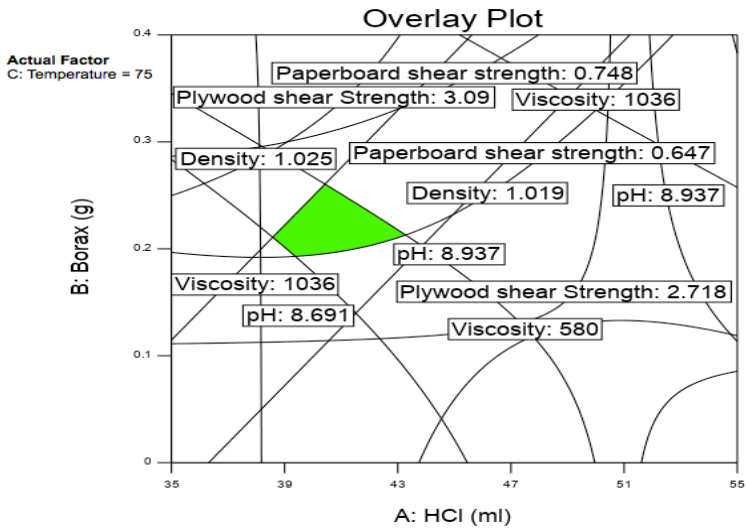

Figure 198: The third criterion overlay figure for HCl gelatinisation.

5.4 Biodiesel, Glycerine and Starch-Based Adhesive Production Cost

The costs of producing biodiesel and glycerine at the laboratory scale are shown in Table 71. Date seed oil was produced process performed at 70 °C, 5 hours extracting time and 1:4 date seed: n-hexane ratio. Transesterification of the oil to produce biodiesel and glycerine was carried out at 65 °C for 2 hours. The production costs were divided into energy consumption and materials cost. Since hexane and methanol can be recovered to 97% and 95%, (section 5.4) their costs were neglected. The cost of energy consumed in producing 100 ml of date seed oil was € 0.68. The cost of energy consumed in transesterification of the oil was € 0.25. The total cost of energy consumed to produce biodiesel and glycerine was € 1.02. The cost of energy consumption for biodiesel purification is meagre, so it was neglected. The energy price in DCU is €0.125 per kWh. The highest cost in the biodiesel and glycerine production process was the cost of oil extraction, which was estimated by two-thirds of the production cost, followed by the transesterification process cost. The cost of sodium hydroxide was the lowest (9% of the total cost). Further investigating of the possibility of reducing the extraction period without affecting the amount of oil may help in reducing this cost.

Table 71: Biodiesel and glycerin production cost.

Process/Material	Energy consumed (kWh)	Process time (h)	Total energy consumed (kWh)	Cost/sample (€)
	(A)	(B)	(C) = (A) × (B)	(D) = (C) × € 0.125
Oil Extraction	1.08	5	5.40	0.68
Transesterification of oil	0.98	2	1.96	0.25
N-Hexane*	----------	---------	----------	~~2.36~~
Methanol*	----------	---------	----------	~~1.53~~
Sodium hydroxide	----------	---------	----------	0.09
Total				1.02

** Hexane and methanol costs were neglected as they can recover at high percentages.*

The adhesive production process from NaOH and HCl gelatinisation at optimum values were carried out at different temperatures. Table 72 describes the starch-based adhesive production cost. The energy consumed to produce the adhesive from NaOH at 85 °C was 0.32 kWh, and 0.25 kWh at 65 °C. In contrast, to produce the adhesive from HCl at 80 and 85 °C, the energy consumption was 0.32 and 0.33 kWh, respectively. The cost of each gelatinisation was € 1.58 /sample of NaOH and € 0.78/sample of HCl. One gram of borax cost was € 0.25. The total cost of producing 40ml of the adhesive from NaOH is between € (1.89-1.98) and from HCl is between € (1.16-1.23).

Table 72: starch-based adhesive production cost based on optimal results.

Process/Materials		Adhesive from NaOH	Adhesive from HCl
Energy consumed at 65 °C (kWh)		0.25	0.26
Energy consumed at 85 °C (kWh)		0.32	0.33
Sodium Hydroxide (€)		1.58/sample	0.78/ sample
Borax (€)		0.25/g	0.25/g
Total cost (€)	1st criteria	1.97	1.23
	2nd criteria	1.98	1.19
	3rd criteria	1.89	1.16

5.5 Preliminary Analysis of Process Boundary

The preliminary analysis of process boundary aims to compare the approach of producing bio-product and their resulting waste. Biogas, starch-based adhesive and digestate were produced from cassava peel and biogas, biodiesel, glycerine and digestate were created from date seeds. The preliminary analysis of the process boundary diagram shown in Figure 199 consists of the production of biogas, starch-based adhesive, oil extraction and

production of biodiesel and glycerine. Waste from these processes includes gaseous emissions and wastewater. The production of raw materials, the energy consumed during the pre-treatment processes and the separation of hexane and methanol were not considered.

Raw materials were prepared using laboratory equipment, minimising the treatment process was taken into account as much as possible to reduce each operation costs, weight loss of raw materials and the amount of waste generated were also minimised. The cassava peel was used immediately in the AD process after extracting the starch, the water produced with the starch was added to the pre-treated peel. The date seeds were washed to purify them from impurities, resulting in a quantity of water discarded to sewage. The biogas production process yielded certain amounts of CO_2, which usually disposed of in air but in quite lower amounts than that generated from fossil fuels. The surplus by products of AD processes (digestate) can be exploited in some fields such as in agricultural applications for soil amendment or as a bio fertiliser or recycle and reuse in the AD process [196, 197]. Each gram of cassava peel yielded between 578.9 to 871.5 ml of CH_4/g-VS based on the optimal results (Table 62). While one gram of date seeds before oil extraction produced 598.8 to 1,073.9 ml of CH_4/g-VS. On the other hand, after oil extraction, these quantities were reduced to 473.7 and 887.6 ml of CH_4/g-VS, based on the optimal results (Tables 64 and 66).

The process of producing date seed oil, biodiesel and glycerine was carried out under reflux conditions, so there were no emissions to the air from these processes. The biodiesel purification process generated wastewater. Every 100 ml of date seed oil production process (approximately 80 ml of biodiesel and 10 ml of glycerin) required 550 g of ground date seed, 2,200ml of n-hexane, 22 ml of methanol and 0.750 g of NaOH. N-Hexane and methanol can be recycled and used several times, depending on the efficiency of the recycling process, which can reach more than 97% and 95%, respectively. The total energy consumed to produce the date seed oil was estimated at 5.4 KWh per cycle (based on five hours extraction time at 70 °C) and 0.98 KWh for the transesterification process at temperature between 60-65 °C. The process of producing 40 ml of the adhesive required a consumption of an amount ranging from 0.25 kWh to 0.33

kWh (depending on the reaction temperature and the type of gelatinisation used) in addition to the gelatinisation (NaOH or HCl) amount and viscosity enhancer (Borax). Since this assessment was implemented at the laboratory scale, further investigation of the life cycle analysis at an industrial scale is required.

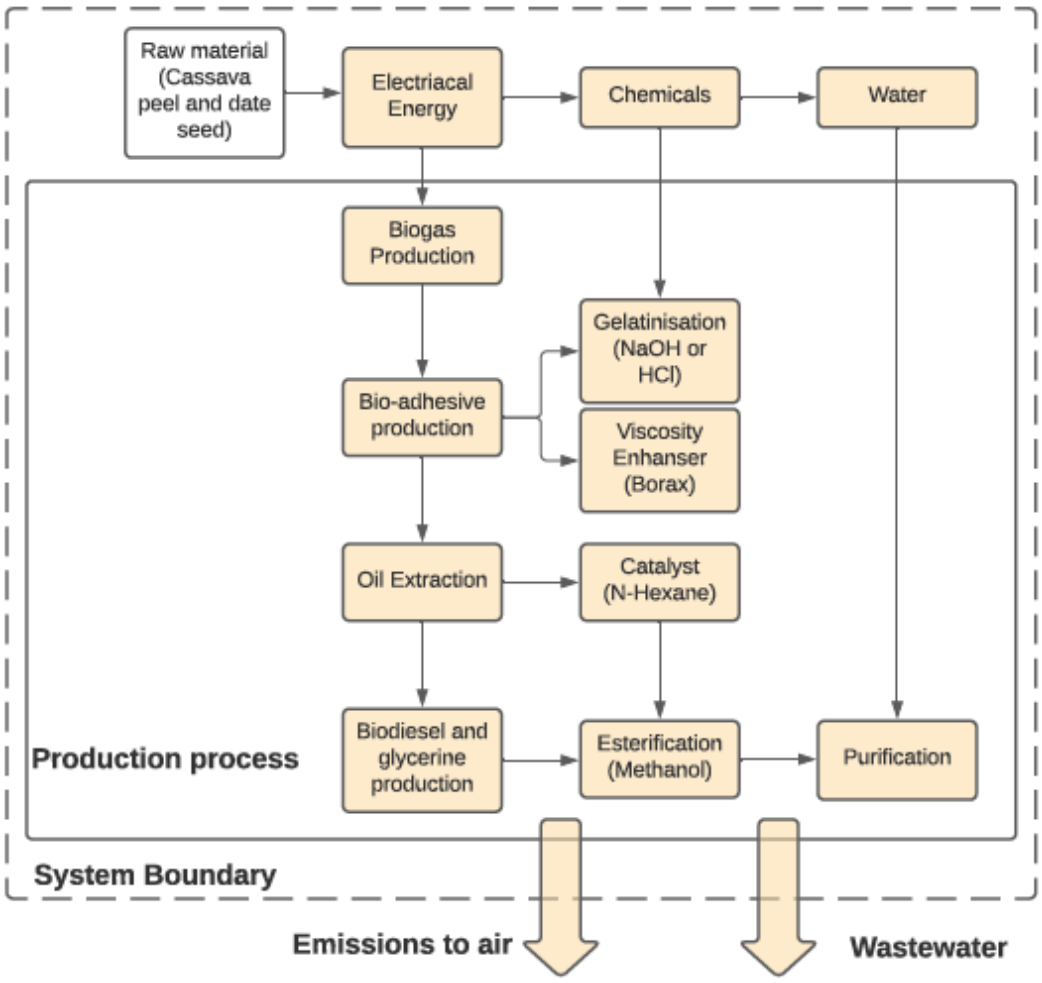

Figure 199: The preliminary analysis of process boundary in this study.

5.6 Summary

The optimisation process of the AD process was carried out to calculate the energy balance at optimum results. Three criteria were defined as follows, the first criterion to improve the quality of biogas and the other two to reduce the operational costs of the process. In the energy balance calculations for cassava peels, the largest energy loss was the first criterion for biogas quality. In contrast, the third criterion had the largest energy gain when the amount of sludge was "in range". As for the energy balance calculations

for date seeds, the second and third criteria (cost criteria) had the same results, so the third criterion was ignored. The energy gain of the second criterion was 131.6% for date seed before oil extraction, while it decreased slightly to 121.5% after oil extraction.
The costs of producing biodiesel and glycerine were calculated on the laboratory scale. The costs of purchasing the n-hexane, used in the oil extraction process and the methanol used in the transesterification processes were neglected due to the possibility of their recovery (by more than 95%).

The process of optimising the adhesive production process was carried out at optimum results. Three criteria were set to improve the quality of the adhesive and reduce the production cost. The first and second criteria were set to improve the quality of the adhesive and the third criterion was aimed to reduce the cost of production by placing all factors at the "minimise". For both gelatinisations, in terms of plywood and paperboard shear strength, the second criterion had the best performance of the adhesive. In contrast, the third criterion had the lowest performance. The production costs of the adhesive from NaOH gelatinisation were higher than the adhesive from HCl gelatinisation due to the difference in the gelatinisation material price.

CHAPTER 6

6 CONCLUSION AND FUTURE WORK

6.1 Conclusions

In this chapter, the main study's conclusions, limitations and required future studies will be discussed. At the end of this chapter, the study's contributions for obtaining a Doctor of Philosophy in addition to the previously mentioned publications will be clarified.

6.1.1 Anaerobic Digestion

The exploitation of cassava peels and date seeds in producing bioenergy contribute in increasing bioenergy dependence and thus reducing dependence on fossil fuel, which contributes in reducing harmful emissions and properly managing waste. In addition to the accumulation of waste in general, fossil fuel emissions and food waste pose environmental and health threats. Therefore, there is an urgent need to move to sustainable and renewable energy with low emissions and to become more environmentally friendly. Food waste from cassava peels and date seeds constitute usable sources of energy.

To obtain the highest quantity and quality biogas, it is necessary to set reaction temperature and sludge/substrate ratio at their optimal values. The energy balance results support AD plants in applying gate fees for accepting the wastes and increasing the contribution of the AD of cassava peels and date seeds with respect to waste management.

The results of the digestate tests confirmed the content of the three basic nutrients of fertiliser. The presence of these elements is important if one was to use them in the agricultural field, as the quality of the organic fertilisers are evaluated based on the presence of these elements. Nitrogen in high proportions was found in all of the digestates resulting from the AD processes. Thus, selling the digestate may minimise the cost of maintaining it and, therefore, improve the AD process's economic feasibility.

The main conclusions of the AD process of cassava peels and date seeds before and after oil extraction can be summarised within the following points:

A) Conclusion of Cassava Peel

- The addition of cassava peel to the sludge led to a noticeable increase in biogas and methane production, as the biogas volume increased more than quadrupled, while the methane percentage increased by 17% (from 53% to 62% at its highest value).
- The impact of the starch on the biogas produced was insignificant.
- Compared to recent studies on the AD biogas of cassava peel, beating pre-treatment by the Hollander beater led to better results regarding the quantity and quality of the biogas.
- The Hollander beater was used in the study as a bi-functional device to treat the cassava peel and extract the starch.
- At 36.5 °C, 2 g-VS and 200 ml of sludge, the highest energy gain was obtained at the optimal result of 2,195 ml Biogas, 1,053.2 ml/g-VS, 60.9% CH_4, 18% CO_2 and 652.4 ml/g-VS of methane.
- The highest energy gains from energy balance calculations for the second and third criteria (cost criteria) was 18.93% and 27.26%, respectively.

B) Conclusion of Date Seed and Extracted Oil Date Seed

- Likewise, date seeds increased the biogas yield by an order of five times.
- The methane percentage increased by 25.6%, reaching 71.1%, compared to 52.9% before adding the date seeds.
- Not exposing the date seed to the treatment processes before the grinding process increased the biogas yield. These treatments may cause a loss in date seed weight and thus a change in their properties.
- The highest energy gain obtained was at the optimal result of 3,325.5 ml of Biogas, 830.5 ml/g-VS of ml/g-VS, 73.4% of CH_4%, 13% CO_2% and 598.8 ml/g-VS of CH_4/g-VS at 36.2 °C, 4.2 g-VS and 101.6 ml of sludge.
- The highest energy gain was 131.6% for the cost criterion, while the gain from the quality criterion was 11.3%.

- The addition of extracted oil date seeds to the sludge increased the yield of biogas and methane values. The amount of biogas increased dramatically from 800 ml before adding the date seeds to 3,534 ml.
- The methane percentage increased by approximately 26.5% when the extracted oil date seeds were added.
- The highest biogas volume at the optimum results of the second Criterion was 2,818.7 ml, the Biogas/g-VS was 686.9, CH_4% was 71.2%, CO_2% was 17.5% CH_4/g-VS was 473.7 ml/g-VS at 34°C, 4.2 g-VS and approximately 128 ml of sludge.
- The energy gain at these values was 121.5%.

Comparing the results of the AD process of date seeds before and after oil extraction led to the following conclusions:

- The volume of biogas decreased by varying ratios. The difference was 14.4% at the highest biogas values of 4,140 ml before extracting oil and 3,543 after the extraction process. The highest difference was 22.7%, while the lowest difference was 6.3%.
- The largest difference in CH_4% was 10.98%, while the lowest difference was 1.12%. The difference between the highest values was around 2.53%.
- In contrast, the percentage of CO_2 emissions resulting from the AD of extracted oil date seeds increased to 15.6% compared to 13% before oil extraction.
- The difference in the amount of CH_4/g-VS produced, ranged from 27% to 8.59%. At the highest CH_4/g-VS values, the difference was about 17%, as it decreased from 1,143.8 ml/g-VS to 949.6 ml/g-VS due to the oil extraction process.

C) Limitations

- The beating pre-treatment does not adequately treat the date seeds due to their hardness.
- The low DM of the digestate confirms the challenges of AD plants on the fees incurred for transporting and storing the digestate.

6.1.2 Biodiesel and Glycerine

A) Main conclusions

- Extracting the dates seed oil using the Soxhlet method at the following conditions: 70 °C, 1:4 ratio of date seeds to the solvent and 5 hours of reaction time, resulted in approximately identical quantities to the optimal results of previous studies.
- The percentage of oil extracted from date seeds was approximately 16% of the mass of date seeds, as each gram of ground date seeds yielded approximately 0.202 ml of oil.
- The percentage of biodiesel produced was 79% of the oil produced, while the glycerine generated, was up about 9% of the oil volume.
- The test results of the biodiesel and glycerine samples were largely identical to the standards.

B) Limitations

- This study is valid to the seeds of date palms, not oil palms, which differ in composition from date palm seeds.

6.1.3 Starch Based Adhesive

A) Main conclusions

- The adhesive produced from cassava starch with basic and acidic gelatinisation showed high adherent properties for the plywood and paperboard specimens.
- The adhesive from NaOH gelatinisation had a higher strength marginal than that of HCl gelatinisation adhesive. However, its production process was more expensive.

B) Limitations

- The adherent of the adhesive produced from cassava starch with NaOH and HCl gelatinisation failed for the plastic specimens.

6.2 Future Study

Further studies are still required with respect of the AD process and the feasibility of producing bio-product from food waste. Many aspects of these processes require more study and research to make AD more efficient, effective and reliable. Some of these aspects can be summarised within the following points:

- Search for more food waste that contains starch or oil in their wastes such as banana peel and fruit seeds to produce multiple forms of renewable energy.
- The digestate resulting from the AD needs further testing and investigation of the feasibility of its application in the agricultural field such as a soil conditioner or as an organic fertiliser.
- Consider the feasibility of extracting other bio-products from cassava peel starch, such as bioplastics and kerosene from date seed oil.
- Investigates the recovery processes of the n-hexane solvent and methanol used in biodiesel and glycerine production on a large scale.
- Apply the AD processes and energy balance calculations on an industrial scale.
- Study the effect of other gelatinisation and viscosity enhancer on the adhesive performance.
- Study the causes of adhesive failure of plastic samples and the possibility of applying different surface preparation methods such as acid etching and mechanical polishing.
- Applying the product life-cycle assessment, considering transportation, export operations and other influence factors.
- Cost analysis of producing biodiesel, glycerine and starch-based adhesive on an industrial scale needs further research regarding the recovery of N-hexane and methanol and the plastic surface preparation costs.

6.3 PhD Research Contribution

This study contributes to adding more knowledge in the field of the AD and the production of several bio-product from food waste in an attempt seeking to provide some solutions to the environmental and health issues as a result of the accumulation of waste and harmful emissions from fossil fuels. The novelty of research for a PhD can be summarised as follows:

- Extracting starch from cassava peel and using it in the adhesive production for the first time and using the remaining peels in the AD process to produce biogas.
- It is the first study that introduced the Hollander beater as a bi-functional to treat cassava peels and isolate the starch.

- The study illustrating the effect of beating pre-treatment by Hollander beater and grinding pre-treatment on the quantity and quality of biogas produced from two types of food waste (cassava peels and date seeds that consumed in large amounts by many nations). Such results have not been determined in the literature thus is a novel contribution.

- It is a unique study to determine the impact of extracting the starch from cassava peel on the biogas' quantity and quality produced from the AD process of cassava peel.

- Only one study was found discussing the effect of biogas produced from grounded date seeds before and after oil extraction, but no study was found discussing this topic without pre-treating process.

- Highlighting the effect of extracting cassava peel starch and date seed oil on the resulting digestate and their effect on the presence of necessary elements. Such information have not been determined in the literature thus is a new contribution to knowledge.

- The comparison of the cassava peel starch adhesive strength of base and acid gelatinisation as an adherent applied to plywood and paperboard specimens is novel for the knowledge.

- The successful application of the DOE technique in designing experiments and analysing results for the AD process of cassava peel and date seeds and starch-based adhesive production.

- The optimisation of the AD process to form optimal bio-products, in order to address the energy/environmental issues raised in the literature. The use of DOE has been minimal in this area, other than its application in DCU, therefore this is novel.

- Finally the calculation of the AD process's energy balance for the two food wastes and production costs of biodiesel, glycerine, and starch-based adhesive material.

References

[1] Hu, H., Wang, L., Lv, S. X., 2020, "Forecasting energy consumption and wind power generation using deep echo state network," Renewable Energy, 154, pp. 598-613.
[2] Zeren, F., Akkuş, H. T., 2020, "The relationship between renewable energy consumption and trade openness: New evidence from emerging economies," Renewable Energy, 147, pp. 322-329.
[3] Matheri, A. N., Mbohwa, C., Ntuli, F., Belaid, M., Seodigeng, T., Ngila, J. C., Njenga, C. K., 2018, "Waste to energy bio-digester selection and design model for the organic fraction of municipal solid waste," Renewable and sustainable energy reviews, 82, pp. 1113-1121.
[4] Sadorsky, P., 2009, "Renewable energy consumption, CO_2 emissions and oil prices in the G7 countries," Energy Economics, 31(3), pp. 456-462.
[5] Chen, Z. M., Chen, P. L., Ma, Z., Xu, S., Hayat, T., Alsaedi, A., 2019, "Inflationary and distributional effects of fossil energy price fluctuation on the Chinese economy," Energy, 187, p. 115974.
[6] Latinwo, G. K., Agarry, S. E., 2015, "Modelling the kinetics of biogas production from mesophilic anaerobic co-digestion of cow dung with plantain peels," International Journal of Renewable Energy Development, 4(1), pp. 55-63.
[7] Adams, S., Klobodu, E. K. M., Apio, A., 2018, "Renewable and non-renewable energy, regime type and economic growth," Renewable Energy, 125, pp. 755-767.
[8] Waseem, M., Manshadi, S. D., 2020, "Electricity grid resilience amid various natural disasters: Challenges and solutions," The Electricity Journal, 33(10), p. 106864.
[9] Abbasi, T., Premalatha, M., Abbasi, S. A., 2011, "The return to renewables: Will it help in global warming control?," Renewable and Sustainable Energy Reviews, 15(1), pp. 891-894.
[10] Owusu, P. A., Asumadu-Sarkodie, S., 2016, "A review of renewable energy sources, sustainability issues and climate change mitigation," Cogent Engineering, 3(1), p. 1167990.
[11] Elum, Z. A., Momodu, A. S., 2017, "Climate change mitigation and renewable energy for sustainable development in Nigeria: A discourse approach," Renewable and Sustainable Energy Reviews, 76, pp. 72-80.
[12] Liu, X., Kong, H., Zhang, S., 2021, "Can urbanisation, renewable energy, and economic growth make environment more eco-friendly in Northeast Asia?," Renewable Energy, 169, pp. 23-33.
[13] Luukkanen, J., Vehmas, J., Kaivo-oja, J., 2021, "Quantification of doughnut economy with the sustainability window method: analysis of development in Thailand," Sustainability, 13(2), p. 847.
[14] Hiloidhari, M., Baruah, D. C., Kumari, M., Kumari, S., Thakur, I. S., 2019, "Prospect and potential of biomass power to mitigate climate change: A case study in India," Journal of Cleaner Production, 220, pp. 931-944.
[15] Popp, J., Lakner, Z., Harangi-Rakos, M., Fari, M., 2014, "The effect of bioenergy expansion: Food, energy, and environment," Renewable and Sustainable Energy Reviews, 32, pp. 559-578.
[16] Akella, A. K., Saini, R. P., Sharma, M. P., 2009, "Social, economical and environmental impacts of renewable energy systems," Renewable Energy, 34(2), pp. 390-396.
[17] Yao, Y., Xu, J. H., Sun, D. Q., 2020, "Untangling global levelised cost of electricity based on multi-factor learning curve for renewable energy: Wind, solar, geothermal, hydropower and bioenergy," Journal of Cleaner Production, 285, p. 124827.

[18] Sachs, J. D., Schmidt-Traub, G., Mazzucato, M., Messner, D., Nakicenovic, N., Rockström, J., 2019, "Six transformations to achieve the sustainable development goals," Nature Sustainability, 2(9), pp. 805-814.
[19] Vural, G., 2020, "How do output, trade, renewable energy and non-renewable energy impact carbon emissions in selected Sub-Saharan African Countries?," Resources Policy, 69, p. 101840.
[20] Wang, B., Wang, Q., Wei, Y. M., Li, Z. P., 2018, "Role of renewable energy in China's energy security and climate change mitigation: An index decomposition analysis," Renewable and sustainable energy reviews, 90, pp. 187-194.
[21] Bonnet, C., Hache, E., Seck, G. S., Simoen, M., Carcanague, S., 2019, "Who's winning the low-carbon innovation race? An assessment of countries' leadership in renewable energy technologies," International Economics, 160, pp. 31-42.
[22] Davis, M., Moronkeji, A., Ahiduzzaman, M. Kumar, A., 2020, "Assessment of renewable energy transition pathways for a fossil fuel-dependent electricity-producing jurisdiction," Energy for Sustainable Development, 59, pp. 243-261.
[23] Hansen, K., Mathiesen, B. V., Skov, I. R., 2019, "Full energy system transition towards 100% renewable energy in Germany in 2050," Renewable and Sustainable Energy Reviews, 102, pp. 1-13.
[24] Perez, A., Garcia-Rendon, J. J., 2020, "Integration of non-conventional renewable energy and spot price of electricity: A counterfactual analysis for Colombia," Renewable Energy, 167, pp. 146-161.
[25] Herbert, G. M., Krishnan, A. U., 2016, "Quantifying environmental performance of biomass energy," Renewable and Sustainable Energy Reviews, 59, pp. 292-308.
[26] "Facts about climate change," Available from: https://spunout.ie/news/climate/10-facts-about-climate-change [Accessed on: 3 June 2021].
[27] Hu, M., Li, R., You, W., Liu, Y., Lee, C. C., 2020, "Spatiotemporal evolution of decoupling and driving forces of CO_2 emissions on economic growth along the Belt and Road," Journal of Cleaner Production, 277, p. 123272.
[28] Rauf, A., Liu, X., Amin, W., Ozturk, I., Rehman, O. U., Sarwar, S., 2018, "Energy and ecological sustainability: challenges and panoramas in belt and road initiative countries," Sustainability, 10(8), p. 2743.
[29] Kaygusuz, K., 2011, "Energy services and energy poverty for sustainable rural development," Renewable and sustainable energy reviews, 15(2), pp. 936-947.
[30] Bergmann, A., Hanley, N., Wright, R., 2006, "Valuing the attributes of renewable energy investments," Energy policy, 34(9), pp. 1004-1014.
[31] Luttenberger, L. R., 2015, "The barriers to renewable energy use in Croatia," Renewable and Sustainable Energy Reviews, 49, pp. 646-654.
[32] Bhattacharya, M., Paramati, S. R., Ozturk, I., Bhattacharya, S., 2016, "The effect of renewable energy consumption on economic growth: Evidence from top 38 countries," Applied Energy, 162, pp. 733-741.
[33] IEA, International Energy Agency, 2013, "Renewable Energy: Medium-Term Market Report," Paris.
[34] Li, L., Lin, J., Wu, N., Xie, S., Meng, C., Zheng, Y., Wang, X., Zhao, Y., 2020, "Review and Outlook on the International Renewable Energy Development," Energy and Built Environment.

[35] "Statistical Review of World Energy – all data 1965-2019, ," Available from: https://www.bp.com/. [Accessed on: 3 June 2021].
[36] Resch, G., Held, A., Faber, T., Panzer, C., Toro, F., Haas, R., 2008, "Potentials and prospects for renewable energies at global scale," Energy policy, 36(11), pp. 4048-4056.
[37] Eurostat, "Energy intensity (nrg_ind_ei)," Available from: https://appsso.eurostat.ec.europa.eu/nui/show.do?dataset=nrg_ind_ei&lang=en [Accessed on: 3 June 2021].
[38] Xingang, Z., Jieyu, W., Xiaomeng, L., Pingkuo, L., 2012, "China's wind, biomass and solar power generation: What the situation tells us?," Renewable and Sustainable Energy Reviews, 16(8), pp. 6173-6182.
[39] Hajinajaf, N., Mehrabadi, A., Tavakoli, O., 2021, "Practical strategies to improve harvestable biomass energy yield in microalgal culture: A review," Biomass and Bioenergy, 145, p. 105941.
[40] Ullah, K., Ahmad, M., Sharma, Vinod K., Lu, P., Harvey, A., Zafar, M., Sultana, S., 2015, "Assessing the potential of algal biomass opportunities for bioenergy industry: a review," Fuel, 143, pp. 414-423.
[41] Joshi, G., Pandey, J. K., Rana, S., Rawat, D. S., 2017, "Challenges and opportunities for the application of biofuel," Renewable and Sustainable Energy Reviews, 79, pp. 850-866.
[42] Carmona-Cabello, M., Garcia, I. L., Leiva-Candia, D., Dorado, M. P., 2018, "Valorisation of food waste based on its composition through the concept of biorefinery," Current Opinion in Green and Sustainable Chemistry, 14, pp. 67-79.
[43] Gupta, V. G., Tuohy, M., Kubicek, C. P., Saddler, J., Xu, F., 2013, Bioenergy research: advances and applications, Newnes.
[44] Massanet-Nicolau, J., Dinsdale, R., Guwy, A., Shipley, G., 2015, "Utilising biohydrogen to increase methane production, energy yields and process efficiency via two stage anaerobic digestion of grass," Bioresource technology, 189, pp. 379-383.
[45] Hunter, S. M., Blanco, E., Borrion, A. S., 2020, "Expanding the Anaerobic Digestion Map: A Review of Intermediates in the Digestion of Food Waste," Science of The Total Environment, 767, p. 144265.
[46] Uzuh, F. D., Toyoda, H., Matsubara, S., 2019, "Innovation for New Anaerobic Domestic Wastewater Treatment Recycling System in Developing Countries," Int J Water Wastewater Treat, 5(1).
[47] Li, J., Li, C., Zhao, L., Pan, X., Cai, G., Zhu, G., 2020, "The application status, development and future trend of nano-iron materials in anaerobic digestion system," Chemosphere, 269, p. 129389.
[48] Abraham, A., Mathew, A. K., Park, H. Choi, O., Sindhu, R., Parameswaran, B., Pandey, A., Park, J. H., Sang, B. I., 2020, "Pre-treatment strategies for enhanced biogas production from lignocellulosic biomass," Bioresource Technology, 301, p. 122725.
[49] Rajagopal, R., Massé, D. I., Singh, G., 2013, "A critical review on inhibition of anaerobic digestion process by excess ammonia," Bioresource technology, 143, pp. 632-641.
[50] Pereira, E. L., Borges, A. C., Heleno, F. F., de Oliveira, K. R., da Silva, G. J., Mounteer, A. H., 2019, "Central composite rotatable design for startup optimisation of anaerobic sequencing batch reactor treating biodiesel production wastewater," Journal of Environmental Chemical Engineering, 7(3), p. 103038.
[51] Huang, H., Ekama, G. A., Biswal, B. K., Dai, J., Jiang, F., Chen, G. H., Wu, D., 2019, "A new sulfidogenic oxic-settling anaerobic (SOSA) process: the effects of sulfur-cycle

bioaugmentation on the operational performance, sludge properties and microbial communities," Water Research, 162, pp. 30-42.
[52] Hoelzle, R. D., Virdis, B., Batstone, D. J., 2014, "Regulation mechanisms in mixed and pure culture microbial fermentation," Biotechnology and bioengineering, 111(11), pp. 2139-2154.
[53] Mladenović, M., Paprika, M., Marinković, A., 2018, "Denitrification techniques for biomass combustion," Renewable and Sustainable Energy Reviews, 82, pp. 3350-3364.
[54] Xu, C. C., Liao, B., Pang, S., Nazari, L., Mahmood, N., Tushar, M. S., Dutta, A., Ray, M. B., 2018, "1.19 Biomass Energy," Cellulose, 40, p. 50.
[55] Srirangan, K., Akawi, L., Moo-Young, M., Chou, C. P., 2012, "Towards sustainable production of clean energy carriers from biomass resources," Applied energy, 100, pp. 172-186.
[56] Peter, O., Mbohwa, C., 2019, "Renewable Energy Technologies In Brief," Renewable energy technologies in briefInternational Journal of Scientific and Technology 8, pp. 1283-1289.
[57] Levidowa, L., Ramanb, S., 2019, "Metamorphosing waste as a resource: Scaling waste management by ecomodernist means.," Geoforum, 98, pp. 108-122.
[58] European, Commission, 2008, "Directive 2008/98/EC of the European Parliament and of the Council of 19 November 2008 on waste and repealing certain Directives. ."
[59] Karthikeyan, L., Suresh, V. M., Krishnan, V., Tudor, T., Varshini, V., 2018, "The management of hazardous solid waste in India: An overview," Environments, 5(9), p. 103.
[60] Potting, J., Hekkert, M. P., Worrell, E., Hanemaaijer, A., 2017, Circular economy: measuring innovation in the product chain (No. 2544), PBL Publishers.
[61] Kanagamani, K., Geethamani, P., Narmatha, M., 2020, "Hazardous Waste Management," Environmental Change and Sustainability, IntechOpen.
[62] Demirbas, A., 2011, "Waste management, waste resource facilities and waste conversion processes," Energy Conversion and Management, 52(2), pp. 1280-1287.
[63] Lundie, S., Peters, G. M., 2005, "Life cycle assessment of food waste management options," Journal of cleaner production, 13(3), pp. 275-286.
[64] Nunes, L. J., Godina, R., Matias, J. C., Catalão, J. P. , 2018, "Economic and environmental benefits of using textile waste for the production of thermal energy," Journal of Cleaner Production, 171, pp. 1353-1360.
[65] Hu, F., Ragauskas, A., 2012, "Pre-treatment and lignocellulosic chemistry," Bioenergy Research, 5(4), pp. 1043-1066.
[66] Cho, E. J., Trinh, L. T. P., Song, Y., Lee, Y. G., Bae, H. J., 2020, "Bioconversion of biomass waste into high value chemicals," Bioresource technology, 298, p. 122386.
[67] Nunes, L. J. R., Causer, T. P., Ciolkosz, D., 2020, "Biomass for energy: A review on supply chain management models," Renewable and Sustainable Energy Reviews, 120, p. 109658.
[68] Nunes, L. J., Goadina R., Matias, J. C., Catalao, J. P., 2016, "Wood pellets as a sustainable energy alternative in Portugal," Renewable Energy, 85, pp. 1011-1016.
[69] Tiwari, S., Ahmed, W., Sarkar, B., 2018, "Multi-item sustainable green production system under trade-credit and partial backordering," Journal of cleaner production, 204, pp. 82-95.
[70] Suurs, R., 2002, "Long distance bioenergy logistics. An assessment of costs and energy consumption for various biomass energy transport chains (NWS-E--2002-01).", Department of Science, Netherlands.

[71] Nguyen, D. H., Chen, H., 2018, "Supplier selection and operation planning in biomass supply chains with supply uncertainty," Computers & Chemical Engineering, 118, pp. 103-117.
[72] Murphy, F., Devlin, G., McDonnell, K., 2014, "Forest biomass supply chains in Ireland: A life cycle assessment of GHG emissions and primary energy balances," Applied Energy, 116, pp. 1-8.
[73] Muscat, A., de Olde, E. M., De Boer, I. J., Ripoll-Bosch, R., 2019, "The battle for biomass: A systematic review of food-feed-fuel competition," Global Food Security, 25, p. 100330.
[74] Scherhaufer, S., Moates, G., Hartikainen, H., Waldron, K., Obersteiner, G., 2018, "Environmental impacts of food waste in Europe," Waste management, 77, pp. 98-113.
[75] Dale, V. H., Kline, K. L., Wright, L. L., Perlack, R. D., Downing, M., Graham, R. L., 2011, "Interactions among bioenergy feedstock choices, landscape dynamics, and land use," Ecological Applications, 21(4), pp. 1039-1054.
[76] Wang, T., Zhai, Y., Zhu, Y., Li, C., Zeng, G., 2018, "A review of the hydrothermal carbonisation of biomass waste for hydrochar formation: Process conditions, fundamentals, and physicochemical properties," Renewable and Sustainable Energy Reviews, 90, pp. 223-247.
[77] Zhang, X., Burchell, J., Mosier, N. S., 2018, "Enzymatic Epoxidation of High Oleic Soybean Oil," ACS Sustainable Chemistry & Engineering, 6(7), pp. 8578-8583.
[78] Akhtar, J., Amin, N. A. S., 2011, "A review on process conditions for optimum bio-oil yield in hydrothermal liquefaction of biomass," Renewable and Sustainable Energy Reviews, 15(3), pp. 1615-1624.
[79] Mehariya, S., Patel, A. K., Obulisamy, P. K., Punniyakotti, E., Wong, J. W., 2018, "Co-digestion of food waste and sewage sludge for methane production: Current status and perspective," Bioresource technology, 265, pp. 519-531.
[80] Kiran, E. U., Trzcinski, A. P., Ng, W. J., Liu, Y., 2014, "Bioconversion of food waste to energy: a review," Fuel, 134, pp. 389-399.
[81] Scharff, H., Van Zomeren, A., Van der Sloot, H. A., 2011, "Landfill sustainability and aftercare completion criteria," Waste Management & Research, 29(1), pp. 30-40.
[82] Lundqvist, J., Unver, O., 2018, "Alternative pathways to food security and nutrition–water predicaments and human behavior," Water Policy, 20(5), pp. 871-884.
[83] Fisgativa, H., Tremier, A., Taher, H., Saoudi, M., Le Roux, S., Dabert, P., 2018, "Biochemical and microbial changes reveal how aerobic pre-treatment impacts anaerobic biodegradability of food waste," Waste management, 80, pp. 119-129.
[84] Sharma, B., Sarkar, A., Singh, P., Singh, R. P., 2017, "Agricultural utilisation of biosolids: A review on potential effects on soil and plant grown," Waste Management, 64, pp. 117-132.
[85] Salemdeeb, R., Vivanco, D. F., Al-Tabbaa, A., Zu Ermgassen, E. K., 2017, "A holistic approach to the environmental evaluation of food waste prevention," Waste management, 59, pp. 442-450.
[86] Banu, J. R., Merrylin, J., Usman, T..M., Kannah, R. Y., Gunasekaran, M., Kim, S. H., Kumar, G., 2019, "Impact of pre-treatment on food waste for biohydrogen production: A review," International Journal of Hydrogen Energy, 45(36), pp. 18211-18225.
[87] Lukic, R., Kljenak, D. V., Jovancevic, D., 2014, "Retail food waste management," Management Research and Practice, 6(4), p. 23.

[88] Filimonau, V., Gherbin, A., 2017, "An exploratory study of food waste management practices in the UK grocery retail sector," Journal of Cleaner Production, 167, pp. 1184-1194.
[89] Stenmarck, Â., Jensen, C., Quested, T., Moates, G., Buksti, M., Cseh, B., Juul, S., Parry, A., Politano, A., Redlingshofer, B., 2016, "Estimates of European food waste levels. IVL Swedish Environmental Research Institute," Public Wageningen Food & Biobased Research-Report. , 2102, p. 39.
[90] Chen, C. R., Chen, R. J., 2018, "Using Two Government Food Waste Recognition Programs to Understand Current Reducing Food Loss and Waste Activities in the US," Sustainability, 10(8), p. 2760.
[91] Buzby, J. C., Bentley, J. T., Padera, B., Ammon, C., Campuzano, J., 2015, "Estimated fresh produce shrink and food loss in US supermarkets," Agriculture, 5(3), pp. 626-648.
[92] Caldeira, C., De Laurentiis, V., Corrado, S., van H., F., Sala, S., 2019, "Quantification of food waste per product group along the food supply chain in the European Union: a mass flow analysis," Resources, Conservation and Recycling, 149, pp. 479-488.
[93] FoodCloud., "The Problem," Available online: https://food.cloud/the-problem/ [Accessed on 28 August 2021].
[94] Whitman, E., 2016, "Oil-Rich Saudi Arabia Wastes Astounding $35 Million In Food Every Day," Available from: https://www.ibtimes.com/oil-rich-saudi-arabia-wastes-astounding-35-million-food-every-day-2282137 [Accessed on: 4 June 2021].
[95] Balkhi, K., 2018, "Ideas to chew on: how to end food waste in Saudi Arabia. The National. ," Available from: www.thenational.ae/business/ideas-to-chew-on-how-to-end-food-waste-in-saudi-arabia-1.705509 [Accessed on: 4 June 2021].
[96] Baig, M. B., Al-Zahrani, K. H., Schneider, F., Straquadine, G. S., Mourad, M., 2019, "Food waste posing a serious threat to sustainability in the Kingdom of Saudi Arabia–A systematic review," Saudi journal of biological sciences, 26(7), pp. 1743-1752.
[97] Ishangulyyev, R., Kim, S., Lee, S. H., 2019, "Understanding food loss and waste—Why are we losing and wasting food?," Foods, 8(8), p. 297.
[98] UN., "Goal 2: Zero Hunger," Available from: https://www.un.org/sustainabledevelopment/hunger/ [Accessed on: 4 June 2021].
[99] Pinto, R. S., dos Santos Pinto, R. M., Melo, F. F., Campos, S. S., Cordovil, C. M., 2018, "A simple awareness campaign to promote food waste reduction in a University canteen," Waste management, 76, pp. 28-38.
[100] Lang, L., Wang, Y., Chen, X., Zhang, Z., Yang, N., Xue, B., Han, W., 2020, "Awareness of food waste recycling in restaurants: evidence from China," Resources, Conservation and Recycling, 161, p. 104949.
[101] Septianto, F., Kemper, J. A., Northey, G., 2020, "Thanks, but no thanks: The influence of gratitude on consumer awareness of food waste," Journal of Cleaner Production, 258, p. 120591.
[102] Alrefai, R., Alrefai, A. M., Benyounis, K. Y., Stokes, J., 2017, "Integration approach of anaerobic digestion and fermentation process towards producing biogas and bioethanol with zero waste: technical," J. Fundam. Renew. Energy Appl, 7(6), p. 243.
[103] Makris, D. P., Şahin, S., 2019, "Polyphenolic Antioxidants from Agri-Food Waste Biomass," Antioxidants, 8(12), p. 642.
[104] Swedan., N., 2020, "Deforestation and land farming as regulators of population size and climate," Acta Ecologica Sinica, 40, pp. 443-450.

[105] Lewis., S. L., Edwards, D. P., Galbraith, D., 2015, "Increasing human dominance of tropical forests," Science, 349(6250), pp. 827-832.
[106] Armenteras, D., Espelta, J. M., Rodríguez, N., Retana, J., 2017, "Deforestation dynamics and drivers in different forest types in Latin America: Three decades of studies (1980–2010)," Global Environmental Change, 46, pp. 139-147.
[107] Watson, J. E., Dudley, N., Segan, D. B., Hockings, M., 2014, "The performance and potential of protected areas," Nature, 515(7525), pp. 67-73.
[108] Tegegne, Y. T., Lindner, M., Fobissie, K., Kanninen, M., 2016, "Evolution of drivers of deforestation and forest degradation in the Congo Basin forests: Exploring possible policy options to address forest loss," Land use policy, 51, pp. 312-324.
[109] Jayathilake, H. M., Prescott, G. W., Carrasco, L. R., Rao, M., Symes, W. S., 2021, "Drivers of deforestation and degradation for 28 tropical conservation landscapes," Ambio, 50, pp. 215-228.
[110] Yaap, B., Struebig, M. J., Paoli, G., Koh, L. P., 2010, "Mitigating the biodiversity impacts of oil palm development," CAB Reviews, 5(19), pp. 1-11.
[111] Hansen, S. B., Padfield, R., Syayuti, K., Evers, S., Zakariah, Z., Mastura, S., 2015, "Trends in global palm oil sustainability research," Journal of cleaner Production, 100, pp. 140-149.
[112] Jamaludin, N. F., Ab Muis, Z., Hashim, H., 2019, "An integrated carbon footprint accounting and sustainability index for palm oil mills," Journal of Cleaner Production, 225, pp. 496-509.
[113] Saswattecha, K., Kroeze, C., Jawjit, W., Hein, L., 2015, "Assessing the environmental impact of palm oil produced in Thailand," Journal of cleaner production, 100, pp. 150-169.
[114] Permpool, N., Bonnet, S., Gheewala, S. H., 2016, "Greenhouse gas emissions from land use change due to oil palm expansion in Thailand for biodiesel production," Journal of Cleaner Production, 134, pp. 532-538.
[115] Gérard, A., Wollni, M., Hölscher, D., Irawan, B., Sundawati, L., Teuscher, M., Kreft, H., 2017, "Oil-palm yields in diversified plantations: Initial results from a biodiversity enrichment experiment in Sumatra, Indonesia," Agriculture, Ecosystems & Environment, 240, pp. 253-260.
[116] Rivera-Méndez, Y. D., Rodríguez, D. T., Romero, H. M., 2017, "Carbon footprint of the production of oil palm (Elaeis guineensis) fresh fruit bunches in Colombia," Journal of cleaner production, 149, pp. 743-750.
[117] Ayompe, L. M., Schaafsma, M., Egoh, B. N., 2020, "Towards sustainable palm oil production: The positive and negative impacts on ecosystem services and human wellbeing," Journal of Cleaner Production, 278, p. 123914.
[118] McCarthy, J. F., 2010, "Processes of inclusion and adverse incorporation: oil palm and agrarian change in Sumatra, Indonesia," The Journal of peasant studies, 37(4), pp. 821-850.
[119] Li, T. M., 2015, Social impacts of oil palm in Indonesia: A gendered perspective from West Kalimantan (Vol. 124), CIFOR.
[120] Bourgis, F., Kilaru, A., Cao, X., Ngando-Ebongue, G.F., Drira, N., Ohlrogge, J. B., Arondel, V., 2011, "Comparative transcriptome and metabolite analysis of oil palm and date palm mesocarp that differ dramatically in carbon partitioning," Proceedings of the National Academy of Sciences, 108(30), pp. 12527-12532.
[121] 2014, " Rainforest News Observatory on world's natural forests ", Available from: https://www.salvaleforeste.it/en/deforestation-blog/3787-deforestation-in-saudi-arabia.html [Accessed on: 4 June 2021].

[122] Aronson, J., Aronson, T. B., Patzelt, M. A., Knees, S., Lewis, G., Lupton, D., Taifour, H., Gardner, M. F., Thompson, H., Al Hatmi, S., Al Khulaidi, A. W., 2016, "Paleorelicts or archaeophytes: enigmatic trees in the Middle East," Journal of Arid Environments 137, pp. 69-82.
[123] Al-Namazi, A. A., Al-Khulaidi, A. W. A., Al-Turki, T., Algarni, S., Al-Sagheer, N. A., 2021, "Natural plant species inventory of hotspot areas in Arabian Peninsula: Southwest Al-Baha region Saudi Arabia," Saudi Journal of Biological Sciences.
[124] Britannica., 2019, ""Date palm"," Available from: https://www.britannica.com/plant/date-palm [accessed on 4 June 2021].
[125] Pennisi, E., 2015, "Researchers solve mystery of the mutated oil palms," Available from: Available from: https://www.sciencemag.org/news/2015/09/researchers-solve-mystery-mutated-oil-palms [accessed on 4 June 2021].
[126] Teixeira, E., Pasquini, D., Curvelo, A., Corradini, E., Belgacem, M., Dufresne, A., 2009, "Cassava bagasse cellulose nanofibrils reinforced thermoplastic cassava starch," Carbohydrate Polymers, 87, pp. 422-431.
[127] Sawyerr, N., Trois, N., Workneh, T., Okudoh, V., 2017, "Co-Digestion of Animal Manure and Cassava Peel for Biogas Production in South Africa," 9th Int'l Conference on Advances in Science, Engineering, Technology & Waste Management (ASETWM-17)Parys, South Africa, pp. 101-106.
[128] Kuiper, L., Ekmekci, B., Hamelinck, C., Hettinga, W., Meyer, S., Koop, K., 2007, "Bio-ethanol from cassava," Ecofys Netherlands BV, 3, pp. 1-38.
[129] Okudoh, V., Trois, C., Workneh, T., Schmidt, S., 2014, "The potential of cassava biomass and applicable technologies for sustainable biogas production in South Africa: A review," Renewable and Sustainable Energy Reviews, 39, pp. 1035-1052.
[130] DAFF, S. A., 2010, "Cassava production guidline. Pretoria, South Africa: service of department of agriculture."
[131] Ghimire, A., , Sen, R., Annachhatre, A., 2015, "Biosolid Management Options in Cassava Starch Industries of Thailand: Present Practice and Future Possibilities," Procedia Chemistry, 14, pp. 66-75.
[132] Sivamani, S., Chandrasekaran, A., Balajii, M., Shanmugaprakash, M., 2018, "Evaluation of the potential of cassava-based residues for biofuels production," Reviews in Environmental Science and Bio/Technology, 17(3), pp. 553-570.
[133] Aro, S., Aletor, V., Tewe, O., Agbede, J., 2010, "Nutritional potentials of cassava tuber wastes: A case study of a cassava starch processing factory in south-western Nigeria," Livestock Research for Rural Development, 22(11), pp. 42-47.
[134] Obadina, O., Oyewole, B., Sanni, O., Abiola, S., 2006, "Fungal enrichment of cassava peels proteins," African Journal of Biotechnology 5(3), pp. 302-304.
[135] Ezekiel O, Aworh O., 2018, "Simultaneous saccharification and cultivation of Candida utilis on cassava peel," Innovative Food Science and Emerging Technologies, 49, pp. 184-191.
[136] Sivamania, S., Archanaa, K., Santhosha, R., Sivarajasekara, N., Prasad, N. , 2018, "Synthesis and characterisation of starch nanoparticles from cassava Peel," Journal of Bioresources and Bioproducts, 3(4), pp. 161-165.
[137] Okoroigw, E., Ofomatah, A., Oparaku, N., 2013, "Biodigestion of cassava peels blended with pig dung for methane generation," African Journal of Biotechnology, 12(40), pp. 5956-5961.

[138] Albokari, M., 2013, "Acclimation of Cassava in Saudi Arabia," Wulfenia, 20(10), pp. 368-381.
[139] TRIDGE, 2019, Available from: https://www.tridge.com/products/mandioca/import/SA [Accessed on: 4 June 2021].
[140] Khan, A. J., Akhtar, S., Al-Matrushi, A.M., Fauquet, C. M., Briddon, R. W., 2013, "Introduction of East African cassava mosaic Zanzibar virus to Oman harks back to "Zanzibar, the capital of Oman"," Virus genes, 46(1), pp. 195-198.
[141] Nkodi, T., Taba, K., Sungula, J., Mulaji, C., Mihigo, S., 2016, "Biogas Production by Co-Digestion of Cassava Peels with Urea," International Journal of Scientific Engineering and Technology, 5(3), pp. 139-141.
[142] Jekayinfa, S., Scholz, V., 2013, "Laboratory Scale Preparation of Biogas from Cassava Tubers, Cassava Peels, and Palm Kernel Oil Residues," Energy Sources, Part A: Recovery, Utilisation, and Environmental Effects, 35(21), pp. 2022-2032.
[143] AbdElgawad, H., Saleh, A. M., Al Jaouni, S., Selim, S., Hassan, M. O., Wadaan, M. A., Shuikan, A. M., Mohamed, H. S., Hozzein, W. N., 2019, "Utilisation of actinobacteria to enhance the production and quality of date palm (Phoenix dactylifera L.) fruits in a semi-arid environment," Science of The Total Environment, 665, pp. 690-697.
[144] Nasiri, A., Taheri-Garavand, A., Zhang, Y. D., 2019, "Image-based deep learning automated sorting of date fruit," Postharvest Biology and Technology, 153, pp. 133-141.
[145] Al-MSSalleM, M. Q., 2020, "The Role of Date Palm Fruit in Improving Human Health," Journal of Clinical & Diagnostic Research, 14(1), pp. 1-6.
[146] Al-MSSalleM, M. Q., 2020, "The Role of Date Palm Fruit in Improving Human Health," Journal of Clinical & Diagnostic Research, 14(1).
[147] Hossain, M. S., Muhammad, G., Amin, S. U., 2018, "Improving consumer satisfaction in smart cities using edge computing and caching: A case study of date fruits classification," Future Generation Computer Systems, 88, pp. 333-341.
[148] Ghnimi, S., Umer, S., Karim, A., Kamal-Eldin, A., 2017, "Date fruit (Phoenix dactylifera L.): An underutilised food seeking industrial valorisation," NFS journal, 6, pp. 1-10.
[149] Lockwood, R., 2013, "Dates: Production, Processing, Food, and Medicinal Values (Medicinal and Aromatic Plants–Industrial Profiles). Edited by A. Manickavasagan, MM Essa and E. Sukumar. Boca Raton, FL, USA: CRC Press (2012), pp. xviii+ 415,£ 89.00. ISBN 978-1-4398-4945-3," Experimental Agriculture, 49(1), pp. 153-153.
[150] Abdulsada, S. A., Al-Mosawi, A. I., Hashim, A. A., 2018, "Date Waste as Environmentally Friendly Composites," Journal of Materials & Metallurgical Engineering, 8(1), pp. 25-30.
[151] Najafi, M. B., 2011, "Date seeds: a novel and inexpensive source of dietary fiber," Proc. International Conference on Food Engineering and Biotechnology, IPCBEF, pp. 323-326.
[152] Mirghani, M. E., 2012, "Processing of date palm kernel (DPK) for production of nutritious drink," Advances in Natural Applied Sciences, 6(5), pp. 575-582.
[153] Alsewailem, F. D., Binkhder, Y. A., 2010, "Preparation and characterisation of polymer/date pits composites," Journal of Reinforced Plastics and Composites, 29(11), pp. 1743-1749.
[154] Mrabet, A., Jiménez-Araujo, A., Guillén-Bejarano, R., Rodríguez-Arcos, R., Sindic, M., 2020, "Date seeds: A promising source of oil with functional properties," Foods, 9(6), p. 787.

[155] Ali, M. A., Al-Hattab, T. A., Al-Hydary, I. A., 2015, "Extraction of date palm seed oil (Phoenix dactylifera) by Soxhlet apparatus," International Journal of Advances in Engineering & Technology, 8(3), p. 261.
[156] Elnajjar, E., Hasan, S., Alnaqbi, A. H., Al Omari, S. A., Al-Zuhair, S., 2018, "Optimising the Extraction of Oils from Date Seeds for Biodiesel Production," International Journal of Environmental Research, 12(1), pp. 101-108.
[157] Azeem, M. W., Hanif, M. A., Al-Sabahi, J. N., Khan, A. A., Naz, S., Ijaz, A., 2016, "Production of biodiesel from low priced, renewable and abundant date seed oil," Renewable energy, 86, pp. 124-132.
[158] Ala'a, H., Jamil, F., Al-Haj, L., Myint, M. T., Mahmoud, E., Ahmad, M. N., Hasan, A. O., Rafiq, S., 2018, "Biodiesel production over a catalyst prepared from biomass-derived waste date pits," Biotechnology Reports, 20, p. e00284.
[159] Al-Farsi, M. A., Lee, C. Y., 2011, "Usage of date (Phoenix dactylifera L.) seeds in human health and animal feed," Nuts and seeds in health and disease prevention, Elsevier, pp. 447-452.
[160] Radeef, W., Shanableh, A., Merabtene, T., "Biogas production through co-digestion of date palm seeds and wastewater treatment sludge," Proc. The 2015 International Conference on Water, Energy, and the Environment.
[161] Gupta, N., Kushwaha, H., 2011, "Date palm as a source of bioethanol producing microorganisms," Date Palm Biotechnology, Springer, pp. 711-727.
[162] Hussain, A., Farooq, A., Bassyouni, M. I., Sait, H. H., El-Wafa, M. A., Hasan, S. W., Ani, F. N., 2014, "Pyrolysis of Saudi Arabian date palm waste: A viable option for converting waste into wealth," Life Science Journal, 11(12), pp. 667-671.
[163] Kriker, A., Debicki, G., Bali, A., Khenfer, M. M., Chabannet, M., 2005, "Mechanical properties of date palm fibres and concrete reinforced with date palm fibres in hot-dry climate," Cement and Concrete Composites, 27(5), pp. 554-564.
[164] Augustia, V., Chafidz, A., Chafidz, A., Setyaningsih, L., Rizal, M., Kaavessina, M., Al Zahrani, S. M., 2018, "Effect of Date Palm Fiber Loadings on the Mechanical Properties of High Density Polyethylene/Date Palm Fiber Composites," Key Engineering Materials, 773, pp. 94-99.
[165] Besbes, S., Drira, L., Blecker, C., Deroanne, C., Attia, H., 2009, "Adding value to hard date (Phoenix dactylifera L.): compositional, functional and sensory characteristics of date jam," Food chemistry, 112(2), pp. 406-411.
[166] FAOSTAT, 2019, "The Food and Agriculture Organisation (FAO). FAOSTAT-FAO Statics Division – Production Quantity/Plywood.," Available from: http://www.fao.org/faostat/en/ - data/FO [Accessed on: 7 June 2021].
[167] Lattieff, F. A., 2016, "A study of biogas production from date palm fruit wastes," Journal of cleaner production, 139, pp. 1191-1195.
[168] Shafiei, M., Karimi, K., Taherzadeh, M. J., 2010, "Palm date fibers: analysis and enzymatic hydrolysis," International journal of molecular sciences, 11(11), pp. 4285-4296.
[169] Al-Khayri, J. M., Jain, S. M., Johnson, D. V., 2015, Date palm genetic resources and utilisation, (Vol. 1). Africa and the Americas: Springer.
[170] FAOSTAT., 2012, "Food and Agricultural Organisation of the United nations.," Available from: http://www.fao.org/faostat/en/? - data/QC, [Accessed on: 4 June 2021].
[171] "Statistical Year Book, Ministry of agriculture, Vol. 52. Kingdom of Saudi Arabia. 2016.," Available from:

https://www.mewa.gov.sa/ar/InformationCenter/Researchs/StaticticsData/Pages/default.aspx [Accessed on: 4 June 2021].
[172] "King Saud University, Date exports in Saudi Arabia in 2019 reached 230 million USD.," Available from: https://news.ksu.edu.sa/en/node/133022 [Accessed on: 4 June 2021].
[173] El-Juhany, L. I., 2010, "Degradation of date palm trees and date production in Arab countries: causes and potential rehabilitation," Australian Journal of Basic and Applied Sciences, 4(8), pp. 3998-4010.
[174] "Ministry of Agriculture (2011) Twenty-fourth statistical yearbook. Total estimated of agricultural crops area and production in Saudi Arabia: estimated area and production of dates crop by region in Saudi Arabia. Department of Economic Studies and Statistics, Ministry of Agriculture, Riyadh, Saudi Arabia, pp 68–70."
[175] "Statistical Year Book, Ministry of agriculture, Kingdom of Saudi Arabia. 2019.," Available from: https://www.mewa.gov.sa/ar/InformationCenter/Researchs/Reports/Pages/default.aspx [Accessed on: 4 June 2021].
[176] Aleid, S. M., Al-Khayri, J. M., Al-Bahrany, A. M., 2015, "Date palm status and perspective in Saudi Arabia," Date palm genetic resources and utilisation, Springer, pp. 49-95.
[177] Assirey, E. A., 2015, "Nutritional composition of fruit of 10 date palm (Phoenix dactylifera L.) cultivars grown in Saudi Arabia," Journal of Taibah University for science, 9(1), pp. 75-79.
[178] "The Iraqi Network for Date Palm," Available from: https://www.iraqi-datepalms.net/assets/uploads/2018/09/Tamor1.pdf [Accseed on: 4 June 2021].
[179] Marib, N. R., Feryal, H. M. S., Essam, F. J., 2009, "Purification and Characterisation of protease from Zahdi dates plam seeds (Phoenix dactylifera L.)," Majallat Baghdād lil-ʻulūm, Journal Baghdad Science, 6(4), pp. 633-639.
[180] AlManhal, J. M., 2007, "Preparation of powdered date juice (molasses) from Al-Zuhdi dates and studying its qualities," Basra Research Journal (Al-Alamiat), University of Basra, Iraq, 33(2B), pp. 30-36.
[181] Shanableh, A., Radeef, W., 2017, "Biogas production from raw and oil-spent date palm seeds mixed with wastewater treatment sludge," Biofuels, 11(6), pp. 1-8.
[182] Sabbagh, S., 2014, "Biological, physical and chemical analyses of salvation dates by radiation As alternatives to fumigants and heat treatments.," University of Aleppo Research Journal, 98, pp. 1-14.
[183] Jaafar, K. A., 2010, "Biogas production by anaerobic digestion of date palm pulp waste," Al-Khwarizmi Engineering Journal, 6(3), pp. 14-20.
[184] Ventura, J. R. S., Yang, B., Lee, Y. W., Lee, K., Jahng, D., 2013, "Life cycle analyses of CO_2, energy, and cost for four different routes of microalgal bioenergy conversion," Bioresource technology, 137, pp. 302-310.
[185] Milledge, J. J., Heaven, S., 2014, "Methods of energy extraction from microalgal biomass: a review," Reviews in Environmental Science and Bio/Technology, 13(3), pp. 301-320.
[186] Milledge, J., Patricia, H., 2018, "Anaerobic digestion and gasification of seaweed," Grand Challenges in Marine Biotechnology, P.H., Rampelotto and A. Trincone, ed.Spinger International Publishing.

[187] Vanegas, C., Bartlett, J., 2013, "Green energy from marine algae: biogas production and composition from the anaerobic digestion of Irish seaweed species," Environmental Technology, 34(15), pp. 2277-2283.
[188] Monlau, F., Sambusiti, C. Barakat, A., Quéméneur, M. Trably, E., Steyer, J. P., Carrère, H., 2014, "Do furanic and phenolic compounds of lignocellulosic and algae biomass hydrolysate inhibit anaerobic mixed cultures? A comprehensive review," Biotechnology Advances, 32, pp. 934-951.
[189] Samaras, V. G., Mathiopoulou, A. I., Sirigou, I. E., Stasinakis, A. S., Lekkas T.D., 2012, "Comparison Of Mesophilic And Thermophilic Sludge Anaerobic Digestion: Role Of Sludge Retention Time, Reactor's Configuration And Sonolysis Pre-Treatment On Process Performance," 3RD International Conference on industrial and Hazardous Waste Management (CRETE 2012), Techn. Univ. of Crete, Chania.
[190] Mao, C., Feng, Y., Wang, X., Ren, G., 2015, "Review on research achievements of biogas from anaerobic digestion," Renewable and Sustainable Energy Reviews, 45, pp. 540-555.
[191] Bowen, E. J., Dolfing, J., Davenport, R. J., Read, F. L., Curtis, T. P., 2014, "Low-temperature limitation of bioreactor sludge in anaerobic treatment of domestic wastewater," Water Science & Technology, 69(5), pp. 1004-1013.
[192] Fisgativa, H., Tremier, A., "Influence of food waste characteristics variations on treatability through an-aerobic digestion," Proc. 16th International Conference: Rural-Urban Symbiosis, RAMIRAN 2015, p. 4.
[193] Yin, Y., Liu, Y. J., Meng, S. J., Kiran, E. U., Liu, Y., 2016, "Enzymatic pre-treatment of activated sludge, food waste and their mixture for enhanced bioenergy recovery and waste volume reduction via anaerobic digestion," Applied Energy, 179, pp. 1131-1137.
[194] Kwietniewska, E., Tys, J., 2014, "Process characteristics, inhibition factors and methane yields of anaerobic digestion process, with particular focus on microalgal biomass fermentation," Renewable and Sustainable Energy Reviews, 34, pp. 491-500.
[195] Møller, J., Boldrin, A., Christensen, T. H., 2009, "Anaerobic digestion and digestate use:Accounting of greenhouse gases and global warming contribution," Waste Management & Research, 27, pp. 813-824.
[196] Lia, Y., Chena, Y., Wuc, J., 2019, "Enhancement of methane production in anaerobic digestion process: A review," Applied Energy, 240, pp. 120-137.
[197] Wua, C., , Huanga, Q., Yua, M., Rena, Y., Wanga, Q. Sakaic, K., 2018, "Effects of digestate recirculation on a two-stage anaerobic digestion system, particularly focusing on metabolite correlation analysis," Bioresource Technology, 251, pp. 40-48.
[198] Fagbohungbe, M. O., Herbert, B. M., Hurst, L., Ibeto, C. N., Li, H., Usmani, S. Q.,, and Semple, K. T., 2017, "The challenges of anaerobic digestion and the role of biochar in optimising anaerobic digestion," Waste management, 61, pp. 236-249.
[199] Rudolfs, W., Amberg, H. R., 1952, "White Water Treatment: I. Factors Affecting Anaerobic Digestion," Sewage and Industrial Wastes, pp. 1108-1120.
[200] Vaneeckhaute, C., Meers, E., Michels, E., Ghekiere, G., Accoe, F., Tack, F. M. , 2013, "Closing the nutrient cycle by using bio-digestion waste derivatives as synthetic fertiliser substitutes: A field experiment," Biomass and Bioenergy, 55, pp. 175-189.
[201] Batstone, D. J., Hülsen, T., Mehta, C. M., Keller, J., 2015, "Platforms for energy and nutrient recovery from domestic wastewater: A review," Chemosphere, 140, pp. 2-11.

[202] Ai, P., Chen, M., Ran, Y., Jin, K., Peng, J., Abomohra, A. E. F., 2020, "Digestate recirculation through co-digestion with rice straw: Towards high biogas production and efficient waste recycling," Journal of Cleaner Production, 263, p. 121441.
[203] Gonzalez-Fernandez, C., Sialve, B., , and Molinuevo-Salces, B., 2015, "Anaerobic digestion of microalgal biomass: challenges, opportunities and research needs," Bioresource technology, 198, pp. 896-906.
[204] Lee, H. V., Hamid, S. B., Zain, S. K., 2014, "Conversion of lignocellulosic biomass to nanocellulose: structure and chemical process," The Scientific World Journal, 2014, p. 631013.
[205] Patinvoh, R. J., Osadolor, O. A., Chandolias, K., Horváth, I. S., Taherzadeh, M. J., 2017, "Innovative pre-treatment strategies for biogas production," Bioresource technology, 224, pp. 13-24.
[206] Karuppiah, T., Azariah, V. E., 2019, "Biomass pre-treatment for enhancement of biogas production," Anaerobic Digestion, IntechOpen.
[207] Şahinkaya, S., Sevimli, M. F., 2013, "Sono-thermal pre-treatment of waste activated sludge before anaerobic digestion," Ultrasonics sonochemistry, 20(1), pp. 587-594.
[208] Karouach, F., Bakraoui, M., El Gnaoui, Y., Lahboubi, N., El Bari, H., 2020, "Effect of combined mechanical–ultrasonic pre-treatment on mesophilic anaerobic digestion of household organic waste fraction in Morocco," Energy Reports, 6, pp. 310-314.
[209] Singh, A., Sevda, S., Abu Reesh, I. M., Vanbroekhoven, K., Rathore, D., Pant, D., 2015, "Biohydrogen production from lignocellulosic biomass: technology and sustainability," Energies, 8(11), pp. 13062-13080.
[210] Rouches, E., Dignac, M. F., Zhou, S., Carrere, H., 2017, "Pyrolysis-GC–MS to assess the fungal pre-treatment efficiency for wheat straw anaerobic digestion," Journal of Analytical and Applied Pyrolysis, 123, pp. 409-418.
[211] Rouches, E., Herpoël-Gimbert, I., Steyer, J. P., Carrere, H., 2016, "Improvement of anaerobic degradation by white-rot fungi pre-treatment of lignocellulosic biomass: a review," Renewable and Sustainable Energy Reviews, 59, pp. 179-198.
[212] Gumisiriza, R., Hawumba, J. F., Okure, M., Hensel, O., 2017, "Biomass waste-to-energy valorisation technologies: a review case for banana processing in Uganda," Biotechnology for biofuels, 10(1), p. 11.
[213] Montingelli, M. E., Benyounis, K. Y., Stokes, J., Olabi, A. G., 2016, "Pre-treatment of macroalgal biomass for biogas production," Energy conversion and management, 108, pp. 202-209.
[214] Reilly, M., Dinsdale, R., Guwy, A., 2015, "Enhanced biomethane potential from wheat straw by low temperature alkaline calcium hydroxide pre-treatment," Bioresource technology, 189, pp. 258-265.
[215] Tumutegyereize, P., Muranga, F. I., Kawongolo, J., Nabugoomu, F., 2011, "Optimisation of biogas production from banana peels: effect of particle size on methane yield," African Journal of Biotechnology, 10(79), pp. 18243-18251.
[216] Kumar, R., Strezov, V., Weldekidan, H., He, J., Singh, S., Kan, T., Dastjerdi, B., 2020, "Lignocellulose biomass pyrolysis for bio-oil production: A review of biomass pre-treatment methods for production of drop-in fuels," Renewable and Sustainable Energy Reviews, 123, p. 109763.

[217] Alvira, P., Tomás-Pejó, E., Ballesteros, M., Negro, M. J. , 2010, "Pre-treatment technologies for an efficient bioethanol production process based on enzymatic hydrolysis: a review," Bioresource technology, 101(13), pp. 4851-4861.
[218] Palmowski, L. M., Müller, J .A., 2000, "Influence of the size reduction of organic waste on their anaerobic digestion," Water science and technology, 41(3), pp. 155-162.
[219] Baruah, J., Nath, B. K., Sharma, R., Kumar, S., Deka, R. C., Baruah, D. C., Kalita, E., 2018, "Recent trends in the pre-treatment of lignocellulosic biomass for value-added products," Frontiers in Energy Research, 6, p. 141.
[220] Mshandete, A., Björnsson, L., Kivaisi, A. K., Rubindamayugi, S. T., Mattiasson, B., 2005, "Enhancement of anaerobic batch digestion of sisal pulp waste by mesophilic aerobic pre-treatment," Water Research, 39(8), pp. 1569-1575.
[221] Karthikeyan, O. P., Trably, E., Mehariya, S., Bernet, N., Wong, J. W., , and Carrere, H., 2018, "Pre-treatment of food waste for methane and hydrogen recovery: a review," Bioresource technology, 249, pp. 1025-1039.
[222] Shah, F. A., Mahmood, Q., Rashid, N., Pervez, A., Raja, I. A., Shah, M. M., 2015, "Co-digestion, pre-treatment and digester design for enhanced methanogenesis," Renewable and Sustainable Energy Reviews, 42, pp. 627-642.
[223] Zhu, J. Y., Wang, G. S., Pan, X. J., Gleisner, R., 2009, "Specific surface to evaluate the efficiencies of milling and pre-treatment of wood for enzymatic saccharification," Chemical Engineering Science, 64(3), pp. 474-485.
[224] Aboderheeba, A. K., 2013, "Novel Approach to Pre-treatment of Agricultural Products and Food Waste to Improve Biogas Production," Doctor of Philosophy, Dublin City University
[225] Rodriguez, C., Alaswad, A., El-Hassan, Z., Olabi, A. G., 2017, "Mechanical pre-treatment of waste paper for biogas production," Waste Management, 68, pp. 157-164.
[226] Tedesco, S., Barroso, T. M., Olabi, A. G., 2014, "Optimisation of mechanical pre-treatment of Laminariaceae spp. biomass-derived biogas," Renewable Energy, 62, pp. 527-534.
[227] Neshat, S. A., Mohammadi, M., Najafpour, G. D., Lahijani, P., 2017, "Anaerobic co-digestion of animal manures and lignocellulosic residues as a potent approach for sustainable biogas production," Renewable and Sustainable Energy Reviews, 79, pp. 308-322.
[228] Palmowski, L. M., Müller, J. A., 2003, "Anaerobic degradation of organic materials-significance of the substrate surface area," Water science and technology, 47(12), pp. 231-238.
[229] Vidal, B. C., Dien, B. S., Ting, K. C., Singh, V., 2011, "Influence of feedstock particle size on lignocellulose conversion—a review," Applied biochemistry and biotechnology, 164(8), pp. 1405-1421.
[230] Sun, Y., Cheng, J., 2002, "Hydrolysis of lignocellulosic materials for ethanol production: a review," Bioresource technology, 83(1), pp. 1-11.
[231] Maurya, D. P., Singla, A., Negi, S., 2015, "An overview of key pre-treatment processes for biological conversion of lignocellulosic biomass to bioethanol," 3 Biotech, 5(5), pp. 597-609.
[232] Silva, G. G., Couturier, M., Berrin, J. G., Buléon, A., Rouau, X., 2012, "Effects of grinding processes on enzymatic degradation of wheat straw," Bioresource technology, 103(1), pp. 192-200.

[233] Dahunsi, S. O., 2019, "Mechanical pre-streatment of lignocelluloses for enhanced biogas production: Methane yield prediction from biomass structural components," Bioresource technology, 280, pp. 18-26.
[234] Tsapekos, P., Kougias, P. G., Angelidaki, I., 2018, "Mechanical pre-treatment for increased biogas production from lignocellulosic biomass; predicting the methane yield from structural plant components," Waste Management, 78, pp. 903-910.
[235] Dell'Omo, P., Froscia, L. S., 2018, "Enhancing Anaerobic Digestion of Wheat Straw through Multistage Milling. Model," Meas. Control C, 79, pp. 127-132.
[236] Tsapekos, P., Kougias, P. G., Angelidaki, I., 2015, "Biogas production from ensiled meadow grass; effect of mechanical pre-treatments and rapid determination of substrate biodegradability via physicochemical methods," Bioresource technology, 182, pp. 329-335.
[237] Zhang, R., Zhang, Z., 1999, "Biogasification of rice straw with an anaerobic-phased solids digester system," Bioresource technology, 68(3), pp. 235-245.
[238] Montingelli, M. E., Tedesco, S., Olabi, A. G., 2015, "Biogas production from algal biomass: A review," Renewable and Sustainable Energy Reviews, 43, pp. 961-972.
[239] Umeghalu, C. E., Chukwuma, E. C., Okonkwo, I. F., Umeh, S. O., 2012, "Potentials for biogas production in Anambra State of Nigeria using cow dung and poultry droppings," International Journal of Veterinary Science, 1(1), pp. 26-30.
[240] Sawyerr, N., Trois, C., Workneh, T., Okudoh, V., 2019, "An overview of biogas production: Fundamentals, applications and future research," International Journal of Energy Economics and Policy, 9(2), pp. 105-116.
[241] Damyanova, S., Beschkov, V., 2020, "Biogas as a Source of Energy and Chemicals," Biorefinery Concepts. Energy and Products. Biorefinery Concepts; IntechOpen: London, UK.
[242] Patterson, T., Esteves, S., Dinsdale, R., Guwy, A., Maddy, J., 2013, "Life cycle assessment of biohydrogen and biomethane production and utilisation as a vehicle fuel," Bioresource technology, 131, pp. 235-245.
[243] Negri, C., Ricci, M., Zilio, M., D'Imporzano, G., Qiao, W., Dong, R., Adani, F., 2020, "Anaerobic digestion of food waste for bio-energy production in China and Southeast Asia: A review," Renewable and Sustainable Energy Reviews, 133, p. 110138.
[244] Gou, C., Yang, Z., Huang, J., Wang, H., Xu, H., Wang, L., 2014, "Effects of temperature and organic loading rate on the performance and microbial community of anaerobic co-digestion of waste activated sludge and food waste," Chemosphere, 105, pp. 146-151.
[245] Xiao, B., Qin, Y., Zhang, W., Wu, J., Qiang, H., Liu, J., Li, Y. Y., 2018, "Temperature-phased anaerobic digestion of food waste: A comparison with single-stage digestions based on performance and energy balance," Bioresource Technology, 249, pp. 826-834.
[246] Kiyasudeen, K., Ibrahim, M. H., Quaik, S., Ismail, S. A., 2016, "An Introduction to Anaerobic Digestion of Organic Wastes. In: Prospects of Organic Waste Management and the Significance of Earthworms," Applied Environmental Science and Engineering for a Sustainable Future. Springer, Cham. , pp. 23-44.
[247] Kaparaju, P. L. N., Rintala, J. A., 2008, "Effects of solid–liquid separation on recovering residual methane and nitrogen from digested dairy cow manure," Bioresource Technology, 99(1), pp. 120-127.
[248] Kariyama, I. D., Zhai, X., Wu, B., 2018, "Influence of mixing on anaerobic digestion efficiency in stirred tank digesters: a review," Water research, 143, pp. 503-517.

[249] Ward, A. J., Hobbs, P.l J., Holliman, P. J., Jones, D. L., 2008, "Optimisation of the anaerobic digestion of agricultural resources," Bioresource technology, 99(17), pp. 7928-7940.
[250] Deepanraj, B., Sivasubramanian, V., Jayaraj, S., 2014, "Biogas generation through anaerobic digestion process-an overview," Research Journal of Chemistry and Environment, 18(5), pp. 80-93.
[251] Leung, D. Y., Wang, J., 2016, "An overview on biogas generation from anaerobic digestion of food waste," International Journal of Green Energy, 13(2), pp. 119-131.
[252] Liu, C. F., Yuan, X. Z., Zeng, G. M., Li, W. W., Li, J., 2008, "Prediction of methane yield at optimum pH for anaerobic digestion of organic fraction of municipal solid waste," Bioresource technology, 99(4), pp. 882-888.
[253] Kondusamy, D., Kalamdhad, A. S., 2014, "Pre-treatment and anaerobic digestion of food waste for high rate methane production–A review," Journal of Environmental Chemical Engineering, 2(3), pp. 1821-1830.
[254] Pramanik, S. K., Suja, F. B., Zain, S. M., Pramanik, B. K., 2019, "The anaerobic digestion process of biogas production from food waste: Prospects and constraints," Bioresource Technology Reports, 20, p. e00284.
[255] Wang, T., Yang, P., Zhang, X., Zhou, Q., Yang, Q., Xu, B., Yang, P., Zhou, T.,, 2018, "Effects of mixing ratio on dewaterability of digestate of mesophilic anaerobic co-digestion of food waste and sludge," Waste and Biomass Valorisation, 9(1), pp. 87-93.
[256] Mu, H., Zhao, C., Zhao, Y., Li, Y., Hua, D., Zhang, X., Xu, H., 2017, "Enhanced methane production by semi-continuous mesophilic co-digestion of potato waste and cabbage waste: Performance and microbial characteristics analysis," Bioresource technology, 236, pp. 68-76.
[257] Zhai, N., Zhang, T., Yin, D., Yang, G., Wang, X., Ren, G., Feng, Y., 2015, "Effect of initial pH on anaerobic co-digestion of kitchen waste and cow manure," Waste management, 38, pp. 126-131.
[258] Pavi, S., Kramer, L. E., Gomes, L. P., Miranda, L. A., 2017, "Biogas production from co-digestion of organic fraction of municipal solid waste and fruit and vegetable waste," Bioresource technology, 228, pp. 362-367.
[259] Shi, X., Guo, X., Zuo, J., Wang, Y., Zhang, M., 2018, "A comparative study of thermophilic and mesophilic anaerobic co-digestion of food waste and wheat straw: process stability and microbial community structure shifts," Waste management, 75, pp. 261-269.
[260] Akila, V., M., A., Sukeetha, D. S., Balakrishnan, S., Ayyasamy, P. M., Rajakumar, S. , 2019, "Biogas and biofertiliser production of marine macroalgae: An effective anaerobic digestion of Ulva sp," Biocatalysis and Agricultural Biotechnology, 18, p. 101035.
[261] Wu, Q., , Shao, W., Xia, N., Wang, P., Kong, F. , 2020, "A separable paper adhesive based on the starch—lignin composite," Carbohydrate Polymers, 229, p. 115488.
[262] Monlau, F., Francavilla, M., Sambusiti, C., Antoniou, N., Solhy, A., Libutti, A., Zabaniotou, A., Barakat, A., Monteleone, M., 2016, "Toward a functional integration of anaerobic digestion and pyrolysis for a sustainable resource management. Comparison between solid-digestate and its derived pyrochar as soil amendment," Applied Energy, 169, pp. 652-662.

[263] O'Brien, B. J., Milligan, E., Carver, J., Roy, E. D., 2019, "Integrating anaerobic co-digestion of dairy manure and food waste with cultivation of edible mushrooms for nutrient recovery," Bioresource technology, 285, p. 121312.
[264] Peng, W., Lü, F., Hao, L., Zhang, H., Shao, L., He, P., 2020, "Digestate management for high-solid anaerobic digestion of organic wastes: A review," Bioresource Technology, 297, p. 122485.
[265] Hung, C. Y., Tsai, W. T., Chen, J. W., Lin, Y. Q., Chang, Y. M., 2017, "Characterisation of biochar prepared from biogas digestate," Waste management, 66, pp. 53-60.
[266] Hübner, T., Mumme, J., 2015, "Integration of pyrolysis and anaerobic digestion–use of aqueous liquor from digestate pyrolysis for biogas production," Bioresource technology, 183, pp. 86-92.
[267] Wei, Y. M., Wu, G., Liang, Q. M., Liao, H., 2012, "China energy report (2012): energy security research," SciencePress, Beijing.
[268] Uthirapandi, V., Suriya, S., Boomibalagan, P., Eswaran, S., Ramya, S. S., Vijayanand, N., Kathiresan, D., 2018, "Bio-fertiliser potential of seaweed liquid extracts of marine macro algae on growth and biochemical parameters of Ocimum sanctum," Journal of Pharmacognosy and Phytochemistry, 7(3), pp. 3528-3532.
[269] Lafleur, B., Thiffault, E., Paré, D., Camiré, C., Bernier-Cardou, M., Masse, S., 2012, "Effects of hog manure application on the nutrition and growth of hybrid poplar (Populus spp.) and on soil solution chemistry in short-rotation woody crops," Agriculture, ecosystems & environment, 155, pp. 95-104.
[270] Nkoa, R., 2014, "Agricultural benefits and environmental risks of soil fertilisation with anaerobic digestates: a review," Agronomy for Sustainable Development, 34(2), pp. 473-492.
[271] Robert P., 2019, "Garden Fundamentals - Become a better gardenerFertiliser," Available from: https://www.gardenfundamentals.com/fertilizing-gardens-right-way/ [Accessed on: 7 June 2021].
[272] "The Official Information Portal on Anaerobic Digestion," Available from: http://www.biogas-info.co.uk/about/digestate/ [Accessed on: 7 June 2021].
[273] Bonten, L. T. C., Zwart, K. B., Rietra, R. P. J. J., Postma, R., De Haas, M. J. G., Nysingh, S. L., 2014, "Bio-slurry as fertiliser: is bio-slurry from household digesters a better fertiliser than manure?: a literature review," No. 1566-7197, Alterra, Wageningen-UR.
[274] "Official Journal of the European Union , Legislation," Available from: https://eur-lex.europa.eu/legal-content/EN/TXT/PDF/?uri=OJ:L:2019:170:FULL&from=EN [Accessed on: 7 June 2021].
[275] Weiland, P., 2010, "Biogas production: current state and perspectives," Applied microbiology and biotechnology, 85(4), pp. 849-860.
[276] Ye, Z., Zhang, L., Huang, Q., Tan, Z., 2019, "Development of a carbon-based slow release fertiliser treated by bio-oil coating and study on its feedback effect on farmland application," Journal of Cleaner Production, 239, p. 118085.
[277] Gutser, R., Ebertseder, T., Weber, A., Schraml, M., Schmidhalter, U., 2005, "Short‐term and residual availability of nitrogen after long‐term application of organic fertilisers on arable land," Journal of Plant Nutrition and Soil Science, 168(4), pp. 439-446.
[278] Chong, C. C., Aqsha, A., Ayoub, M., Sajid, M., Abdullah, A. Z., Yusup, S., Abdullah, B., 2020, "A review over the role of catalysts for selective short-chain polyglycerol production

from biodiesel derived waste glycerol," Environmental Technology & Innovation, 19, p. 100859.
[279] Noor, C. M., Noor, M. M., Mamat, R., 2018, "Biodiesel as alternative fuel for marine diesel engine applications: A review," renewable and sustainable energy reviews, 94, pp. 127-142.
[280] Ramadhas, A. S., Muraleedharan, C., Jayaraj, S., 2005, "Performance and emission evaluation of a diesel engine fueled with methyl esters of rubber seed oil," Renewable energy, 30(12), pp. 1789-1800.
[281] Kawentar, W. A., Budiman, A., 2013, "Synthesis of biodiesel from second-used cooking oil," Energy Procedia, 32, pp. 190-199.
[282] Balasubramanian, D., Kamaraj, S., Krishnamoorthy, R., 2020, "Synthesis of Biodiesel from Waste Cooking Oil by Alkali Doped Calcinated Waste Egg Shell Powder Catalyst and Optimisation of Process Parameters to Improve Biodiesel Conversion," No. 0148-7191, SAE Technical Paper.
[283] Mahmudul, H. M., Hagos, F. Y., Mamat, R., Adam, A .A., Ishak, W. F., Alenezi, R., 2017, "Production, characterisation and performance of biodiesel as an alternative fuel in diesel engines–A review," Renewable and Sustainable Energy Reviews, 72, pp. 497-509.
[284] Chuah, L. F., Klemeš, J. J., Yusup, S., Bokhari, A., Akbar, M. M., 2017, "A review of cleaner intensification technologies in biodiesel production," Journal of cleaner production, 146, pp. 181-193.
[285] Atabani, A. E., Silitonga, A. S., Badruddin, I. A., Mahlia, T. M., Masjuki, H. H., Mekhilef, S., 2012, "A comprehensive review on biodiesel as an alternative energy resource and its characteristics," Renewable and sustainable energy reviews, 16(4), pp. 2070-2093.
[286] Alaswad, A., Dassisti, M., Prescott, T., Olabi, A. G., 2015, "Technologies and developments of third generation biofuel production," Renewable and Sustainable Energy Reviews, 51, pp. 1446-1460.
[287] Borugadda, V. B., Goud, V. V., 2016, "Improved thermo-oxidative stability of structurally modified waste cooking oil methyl esters for bio-lubricant application," Journal of Cleaner Production, 112, pp. 4515-4524.
[288] Ghayal, D., Pandit, A. B., Rathod, V. K., 2013, "Optimisation of biodiesel production in a hydrodynamic cavitation reactor using used frying oil," Ultrasonics sonochemistry, 20(1), pp. 322-328.
[289] Chuah, L. F., Yusup, S., AzizAbdul, R. A., Klemeš, J. J., Bokhari, A., Abdullah, M. Z., 2016, "Influence of fatty acids content in non-edible oil for biodiesel properties," Clean Technologies and Environmental Policy, 18(2), pp. 473-482.
[290] Lin, L., Cunshan, Z., Vittayapadung, S., Xiangqian, S., Mingdong, D., 2011, "Opportunities and challenges for biodiesel fuel," Applied energy, 88(4), pp. 1020-1031.
[291] Muanruksa, P., Kaewkannetra, P., 2020, "Combination of fatty acids extraction and enzymatic esterification for biodiesel production using sludge palm oil as a low-cost substrate," Renewable Energy, 146, pp. 901-906.
[292] Amani, M. A., Davoudi, M. S., Tahvildari, K., Nabavi, S. M., and Davoudi, M. S., 2013, "Biodiesel production from Phoenix dactylifera as a new feedstock," Industrial Crops and Products, 43, pp. 40-43.
[293] Jamil, F., Ala'a, H., Al-Haj, L., Al-Hinai, M. A., Hellier, P., Rashid, U., 2016, "Optimisation of oil extraction from waste "Date pits" for biodiesel production," Energy Conversion and Management, 117, pp. 264-272.

[294] Singh, D., Sharma, D., Soni, S. L., Inda, C. S., Sharma, S., Sharma, P. K., Jhalani, A., 2021, "A comprehensive review of physicochemical properties, production process, performance and emissions characteristics of 2nd generation biodiesel feedstock: Jatropha curcas," Fuel, 285, p. 119110.
[295] Rajalingam, A., Jani, S. P., Kumar, A. S., and Khan, M. A., 2016, "Production methods of biodiesel," J. Chem. Pharm. Res, 8(3), pp. 170-173.
[296] Xiao, X., Yan, B., Fu, J., Xiao, X., 2015, "Absorption and recovery of n-hexane in aqueous solutions of fluorocarbon surfactants," Journal of Environmental Sciences, 37, pp. 163-171.
[297] Boutekedjiret, C., Vian, M. A., Chemat, F., 2014, "Terpenes as green solvents for natural products extraction," In Alternative Solvents for Natural Products Extraction, Springer, pp. 205-219.
[298] Zamir, M., Halladj, R., Sadraei, M., Nasernejad, B., 2012, "Biofiltration of gas-phase hexane and toluene mixture under intermittent loading conditions," Process Safety and Environmental Protection, 90(4), pp. 326-332.
[299] Heymes, F., Demoustier, P. M., Charbit, F., Fanlo, J.L., Moulin, P., 2006, "Recovery of toluene from high temperature boiling absorbents by pervaporation," Journal of membrane science, 284(1-2), pp. 145-154.
[300] Heymes, F., Demoustier, P. M., Charbit, F., Fanlo, J. L., Moulin, P., Manno-Demoustier, P., Charbit, F., Fanlo, J. L., Moulin, P., 2006, "A new efficient absorption liquid to treat exhaust air loaded with toluene," Chemical Engineering Journal, 115(3), pp. 225-231.
[301] Wu, G., Li, X., Coulon, F., Li, H., Lian, J., Sui, H., 2011, "Recycling of solvent used in a solvent extraction of petroleum hydrocarbons contaminated soil," Journal of hazardous materials, 186(1), pp. 533-539.
[302] Emamgholivand, A., Ghobadian, B., Abbaszadeh, A., 2012, "Simulation and Study of Methanol Recovery Process in Biodiesel Production," European Workshop on Renewable Energy SystemsAntalya.
[303] Al-Mawali, K. S., Osman, A. I., Ala'a, H., Mehta, N., Jamil, F., Mjalli, F., Vakili-Nezhaad, G. R., Rooney, D. W., 2021, "Life cycle assessment of biodiesel production utilising waste date seed oil and a novel magnetic catalyst: A circular bioeconomy approach," Renewable Energy, 170, pp. 832-846.
[304] Marchetti, J. M., Miguel, V. U., Errazu, A. F., 2007, "Possible methods for biodiesel production," Renewable and sustainable energy reviews, 11(6), pp. 1300-1311.
[305] Jitputti, J., Kitiyanan, B., Rangsunvigit, Pr., Bunyakiat, K., Attanatho, L., Jenvanitpanjakul, P., 2006, "Transesterification of crude palm kernel oil and crude coconut oil by different solid catalysts," Chemical Engineering Journal, 116(1), pp. 61-66.
[306] Wan Isahak, W. N. R., Che Ramli, Z.A., Ismail, M., Mohd Jahim, J., Yarmo, M. A., 2015, "Recovery and purification of crude glycerol from vegetable oil transesterification," Separation & Purification Reviews, 44(3), pp. 250-267.
[307] Isahak, W. N. R. W., Ismail, M., Yarmo, M. A., Jahim, J.M., Salimon, J., 2010, "Purification of crude glycerol from transesterification RBD palm oil over homogeneous and heterogeneous catalysts for the biolubricant preparation," Journal of Applied Sciences, 10(21), pp. 2590-2595.
[308] Hájek, M., Skopal, F., 2010, "Treatment of glycerol phase formed by biodiesel production," Bioresource technology, 101(9), pp. 3242-3245.

[309] Baabad, M., Ismail, M., "Biodiesel production using potassium based heterogeneous catalyst on γ-alumina support," Proc. In Proceedings on 15th Regional Symposium on Chemical Engineering (RSCE) in conjunction with the 22nd Sym posium of Malaysian Chemical Engineers (SOMChe) (pp. 911-916).
[310] Duncan, J., 2003, "Costs of Biodiesel Production. Energy Efficiency and Conservation Authority, New Zealand."
[311] Thompson, J. C., He, B. B., 2006, "Characterisation of crude glycerol from biodiesel production from multiple feedstocks," Applied engineering in agriculture, 22(2), pp. 261-265.
[312] Isahak, W. N. R. W., Ismail, M., Yarmo, M.A., Jahim, J.M., Salimon, J., "Crude glycerol purification and treatment for bio-lubricant preparation. ," Proc. Proceedings on Chemical Engineering (RSCE). University of Santo Tomas, Manila December 1–2, 2009.
[313] Chiu, C. W., Dasari, M. A., Sutterlin, Willam, R. Suppes, G. J., 2006, "Removal of residual catalyst from simulated biodiesel's crude glycerol for glycerol hydrogenolysis to propylene glycol," Industrial & engineering chemistry research, 45(2), pp. 791-795.
[314] Hui, Y. H., 1996, In Bailey's Industrial Oil and Fat Products: Industrial and Consumer Non-edible products from Oils and Fats., John Wiley and Sons, New York.
[315] Hammond, G. P., Li, B., 2016, "Environmental and resource burdens associated with world biofuel production out to 2050: footprint components from carbon emissions and land use to waste arisings and water consumption," Gcb Bioenergy, 8(5), pp. 894-908.
[316] Lu, J., Liu, Z., Zhang, Y., Li, B., Lu, Q., Ma, Y., Shen, R., Zhu, Z., 2017, "Improved production and quality of biocrude oil from low-lipid high-ash macroalgae Enteromorpha prolifera via addition of crude glycerol," Journal of Cleaner Production, 142, pp. 749-757.
[317] Guerrero-Urbaneja, P., García-Sancho, C., Moreno-Tost, R., Mérida-Robles, J., Santamaría-González, J., Jiménez-López, A., Maireles-Torres, P., 2014, "Glycerol valorization by etherification to polyglycerols by using metal oxides derived from MgFe hydrotalcites," Applied Catalysis A: General, 470, pp. 199-207.
[318] Siew, K. W., Lee, H. C. Gimbun, J., Chin, S. Y., Khan, M. R., Taufiq-Yap, Y. H., Cheng, C. K., 2015, "Syngas production from glycerol-dry (CO_2) reforming over La-promoted Ni/Al2O3 catalyst," Renewable Energy, 74, pp. 441-447.
[319] Jamil, F., Saxena, S. K., Ala'a, H., Baawain, M., Al-Abri, M., Viswanadham, N., Kumar, G., Abu-Jrai, A. M., 2017, "Valorisation of waste "date seeds" bio-glycerol for synthesising oxidative green fuel additive," Journal of cleaner production, 165, pp. 1090-1096.
[320] Board, N. B., 2018, "US Biodiesel and Renewable Diesel Production Statistics According NBB. Diamond Producers Association."
[321] Zhang, M., Wu, H., 2015, "Effect of major impurities in crude glycerol on solubility and properties of glycerol/methanol/bio-oil blends," Fuel, 159, pp. 118-127.
[322] Levi, P. G., Cullen, J. M., 2018, "Mapping global flows of chemicals: from fossil fuel feedstocks to chemical products," Environmental science & technology, 52(4), pp. 1725-1734.
[323] Kośmider, A., Leja, K., Czaczyk, K., 2011, "Improved utilisation of crude glycerol by-product from biodiesel production," **In** Biodiesel-Quality, emissions and by-products. Rijeka. IntechOpen. (pp. 341-364).
[324] Hansen, C. F., Hernandez, A., Mullan, B. P., Moore, K., Trezona-Murray, M., King, R. H., Pluske, J. R., 2009, "A chemical analysis of samples of crude glycerol from the production of biodiesel in Australia, and the effects of feeding crude glycerol to growing-finishing pigs on

performance, plasma metabolites and meat quality at slaughter," Animal Production Science, 49(2), pp. 154-161.
[325] Adnan, N. A. A., Suhaimi, S. N., Abd-Aziz, S., Hassan, M. A., Phang, L. Y., 2014, "Optimisation of bioethanol production from glycerol by Escherichia coli SS1," Renewable energy, 66, pp. 625-633.
[326] Emblem, A., Emblem, H., 2012, Packaging technology: Fundamentals, materials and processes, Woodhead publishing Limited. TJ International Ltd, Padstow, Cornwall, UK, UK.
[327] Yin, H., Zheng, P., Zhang, E., Rao, J., Lin, Q., Fan, M., Zhu, Z., Zeng, Q., Chen, N., 2020, "Improved wet shear strength in eco-friendly starch-cellulosic adhesives for woody composites," Carbohydrate Polymers, 250, p. 116884.
[328] Yap, Y. L., Toh, W., Koneru, R., Lin, R., Chan, K. I., Guang, H., Chan, W. Y. B., Teong, S. S., Zheng, G., Ng, T. Y., 2020, "Evaluation of structural epoxy and cyanoacrylate adhesives on jointed 3D printed polymeric materials," International Journal of Adhesion and Adhesives, 100, p. 102602.
[329] Kadam, S. U., Tiwari, B. K., O'Donnell, C. P., 2015, "Improved thermal processing for food texture modification," Modifying Food Texture, Elsevier, pp. 115-131.
[330] Nasiri, A., Wearing, J., Dubé, M. A., 2020, "Using Lignin to Modify Starch-Based Adhesive Performance," ChemEngineering, 4(1), p. 3.
[331] Oghenejoboh, K. M., 2012, "Effects of starch fermentation on the shelf-life of cassava starch based adhesive," Biotechnology Journal International, 2(4), pp. 257-268.
[332] Ayoola, A. A., Fayomi, O.S.I., Akande, I.G., Adeeyo, O.A., Obanla, O.R., Abatan, O.G., Babatunde, D.E., Olawepo, V.A., Fagbiele, O.O., Olomo, V.D., "Production of Adhesive from Cassava Starch," Proc. Journal of Physics: Conference Series, IOP Publishing, p. 032079.
[333] Gunorubon, A. J., 2012, "Production of cassava starch-based adhesive," Research Journal in Engineering and Applied Sciences, 1(4), pp. 219-214.
[334] Omotioma, M., Mba, G. O., Okonkwo, O. F., Okoye, C. O., 2012, "Rheological characteristics of adhesive material produced from locally sourced cassava starch," International Journal of Environmental Science, Management and Engineering Research, 1(6), pp. 211-213.
[335] Zhu, F., 2015, "Composition, structure, physicochemical properties, and modifications of cassava starch," Carbohydrate polymers, 122, pp. 456-480.
[336] Padi, R. K., Chimphango, A., 2021, "Comparative sustainability assessments for integrated cassava starch wastes biorefineries," Journal of Cleaner Production, 290, p. 125171.
[337] Sun, Y., Gu, J., Tan, H., Zhang, Y., Huo, P., 2018, "Physicochemical properties of starch adhesives enhanced by esterification modification with dodecenyl succinic anhydride," International journal of biological macromolecules, 112, pp. 1257-1263.
[338] Qiao, Z., Gu, J., Lv, S., Cao, J., Tan, H., Zhang, Y. , 2015, "Preparation and properties of isocyanate prepolymer/corn starch adhesive," Journal of Adhesion Science and Technology, 29(13), pp. 1368-1381.
[339] Awaja, F., Gilbert, M., Kelly, G., Fox, B., Pigram, P.l J., 2009, "Adhesion of polymers," Progress in polymer science, 34(9), pp. 948-968.
[340] Pinto, A. M. G., Magalhaes, A. G., da Silva, F. G., Baptista, A. P. M., 2008, "Shear strength of adhesively bonded polyolefins with minimal surface preparation," International Journal of Adhesion and Adhesives, 28(8), pp. 452-456.

[341] Jelušič, P., Kravanja, S., 2018, "Flexural analysis of laminated solid wood beams with different shear connections," Construction and Building Materials, 174, pp. 456-465.
[342] Shokrian, M. D., Shelesh-Nezhad, K., Najjar, R., 2019, "The effects of Al surface treatment, adhesive thickness and microcapsule inclusion on the shear strength of bonded joints," International Journal of Adhesion and Adhesives, 89, pp. 139-147.
[343] Sundriyal, P., Pandey, M., Bhattacharya, S., 2020, "Plasma-assisted surface alteration of industrial polymers for improved adhesive bonding," International Journal of Adhesion and Adhesives, 101, p. 102626.
[344] Xu, Y., Li, H., Shen, Y., Liu, S., Wang, W., Tao, J., 2016, "Improvement of adhesion performance between aluminum alloy sheet and epoxy based on anodising technique," International Journal of Adhesion and Adhesives, 70, pp. 74-80.
[345] Rechner, R., Jansen, I., Beyer, E., 2010, "Influence on the strength and aging resistance of aluminium joints by laser pre-treatment and surface modification," International Journal of Adhesion and Adhesives, 30(7), pp. 595-601.
[346] Zielecfei, W., Pawlus, P., Perłowski, R., Dzierwa, A., 2013, "Surface topography effect on strength of lap adhesive joints after mechanical pre-treatment," Archives of Civil and Mechanical Engineering, 13, pp. 175-185.
[347] Guo, L., Liu, J., Xia, H., Li, X., Zhang, X., Yang, H., "Effects of surface treatment and adhesive thickness on the shear strength of precision bonded joints," Polymer Testing, 94, p. 107063.
[348] Thornton, C., Cummins, S. J., Cleary, P. W., 2017, "On elastic-plastic normal contact force models, with and without adhesion," Powder Technology, 315, pp. 339-346.
[349] Boutar, Y., Naïmi, S., Mezlini, S., Ali, M. B. S., 2016, "Effect of surface treatment on the shear strength of aluminium adhesive single-lap joints for automotive applications," International Journal of Adhesion and Adhesives, 67, pp. 38-43.
[350] Budhe, S., Ghumatkar, A., Birajdar, N., Banea, M. D., 2015, "Effect of surface roughness using different adherend materials on the adhesive bond strength," Applied Adhesion Science, 3(1), pp. 1-10.
[351] Li, X., Dong, M., Jiang, D., Li, S., Shang, Y., 2020, "The effect of surface roughness on normal restitution coefficient, adhesion force and friction coefficient of the particle-wall collision," Powder Technology, 362, pp. 17-25.
[352] Mittal, K. L., 2014, Polymer surface modification: relevance to adhesion (Vol. 3). CRC Press.
[353] Deng, S., Djukic, L., Paton, R., Ye, L., 2015, "Thermoplastic–epoxy interactions and their potential applications in joining composite structures–A review," Composites Part A: Applied Science and Manufacturing, 68, pp. 121-132.
[354] Chen, X., Zhang, Z., Jin, X., Xiao, M., Guo, H., Ma, Z., 2018, "Simulation method for precision bonding structure with micron scale adhesive layer," Procedia CIRP, 76, pp. 100-105.
[355] Akhavan-Safar, A., Ayatollahi, M. R., da Silva, L. F. M., 2017, "Strength prediction of adhesively bonded single lap joints with different bondline thicknesses: A critical longitudinal strain approach," International Journal of Solids and Structures, 109, pp. 189-198.
[356] Da Silva, L. F. M., Rodrigues, T. N. S. S., Figueiredo, M. A. V., De Moura, M. F. S. F., Chousal, J. A. G., 2006, "Effect of adhesive type and thickness on the lap shear strength," The journal of adhesion, 82(11), pp. 1091-1115.

[357] Liao, L., Huang, C., Sawa, T., 2013, "Effect of adhesive thickness, adhesive type and scarf angle on the mechanical properties of scarf adhesive joints," International Journal of Solids and Structures, 50(25-26), pp. 4333-4340.
[358] Borsellino, C., Urso, S., Alderucci, T., Chiappini, G., Rossi, M., Munafò, P., 2021, "Temperature effects on failure mode of double lap glass-aluminum and glass-GFRP joints with epoxy and acrylic adhesive," International Journal of Adhesion and Adhesives, 105, p. 102788.
[359] Manohar, K. R., Raghunadh, Y. M., Kumar, B. K., Ranganath, L., Koteswararao, B., 2019, "Experiment Analysis To Examine The Effects Of Adhesive And Adherent Type Of Geometrical Configuration On Joint Failure Loads," Materials Today: Proceedings, 18, pp. 4665-4674.
[360] Chen, L., Zhou, Z., Liu, G., Cui, X., Dong, Q., Cao, H., 2020, "Effects of substrate materials and liner thickness on the adhesive strength of the novel thin spray-on liner," Advances in Mechanical Engineering, 12(2), pp. 1-13.
[361] Campbell, F. C., 2004, "Adhesive Bonding and Integrally Cocured Structure: A Way to Reduce Assembly Costs through Parts Integration," Manufacturing Processes for Advanced Composites; Elsevier Science: Amsterdam, The Netherlands, pp. 241-301.
[362] Bekhta, P., Sedliačik, J., Bekhta, N., 2020, "Effect of Veneer-Drying Temperature on Selected Properties and Formaldehyde Emission of Birch Plywood," Polymers, 12(3), p. 593.
[363] Almeshal, I., Tayeh, B. A., Alyousef, R., Alabduljabbar, H., Mohamed, A. M., Alaskar, A., 2020, "Use of recycled plastic as fine aggregate in cementitious composites: A review," Construction and Building Materials, 253, p. 119146.
[364] Kelly, T. J., Smith, D. L., Satola, J., 1999, "Emission rates of formaldehyde from materials and consumer products found in California homes," Environmental Science & Technology, 33(1), pp. 81-88.
[365] Cakiroglu, E. O., Demir, A., Aydin, I., 2019, "Comparison of birch and beech wood in terms of economic and technological properties for plywood manufacturing," Drvna industrija: Znanstveni časopis za pitanja drvne tehnologije, 70(2), pp. 169-174.
[366] Biziks, V., Andersons, B., Beļkova, Ļ., Kapača, E., Militz, H., 2013, "Changes in the microstructure of birch wood after hydrothermal treatment," Wood science and technology, 47(4), pp. 717-735.
[367] "Plastics-the Facts 2019, An analysis of European plastics production, demand and waste data, 2019," Available from: https://www.plasticseurope.org/application/files/9715/7129/9584/FINAL_web_version_Plastics_the_facts2019_14102019.pdf [Accessed on: 7 June 2020].
[368] Subramanian, P. M., 2000, "Plastics recycling and waste management in the US," Resources, Conservation and Recycling, 28(3-4), pp. 253-263.
[369] Onusseit, H., 2006, "The influence of adhesives on recycling," Resources, Conservation and Recycling, 46(2), pp. 168-181.
[370] Bajpai, P., 2018, Biermann's Handbook of Pulp and Paper: Volume 1: Raw Material and Pulp Making, Elsevier.
[371] Zhang, J., Xu, J., Wang, D., Ren, N., 2016, "Anaerobic Digestion of Cassava Pulp with Sewage Sludge Inocula," BioResources, 11(1), pp. 451-465.

[372] Panichnumsin, P., Nopharatana, A., Ahring, B., Chaiprasert, P., 2010, "Production of methane by co-digestion of cassava pulp with various concentrations of pig manure," biomass and bioenergy 34, pp. 1117-1124.
[373] Glanpracha, N., Annachhatre, A., 2016, "Anaerobic co-digestion of cyanide containing cassava pulp with pig manure," Bioresource Technology 214, pp. 112-121.
[374] Vasudeo, C. G., 2016, "Optimisation of Ultrasound-Assisted Extraction (UAE) of Starch from Cassava (Manihot esculenta Grantz) using Response Surface Methodology (RSM) Technique. Indian Institute of Crop Processing Technology (IICPT), Ministry of Food Processing Industries, Thanjavur, Tamil Nadu ".
[375] Montingelli, M. E., Benyounis, K. Y., Quilty, B. Stokes, J., Olabi, A. G., 2017, "Influence of mechanical pre-treatment and organic concentration of Irish brown seaweed for methane production," Energy, 118, pp. 1079-1089.
[376] Logan, M., Safi, M., Lens, P., Visvanathan, C., 2019, "Investigating the performance of internet of things based anaerobic digestion of food waste," Process Safety and Environmental Protection, 127, pp. 277-287.
[377] 1993, "Official methods and recommended practices of the American Oil Chemist sample. Am 2-93. Determination of oil content in oilseeds. American Oil Chemists Society, 4th ed. Champaign, IL: AOCS Press.."
[378] Gopalasatheeskumar, K., 2018, "Significant Role Of Soxhlet Extraction Process In Phytochemical Research," Mintage Journal of Pharmaceutical & Medical Sciences, 7(1), pp. 43-47.
[379] Guimarães, A. C. R., Costa, K. Á., de Miranda Reis, M., Santana, C. S. A., Castro, C. D., 2021, "Study of controlled leaching process of steel slag in soxhlet extractor aiming employment in pavements," Transportation Geotechnics, 27, p. 100485.
[380] ASTM D906-20, 2007, "Standard Test Method for Strength Properties of Adhesives in Plywood Type Construction in Shear by Tension Loading. ASTM West Conshohocken, PA."
[381] ASTM D3163-01, 2014, "Standard test method for determining strength of adhesively bonded rigid plastic lap-shear joints in shear by tension loading. ASTM West Conshohocken, PA."
[382] Mahrdt, E., Pinkl, S., Schmidberger, C., van Herwijnen, H. W., Veigel, S., Gindl-Altmutter, W., 2016, "Effect of addition of microfibrillated cellulose to urea-formaldehyde on selected adhesive characteristics and distribution in particle board," Cellulose, 23(1), pp. 571-580.
[383] ASTM D792-20, 2007, "Standard Test Methods for Density and Specific Gravity (Relative Density) of Plastics by Displacement. ASTM West Conshohocken, PA."
[384] Akpabio, U. D., Akpakpan, A. E.,Udo, I. E., Nwokocha, G. C., 2012, "Comparative study on the physicochemical properties of two varieties of cassava peels (Manihot utilissima Pohl)," International Journal of Environment and Bioenergy, 2(1), pp. 19-32.
[385] Adekunle, A., Orsat, V., Raghavan, V., 2018, "Lignocellulosic bioethanol: A review and design conceptualisation study of production from cassava peels," Renewable and Sustainable Energy Reviews, 64, pp. 518-531.
[386] Kohli, D., Champawat, P. S., Mudgal, V. D., , and Jain, S. K., Tiwari, B. K., 2021, "Advances in peeling techniques for fresh produce," Journal of Food Process Engineering, p. e13826.

[387] Toreci, I., Droste, R. L., Kennedy, K. J., 2011, "Mesophilic Anaerobic Digestion with High‐Temperature Microwave Pre-treatment and Importance of Inoculum Acclimation," Water environment research, 83(6), pp. 549-559.
[388] Wilkins, D., Rao, S., Lu, X., Lee, P. K., 2015, "Effects of sludge inoculum and organic feedstock on active microbial communities and methane yield during anaerobic digestion," Frontiers in microbiology, 6, p. 1114.
[389] Srisowmeya, G., Chakravarthy, M., Devi, G. N., 2019, "Critical considerations in two-stage anaerobic digestion of food waste–A review," Renewable and Sustainable Energy Reviews, 119, p. 109587.
[390] Igoni, A. H., Abowei, M. F. N., Ayotamuno, M. J., Eze, C. L., 2008, "Effect of total solids concentration of municipal solid waste on the biogas produced in an anaerobic continuous digester," Agricultural Engineering International: CIGR Journal, X, pp. 1-11.
[391] Deublein, D., Steinhauser, A., 2011, Biogas from waste and renewable resources: an introduction, John Wiley & Sons.
[392] Hobbs, S. R., Landis, A. E., Rittmann, B. E., Young, M. N., Parameswaran, P., 2018, "Enhancing anaerobic digestion of food waste through biochemical methane potential assays at different substrate: inoculum ratios," Waste management, 71, pp. 612-617.
[393] De la Rubia, M. Á., Walker, M., Heaven, S., Banks, C. J., Borja, R., 2010, "Preliminary trials of in situ ammonia stripping from source segregated domestic food waste digestate using biogas: effect of temperature and flow rate," Bioresource technology, 101(24), pp. 9486-9492.
[394] Dahlin, J., Herbes, C., Nelles, M., 2015, "Biogas digestate marketing: Qualitative insights into the supply side," Resources, Conservation and Recycling, 104, pp. 152-161.
[395] Alrefai, A. M., Alrefai, R., Benyounis, K. Y., Stokes, J., 2019, "The Environmental Challenges Associated With the Anaerobic Digestion Process when Applied Extensively," Encyclopedia of Renewable and Sustainable Materials, 1, pp. 279-286.
[396] Alrefai, R., Alrefai, A. M., Benyounis, K. Y., Stokes, J., 2019, "The Production of Biogas, Biodiesel as High-Value Bio-Based Product and Multiple Bio-Products Through an Integration Approach of the Anaerobic Digestion and Fermentation Processes," Encyclopedia of Renewable and Sustainable Materials, 1, pp. 686-694.
[397] Sakthivel, R., Ramesh, K., Purnachandran, R., Shameer, P. M., 2018, "A review on the properties, performance and emission aspects of the third generation biodiesels," Renewable and Sustainable Energy Reviews, 82, pp. 2970-2992.
[398] ASTM D6751-20a, 2020, "Standard Specification for Biodiesel Fuel Blend Stock (B100) for Middle Distillate Fuels, ASTM International, West Conshohocken, PA.."
[399] European Standard EN 14214, 2008, "Automotive fuels. Fatty acid methylesters (FAME) for diesel engines. Requirements and test methods."
[400] Knothe, G., Dunn, R. O., Bagby, M. O., 1997, "Biodiesel: the use of vegetable oils and their derivatives as alternative diesel fuels," ACS Publications.
[401] Rashid, U., Anwar, F., Knothe, G., 2011, "Biodiesel from Milo (Thespesia populnea L.) seed oil," biomass and bioenergy, 35(9), pp. 4034-4039.
[402] de Oliveira Filho, W. P., Borges, D. L., Saint'Pierre, T. D., Dupim, M., Vale, F., Marques, B., Medeiros, F. R., 2017, "Assessment of the equivalence and correlation between total sulfur determination methods in biodiesel: An use of isotope dilution inductively coupled plasma mass spectrometry," Fuel, 202, pp. 227-232.

[403] Canakci, M., Sanli, H., 2008, "Biodiesel production from various feedstocks and their effects on the fuel properties," Journal of industrial microbiology & biotechnology, 35(5), pp. 431-441.
[404] Ahmad, J., Yusup., Bokhari, A., Kamil, R. N. M., 2014, "Study of fuel properties of rubber seed oil based biodiesel," Energy Conversion and Management, 78, pp. 266-275.
[405] Lee, S. W., Tanaka, D., Kusaka, J., Daisho, Y., 2002, "Effects of diesel fuel characteristics on spray and combustion in a diesel engine," JSAE review, 23(4), pp. 407-414.
[406] Choi, C. Y., Reitz, R. D., 1999, "A numerical analysis of the emissions characteristics of biodiesel blended fuels," J. Eng. Gas Turbines Power, 121(1), pp. 31-37.
[407] Saidur, R., BoroumandJazi, G., Mekhilef, S., Mohammed, H. A., 2012, "A review on exergy analysis of biomass based fuels," Renewable and Sustainable Energy Reviews, 16(2), pp. 1217-1222.
[408] Saxena, R. C., Adhikari, D. K., Goyal, H. B., 2009, "Biomass-based energy fuel through biochemical routes: A review," Renewable and sustainable energy reviews, 13(1), pp. 167-178.
[409] Szybist, J. P., Song, J., Alam, M. Boehman, A. L., 2007, "Biodiesel combustion, emissions and emission control," Fuel processing technology, 88(7), pp. 679-691.
[410] Catoire, L., Paulmier, S., Naudet, V., 2006, "Estimation of closed cup flash points of combustible solvent blends," Journal of Physical and Chemical Reference Data, 35(1), pp. 9-14.
[411] Catoire, L., Paulmier, S., Naudet, V., 2006, "Experimental determination and estimation of closed cup flash points of mixtures of flammable solvents," Process safety progress, 25(1), pp. 33-39.
[412] do Nascimento, D. C., Carareto, N. D. D.,, and Neto, A. M. B., Gerbaud, V., da Costa, M. C., 2020, "Flash point prediction with UNIFAC type models of ethylic biodiesel and binary/ternary mixtures of FAEEs," Fuel, 281, p. 118717.
[413] Saifuddin, N., Refal, H., Kumaran, P., 2014, "Rapid purification of glycerol by-product from biodiesel production through combined process of microwave assisted acidification and adsorption via chitosan immobilised with yeast," Research Journal of Applied Sciences, Engineering and Technology, 7(3), pp. 593-602.
[414] Yang, L., Liu, J. J., Du, C. C., Qiang, Y., 2013, "Preparation and properties of cornstarch adhesives," Advance Journal of Food Science and Technology, 5(8), pp. 1068-1072.
[415] Yamamoto, H., Makita, E., Oki, Y., Otani, M., 2006, "Flow characteristics and gelatinisation kinetics of rice starch under strong alkali conditions," Food Hydrocolloids, 20(1), pp. 9-20.
[416] Bhambure, S., Mallick, P. K., 2012, "Effect of Temperature Variation on Stresses in Adhesive Joints between Magnesium and Steel," SAE International Journal of Materials and Manufacturing, 5(2), pp. 410-417.
[417] Jin, Y., Cheng, X., Zheng, Z., 2010, "Preparation and characterisation of phenol–formaldehyde adhesives modified with enzymatic hydrolysis lignin," Bioresource Technology, 101(6), pp. 2046-2048.
[418] Ortiz-Fernández, A., Ríos-Soberanis, C. R., Chim-Chi, Y. A., Moo-Huchin, V. M., Estrada-León, R. J., Pérez-Pacheco, E., 2020, "Optimisation of biodegradable starch adhesives using response surface methodology," Polymer Bulletin, pp. 1-21.

[419] Wang, S., Copeland, L., 2015, "Effect of acid hydrolysis on starch structure and functionality: A review," Critical reviews in food science and nutrition, 55(8), pp. 1081-1097.
[420] Yu, H., Fang, Q., Cao, Y., Liu, Z., 2016, "Effect of HCl on starch structure and properties of starch-based wood adhesives," BioResources, 11(1), pp. 1721-1728.
[421] Xing, J., Li, T., Yu, Y., Chen, C., Chang, J., 2018, "Development and characterisation of a new bio-adhesive for wood using cassava starch and bio-oil," International Journal of Adhesion and Adhesives, 87, pp. 91-97.
[422] Khoon, P., A., Choy Sin, L., Sit Foon, C., Cheng Hock, C., 2014, "Polyurethane wood adhesive from palm oil-based polyester polyol," Journal of Adhesion Science and Technology, 28(11), pp. 1020-1033.
[423] Shen, Y., Linville, J., L., Urgun-Demirtas, M., Mintz, M. M., Snyder, S. W., 2015, "An overview of biogas production and utilisation at full-scale wastewater treatment plants (WWTPs) in the United States: challenges and opportunities towards energy-neutral WWTPs," Renewable and Sustainable Energy Reviews, 50, pp. 346-362.
[424] Gowe, C., 2015, "Review on potential use of fruit and vegetables by-products as a valuable source of natural food additives," Food Science and Quality Management, 45, pp. 47-61.
[425] McDonnell, D., Burke, M., Dowdall, J., Foster, P., Mahon, K. , 2018, "Guidelines for Anaerobic Digestion in Ireland," Available from: http://www.cre.ie/web/wp-content/uploads/2018/03/Guidelines-for-Anaerobic-Digestion-in-Ireland_Final.pdf [Accessed on: 7 June 2021].
[426] Vilanova, P., Noche, B., 2016, "A review of the current digestate distribution models: storage and transport," The 8 International Conference th on Waste Management and The Environment (WM 2016), WIT press, Valencia, Spain.
[427] Mouat, A., Barclay, A., Mistry, P., Webb, J., "Digestate Market Development in Scotland," Natural Scotland, Scottish government: Inverness, UK, 2010.
[428] Wang, D., Xi, J., Ai, P., Yu, L., Zhai, H., Yan, S., Zhang, Y., 2016, "Enhancing ethanol production from thermophilic and mesophilic solid digestate using ozone combined with aqueous ammonia pre-treatment," Bioresource Technology, 207, pp. 52-58.
[429] Braun, R., Wellinger, A., "Potential of co-digestion," Proc. . International Energy Agency (IEA), Bioenergy; 2009.

Appendix (A)
Additional Equipment and devices

Hollander Beater

Mechanical pre-treatment is the treatment method that used in the experiment represented in beating and grinding treatment. The beating pre-treatment was performed by using Hollander Beater that illustrated in Figure 200. It is a device that used to beats and slices the cassava peel into small particles in order to increase the surface area and reduce the degree of polymerisation. It is composed from drum, motor and a V-belt. It is provider with slot that opened/closed manually for drainage and a scale to control the gap between the bottom surface of the device and the drum.

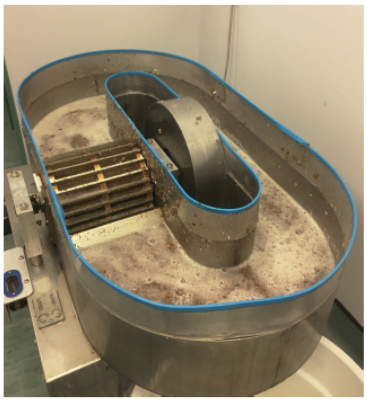

Figure 200: The Hollander beater.

Grinding Mill Machine

The date seeds were treated by grinding pre-treatment method using a 400 mm vertical Diamant grinding mill machine. The grinding process aimed to reduce the size of date seed and convert them into powder to facilitate the feeding of bacteria. This machine is available in different sizes 300, 400 and 500 mm diameter. It is also distinguished by its ability to grind grains and stones at the required sizes.

Water Baths

To maintain the reactors at specified temperatures in mesophilic condition, five water baths were used in this study. The temperatures were set at the three different temperatures, 34, 37, and 40 ºC. Figure 201 shows the water bath that set at 37 ºC. Water baths and reactors were monitored

on a daily basis for safety, temperature assurance and shaking the flasks. They were filled regularly by water to ensure that the heat was distributed evenly over samples and they not affected by the water shortage. The water baths were provided with plastic covers on the top that tightened two sides to prevent reactors movement. The capacity of each water bath was 12 reactors. The water bath setting range is +10 to +95 ºC ± 0.1 ºC.

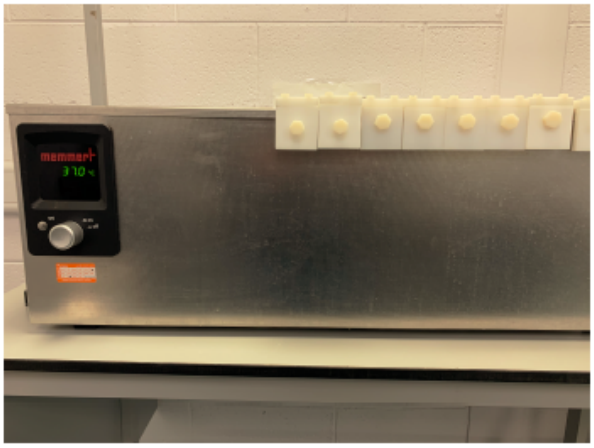

Figure 201: Water bath.

Laboratory Oven

The drying oven VENTI-Line with a maximum temperature of 300 ºC shown in Figure 202, was used to remove moisture from the samples and dry them to calculate DM. The temperature was adjusted to 105 ºC for 24 hours. The samples weight after the 24 hours were measured every 60 minutes until its weight became constant.

Figure 202: Laboratory oven.

Laboratory Furnace

The high temperature Nabertherm furnace with maximum temperature of 3,000 ºC shown in Figure 203, was used to burn the dried samples. The temperature set at 575 ºC for four hours. The resulted ash was weighted to determine the total solid and volatile solid of all samples.

Figure 203: Laboratory furnace.

Electric Pump

The vacuum pump was used to push the nitrogen into the reactors and then withdraw it. The purpose of that was to apply the AD condition by discharging the system from air and gases, especially O_2. The vacuum pump helps in speeding up the discharging air from the reactors and keeps the reactor free of air. Figure 204 demonstrates the vacuum pump used in the experimental works.

Figure 204: Vacuum pump.

Volumetric cylinder

Figure 205 displays the biogas measurement system that consists of volumetric cylinder and round bottom flask. The cylinder was filled by water, when the biogas pumped to the cylinder the water raised. The difference between water levels represents the biogas volume**.**

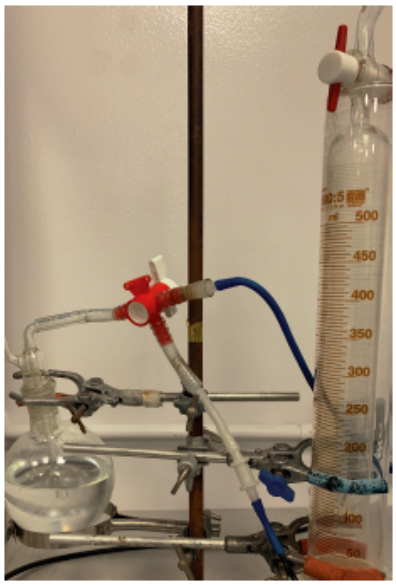

Figure 205: Volumetric cylinder.

Weighing Scales

They are electronic weighing scales used to calculate the samples weight in both wet and dry form. They used to measure cassava peels and date seeds weight before the treatment process, starch and other materials. Beakers as well measured before and after filled to ensure the exact readings. The weighing scales used have ranges from 0 to 11 kg ± 0.1 g with 0.1 readability and from 0 to 210 g ± 0.01 g with 0.01 readability. Figure 206 shows the scale used for light weights.

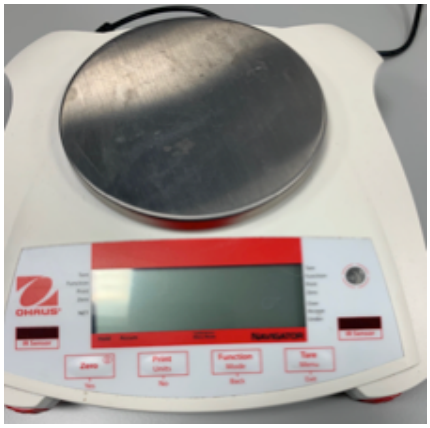

Figure 206: electronic scale.

Biogas analyser

BIOGAS 5000 portable gas analyser (Geo-tech) (CH_4% and CO_2% accuracy ± 0.5%) was used to analyse the biogas produced and to measure the percentage of biogases: CH_4, CO_2, O_2, and H_2S. Figure 207 shows the Biogas analyser device. The device was calibrated after each run by measuring the percentage of oxygen in the air to ensure the measurements accuracy. It is also periodically calibrated by the manufacturer company.

Figure 207: Biogas analyser.

Valve

Three-way valve was used in the study to adjust the biogas movement between the reactors and the aluminium bag. The three-way valve connects to an aluminium bag via tube.

Biogas Bags

The aluminium bags use to store and maintain biogases. Each bag was connected to one reactor. The bags were tightly closed, so that not to allow any leakage of gas, prevent air entering into the bags and for safety precautions. Codes were placed on bags to distinguish between them. The bags were filled with nitrogen from a nitrogen cylinder, then discharged to clean the bags from impurities such as O_2 and air. Figure 208 shows the 5L aluminium bag from Sigma-Aldrich Chemical Co.

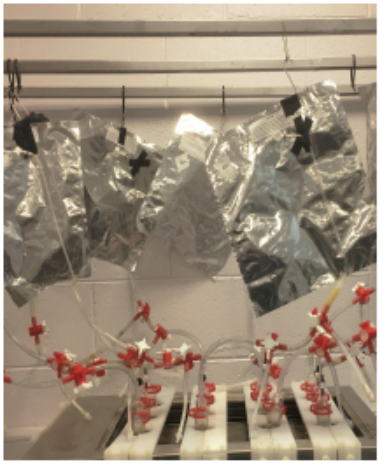

Figure 208: Biogas bag.

Nitrogen Gas Cylinder

The fermentation process occurs in a free O_2 environment under the AD. Nitrogen was used to remove gases present in the fermentation environment.

Round Bottom flask

The round bottom flask was used in the preparation of the AD environment. It is connected to the electric pump by a tube. The electric pump extracts and releases the gas to the flask. The bubble in the flask represents the air being released and the water helps in preventing air from flowing back into the system. The round bottom flask is shown in Figure 209.

Figure 209: Round bottom flask.

Conical Flask

Conical flask that illustrates in Figure 210 is considered as a digester. In these flasks, four decomposition stages (hydrolysis, acidogenesis, acetogenesis, and methanogenesis) occur in the AD environment. All flasks filled with a mixture of feedstock, water and sludge. They were placed in the water baths to maintain the setting temperature. Red clips located on the neck of flask were used to prevent leakage of biogases.

Figure 210: Conical Flask.

Glassware

Other glassware used during the experiment included: dish plate, low and tall beakers illustrate in Figure 211 (250, 2,000, 3,000 and 5,000) ml. These glasswares were used for the purpose of preparing, measuring and pouring the samples.

Figure 211: Glasswares.

pH meter

Hanna Precision pH meter (accuracy ± 0.01) model pH 213 shown in Figure 212, was used in the study. The device measures the pH of the sludge and digestate produced for all samples. It was calibrated before and during the experiments by measuring known pH substances to calibrate the device.

Figure 212: pH meter.

Energy meter

Energy consumption during AD process was measured by aiming of energy meter an accuracy of ± 0.01 kWh. Energy consumption of water baths was measured at the three target temperatures over a period of 21 days. Daily consumption was recorded at the same time to observe the daily consumption of each water bath.

Soxhlet Device

For the purpose of extracting the oil from the date seeds, the Soxhlet device shown in Figure 32 (chapter 3) was used. The device consists of several main parts, still pot, thimble, siphon, condenser and water inlet and outlet slots.

Condenser

Figure 213 shows the reflux condenser of sizes 40/38 and 24/29 that used in the study with water in and out slots.

Figure 213: Soxhlet Reflux Condenser.

Extraction Thimble

The soluble substances are placed in the pure cotton cellulose thimbles as demonstrated in Figure 214 to extracted the oil by solvent extraction. Extraction thimble sizes 33×80 mm and 33×100 mm were used in the process of extracting oil from date seeds.

Figure 214: Cotton extraction thimble.

Rotary Evaporator

BUCHI water bath B-480 rotary evaporator as shown in Figure 215 was used to separate the oil from the solvent and in separation of alcohol from the bio diesel and glycerine mixture.

Figure 215: Rotary evaporator.

Funnel Extractor

The Funnel extractor in Figure 216 was used in order to separate the bio diesel and glycerine according to the difference in their density.

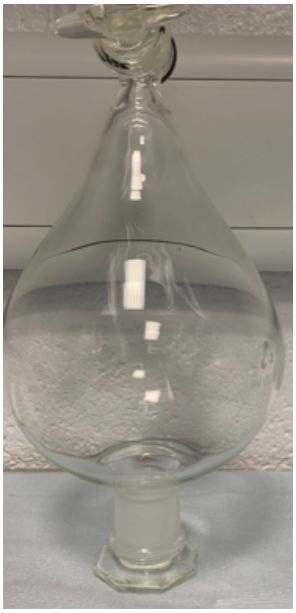

Figure 216: Funnel extractor.

Density Kit

Avery Berkel density kit as shown in Figure 217 was used to calculate the adhesive's samples density. The weighing scale was zeroed after each measurement to ensure that the reading accuracy.

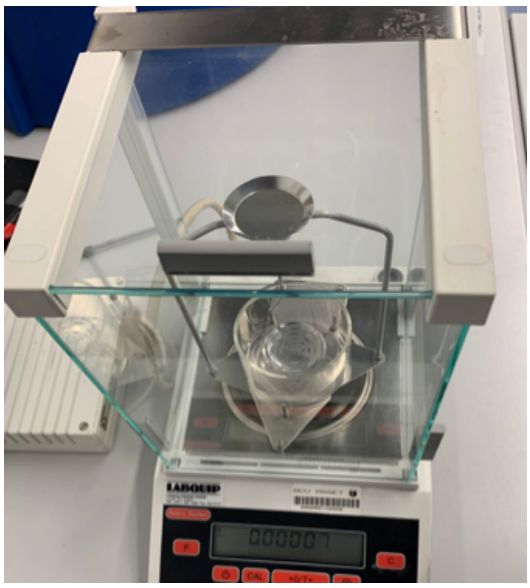

Figure 217: density kit.

Viscometer

Figure 218 shows the Rheology International Viscometer that used in measuring the viscosity of starch-based adhesives. The device accuracy is ±1%, the device was auto zeroed after each measurement to ensure the accuracy of readings.

Figure 218: Rheology International Viscometer.

Shear Strength

Zwick/Roell universal electromechanical testing machine (model Z5) was used to measure the shear strength of plywood, plastic, and paperboard samples. The machine has high measured-value accuracy over a wide measurement range with sampling rates of 400 kHz and 24-bit resolution. After each measurement, the grips were setting to the start position and zeroing the force for ensuring accuracy. Figure 219 Shows the Zwick/Roell testing machine.

Figure 219: Shear strength tesing machine.

Roughness meter

Figure 220 illustrates the Surface Roughness Tester TR-200 that used in measuring the surfaces roughness of plywood, plastic and paperboard. The roughness measurement accuracy is 0.001 µm. The accuracy of the instrument was tested periodically by measuring the surface roughness of the reference sample.

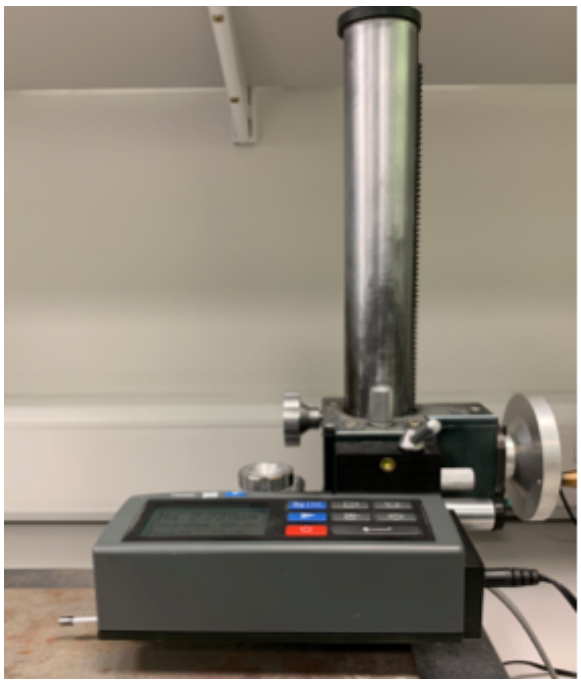

Figure 220: Surface Roughness tester meter TR200

Appendix (B)
Digestate Tests certificates

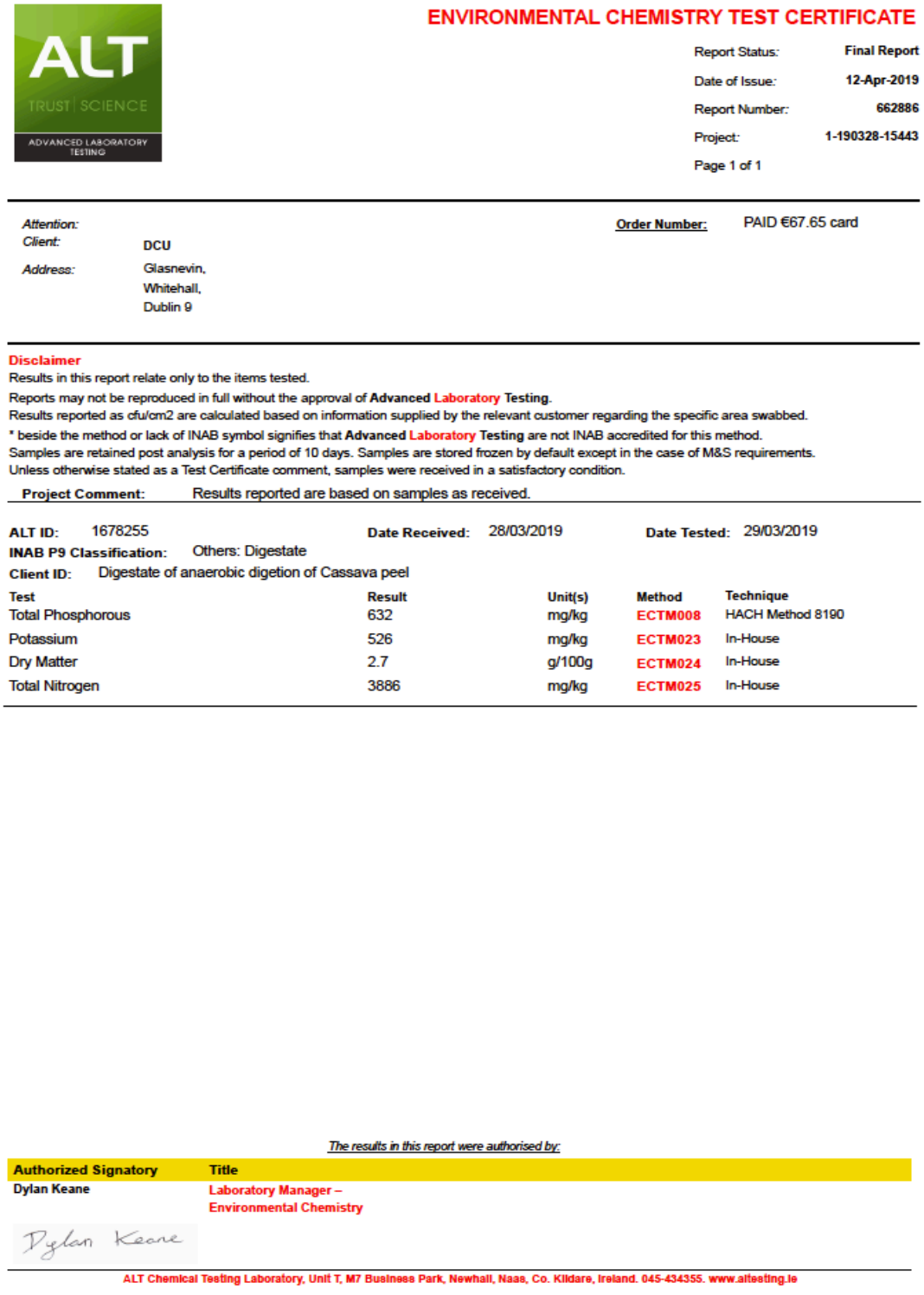

ENVIRONMENTAL CHEMISTRY TEST CERTIFICATE

Report Status: Final Report
Date of Issue: 12-Apr-2019
Report Number: 662886
Project: 1-190328-15443
Page 1 of 1

Attention:
Client: DCU
Address: Glasnevin, Whitehall, Dublin 9

Order Number: PAID €67.65 card

Disclaimer
Results in this report relate only to the items tested.
Reports may not be reproduced in full without the approval of Advanced Laboratory Testing.
Results reported as cfu/cm2 are calculated based on information supplied by the relevant customer regarding the specific area swabbed.
* beside the method or lack of INAB symbol signifies that Advanced Laboratory Testing are not INAB accredited for this method.
Samples are retained post analysis for a period of 10 days. Samples are stored frozen by default except in the case of M&S requirements.
Unless otherwise stated as a Test Certificate comment, samples were received in a satisfactory condition.

Project Comment: Results reported are based on samples as received.

ALT ID: 1678255 Date Received: 28/03/2019 Date Tested: 29/03/2019
INAB P9 Classification: Others: Digestate
Client ID: Digestate of anaerobic digetion of Cassava peel

Test	Result	Unit(s)	Method	Technique
Total Phosphorous	632	mg/kg	ECTM008	HACH Method 8190
Potassium	526	mg/kg	ECTM023	In-House
Dry Matter	2.7	g/100g	ECTM024	In-House
Total Nitrogen	3886	mg/kg	ECTM025	In-House

The results in this report were authorised by:

Authorized Signatory	Title
Dylan Keane	Laboratory Manager – Environmental Chemistry

Dylan Keane

ALT Chemical Testing Laboratory, Unit T, M7 Business Park, Newhall, Naas, Co. Kildare, Ireland. 045-434355. www.altesting.ie

Figure 221: Digestate test result certificate that produced from AD of the cassava peel.

ENVIRONMENTAL CHEMISTRY TEST CERTIFICATE

Report Status: **Final Report**
Date of Issue: **25-Mar-2019**
Report Number: **651670**
Project: **1-190311-05470**
Page 1 of 1

Attention:
Client: **DCU**
Address: Glasnevin,
Whitehall,
Dublin 9

Order Number: PAID €67.65

Disclaimer
Results in this report relate only to the items tested.
Reports may not be reproduced in full without the approval of **Advanced** Laboratory **Testing**.
Results reported as cfu/cm2 are calculated based on information supplied by the relevant customer regarding the specific area swabbed.
* beside the method or lack of INAB symbol signifies that **Advanced** Laboratory **Testing** are not INAB accredited for this method.
Samples are retained post analysis for a period of 10 days. Samples are stored frozen by default except in the case of M&S requirements.
Unless otherwise stated as a Test Certificate comment, samples were received in a satisfactory condition.

ALT ID: 1652799 **Date Received:** 11/03/2019 **Date Tested:** 14/03/2019
INAB P9 Classification: Others: Digestate
Client ID: Biofertilizer of Anerobic digestion of date seed.

Test	Result	Unit(s)	Method	Technique
Total Phosphorous	347	mg/kg	ECTM008	HACH Method 8190
Potassium	382	mg/kg	ECTM023	In-House
Dry Matter	1.7	g/100g	ECTM024	In-House
Total Nitrogen	2322	mg/kg	ECTM025	In-House

The results in this report were authorised by:

Authorized Signatory	Title
Dylan Keane	Laboratory Manager – Environmental Chemistry

Dylan Keane

ALT Chemical Testing Laboratory, Unit T, M7 Business Park, Newhall, Naas, Co. Kildare, Ireland. 045-434355. www.altesting.ie

Figure 222: Digestate test result certificate that produced from AD of the date seed.

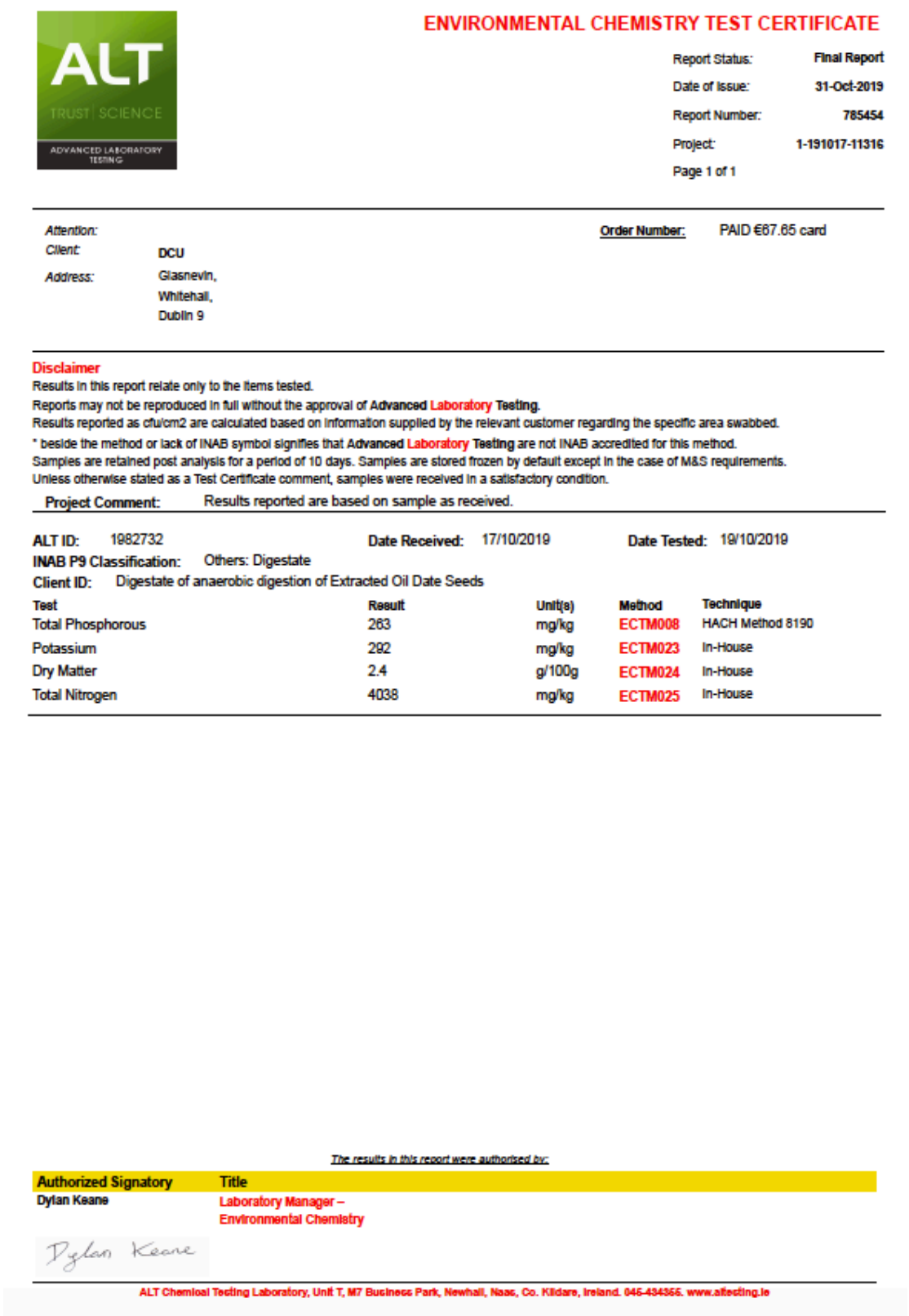

ENVIRONMENTAL CHEMISTRY TEST CERTIFICATE

Report Status: Final Report
Date of Issue: 31-Oct-2019
Report Number: 785454
Project: 1-191017-11316
Page 1 of 1

Attention:
Client: DCU
Address: Glasnevin, Whitehall, Dublin 9

Order Number: PAID €67.65 card

Disclaimer
Results in this report relate only to the items tested.
Reports may not be reproduced in full without the approval of Advanced Laboratory Testing.
Results reported as cfu/cm2 are calculated based on information supplied by the relevant customer regarding the specific area swabbed.
* beside the method or lack of INAB symbol signifies that Advanced Laboratory Testing are not INAB accredited for this method.
Samples are retained post analysis for a period of 10 days. Samples are stored frozen by default except in the case of M&S requirements.
Unless otherwise stated as a Test Certificate comment, samples were received in a satisfactory condition.

Project Comment: Results reported are based on sample as received.

ALT ID: 1982732 Date Received: 17/10/2019 Date Tested: 19/10/2019
INAB P9 Classification: Others: Digestate
Client ID: Digestate of anaerobic digestion of Extracted Oil Date Seeds

Test	Result	Unit(s)	Method	Technique
Total Phosphorous	263	mg/kg	ECTM008	HACH Method 8190
Potassium	292	mg/kg	ECTM023	In-House
Dry Matter	2.4	g/100g	ECTM024	In-House
Total Nitrogen	4038	mg/kg	ECTM025	In-House

The results in this report were authorised by:

Authorized Signatory	Title
Dylan Keane	Laboratory Manager – Environmental Chemistry

Dylan Keane

ALT Chemical Testing Laboratory, Unit T, M7 Business Park, Newhall, Naas, Co. Kildare, Ireland. 045-434355. www.altesting.ie

Figure 223: Digestate test result certificate that produced from AD of the extracted oil date seed.

Appendix (C)
Biodiesel and Glycerine Tests Results

مطابقة
MOTABAQAH
الشركة السعودية للمختبرات الخاصة
Saudi Specialized Laboratories Co.

مختبر فحص المواد البترولية - الدمام
Petroleum Testing Laboratory - Dammam

Page No.: Page 1 of 2
Report No.: 430657
Issuance Date: 15-Jun-2020

تقرير اختبار / Test Report

Customer Information			
Company Name	Alla Mohammed Alrefai		
Company Address	Jeddah, Saudi Arabia,		
Contact Person	Alla Mohammed Alrefai		
Telephone/Fax/Email	alaa.alrefai2@mail.dcu.ie Tel # 0505657685		
Sample Information			
Sample Description	Biodiesel Extracted from Sagai Date Seed Oil		
Client Sample ID	Biodiesel	Date Sampled	03-Jun-2020
Number of Samples	1 Container	Date Received	03-Jun-2020
Sampled By	Customer	Date Tested	03,15-June-2020

Name of Analysis	Test Method	Results	Unit
Acid Number	ASTM D664	0.01	mgKOH/g
Cetane Index, Calculated	ASTM D976	47.6	
Sulfur Content, EDXRF	ASTM D4294	0.005	%mass
Initial Boiling Point IBP *	ASTM D2887	86	°C
10% Recovery *	ASTM D2887	289	°C
20% Recovery *	ASTM D2887	290	°C
30% Recovery *	ASTM D2887	320	°C
40% Recovery *	ASTM D2887	348.5	°C
50% Recovery *	ASTM D2887	369.5	°C
60% Recovery *	ASTM D2887	370	°C
70% Recovery *	ASTM D2887	371	°C
80% Recovery *	ASTM D2887	371	°C
90% Recovery *	ASTM D2887	371.5	°C
95% Recovery *	ASTM D2887	373.5	°C
Final Boiling Point FBP *	ASTM D2887	439	°C
Appearance	Visual	Hazy Liquid	
Cloud Point	ASTM D5773	0	°C
Color	Visual	Yellowish	
Density @ 15°C	ASTM D4052	890	kg/m3
Flash Point, SETA *	ASTM D3828	147	°C
Pour Point	ASTM D5949	-2.0	°C
Viscosity Kinematic @ 40°C	ASTM D7042	4.11	cSt

Comment

Test results relate only to the sample as received by the laboratory and MI Labs accepts no liability for the traceability or quality of samples prior to receipt by the laboratory.

SIMDIS ASTM D2887 Report Attached. Sample was diluted (DF-3) with carbon disulfide CS2.

End of test report

Testing

الشركة السعودية للمختبرات الخاصة
Saudi Specialized Laboratories Co.
مطابقة MOTABAQAH
مختبر فحص المواد البترولية
Petroleum Testing Lab
1010225110 س.ت

ترقيع المخول / Authorized Signatory
Joel Deocares
المدير الفني / Technical Manager

22nd Street Dammam 1st Industrial Area, Kingdom of Saudi Arabia
Tel (+966920029293) / Fax (+966138143417) F/7.8/1.01 Rev. 00 05/05/2019

Figure 224: Biodiesel test results.

مطابقة
MOTABAQAH
الشركة السعودية للمختبرات الخاصة
Saudi Specialized Laboratories Co.

مختبر فحص المواد البترولية - الدمام
Petroleum Testing Laboratory - Dammam

Page No.: Page 1 of 1
Report No.: 430658
Issuance Date: 15-Jun-2020

تقرير اختبار / Test Report

Customer Information			
Company Name	Alla Mohammed Alrefai		
Company Address	Jeddah, Saudi Arabia,		
Contact Person	Alla Mohammed Alrefai		
Telephone/Fax/Email	alaa.alrefai2@mail.dcu.ie Tel # 0505657685		
Sample Information			
Sample Description	Glycerine Extracted from Sagai Date Seed Oil		
Client Sample ID	Glycerine	Date Sampled	03-Jun-2020
Number of Samples	1 Container	Date Received	03-Jun-2020
Sampled By	Customer	Date Tested	03,15-June-2020

Name of Analysis	Test Method	Results	Unit
pH Value @ 20°C (10%)	ASTM E70	9.16	
Appearance	Visual	Gelatinous at room temp.	
Color	Visual	Brownish	
Density @ 15°C	ASTM D4052	1.047	g/ml
Flash Point, SETA *	ASTM D3828	149.5	°C
Water Content, Karl Fischer	ASTM D6304	38	%

Comment

Test results relate only to the sample as received by the laboratory and MI Labs accepts no liability for the traceability or quality of samples prior to receipt by the laboratory.

End of test report

GAC ACCREDITATION CENTER GAC
Testing
ISO/IEC 17025:2017
ATL 0089

اللجنة السعودية للاعتماد
Saudi Accreditation Committee
Testing Laboratory TL00004

الشركة السعودية للمختبرات الخاصة
Saudi Specialized Laboratories Co.
مطابقة MOTABAQAH
مختبر فحص المواد البترولية
Petroleum Testing Lab
1010225110 : س.ت

توقيع المخول / Authorized Signatory
Joel Deocares
المدير الفني / Technical Manager

Test with "*" denotes non-accredited tests. Test with "**" denotes subcontracted tests.
Test Report relates only to the item(s) tested on specified Standard Test Method(s) and specific clause(s).
Test Report shall not be reproduced, except in full, without written approval of Motabaqah.
Unless requested for return, Test Item(s) are destroyed and discarded 90 days after Test Report Date.
Test conducted may form into unusble and dangerous item(s). Motabaqah, do not assume liability resulting from the use of the returned item(s).

Figure 225: Glycerine test results.